

Max-Planck-Institut für  
molekulare Physiologie



Technische Universität  
Dortmund

# **Novel Transition Metal-Free C–H Bond Functionalization Methods for Biologically Important Heterocycles Synthesis**

## **Dissertation**

For the achievement of the academic degree of the  
**Doctor in Natural Science**  
(Dr. rer. Nat.)

Submitted to  
The Faculty of Chemistry and Chemical Biology  
Technical University of Dortmund

By  
**Mahesh Puthanveedu, M.S.**  
from Mannarkkad, India

Dortmund 2021







The work presented in this thesis was performed during the time period from July 2018 to November 2021 under the supervision of Prof. Dr. Dr. h.c. Herbert Waldmann and the guidance of Prof. Dr. Andrey P. Antonchick at the Faculty of Chemistry and Chemical Biology of the Technical University Dortmund and the Max Planck Institute of Molecular Physiology, Dortmund.

Dean: Prof. Dr. S. M. Kast

1<sup>st</sup> Examiner: Prof. Dr. Dr. h.c. H. Waldmann

2<sup>nd</sup> Examiner: Prof. Dr. A. P. Antonchick



Results presented in this thesis contributed to the following publications:

1. Mahesh Puthanveedu, Vasiliki Polychronidou, and Andrey P. Antonchick, “Catalytic Selective Metal-Free Cross-Coupling of Heteroaromatic *N*-Oxides with Organosilanes”, *Org. Lett.* **2019**, *21*, 3407–3411.
2. Mahesh Puthanveedu, Vladislav Khamraev, Lukas Brieger, Carsten Strohmann, and Andrey P. Antonchick; “Electrochemical Dehydrogenative C(sp<sup>2</sup>)-H Amination”, *Chem. Eur. J.* **2021**, *27*, 8008-8012.
3. Fabian Wessler, Daniel Riege, Mahesh Puthanveedu, Jonas Halver, Eva Müller, Jessica Bertrand, Andrey P. Antonchick, Sonja Sievers, Herbert Waldmann, Dennis Schade, “Probing embryonic mesodermal differentiation enables identification of small molecule bone morphogenetic protein activators”, *manuscript submitted*.





*Dedicated to my family*



# Table of Contents

Table of Contents	I
Abstract	V
Zusammenfassung	VII
1. Introduction	3
1.1 C–H functionalization	3
1.1.1 Transition metal-free C–H functionalization	5
1.1.2 Transition metal free C–H functionalization of heteroaromatic <i>N</i> -oxides	9
1.1.3 Electrochemical C–H functionalization in the absence of transition metal catalysts	17
1.1.4 Electrochemical direct C–H bond amination methods	20
2 Objectives	29
3 Cross-Coupling of Heteroaromatic <i>N</i> -oxides with Organosilanes	33
3.1 C–H Benzylation	33
3.1.1 Introduction	33
3.1.2 Motivation and objectives	36
3.1.3 Initial results and optimization	37
3.1.4 Scope of heterocyclic <i>N</i> -oxides and benzytrimethylsilanes	40
3.1.5 Mechanistic considerations	43
3.1.6 Identification of biological activity	46
3.2 C–H Alkynylation	48
3.2.1 Introduction	48
3.2.2 Motivation and objectives	49
3.2.3 Initial results and optimization	50
3.2.4 Scope of heterocyclic <i>N</i> -oxides	52
3.2.5 Mechanistic considerations	53
3.2.6 Identification of biological activity	54
4 Electrochemical Dehydrogenative Amination	59
4.1 Introduction	59
4.2 Intramolecular amination	61
4.2.1 Motivation and objectives	61

4.2.2	Initial results and optimization	63
4.2.3	Scope of intramolecular amination	65
4.2.4	Mechanistic considerations	67
4.3	Intermolecular amination	73
4.3.1	Motivation and objectives	73
4.3.2	Initial results and optimization	75
4.3.3	Scope of intermolecular amination	76
4.3.4	Identification of biological activity	77
5	Synthesis of Bioactive Compounds <i>via</i> C–H Amination	81
5.1	Introduction	81
5.2	Identification of a novel osteogenic BMP activator chemotype	82
5.3	Design, synthesis and biological evaluation of chromone derivatives	83
6	Summary	91
7	Experimental Part	95
7.1	General	95
7.2	Experimental part for the cross-coupling	97
7.2.1	General procedures	97
7.2.2	Physical data of products	99
7.3	Experimental part for the electrochemical amination	112
7.3.1	General procedures	112
7.3.2	Electrolytic parameters of reaction	114
7.3.3	Evidences for nitrenium ion intermediate	115
7.3.4	Physical data of products	117
7.3.5	Crystal data	135
7.4	Experimental part for the synthesis of bioactive chromones	137
7.4.1	General procedures	137
7.4.2	Physical data of products	139
8	References	145
9	Appendix	i
9.1	List of Abbreviations	i

9.2	Acknowledgement	v
9.3	Curriculum Vitae	vii
9.4	Eidesstattliche Versicherung (Affidavit)	ix



## Abstract

The development of transition metal-free reaction methodologies for the direct functionalization of C–H bonds is an attractive area of research. These reactions offer atom-economic methods for the synthesis and functionalization of valuable organic molecules in the absence of precious metal catalysts under mild conditions. Novel methodologies have been established for biologically important nitrogen containing molecules (Figure 1). A regioselective cross-coupling method for the benzylation and alkynylation of privileged heterocyclic scaffolds like quinolines, isoquinolines and pyridines were evaluated under organocatalytic conditions. Oxidized *N*-heterocyclic compounds were reacted with organosilanes in presence of a fluoride catalyst. This method offers a highly selective route to access C<sub>1</sub>-benzylated isoquinolines, C<sub>2</sub>-benzylated quinolines and pyridines. Additionally, a unique sigma bond metathesis strategy is explored to obtain symmetrically disubstituted acetylenes containing privileged scaffolds (Chapter 3).

Electroorganic chemistry has witnessed a renewed interest in recent years because of its profound advantages over other methods such as oxidants mediated oxidative coupling reactions. Many oxidants used in the organic reactions are potentially hazardous and even toxic. The risk of handling such oxidants in stoichiometric amounts is high. Alternatively, electricity itself can be employed as sole oxidant to carry out many redox reactions. Combining the field of transition metal-free C–H functionalization chemistry with the revived electroorganic chemistry offers unique advantages. Inspired by this proposal, an electrochemical dehydrogenative amination including both intramolecular and intermolecular variants have been established. Detailed mechanism involving a nitrenium ion intermediate has been proposed revealing the possible generation of nitrenium ion intermediates under electrochemical oxidative conditions for the first time (Chapter 4).

Direct C–H bond functionalization methods frequently give access to the kind of molecules which were never accessed before. These molecules however might be relevant in terms of biological properties. Therefore, the evaluation of bioactivities for novel molecules synthesized by direct C–H bond functionalization methods are highly significant. A novel physiological, morphogenic cellular screening system that is focused on the bone morphogenetic pathway revealed chromones as potential BMP activator chemotypes. The key step in the synthesis of these chromone compounds is an oxidative C–H amination in presence of molecular iodine and base. The active

hits were resynthesized in adequate amounts for *in vitro* and *in vivo* studies. Additionally, based on the molecular structure of active hits, novel derivatives were designed and synthesized. Afterwards, biological experiments were carried out in collaboration to understand the structure activity relationship of various chromones as BMP effectors (Chapter 5).

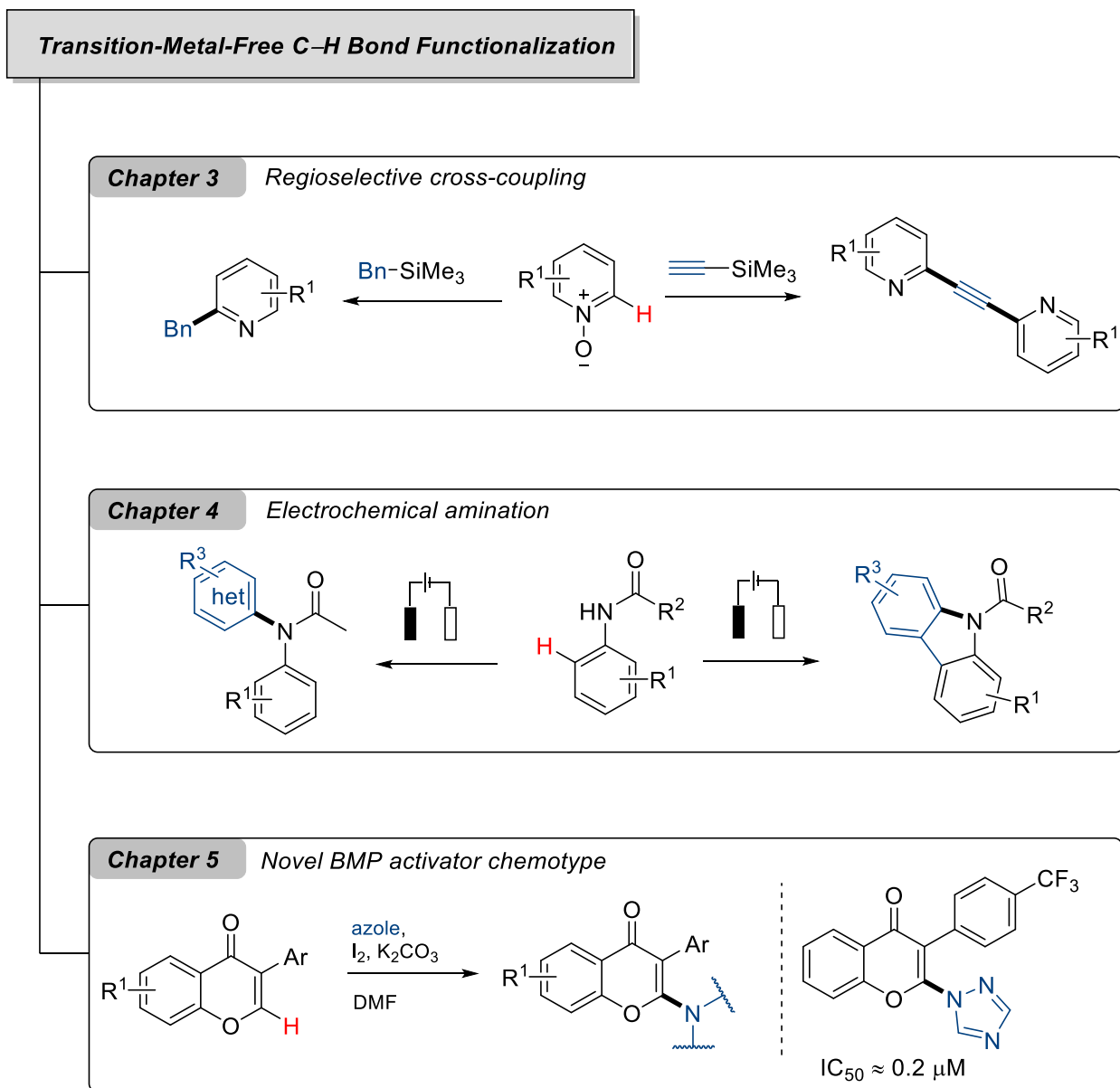


**Figure 1** Overview of the projects described in this thesis



## Zusammenfassung

Die Entwicklung von Übergangsmetallfreien Reaktionsmethoden für die direkte Funktionalisierung von C–H-Bindungen ist ein attraktives Forschungsgebiet. Diese Reaktionen bieten verbesserte, atomökonomische Methoden für die Synthese und Funktionalisierung wertvoller organischer Moleküle in Abwesenheit von Edelmetallkatalysatoren unter relativ milden Bedingungen. In diesem Zusammenhang wurden neue Methoden für biologisch relevante stickstoffhaltige Moleküle entwickelt (Abbildung 1). Zunächst wurde eine regioselektive Kreuzkupplungsmethode für die Benzylierung und Alkynylierung privilegierter heterozyklischer Strukturgerüste wie Chinoline, Isochinoline und Pyridine unter organokatalytischen Bedingungen untersucht. Voroxidierte *N*-heterozyklische Verbindungen wurden mit Organosilanen in Anwesenheit eines Fluoridaktivators umgesetzt. Diese Methode bietet einen hochselektiven Zugang zu C<sub>1</sub>-benzylierten Isochinolinen, C<sub>2</sub>-benzylierten Chinolinen und Pyridinen. Zusätzlich wird eine einzigartige Sigma-Bindungs-Metathesestrategie untersucht, um symmetrisch disubstituierte Acetylene zu erhalten, die an beiden Enden privilegierte Gerüste aufweisen. Diese Verbindungen wurden auch auf potenzielle Bioaktivität untersucht (Kapitel 3). Die elektroorganische Chemie hat in den letzten Jahren aufgrund ihrer tiefgreifenden Vorteile gegenüber anderen Methoden, wie z. B. durch chemische Oxidationsmittel vermittelte oxidative Kupplungsreaktionen, ein neues Interesse geweckt. Viele verwendeten Oxidationsmittel in organischen Reaktionen sind potenziell gefährlich und sogar giftig. Der Umgang mit solchen Oxidationsmitteln in stöchiometrischen Mengen ist mit hohem Risiko verbunden. Alternativ kann Elektrizität selbst als gezieltes Oxidationsmittel eingesetzt werden, um viele Redoxreaktionen durchzuführen. Die Kombination von Übergangsmetallfreien C–H-Funktionalisierungsschemie mit der wiederbelebten elektroorganischen Chemie bietet einzigartige Vorteile. Inspiriert von diesem Ansatz wurde eine elektrochemische dehydrierende Aminierung entwickelt, die sowohl intramolekulare als auch intermolekulare Varianten umfasst. Ein detaillierter Mechanismus, an dem ein Nitrenium-Ionen-Zwischenprodukt beteiligt ist, welcher zum ersten Mal die mögliche Bildung von Nitrenium-Ionen Zwischenprodukten unter elektrochemischen oxidativen Bedingungen aufzeigt, wurde vorgeschlagen (Kapitel 4).

Direkte C–H-Bindungsfunktionalisierungsmethoden ermöglichen häufig den Zugang zu Molekülen, die bisher nicht bzw. erschwert zugänglich waren. Diese Moleküle könnten jedoch im

Hinblick auf biologische Eigenschaften von hoher Bedeutung sein. Daher ist die Untersuchung der Bioaktivität neuartiger Moleküle, die mit Hilfe direkter C–H-Bindungsfunktionalisierungsmethoden synthetisiert wurden, von großer Bedeutung. Ein neuartiges physiologisches, morphogenetisches zelluläres Screening-System, das sich auf den Knochenmorphogenese-Weg (BMP-Weg) konzentriert, hat zum Beispiel Chromone als potenziellen BMP-Aktivator-Chemotyp enthüllt. Der Schlüsselschritt bei der Synthese dieser Chromonverbindungen ist eine oxidative CH-Aminierung in Gegenwart von molekularem Jod und einer Base. Die aktiven Verbindungen wurden in ausreichenden Mengen für In-vitro- und In-vivo-Studien resynthetisiert. Darüber hinaus wurden auf der Grundlage der Molekularstruktur der aktiven Moleküle neue Derivate entworfen und synthetisiert. Anschließend wurden in Zusammenarbeit biologische Experimente durchgeführt, um die Struktur-Aktivitäts-Beziehung der verschiedenen Chromone als BMP-Effektoren zu analysieren.

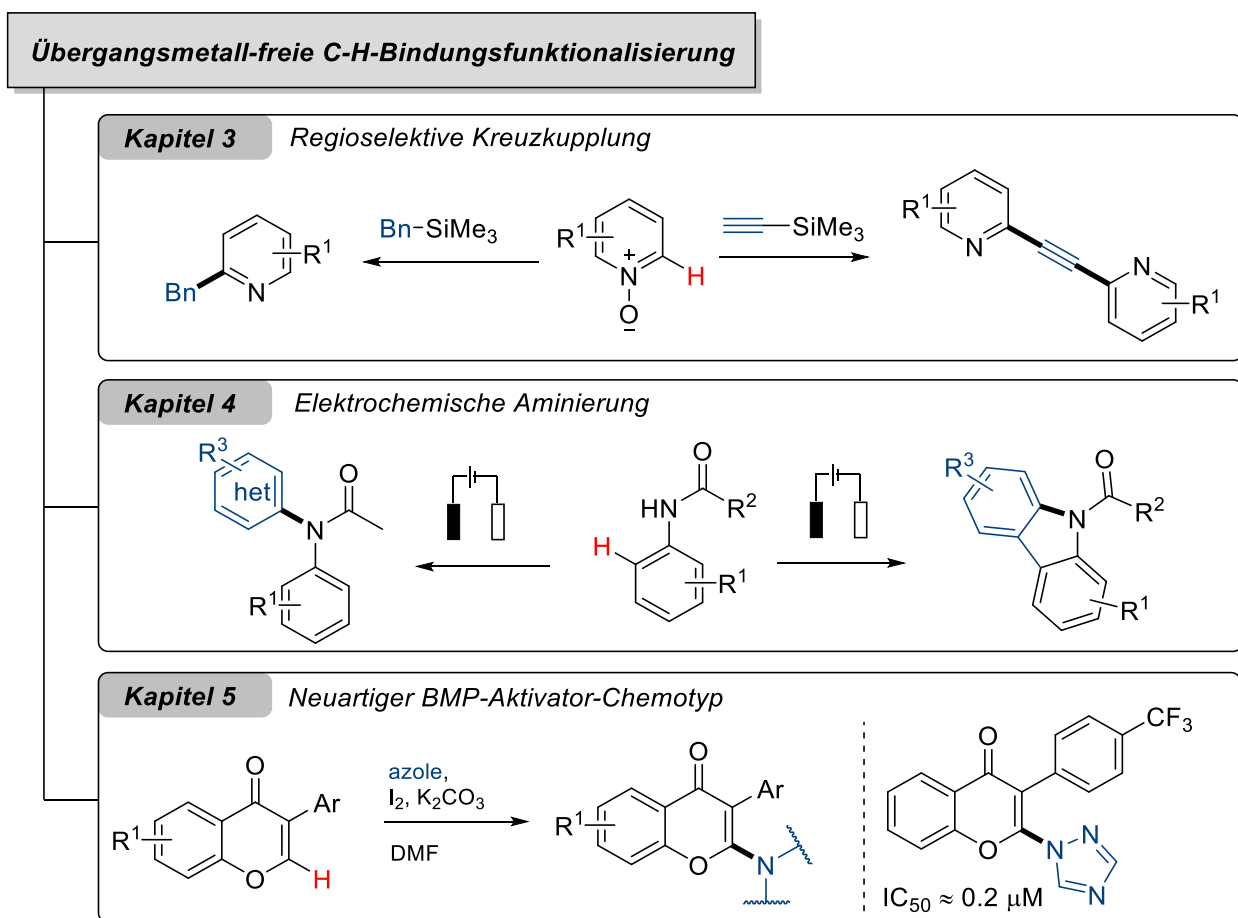


**Abbildung 1** Überblick über die in dieser Arbeit beschriebenen Projekte

**Introduction**

---



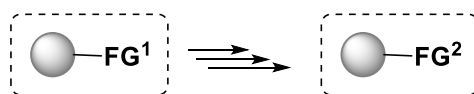
# 1. Introduction

## 1.1 C–H functionalization

Direct C–H bond functionalization methods have attracted the attention of the synthetic community because of their undisputed advantages over the traditional methods. Since the 1960s, following the discovery of Shilov's platinum chemistry, this research area has experienced tremendous developments.<sup>[1]</sup> Considering their new-found applications in synthetic organic chemistry and medicinal chemistry such as late-stage functionalization, researchers around the globe continue to develop novel reactions as well as solve existing challenges in this field.<sup>[2]</sup> C–H functionalization is used to directly functionalize otherwise unreactive C–H bonds without the requirement of their pre-functionalization. This offers a number of advantages over traditional methods of organic synthesis (Scheme 1.1). Development of atom and step economical reactions were realized with minimal amounts of waste generation in the form of reaction by-products. In addition, from the sustainability point of view, the catalytic C–H functionalization methods offer milder conditions, more efficient routes in comparison to cross-coupling reactions. Due to their large functional group tolerance and cost effectiveness up to an extent, these methodologies are highly significant for the synthesis and functionalization of biologically relevant natural products and pharmaceuticals.<sup>[3]</sup>

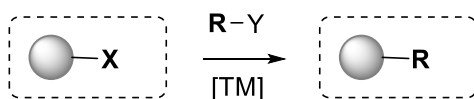
### Conventional methods:

1) FG transformations



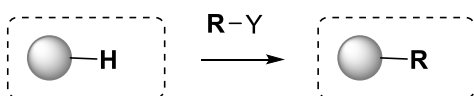
- x multi-step procedure
- x waste generation
- x selectivity

2) Cross-coupling reactions



- x atom and step economy
- x waste generation
- ✓ better selectivity

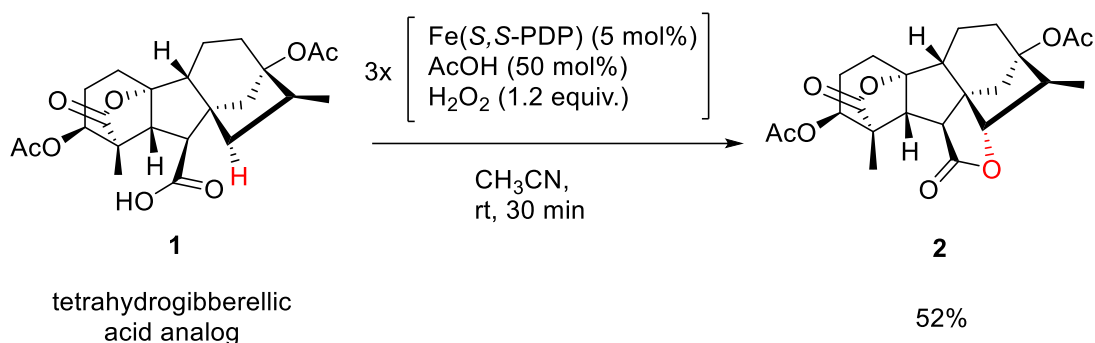
### C–H functionalization:



- ✓ atom and step economy
- ✓ less waste
- ✓ sustainability
- ✓ better selectivity

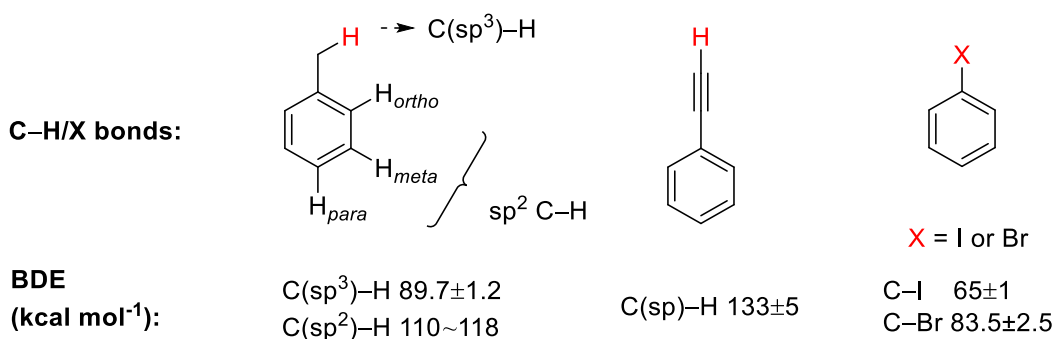
**Scheme 1.1** Progress in organic synthesis towards C–H functionalization

Techniques like late-stage functionalization enable synthesis of large numbers of derivatives from the same intermediate *via* direct functionalization of carbon-hydrogen bonds<sup>[4]</sup> and hence helping in the structure-activity relationship studies during drug discovery. In short, a method once considered as highly challenging and less practical is now becoming an important aspect of synthetic route design and offers a new set of retrosynthetic connections for molecularly diverse architectures (Scheme 1.2).<sup>[5]</sup>



**Scheme 1.2** Late-stage functionalization of a complex organic molecule

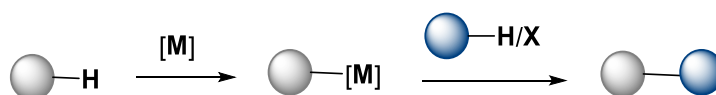
However, the challenges to overcome in the area of C–H activation/functionalization chemistry are still many in terms of industrial applications. The limitations pertaining to catalytic C–H functionalization methods are mainly attributed to the ubiquitous nature of carbon-hydrogen bonds, their relatively higher bond dissociation energies and lack of major electronic differences between various C–H bonds. These challenges ultimately result in harsh reaction conditions. Moreover, C–H functionalization methods advancing the sustainability of chemical reactions are also an active area of research “to meet the chemistry needs of the present without compromising those of future” (Scheme 1.3).<sup>[6]</sup>



**Scheme 1.3** Relative bond dissociation energies (BDEs) of different C–H/X bonds

The majority of developed C–H functionalization methodologies use various transition metal catalysts (TM) in order to facilitate the activation of inert and thermodynamically stable C–H bonds. In this regard, a large number of site-selective transformations have been realized employing external or internal directing group coordination chemistry.<sup>[7]</sup> This not only includes selective functionalization of adjacent C–H bonds to the coordinating group, but also C–H bonds located at remote positions of coordinating functionalities.<sup>[8]</sup> Currently, the development of enantioselective reactions by means of C–H activation has gained attention as well.<sup>[9]</sup> Despite the undisputed advantages over other existing methods C–H activation has its own shortcomings (Scheme 1.4). Most of these methods necessitate the use of precious transition metal catalysts. With a clear focus on sustainable chemistry for the future, it is obvious that dependence on such scarce metals should be minimized. Many such literature methods employ high catalyst loadings of high valent transition metals as well. In general, these methods also employ high temperatures and solvents which are not well suited for green and sustainable chemistry. Another problem is the dependence on hazardous oxidants for the completion of catalytic cycles. Also, additional directing group manipulations are required for selective insertion of functional groups. However, a large number of methods have already been published with improved sustainability parameters for C–H activation in the past two decades.<sup>[10]</sup> These include methodologies using early transition metals, reduced catalyst loading and alternative oxidant systems are to name a few. Catalysis under mild and efficient reaction conditions in environmentally friendly solvents as well as innate functional group directed transformations are also gaining attention.<sup>[11]</sup>

Key issues of C–H Activation:



- precious transition metals
- stoichiometric oxidants
- sensitive reactions
- directing groups
- metal impurities in final products

**Scheme 1.4** Key challenges of sustainable C–H functionalization methods

### 1.1.1 Transition metal-free C–H functionalization

An appealing alternative could be the development of a greater number of C–H functionalization reactions in the absence of any transition metals.<sup>[12]</sup> New avenues in this field of research like

organocatalytic and oxidative C–H functionalizations are progressing rapidly (Figure 1.1). As two significant areas of modern organic chemistry, C–H functionalization and transition metal-free (TM-free) catalysis results in the development of viable, green, selective and efficient transformations. In addition, such methods allow synthesis of important intermediates of pharmaceuticals without the high risk of contamination with heavy metal impurities. Otherwise removal of these impurities from the final products are a time consuming and cost-ineffective process.

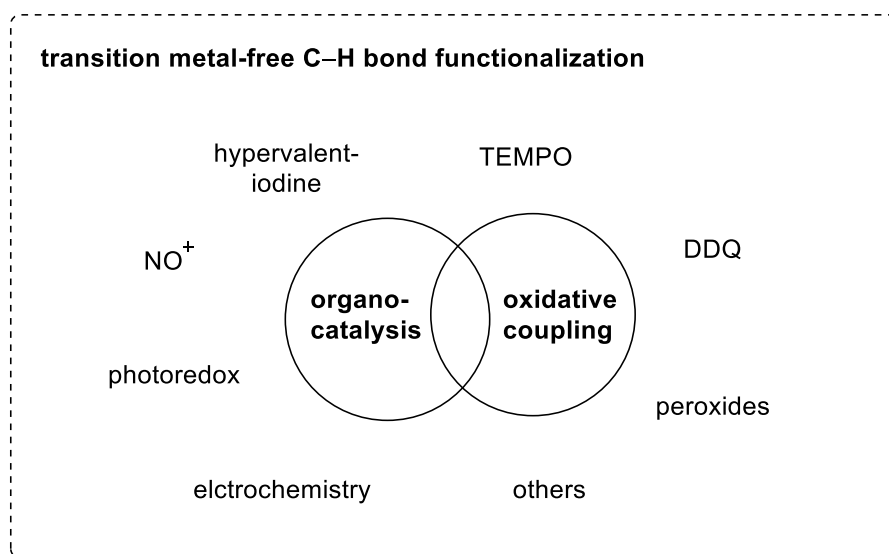


**Figure 1.1** Methods of TM-free C–H bond functionalizations

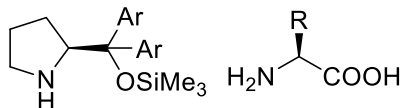
Despite the advances made in the past couple of decades, more selective and efficient methods are in high demand at present. In this context, rapid advances in the area of organocatalysis along with other transition metal-free methodologies are well foreseeable.<sup>[13]</sup> According to existing literature reports, transition metal-free C–H functionalization reactions can be broadly categorized as organocatalytic methods and oxidative C–H functionalization reactions such as oxidative homo- and hetero- couplings. The former class visibly involves a complete catalytic cycle while the latter could be oxidation-initiated C–C or C–X bond forming reactions.<sup>[14]</sup>

There are different classes of organocatalysts employed in inert C–H functionalization reactions.<sup>[15]</sup> A renaissance in electroorganic synthesis and growing popularity of photoredox catalysis are also complimenting organocatalytic research well.<sup>[16-17]</sup> Oxidative C–H bond



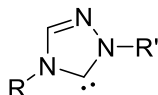
functionalization reactions are also gaining significant popularity owing to their ability to carry out efficient organic transformations without the requirement of pre-functionalization.

#### Aminocatalysts

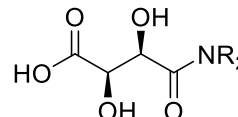


Ar = 3,5-(CF<sub>3</sub>)<sub>2</sub>C<sub>6</sub>H<sub>3</sub>

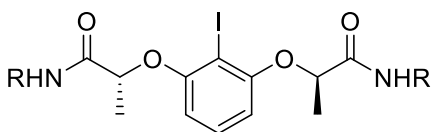
#### N-heterocyclic carbene



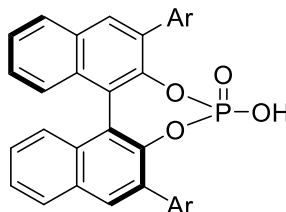
#### Bronsted acid catalyst



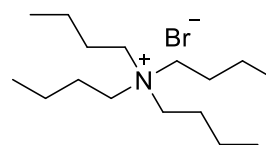
#### Iodoarene catalysts



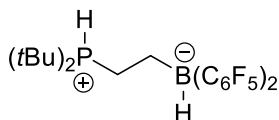
#### Phosphoric acid catalyst



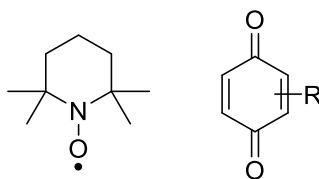
#### Phase transfer catalyst



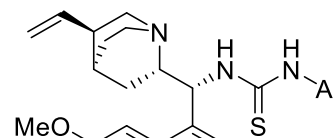
#### Frustrated Lewis pairs



#### Electroorganic catalysts

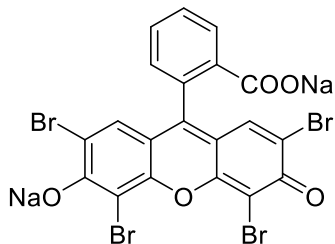


#### Thiourea catalyst

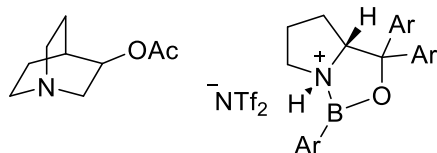


Ar = 2,4,6-(CH<sub>3</sub>)<sub>3</sub>C<sub>6</sub>H<sub>2</sub>

#### Photoredox organocatalysts



#### Other organocatalysts



#### Oxidants

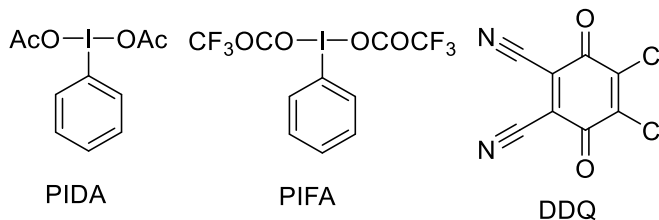
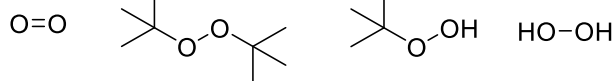
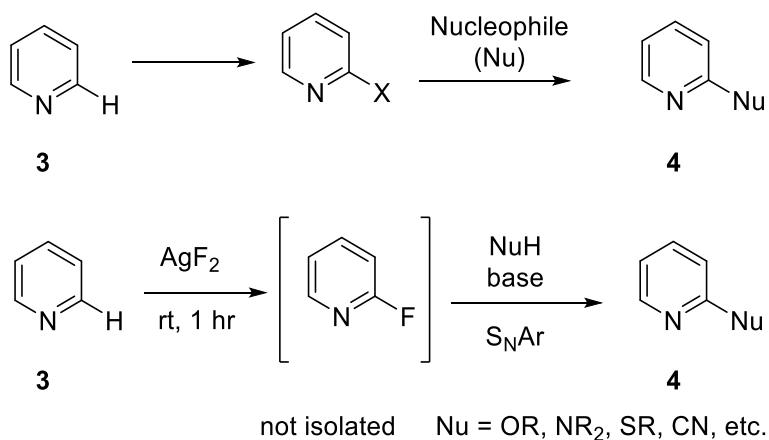


**Figure 1.2** Representative organocatalysts and oxidants for C–H bond functionalization

The amounts of waste generated is significantly lower. However, to functionalize stable C–H bonds is a challenge. For this reason, the electron/hydrogen transfer reagents are employed to significantly increase the acidity of C–H bonds and to decrease the BDE in oxidative C–H functionalization as in the case of photoredox or electroorganic catalysis. Taking advantage of this chemistry, various chemicals like 2,3-dichloro-5,6-dicyano-1,4-benzoquinone (DDQ), 2,2,6,6-tetramethylpiperidin-1-yl)oxyl (TEMPO), phenyl iodine (III) diacetate (PIDA), bis(trifluoroacetoxy)iodo)benzene (PIFA), nitrosonium salts, etc. are used for oxidative homocoupling and heterocoupling reactions in the absence of any transition metals (Figure 1.2).<sup>[18]</sup>

Innate C–H functionalization reactions are based on their innate reactivity at certain positions of molecules as in the case of heteroaromatic *N*-oxide chemistry, aromatic substitution reactions, sulfoxides directed C–H couplings for example.<sup>[19-23]</sup> In this regard, heterocyclic *N*-oxides are an important class of substrates in organic chemistry and they are well studied chemicals for direct C–H functionalization methods to obtain densely functionalized nitrogen heterocycles. They are also present in some biologically active natural products and synthetic drugs.<sup>[24]</sup> A general route for the synthesis of C<sub>2</sub> substituted pyridine or quinoline compounds is the nucleophilic substitution of corresponding heteroaryl halides. However, these reactions usually require pre-functionalization, harsh conditions and still the yield of reactions are quite low in most of the cases (Scheme 1.5).



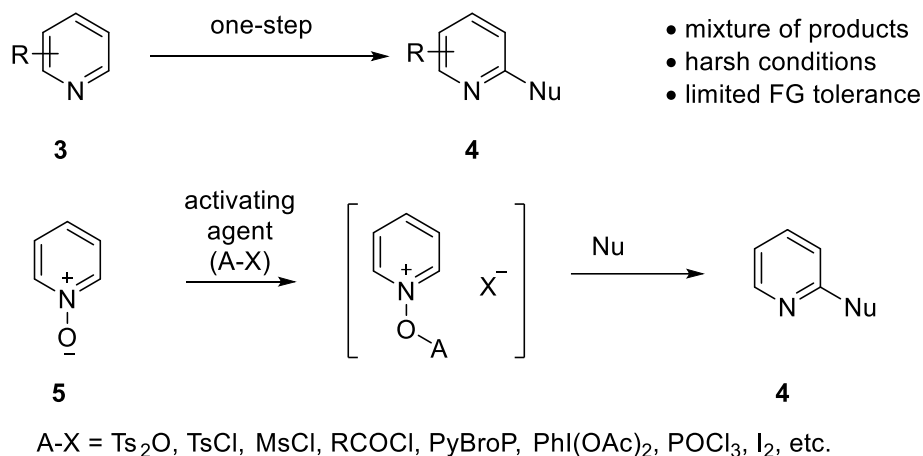
**Scheme 1.5** Nucleophilic substitution of 2-halo-heteroarenes

Hartwig's group used a combination of fluorination and a following nucleophilic aromatic substitution for the site-selective late-stage functionalization of nitrogen containing aromatic

compounds. The reaction is broadly applicable for the  $\alpha$ -functionalization of pyridine containing compounds (**3**) and various nucleophiles like cyano-, amino-, thio-, etc. could be employed to obtain corresponding C<sub>2</sub>-substituted pyridines (**4**) (Scheme 1.5).<sup>[25]</sup>

### 1.1.2 Transition metal free C–H functionalization of heteroaromatic *N*-oxides

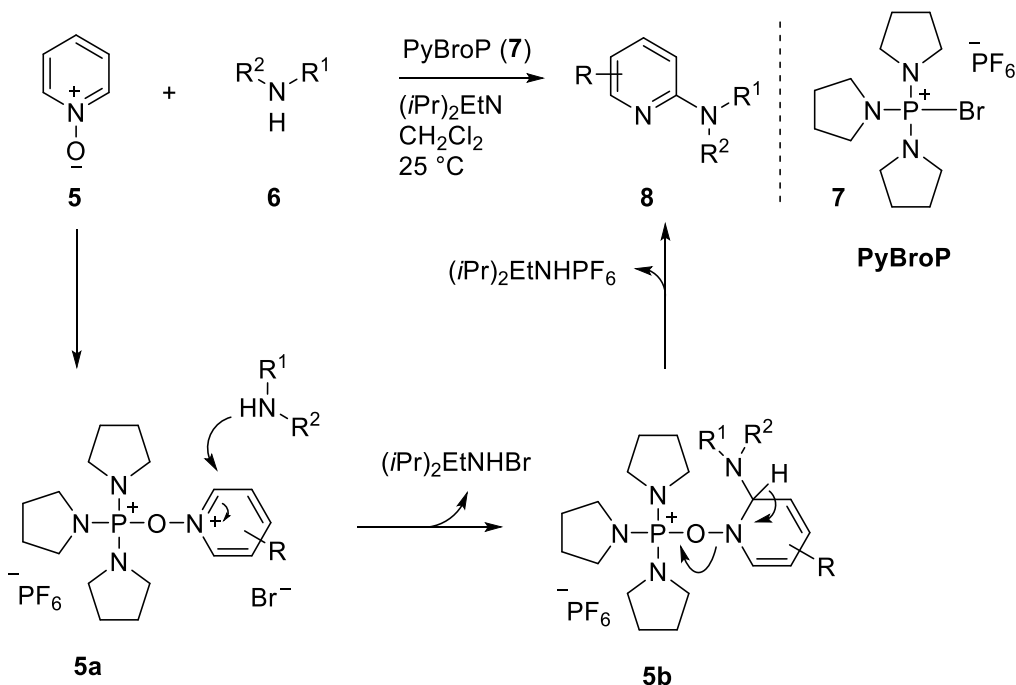
Another strategy is to start with *N*-oxides in the presence of an activating agent, which will eventually increase the electrophilic nature of the 2-position. Hence, reactions will occur under relatively mild conditions. However, there are chances of undesired side reactions in presence of activating agents and 2- or 4- position selectivity is challenging to control in this type of *cine*-substitution reactions. (Scheme 1.6).<sup>[26]</sup>



**Scheme 1.6** Nucleophilic substitution reactions of pyridine and heteroaromatic *N*-oxides

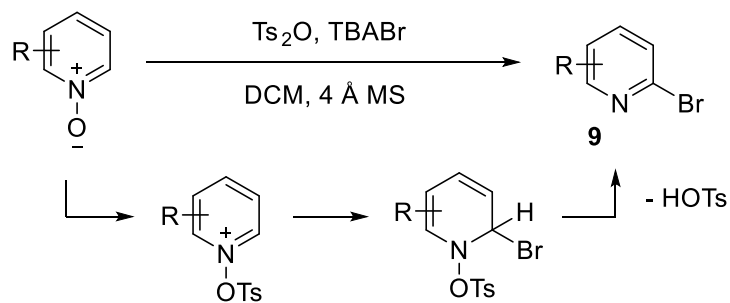
Many efficient deoxygenative functionalization reactions have been reported following this strategy. Among these, phosphorus containing activating groups are attractive reagents as the formation of strong phosphorus-oxygen bonds will drive the reaction to proceed. On this basis, Londregan and co-workers developed a facile amination strategy for the synthesis of 2-aminopyridines using commercially available bromo-tris-pyrrolidino-phosphonium hexafluorophosphate (PyBroP, **7**) as activating agent. The reaction had a diverse substrate scope and could be used for the synthesis of various C<sub>2</sub>-aminated pyridines and quinolines. The reaction was proposed to proceed through the formation of intermediate **5a**. The nucleophilic attack of amine to the intermediate and following rearomatization resulted in the formation of selective amination products (**8**).<sup>[27]</sup> In a following report by the same group, this method was further extended to

various carbon, sulfur and oxygen nucleophiles to obtain selectively C<sub>2</sub>-substituted nitrogen heterocyclic compounds (Scheme 1.7).<sup>[28-29]</sup>



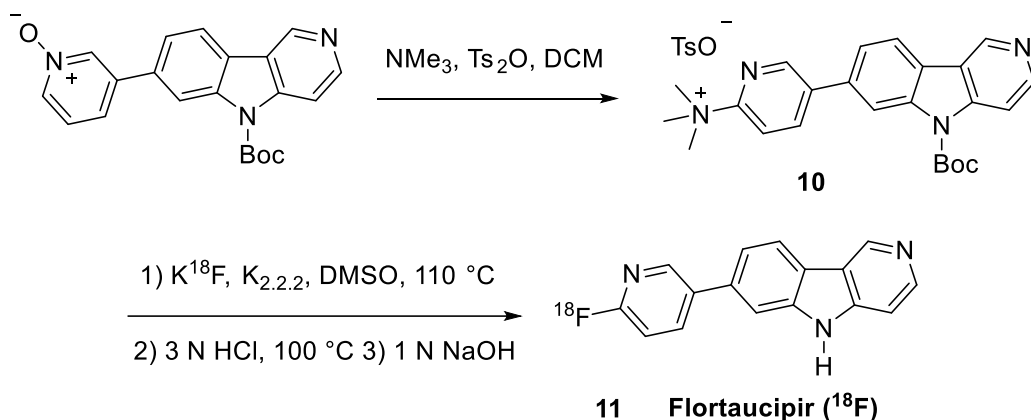
**Scheme 1.7** C–H functionalization of heteroaromatic *N*-oxides using activating agent

Baran group developed a mild and efficient approach for the regioselective bromination of azine *N*-oxides using tosic anhydride as activator. The methodology was successful for the bromination of diverse quinolines and isoquinolines. However, the reaction scope was not extendable to pyridine *N*-oxides. The authors also presented a one-pot oxidation-bromination strategy as well as a chlorination reaction using tetrabutylammonium chloride to demonstrate the versatility of the developed method (Scheme 1.8).<sup>[30]</sup>

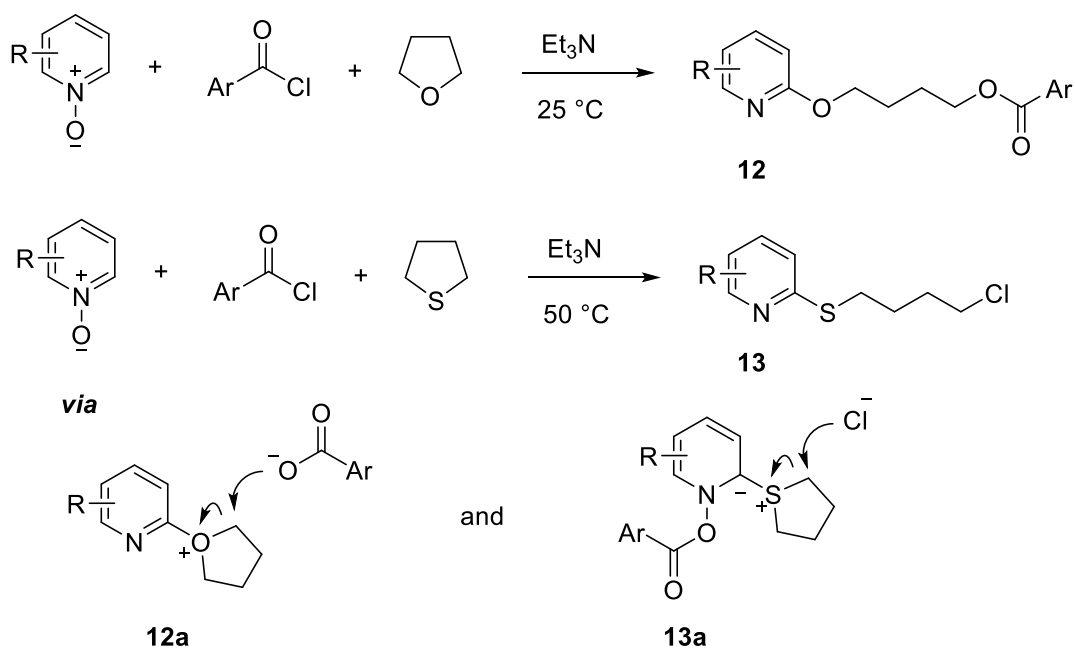


**Scheme 1.8** Regioselective C–H bromination of heteroaromatic *N*-oxides

In case of fluorination, a direct approach was not feasible because of the low nucleophilic reactivity of fluoride ions. Hence, the pyridine *N*-oxides were first converted into 2-pyridylalkylammonium salts (**10**). These salts are isolable and treating them with nucleophilic fluorine reagents like tetrabutylammonium fluoride or potassium fluorides give access to 2-fluoropyridine compounds. Interestingly, this method can be used in the synthesis of flortaucipir ( $^{18}\text{F}$ ) employing  $\text{K}^{18}\text{F}$  in the presence of Kryptofix 2.2.2. Flortaucipir ( $^{18}\text{F}$ ) (**11**) is a radioactive diagnostic agent used for brain imaging with the help of positron emission tomography (PET) (Scheme 1.9).<sup>[31]</sup>



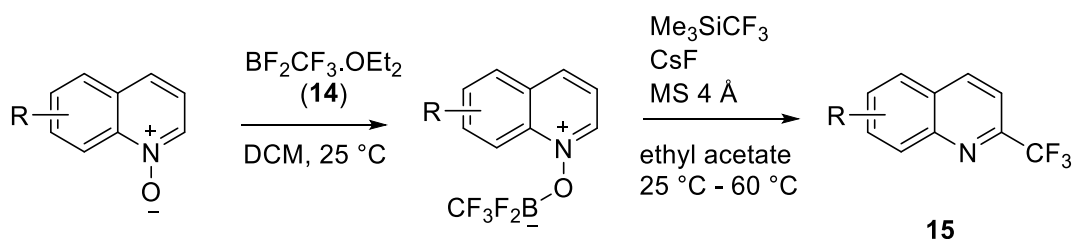
**Scheme 1.9** Application of regioselective C–H fluorination in synthesis



**Scheme 1.10** Three component reaction of *N*-oxides, acyl chlorides and cyclic (thio)ethers

Tomkinson's group revealed a strategy to introduce complex substituents at C<sub>2</sub>-position of electron deficient pyridines through novel three component reactions. The reaction proceeds in presence of acyl chlorides as an activating agent and triethylamine as base. The product formation while using cyclic ethers such as tetrahydrofuran as nucleophile was different from those while using cyclic sulfides (**12**, **13**). The reason was proposed to be the nucleophilic attack of chloride ion to the reaction intermediate (**12a**) instead of the acyloxy anion (**13a**) in the latter case (Scheme 1.10).<sup>[32-33]</sup>

A highly regioselective direct C–H trifluoromethylation of pyridine, quinoline, isoquinoline and two or three nitrogen containing aromatic *N*-oxides was discovered by Kuninobu and Kanai *et al.* trifluoromethyldifluoroborane (**14**) was found to be an effective activating reagent to drive reaction under mild conditions even for gram-scale reactions with an impressive scope. The methodology possesses high potential considering the abundance of trifluoromethyl group in biologically active molecules (Scheme 1.11).<sup>[34]</sup>

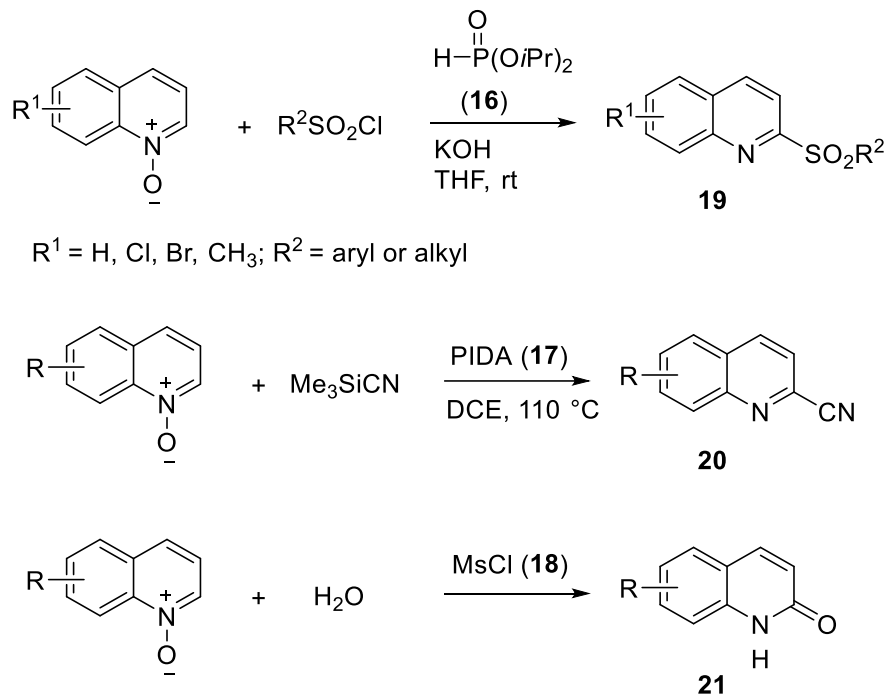


**Scheme 1.11** Direct C–H trifluoromethylation of *N*-oxides using trifluoromethyldifluoroborane

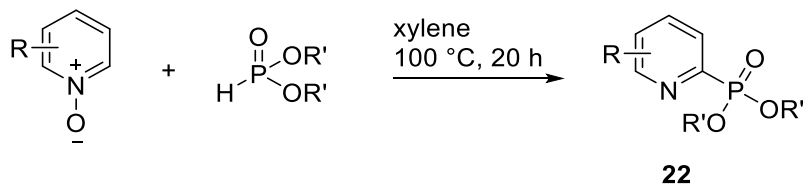
External activating group strategies for the site-selective C–H functionalization of *N*-oxides have been explored to access diversely functionalized nitrogen heterocycles. Moreover, the formation of new C–C, C–S, C–O, etc. (**19-21**) have been achieved *via* the direct functionalization of C–H bonds. Even though the transition metals are employed in many reported reactions, several metal-free alternatives are also available for a wide range of transformations in this class of reactions. In addition to common external activation reagents such as PyBroP, PPh<sub>3</sub>, anhydrides, *H*-phosphonates, hypervalent iodine reagents and acid chlorides (**16-18**) have also been employed successfully to achieve useful functionalizations (Scheme 1.12).<sup>[35-37]</sup>

On the other hand, reactions have also been developed where the use of external activating agents have been negotiated by employing reagents which can simultaneously act as nucleophile source

and activating agent. For instance, dialkyl phosphonates are common activating reagents for nucleophilic *cine*-substitution reactions of *N*-oxides to introduce a phosphonate group at  $\alpha$ -position (Scheme 1.13).<sup>[38-39]</sup>

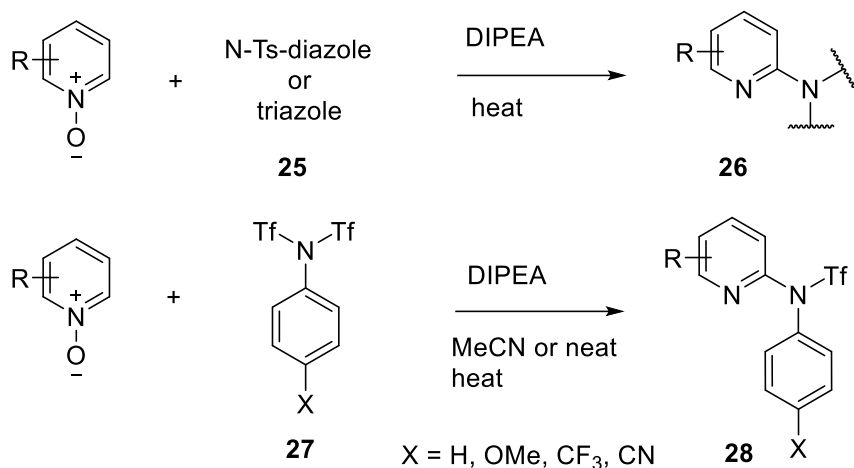
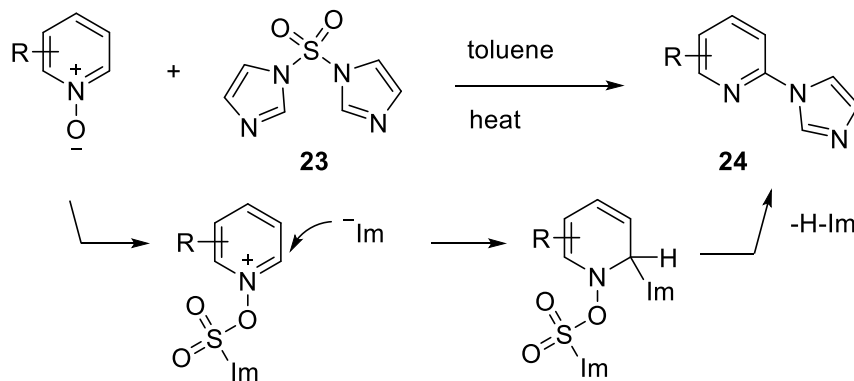


**Scheme 1.12** Other external activation reagents for C–H functionalization of *N*-oxides



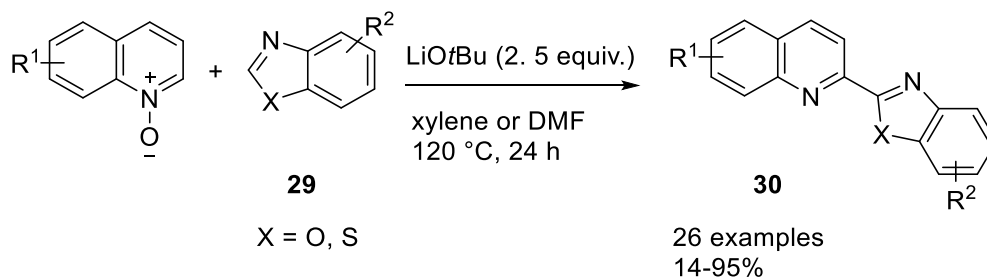
**Scheme 1.13** *cine*-substitution reactions of *N*-oxides with dialkyl phosphonates

Keith *et al.* revealed a method to access  $\alpha$ -imidazole substituted *N*-heteroarenes in presence of commercially available sulfuryl diimidazole (**23**). The reaction showed high site selectivity.<sup>[40]</sup> Later, it was also shown that *N*-tosylated triazoles and diazoles (**25**) can also be used as *N*-heterocycle source in presence of base. Similarly, heating *N*-aryltriflimides (**27**) with heteroaromatic *N*-oxides in presence of diisopropylethylamine yielded *N*-aryltriflamidoazines. However, because of the harsh reaction conditions and low functional group tolerance, the applications of this methodology are limited. (Scheme 1.14).<sup>[41-42]</sup>



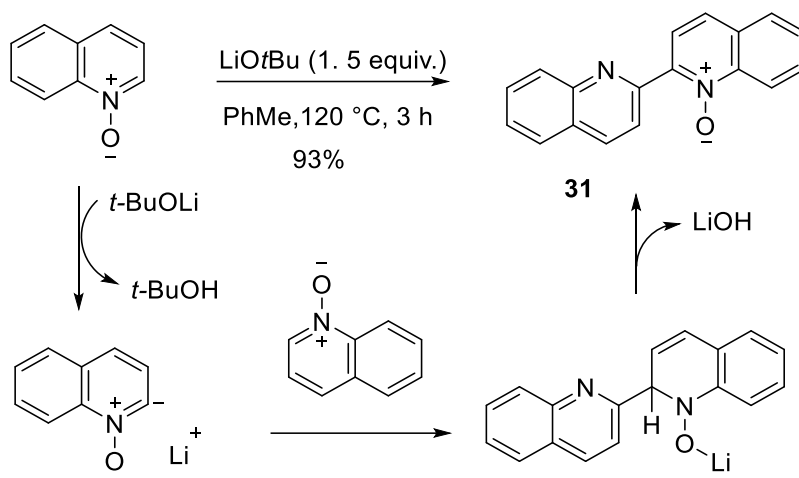
**Scheme 1.14** Amination reactions of *N*-oxides in the absence of external activation

In many cases, a strong base can initiate the reaction by abstracting a proton from  $\alpha$ -position of azine-*N*-oxides. Following nucleophilic attack of the dehydrogenative coupling partner to the resultant carbanion yields the biheteroaryl compounds (**30**). This methodology provides easy and efficient access to introduce heteroaromatic compounds to the *ortho* position of *N*-oxides (Scheme 1.15 and Scheme 1.16).<sup>[43]</sup>

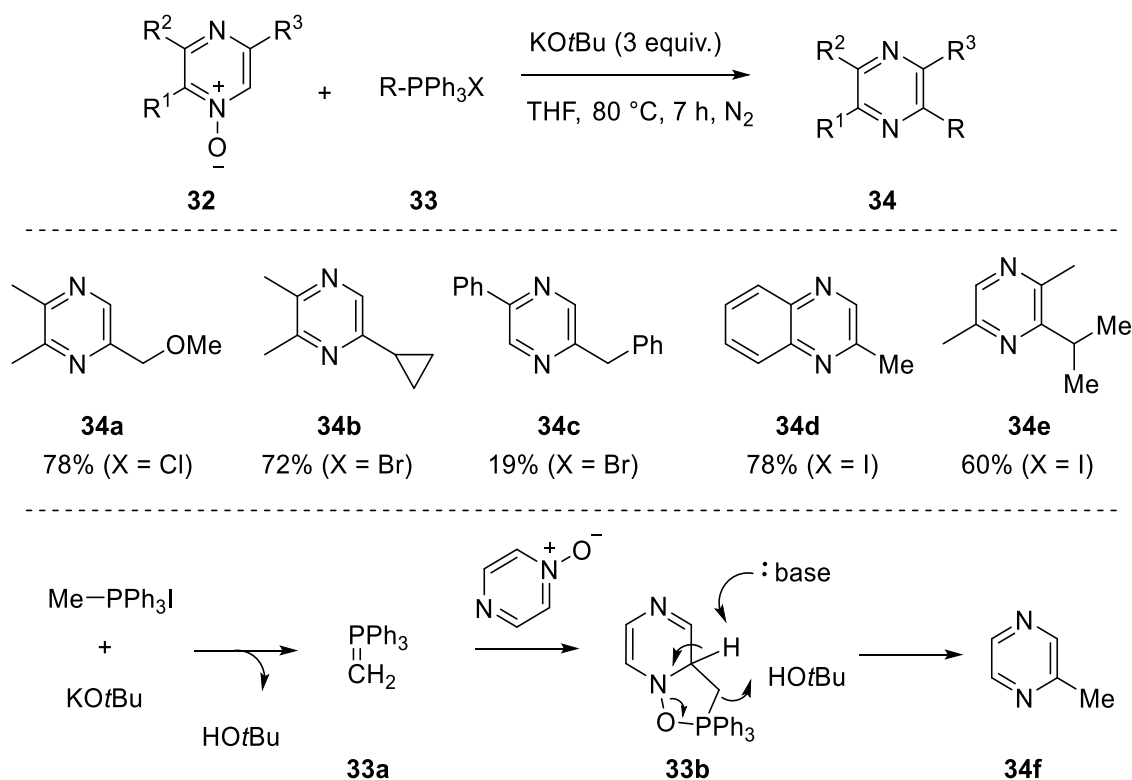


**Scheme 1.15** Base mediated *ortho* C–H functionalization of azine *N*-oxides





**Scheme 1.16** Base mediated homocoupling of azine *N*-oxides

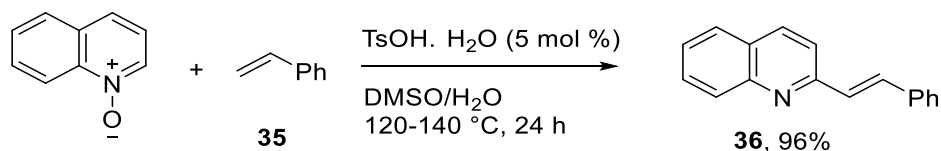


**Scheme 1.17** Regioselective C<sub>2</sub>-alkylation of diazine *N*-Oxides using Wittig reagents

In another approach an active nucleophilic species is generated *in situ* in presence of a base. This further attacks the *ortho*- position of heterocyclic *N*-oxide and ultimately leads to desired product formation.<sup>[44]</sup> Taking inspiration from Cho's alkylation approach employing diborylalkanes as alkylating agents, Kim, Han and co-workers reported a metal-free deoxygenative alkylation

strategy for pyridine, quinoline *N*-oxides and diazene *N*-oxides. The method demonstrates the potential of Wittig reagents (**33**) in site-selective metal-free C–H bond functionalization. Wittig reagent reacts with the heteroaromatic *N*-oxides to generate intermediate **33b**, from which the proton abstraction by the base yield the desired products. Various C<sub>2</sub>-alkylated diazine compounds (**34a-f**) were accessible *via* this method (Scheme 1.17).<sup>[45-47]</sup>

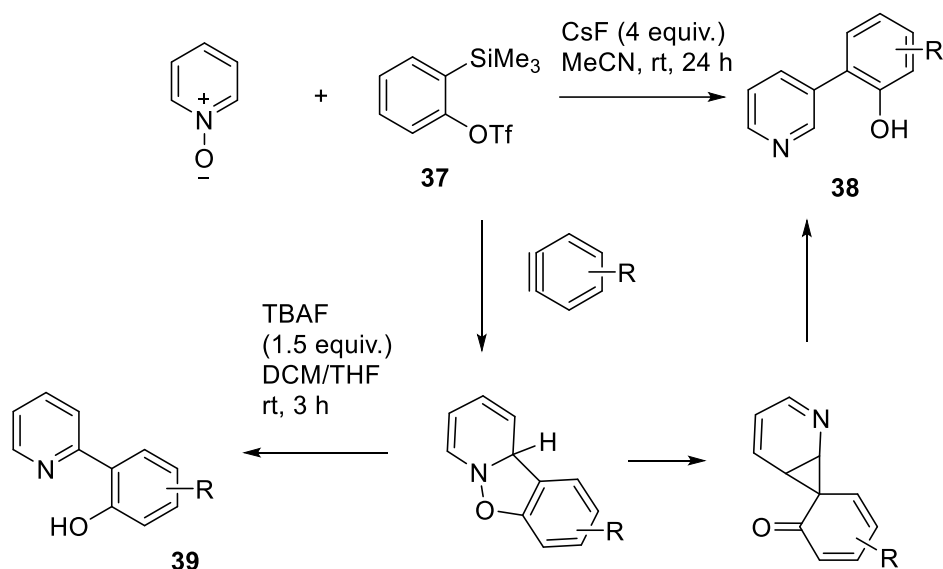
Heteroaromatic *N*-oxides are also 1,3-dipoles. This property has been exploited to develop novel methods of C–H functionalization reactions *via* 1,3-dipolar cycloadditions. In many cases, the intermediate cycloadduct undergoes further modifications to form more stable final products. Methodologies for the C<sub>2</sub>-alkenylation of *N*-oxide containing heterocycles using activated olefins are available in literature.<sup>[48-49]</sup> However, unactivated olefins (**35**) have also been successfully used for alkenylation reactions under Brønsted acid catalysis (Scheme 1.18).<sup>[50]</sup>



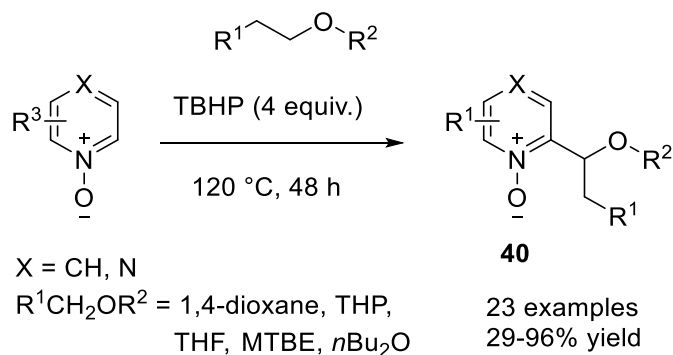
**Scheme 1.18.** 1,3-dipolar cycloaddition for alkenylation of *N*-oxides

Similarly, C<sub>2</sub>- and C<sub>3</sub>- arylations of azaarene *N*-oxides are also reported in reactions involving formation of aryne intermediate. The reaction offers a metal-free route to access hydroxyphenyl pyridines in presence of silylaryl triflates as a precursor for benzyne intermediate. Larock group revealed a methodology in which treating pyridine *N*-oxides with silylaryl triflates in presence of cesium fluoride (CsF) provided 3-(2-hydroxyphenyl)pyridines (**38**).<sup>[51]</sup> Liu's group modified the conditions by introducing a base to obtain 2-(2-hydroxyphenyl) substituted pyridines (**39**) (Scheme 1.19).<sup>[32]</sup>

Free radical intermediates are highly reactive reaction intermediates and they have been used widely in the functionalization of otherwise non-reactive C–H bonds. In this regard, cross dehydrogenative non deoxygenative coupling (CDC) reactions between azine *N*-oxides and ethers have been reported recently. The reaction occurs in presence of *tert*-butyl hydroperoxide as a radical initiator to generate alkyl radical intermediates. This intermediates further undergo coupling with heterocyclic *N*-oxides and results in non-deoxygenative C–H alkylation (Scheme 1.20).<sup>[52]</sup>



**Scheme 1.19** Benzyne mediated C–H functionalization of pyridine *N*-oxides



**Scheme 1.20** Nondeoxygenative C–H functionalization via radical intermediates

### 1.1.3 Electrochemical C–H functionalization in the absence of transition metal catalysts

Electricity as an electron source for carrying out direct functionalization of inert C–H bonds have attracted attention in recent years. This is mainly attributed to their environmentally benign properties.<sup>[53]</sup> Electrochemistry also allows versatile and nonclassical disconnection approaches for retrosynthesis in an atom efficient manner. Conventionally used redox reagents are hazardous and toxic. Usage of such chemicals in stoichiometric amounts at higher temperature involves a great risk. Many of the common redox reagents like lead acetate, osmium tetroxide, sodium hydride, etc. and radical initiators like azobisisobutyronitrile (AIBN) are the recommended

reagents. For these reasons, organic chemists are showing a renewed interest in electrochemistry.<sup>[54]</sup> In addition to the safety, atom efficiency and mild reaction conditions, the electrochemical methods for organic synthesis possess other advantages as well. As electricity is a syringe pump of electrons with numerous variables, it can help chemists to develop unprecedented redox reactions. Electrochemistry can overcome the limitations of synthetic route design based on redox potentials of available oxidizing and reducing agents. In addition, reaction kinetics could also be improved. Recently, there are a number of reports showcasing the potential of electroorganic synthesis in transition metal catalyzed cross-coupling reactions as a terminal oxidant in complex catalytic cycles.<sup>[55]</sup>

In comparison to a classical organic reaction, there are a number of variable reaction parameters and cell types for an electrochemical reaction set up. The electrolysis can be carried out in an undivided cell or in a divided cell. The undivided cell electrolysis involves only one chamber where all the reagents, solvents, catalyst, etc. are put together to carry out the electrolysis. This setup is preferred in terms of ease of set up. However, it is not always possible to carry out electrolysis in a single cell altogether because of the undesired side reactions from counter electrodes. In this case, the cells need to be separated by a semipermeable membrane to avoid such side reactions (Figure 1.3).<sup>[56]</sup>

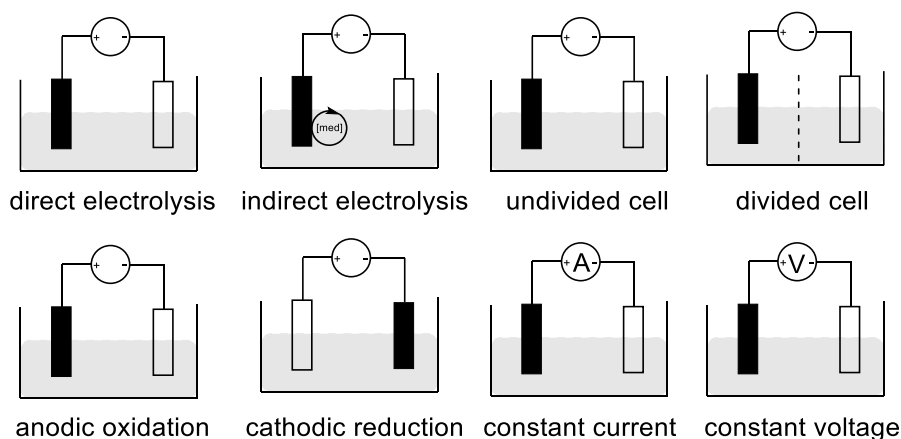
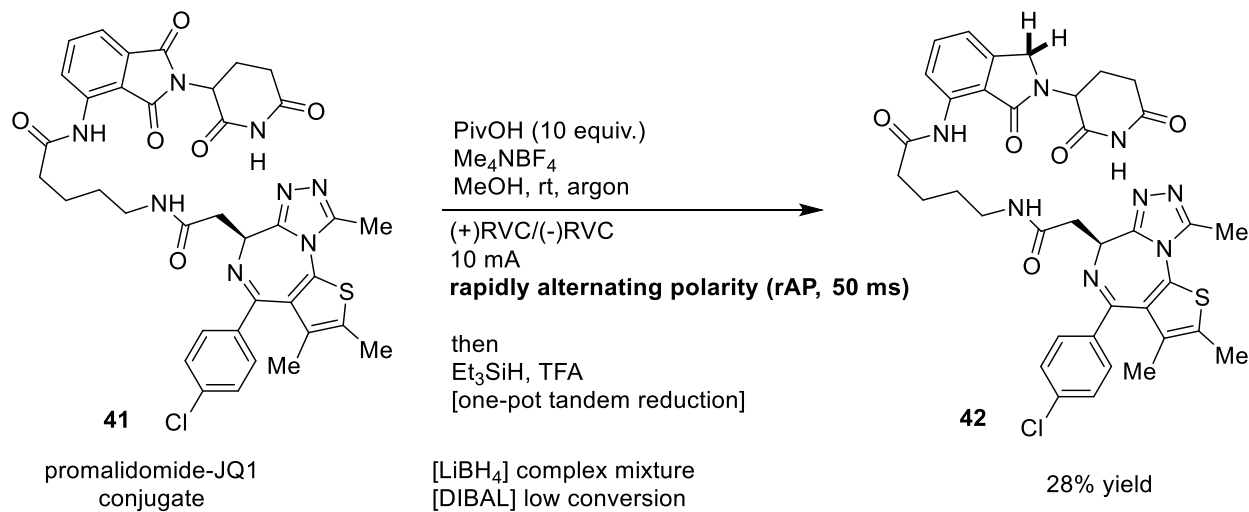


**Figure 1.3** Types of electrolysis for electrochemical reactions

A redox mediator could be employed for electrolysis if the direct electrolysis is not feasible.<sup>[57]</sup> It will undergo single electron transfer (SET) on the electrode surface which further oxidizes or reduces the substrate to initiate desired chemical transformations. Variation and modifications in

the electrochemical parameters, cell types and electrode arrangements are allowing electroorganic chemists to discover novel reactivities of organic molecules including PROTACs in a highly selective manner as shown in the Scheme 1.21.<sup>[58]</sup>



**Scheme 1.21** Chemoselective electrochemical reduction of a PROTAC-relevant molecule

Application of electrochemistry in organic synthesis has a long history. In the 1830s, Faraday pioneered the application of electric current for preparative organic chemistry.<sup>[59]</sup> After a decade, Kolbe's electrolysis was discovered for the decarboxylative C–C bond formation *via* anodic oxidation of carboxylic acids.<sup>[60]</sup> An important milestone in this area was achieved when the concept of redox mediator was introduced in the mid-20<sup>th</sup> century.<sup>[61]</sup> Soon after, various powerful redox catalysts such as triarylamine mediators and nitroxyl radical mediators were applied in electrosynthesis.<sup>[56]</sup> Also, transition metals and halide mediators are playing a significant role as redox mediators in electrosynthesis. Moeller's work on chiral electrodes in the 1970s opened up a new area of asymmetric electrosynthesis.<sup>[62]</sup>

Yoshida and co-worker's enormous contributions include the electroauxillary concept to decrease the redox potential of compounds by introduction of special functional groups and cation pool strategy to carry out electrolysis at lower temperatures.<sup>[63]</sup> Now, researchers are showing a renewed interest in the area of electroorganic synthesis. Baran's electrooxidation methods for unreactive C–H bonds, Waldvogel's studies on biaryl coupling reactions, Ackermann and Mei's work on C–H activation using transition metals, cross dehydrogenative coupling reactions (CDC) developed by Lei *et al.*, Xu's work on electrochemical generation of nitrogen centered radicals

and Lin's asymmetric electrocatalytic methods are promoting this field. In the context of scale-up and efficiency, development of electrochemical reactions under flow conditions is an advancing field.<sup>[54, 64-66]</sup> The likes of Noël and Wirth are making significant contributions for electroorganic synthesis under flow conditions.<sup>[67-68]</sup> Photo-electrochemistry methods combine the power of light and electricity to enable powerful transformations which would have been extremely challenging otherwise. This research area is making rapid progress as indicated by the reports from Lambert group and Wickens group.<sup>[69]</sup> Moreover, availability of standardized commercial equipment has made the adoption of electroorganic synthesis easier and reproducible in research laboratories and chemical industries. These factors have allowed electrochemistry to become more accessible and enabled the application of novel chemistry.

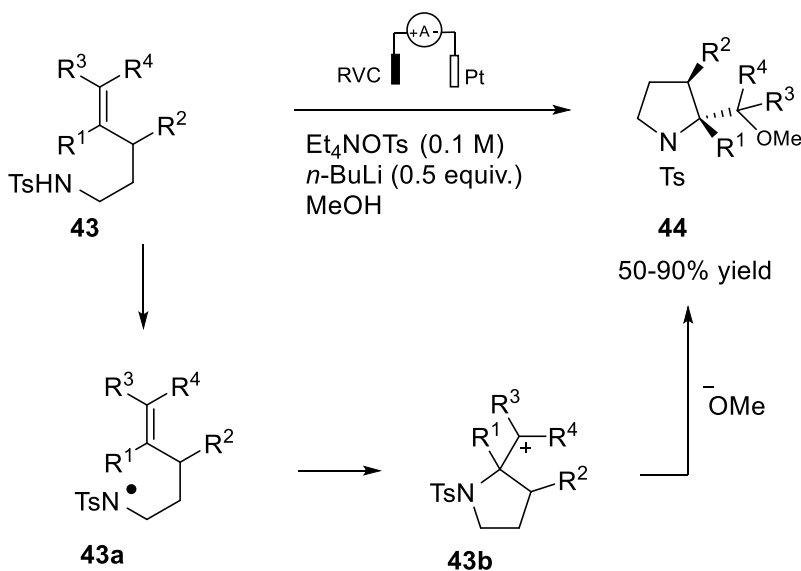
#### 1.1.4 Electrochemical direct C–H bond amination methods

As two complementary research areas, electroorganic synthesis and C–H functionalization methods go hand in hand. Numerous discoveries in this field have allowed more efficient and green synthetic routes. Among them, electrochemical C–H bond amination in the absence of transition metals as redox mediators is one of the prominent areas of research. Nitrogen-containing compounds are of great importance when it comes to biologically active molecules. Direct formation of C–N bond *via* inert C–H bond functionalization is an important strategy for synthesis and derivatization of *N*-heterocyclic compounds. To carry out these transformations in the absence of any transition metals and hazardous redox reagents is highly appealing.<sup>[56]</sup>

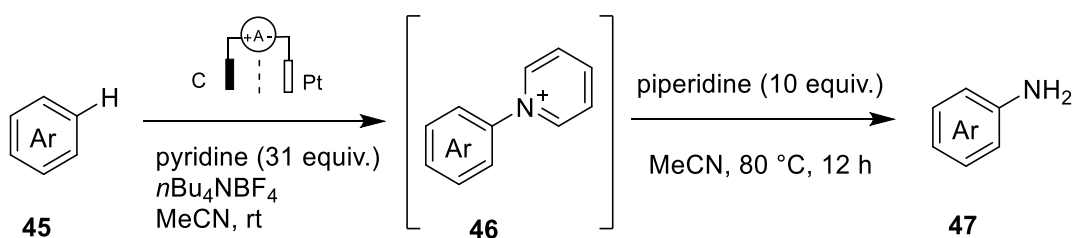
Direct electrolysis is a simple setup electrolysis where the substrates are oxidized or reduced directly at the electrode surface in a chemical transformation. However, the risk of side reactions is more if there are other redox active substrates inside the cell or if the products formed can further undergo overoxidations. Nevertheless, by careful optimization of reaction parameters, many useful intramolecular and intermolecular C–H amination methodologies are reported in literature. To this end, Moeller's report on synthesis of *N*-tosyl pyrrolidines (**44**) by intramolecular coupling of electrochemically generated sulfonamidyl radical (**43a**) to olefins is highly relevant (Scheme 1.22).<sup>[70]</sup>

Later in 2013, Yoshida and coworkers revealed an efficient amination of arenes using pyridines. Selective anodic oxidation of arenes in a divided cell in presence of pyridine generates *N*-

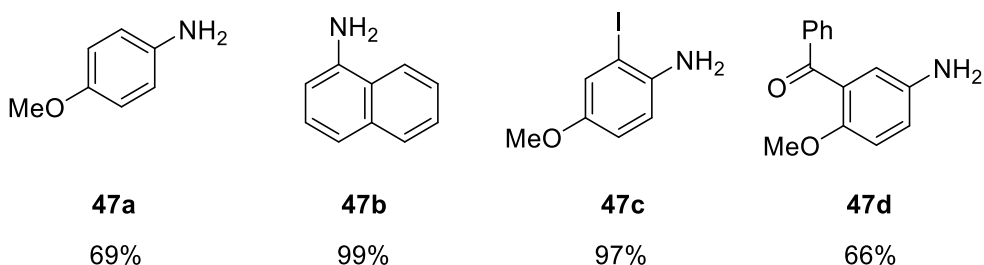
arylpyridinium ions (**46**). Reacting this intermediate with an alkylamine furnished the aromatic primary amines (**47**) under mild conditions. However, the reaction conditions are mostly compatible with activated arenes containing electron donating groups (**47a-d**) while the unactivated arenes are less favored for amination (Scheme 1.23).<sup>[71]</sup>



**Scheme 1.22** Direct electrolysis of *N*-sulfonamidyl group for pyrrolidine synthesis



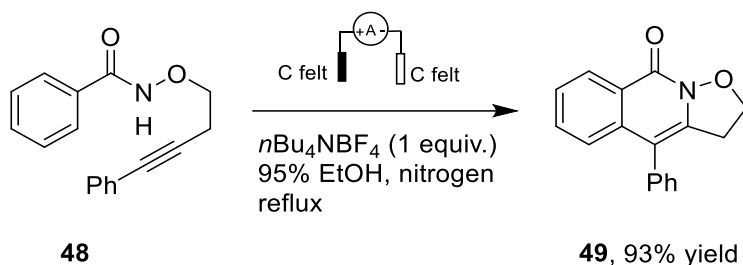
selected examples:



**Scheme 1.23** Yoshida's C-H amination of electron rich arenes via *N*-arylpyridinium ions

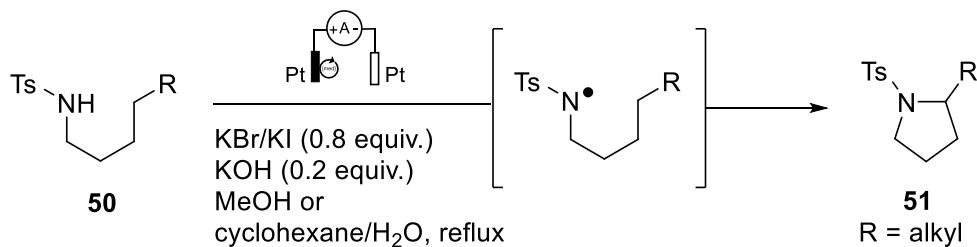
Recently, a metal-free approach to synthesize isoxazolidine-fused isoquinoline-1(2*H*)-ones (**49**) was demonstrated by Li and coworkers. The reaction takes place *via* direct electrolysis of *N*-alkoxy amide scaffolds (**48**) in 95% ethanol as green solvent (Scheme 1.24). Generation of *N*-centered radicals through indirect electrolysis is an important strategy for C–H bond amination reactions.

[72]



**Scheme 1.24** Tricyclic *N*-heterocycles via cascade cyclization

As mentioned earlier, employing a redox mediator as an electrocatalyst has its own advantages. Many reactions have been developed with high selectivity under milder conditions using this approach. One of the earliest reports is when Shono demonstrated electrolysis of tosylamides (**50**) in presence of halide mediators and base to furnish pyrrolidines as in Hofmann-Löffler-Freytag-type cyclization (Scheme 1.25).<sup>[73]</sup>

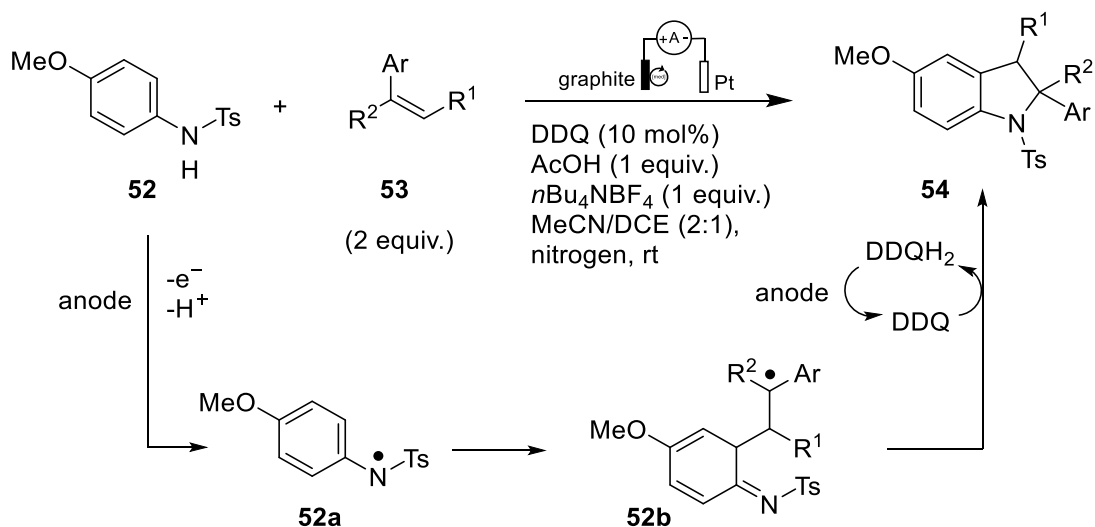


**Scheme 1.25** Electrochemical Hofmann-Löffler-Freytag-type cyclization

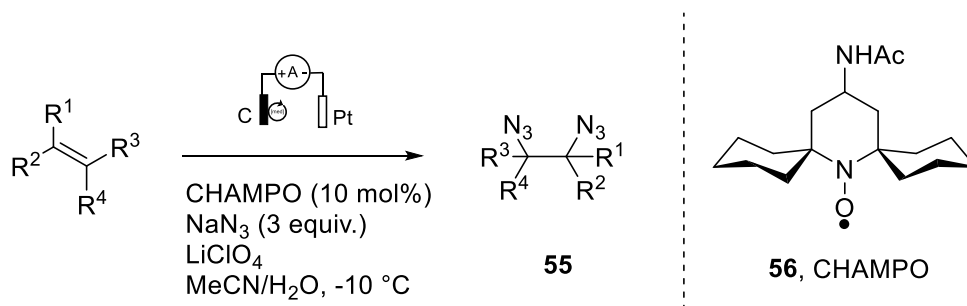
Very recently an intermolecular [3+2] annulation for the synthesis of indolines was discovered by Lei and co-workers. The methodology uses DDQ as an electrocatalyst. The same reaction in the absence of a redox catalyst proceeds with a much lower yield. Mechanistically a *N*-radical formed (**52a**) *via* anodic oxidation is proposed to resonate to form the C-radical (**52b**). This after radical addition with the olefin followed by a second oxidation by DDQ or anode provides the indoline products (**54**) (Scheme 1.26).<sup>[74]</sup>



In an attempt to obtain radical diazidation of alkenes using TEMPO as a redox catalyst, Lin *et al.* observed the azidoxygenation reaction to be favored over diazidation. This eventually requires stoichiometric amounts of TEMPO because of its consumption during the reaction.<sup>[75]</sup> To overcome this issue and to obtain diazidation products under metal-free conditions, the authors synthesized a number of analogues of TEMPO with an increased steric crowd at the *N*-oxyl center. This revealed cyclohexane-substituted (4-acetamidopiperidin-1-yl)oxyl (**56**, CHAMPO) as an efficient catalyst for the diazidation of various types of alkenes effectively (Scheme 1.27).<sup>[76]</sup>

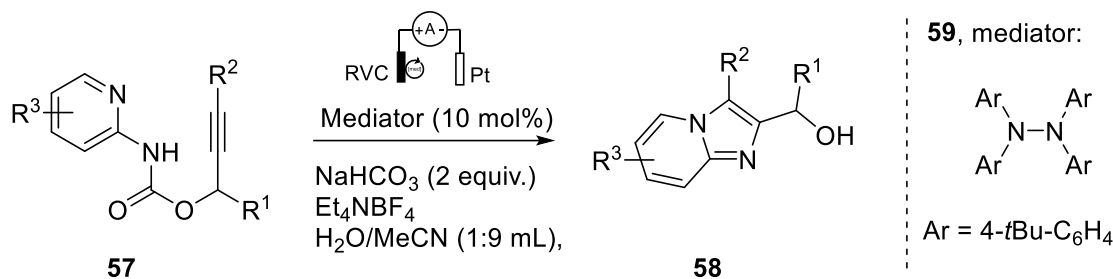


**Scheme 1.26** DDQ mediated [3+2] annulation for the synthesis of indolines

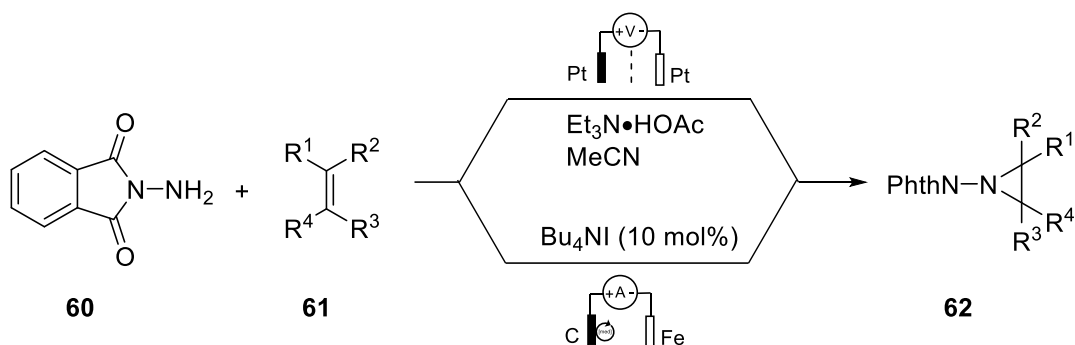


**Scheme 1.27** CHAMPO as an efficient catalyst for the diazidation

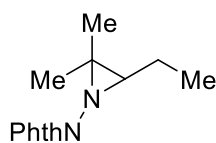
A novel tetraarylhydrazine catalyst (**59**) capably catalyzed intramolecular [3+2] annulation to yield imidazo-fused heteroaromatic compounds (**58**). The reaction proceeds between *N*-centered radical and *C*-radical generated by indirect electrolysis in presence of base under constant current electrolysis under reflux temperature (Scheme 1.28).<sup>[77]</sup>



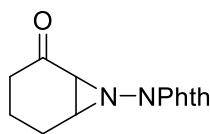
**Scheme 1.28** Tetraarylhiazine as redox mediator for *N*-heteroaryl synthesis



selected examples:

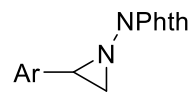


**62a**, 91%



**62b**, 78%

mediated electrolysis:



Ar = **62d**, 4-FC<sub>6</sub>H<sub>4</sub>, 63%

Ar = **62e**, 2-BrC<sub>6</sub>H<sub>4</sub>, 57%

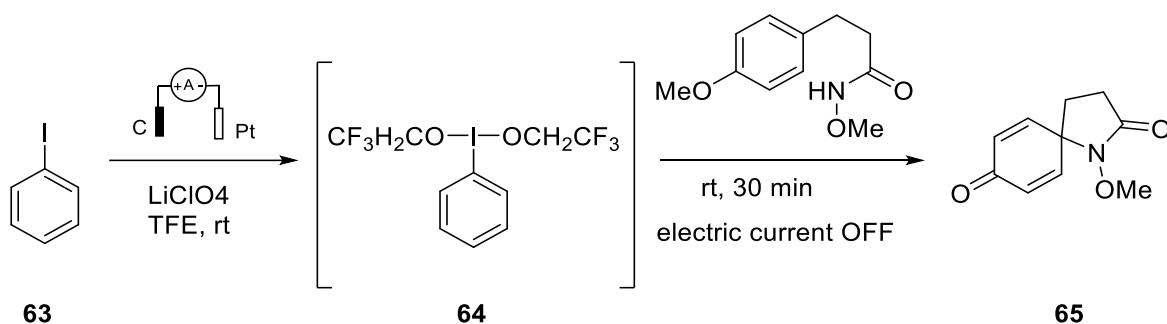
direct electrolysis

**Scheme 1.29** Electrochemical generation of nitrene intermediate for synthesis of aziridines

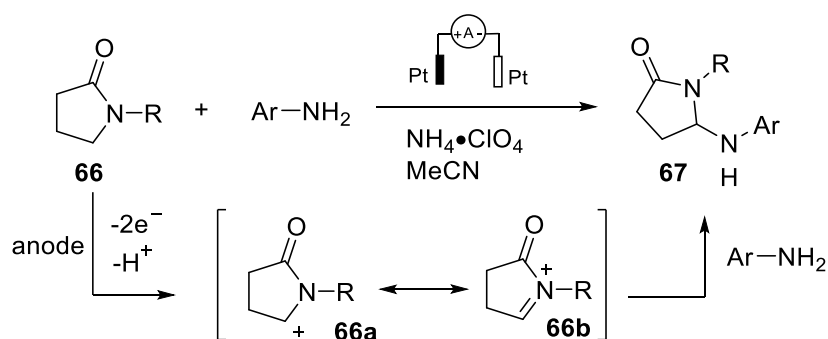
Electrochemical generation of nitrene and nitrenium species enable many interesting amination reactions. Harsh oxidizing agents such as lead tetraacetate (Pb(OAc)<sub>4</sub>) had been used to generate reactive intermediate nitrene from *N*-aminophthalimide (**60**). Yudin's group revealed that under constant potential electrolysis of +1.8 V (vs Ag/AgCl), it is possible to generate such intermediates and can be applied for the aziridination of olefins (**62**). The concept of overpotential was brilliantly exploited to obtain aziridines from electron rich olefins which have more or less similar oxidation potential as that of phthalimide moiety.<sup>[78]</sup> The reaction conditions were modified by Little, Zeng and coworkers to make it more accessible. A redox mediator in the form of tetrabutylammonium

iodide was employed to carry out electrolysis under constant current in an undivided cell using cheaper electrodes (Scheme 1.29).<sup>[79]</sup> Halogens are used as electrochemical mediators in many other reactions as well.

The concept of electrochemical generation of hypervalent iodine and subsequent use of it to carry out important transformations has been studied in detail. One such example is for the oxidative spirocyclization reaction for azacyclic derivatives as reported by Nishiyama group. Electrolysis of iodobenzene in presence of trifluoroethanol as solvent results in the formation of hypervalent iodine intermediate (**64**). This acts as an oxidizing agent to generate nitrenium ion intermediate from alkoxy amide substrate. The following nucleophilic attack of the aromatic ring resulted in the spirocyclic product which are synthetic intermediates (**65**) of complex bioactive compounds (Scheme 1.30).<sup>[80]</sup>



**Scheme 1.30** Electrochemical generation of a hypervalent iodine reagent and its application

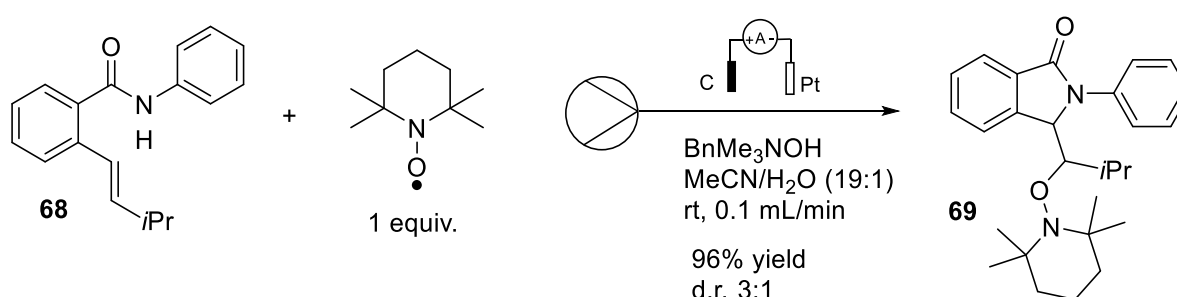


**Scheme 1.31** Shono type electrochemical amination of  $\gamma$ -lactams

Shono oxidation is a classical approach to functionalize  $\alpha$ -position of *N*-acyl compounds. Usually anodic oxidation of compounds ultimately results in the formation of iminium ions and alcoholic solvent attacks the iminium carbon to get corresponding functionalized products. Numerous

modifications of this method have been reported over years. Direct C–H amination reactions of *N*-methyl pyrrolidones (**66**) involving an iminium cation (**66b**) under metal-free conditions have also been reported recently (Scheme 1.31).<sup>[81]</sup>

Flow chemistry has gained significant attention owing to its unique advantages over conventional flask methods. Efficient scale up and reproductivity of electrochemical reactions with control over reactivities can be achieved through combining it with continuous flow synthesis. Wirth *et al.* designed an interesting electrochemical microflow reactor and demonstrated its efficiency by successfully generating nitrogen and sulfur radicals for the synthesis of corresponding heterocycles. For instance, an intramolecular reaction of electrochemically generated *N*-acyl radical in flow reacts with alkene and following radical coupling of TEMPO give rise to corresponding TEMPO substituted *N*-aryl isoindolinones (**69**) (Scheme 1.32).<sup>[82]</sup>



**Scheme 1.32** Isoindolinone synthesis in an electrochemical flow microreactor

It is noteworthy to mention that care should be taken to categorize a reaction as a transition metal free reaction. The starting material preparation before the key C–H bond functionalization step might involve a transition metal. It is possible to carry forward trace amounts of these metals for the next steps as well. In a way, it is more correct to coin the term “externally added TM-free C–H bond functionalization”. A number of studies related to TM-free cross coupling reactions such as organocatalytic Suzuki-Miyaura coupling are considered doubtful in this aspect.<sup>[83]</sup> Even the metal contaminated magnetic stir bars seemed to catalyze the classic cross-coupling reactions to an extent.<sup>[84]</sup> These studies however are still beneficial for the science to develop new reactions with extremely low catalytic loading of expensive and precious transition metals.

**Objectives**

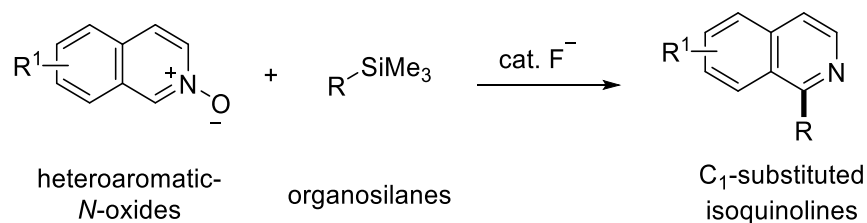
---



## 2 Objectives

Organocatalysis and oxidative coupling reactions allow access to novel organic molecules without the use of any transition metal catalysts. Requirement for the pre-functionalization of starting materials in conventional cross-coupling reactions will increase the number of steps to synthesize a desired product. In this aspect, development of novel direct C–H functionalization methods in a transition metal-free manner is highly advantageous. These methods do not need harsh reaction conditions and pre-functionalization of starting materials to corresponding halides or other functionalities. Instead, direct coupling reaction between the non-pre-functionalized substrates could be achieved. Considering these benefits, efforts will be made to develop novel reaction methodologies of this class especially for the easier access to highly functionalized nitrogen-containing compounds.

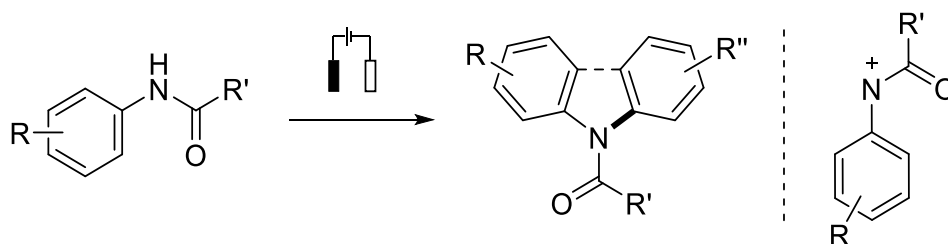
Isoquinoline and other closely related nitrogen heterocycles are abundant in natural products and synthetic pharmaceuticals. Chemical architectures of naturally occurring alkaloids such as papaverine and noscapine are based on a C<sub>1</sub>-benzylic substitution of isoquinoline and tetrahydroisoquinoline moieties. To access these classes of compounds methodologies based on organocatalytic inert C–H functionalization are rare. Keeping this in mind, development of a cross-coupling method between heteroaromatic *N*-oxides and organosilanes was proposed. This method will provide easy access to benzylated *N*-heterocycles without the use of expensive transition metals. Furthermore optimization, evaluation of the scope and mechanistic studies were also planned. The feasibility of methodology to enable alkylation of *N*-heterocyclic compounds will be examined.



**Scheme 2.1** Regioselective cross-coupling of *N*-oxides with organosilanes

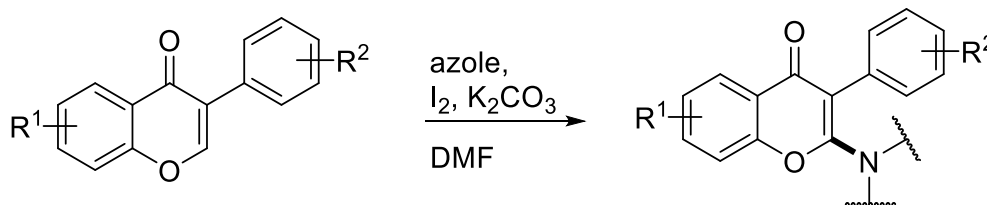
Nitrenium ions are important reaction intermediates and development of methods to access these intermediates electrochemically would help to access various *N*-heterocycles in a sustainable

manner. The existing methodologies for the electrochemical C–H bond amination based on nitrenium ion generation use stoichiometric quantities of redox mediators and electrolytes. Therefore, a novel direct electrolytic amination method involving an electrochemically generated nitrenium ion intermediate was proposed. The feasibility of the proposed reaction will be tested. The optimization of reaction conditions as well as substrate scope evaluation will be carried out. The compatibility of the methodology for both intramolecular and intramolecular aminations needed to be examined.



**Scheme 2.2** Electrochemical dehydrogenative C–H bond aminations

A 2015 report based on oxidative C–H amination of chromones using azoles as coupling partner reported a number of novel C<sub>2</sub>-aminated chromones as Hedgehog inhibitors. Later on, a novel biological assay found these compounds to be potent bone morphogenetic pathway effectors. Based on these results, the synthesis of the most active analogue for various biological studies will be carried out. In addition, to have a better insight into the structure-activity relationship, synthesis of a number of closely related analogues will be carried out to evaluate their biological effects. Also, the compounds lacking specific substituents are required for chemical biology studies as inactive probes.



**Scheme 2.3** Design and synthesis of C<sub>2</sub>-aminated chromones

All novel molecules obtained during the reaction developments, substrate scope evaluation and mechanistic studies would be submitted to the COMAS (Compound Management and Screening Centre) in Dortmund.



## Chapter 3

---

### Cross-Coupling of heteroaromatic *N*-oxides with organosilanes

---

(Parts of this chapter have already been published: Mahesh Puthanveedu, Vasiliki Polychronidou, and Andrey P. Antonchick, *Org. Lett.* **2019**, *21*, 3407–3411.)



### 3 Cross-Coupling of Heteroaromatic *N*-oxides with Organosilanes

#### 3.1 C–H Benzylation

##### 3.1.1 Introduction

Nitrogen containing heteroaromatic compounds are important scaffolds in organic chemistry. They are encountered very often in bioactive natural products and synthetic drugs. Therefore, their synthesis and direct functionalization reactions are of particular interest. Direct C–H functionalization methods are gaining popularity in drug discovery and process chemistry because of their unique advantages. Application of this methodology to synthesize and functionalize pharmaceutical compounds allows atom economic production of drugs in a sustainable way. Not only that, C–H functionalization methods allow faster structure activity relationship studies and in some cases synthesis of previously inaccessible analogues. Privileged scaffolds such as quinoline, isoquinoline and pyridine are highly relevant in medicinal chemistry. Direct C–H bond functionalization reactions of these scaffolds have been studied widely in recent years with most of them using precious transition metals as catalysts.

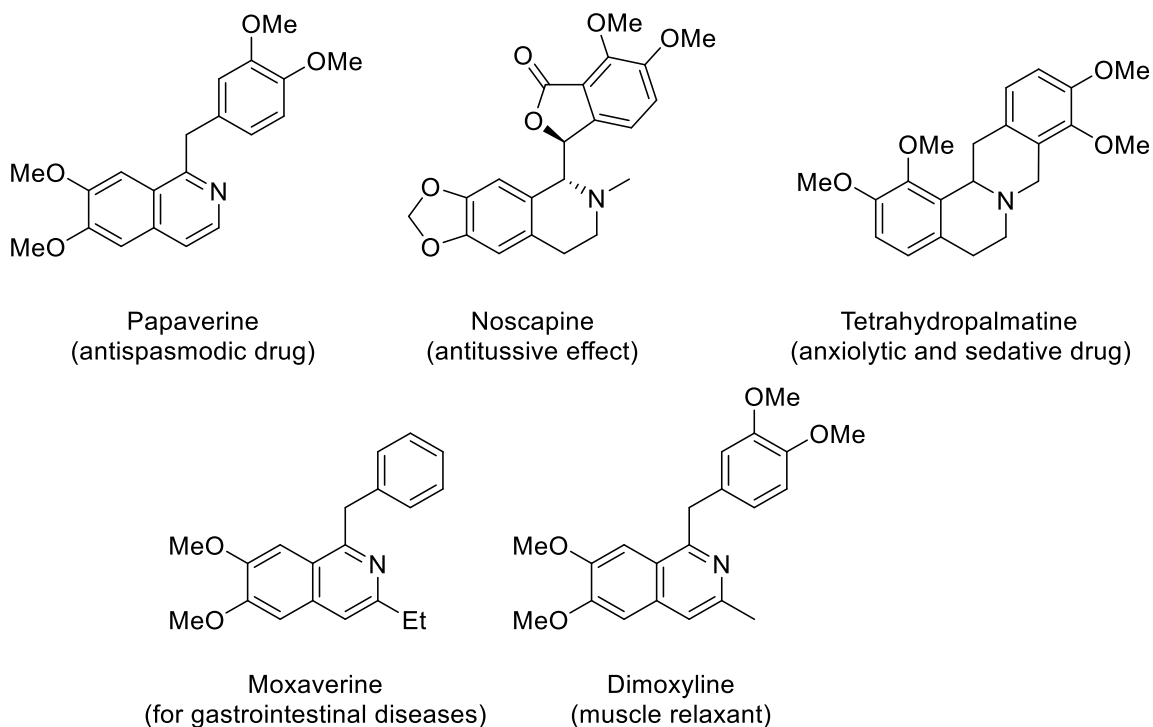
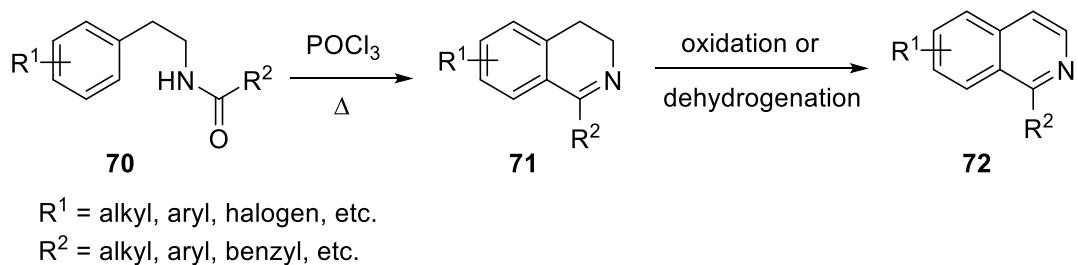


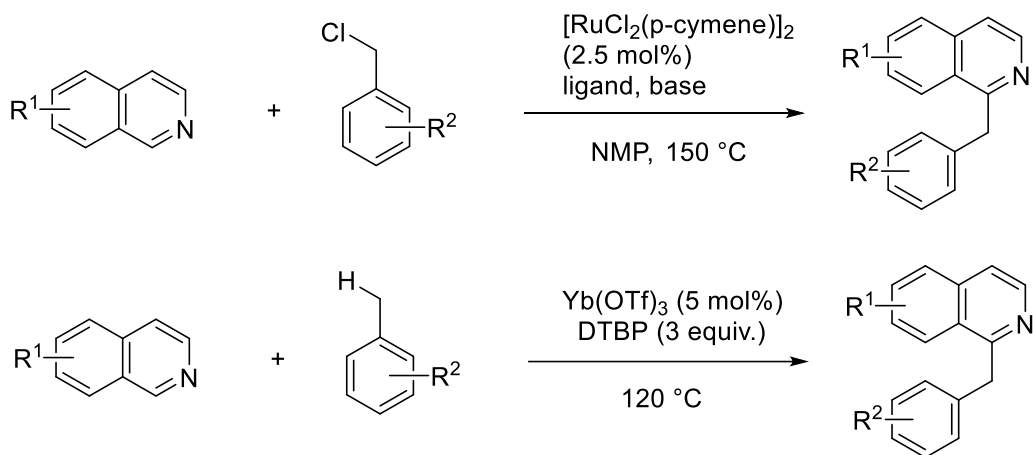
**Figure 3.1** Representative bioactive compounds having benzyl substituted *N*-heterocycle

In this regard a transition metal-free approach for the synthesis of benzylated nitrogen heterocycles *via* direct C–H bond functionalization was highly demanding. This is because many naturally occurring alkaloids and synthetic drugs such as papaverine, berberine, moxaverine, etc. carries benzylated azacycles, especially isoquinoline, as a key scaffold in their structure (Figure 3.1). Historically, isoquinoline derivatives were synthesized using classical Bischler-Napieralski cyclization reactions (Scheme 3.1).



**Scheme 3.1** Bischler-Napieralski cyclization reactions for isoquinoline synthesis

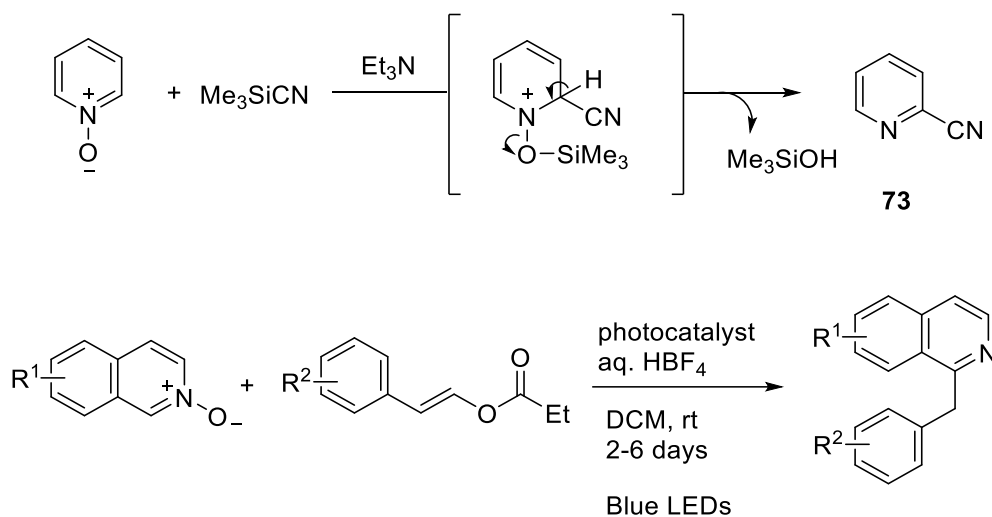
With the rapid development of cross-coupling chemistry, approaches to readily synthesize benzylated isoquinolines and the natural products within the class were revealed. These methodologies however demand harsh reaction conditions, highly expensive metal catalysts and specific metal coordination ligands.<sup>[85]</sup>



**Scheme 3.2** Transition metal mediated direct C–H benzylation of isoquinolines

Minisci reaction is a radical functionalization method to obtain functionalized pyridines in presence of a radical source. This concept has been modified by several groups to obtain various functionalized nitrogen heterocycles *via* C–H bond functionalization methods.<sup>[86]</sup> However, more

than one reactive position for radical reactions as in the case of quinoline (C<sub>2</sub>- and C<sub>4</sub>-) will result in the formation of a mixture of regioisomers. One such successful example of a selective Minisci type C–H benzylation is an oxidative decarbonylative coupling of aliphatic aldehydes with azaarenes in presence of di-*tert*-butyl peroxide as radical initiator and oxidant.<sup>[87]</sup> An independent report from Liu and coworkers used simple methyl arenes as coupling partner for azacycles enabling a cross dehydrogenative coupling (CDC) for the synthesis of C<sub>1</sub>-benzyl isoquinolines (**75**). The reaction proceeds in the presence of catalytic amounts of ytterbium triflate and di-*tert*-butyl peroxide as oxidant (Scheme 3.2).<sup>[88]</sup>



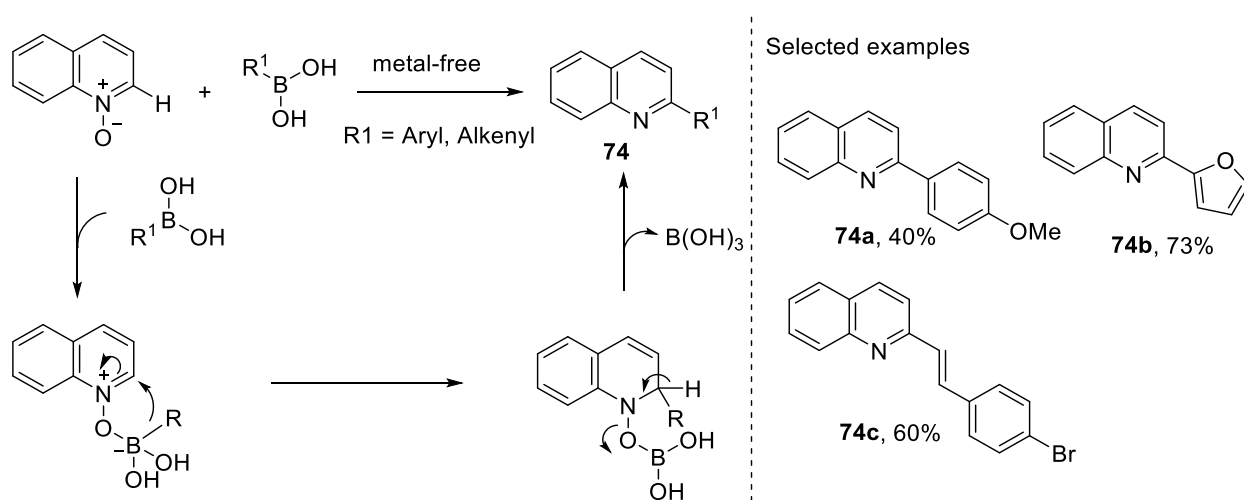
**Scheme 3.3** Regioselective benzylation of heteroaromatic *N*-oxides

Because of the advantages such as improved regioselectivity and step economy of deoxygenative functionalization, heteroaromatic *N*-oxides have gained importance as substrates to synthesize functionalized nitrogen heterocycles. On the other hand, organosilanes are a class of stable, affordable and less toxic alternatives for cross-coupling reactions. Trimethylsilyl cyanide has been successfully employed for the direct deoxygenative *cine*- C–H cyanation of pyridine *N*-oxides to afford 2-cyanopyridine compounds (**73**).<sup>[89]</sup> Murakami, Miura and coworkers developed a strategy to synthesize benzylated and secondary alkyl substituted pyridines by means of photocatalysis. The authors proposed a radical species generated photocatalytically from alkenes will be highly electrophilic. It will then react with pyridine *N*-oxide followed by intramolecular radical addition to *ortho*- position and consequent elimination of a carbonyl compound to furnish C<sub>2</sub>-alkylated pyridine compounds.<sup>[90]</sup> However, the long reaction time up to 7 days of stirring at room

temperature might interrupt adopting this strategy largely for benzyl pyridine synthesis by organic chemists (Scheme 3.3).

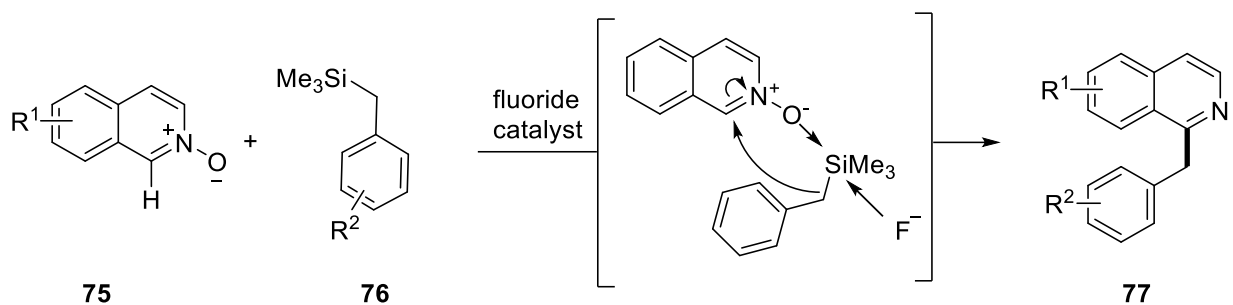
### 3.1.2 Motivation and objectives

Bering and Antonchick revealed a facile strategy for the C–H bond functionalization of quinoline *N*-oxides using boronic acids as a coupling partner. The methodology enabled transition metal and external oxidant free synthesis of C<sub>2</sub>-(hetero)arylated and alkenylated quinolines in an efficient manner. Interestingly, the reaction design was based on an analogy of the structure of quinoline *N*-oxides to a key reaction intermediate formed during the Petasis reaction. This was the first instance of application of the Petasis reaction for direct functionalization of heterocycles. Even though the scope of reaction was broad with respect to quinolines, (hetero)aromatic compounds and alkenes, the reaction was not applied to isoquinoline and pyridine scaffolds. In addition, only C(sp<sup>2</sup>)-C(sp<sup>2</sup>) bond formation was successful under reported conditions (**74**) (Scheme 3.4).



**Scheme 3.4** Regioselective arylation and alkenylation of *N*-oxides with boronic acids

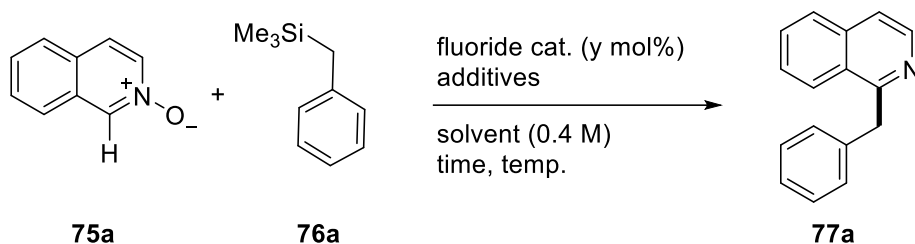
Considering the abundance of various C<sub>2</sub>-substituted nitrogen heterocycles such as isoquinolines and pyridines, novel approaches based on the concept of transition metal-free C–H functionalization methods would be highly appealing. As in the case of boronic acids, organosilicon compounds are also important coupling partners to make new C–C bonds *via* cross-coupling reactions. Based on this similarity, it was hypothesized that replacing boronic acids with organosilicon compounds could help to overcome the limitations of known methods (Scheme 3.5).



**Scheme 3.5** Proposed benzylation of isoquinoline *N*-oxides using organosilanes

### 3.1.3 Initial results and optimization

The feasibility of proposed cross-coupling reaction was examined by reacting isoquinoline *N*-oxide with benzyltrimethylsilane in presence of substoichiometric amount of tetrabutylammonium fluoride (TBAF) under air at room temperature using tetrahydrofuran (THF) as solvent (Table 3.2). Fluoride activation is important to initiate the reaction. Nucleophilic attack of isoquinoline *N*-oxide to this activated silane complex and following nucleophilic migration of benzyl group was proposed to furnish benzylated isoquinoline product. As proposed, a trace amount of desired product formation was observed upon initial screening (entry 1 and entry 2). From screening a number of solvents, either THF or dimethylformamide (DMF) were found to be most suitable (entry 3-5). However, in all cases additional undesired products were also observed. Careful isolation and characterization of side products from the reaction identified two major side products impacting the better conversion of starting materials to desired product. One of them was 1-benzoylisoquinoline which was formed by the oxidation at the benzylic position of the formed product. However, this side reaction was suppressed to a large extent by carrying out the reaction under argon atmosphere. 45% yield of product was obtained by reacting isoquinoline *N*-oxide with benzyltrimethylsilane under argon atmosphere in presence of 10 mol% of TBAF as catalyst and DMF as solvent (entry 6). Increased catalyst loading was not beneficial and furnished lower yields of product (entry 7). Using 3 equivalents of silane coupling partner was found to be advantageous. Addition of TBAF made the reaction vial hot. But lowering the temperature during the catalyst addition did not facilitate better conversion (entry 8). Another important observation made was that the benzylated isoquinoline *N*-oxides are also formed in high quantities during reaction. The main target was to develop the deoxygenative C–H functionalization to directly obtain C<sub>1</sub>-functionalized isoquinolines. So, the efforts were directed towards *in situ* reduction of unreduced

**Table 3.1** Representative conditions of the optimization for the cross-coupling.<sup>[a]</sup>

Entry	76a (equiv.)	Cat. (mol%)	Additives (equiv.)	Temp. (°C)	Solvent (1 mL)	Time (h)	Yield (%) <sup>[b]</sup>
1 <sup>[c]</sup>	2	TBAF (10)		rt	THF	24	trace
2 <sup>[c]</sup>	2	TBAF (10)		rt	DMF	24	trace
3	2	TBAF (10)		rt	NMP	24	n.d.
4	2	TBAF (10)		rt	EtOH	24	n.d.
5	3	TBAF (10)		rt	THF	6	37
6	3	TBAF (10)		rt	DMF	6	45
7	3	TBAF (20)		rt	DMF	6	19
8	3	TBAF (10)		0 → rt	DMF	6	trace
9	3	TBAF (10)	PhB(OH) <sub>2</sub> (2)	rt	DMF	24	trace
10 <sup>[d]</sup>	3	TBAF (10)	Et <sub>3</sub> SiH (5)	rt	DMF	12	59
11 <sup>[d]</sup>	3	TBAF (10)	Et <sub>3</sub> SiH (5)	rt	DMF	24	62
12 <sup>[e]</sup>	3	TBAF (10)	Et <sub>3</sub> SiH (5)	rt	DMF	24	41
<b>13<sup>[f]</sup></b>	<b>3</b>	<b>TBAF (10)</b>	<b>Et<sub>3</sub>SiH (5)</b>	<b>rt</b>	<b>DMF</b>	<b>24</b>	<b>78</b>
14	3	CsF (10)	Et <sub>3</sub> SiH (5)	rt	DMF	24	30
15	3	TBAT (10)	Et <sub>3</sub> SiH (5)	rt	DMF	24	29
16	3	TBAF (10)	Et <sub>3</sub> SiH (5)	rt	THF	24	7
17	3	TBAF (10)	Et <sub>3</sub> SiH (5)	rt	DCE	24	n.d.
18	3	TBAF (10)	Et <sub>3</sub> SiH (5)	rt	Dioxane	24	7



Entry	76a (equiv.)	Cat. (mol%)	Additives (equiv.)	Temp. (°C)	Solvent (1 mL)	Time (h)	Yield (%) <sup>[b]</sup>
19	3	TBAF (10)	Et <sub>3</sub> SiH (5)	rt	EtOAc	24	12
20	3	TBAF (10)	Et <sub>3</sub> SiH (7)	rt	DMF	24	66
21	3	TBAF (10)	Et <sub>3</sub> SiH (10)	rt	DMF	24	68
22	3	TBAF (10)	Et <sub>3</sub> SiH (3)	rt	DMF	24	65
23	3	TBAF (10)	PMHS (1)	rt	DMF	24	trace
24	3	TBAF (10)	PhMe <sub>2</sub> SiH (5)	rt	DMF	24	58
25	3	TBAF (10)	Me <sub>3</sub> Si-SiMe <sub>3</sub>	rt	DMF	24	42
26	3		Et <sub>3</sub> SiH (5)	rt	DMF	24	n.d.

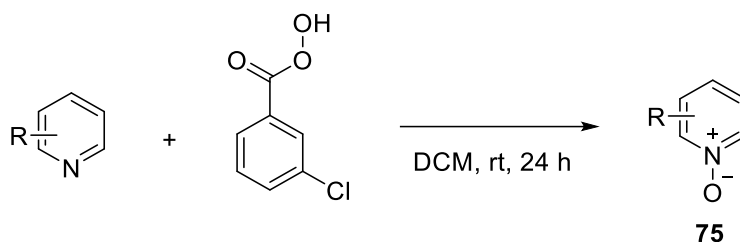
<sup>[a]</sup>Reaction conditions: **75a** (0.4 mmol), solvent (0.4 M), argon. <sup>[b]</sup>yields are given for isolated products (**77a**) after column chromatography. <sup>[c]</sup>under air atmosphere. <sup>[d]</sup>Et<sub>3</sub>SiH was added before the TBAF addition. <sup>[e]</sup>Et<sub>3</sub>SiH after 12 h. <sup>[f]</sup>Et<sub>3</sub>SiH just after TBAF addition. TBAF = tetrabutylammonium fluoride. PMHS = polymethylhydrosiloxane. TBAT = tetrabutylammonium difluorotriphenylsilicate. rt = room temperature (~28 °C). n.d. = not detected.

product to C<sub>1</sub>-benzyl isoquinolines. Along this line, various additives were screened (entry 9-25). It was noted that silyl hydride as additives lead to formation of desired product in higher yields. 5 equivalents of triethylsilane (Et<sub>3</sub>SiH) was added to a mixture of isoquinoline *N*-oxide and benzyltrimethylsilane. After addition of 10 mol% of TBAF the reaction mixture was stirred under argon for 12 hours to isolate 59% of cross-coupled product (entry 10). Increasing the reaction time to 24 hours resulted in a slightly higher yield of product (entry 11). Interestingly, time of addition of triethylsilane was crucial for optimal yield of product. A diminished yield was observed when Et<sub>3</sub>SiH was added after 12 hours of stirring of starting materials with catalyst (entry 12). The optimal yield of 78% of desired product was obtained when the additive was added just after the addition of catalytic fluoride source, which was found to be TBAF (entry 13). Other fluoride sources such as cesium fluoride (CsF) and tetrabutylammonium difluorotriphenylsilicate (TBAT) were also examined (entry 14 and entry 15). In addition to Et<sub>3</sub>SiH, other silane compounds such as dimethylphenylsilane, hexamethyldisilane, polymethylhydrosiloxane (PMHS), etc. were also evaluated for the efficacy in this reaction (entry 22-25). Similarly, using THF, ethyl acetate (EtOAc) or dioxane as solvents were not ideal. The best condition was found to be cross-coupling

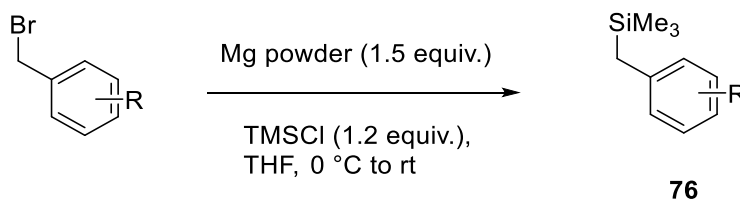
in presence of TBAF and Et<sub>3</sub>SiH using DMF as solvent, stirring at room temperature under argon atmosphere for 24 hours. A reaction in the absence of any catalysts did not furnish 1-benzylsioquinoline (entry 26).

### 3.1.4 Scope of heterocyclic *N*-oxides and benzyltrimethylsilanes

With the optimal reaction conditions in hand, the substrate scope of reaction was examined. All the heterocyclic *N*-oxides were synthesized by reacting them with *meta*-chloroperbenzoic acid (*m*CPBA) (Scheme 3.6).<sup>[28]</sup> Various substituted benzyltrimethylsilane derivatives are prepared by reacting trimethylsilyl chlorides with *in situ* generated Grignard reagents of corresponding benzyl bromides (Scheme 3.7).<sup>[91]</sup>



**Scheme 3.6** Preparation of heteroaromatic *N*-oxides



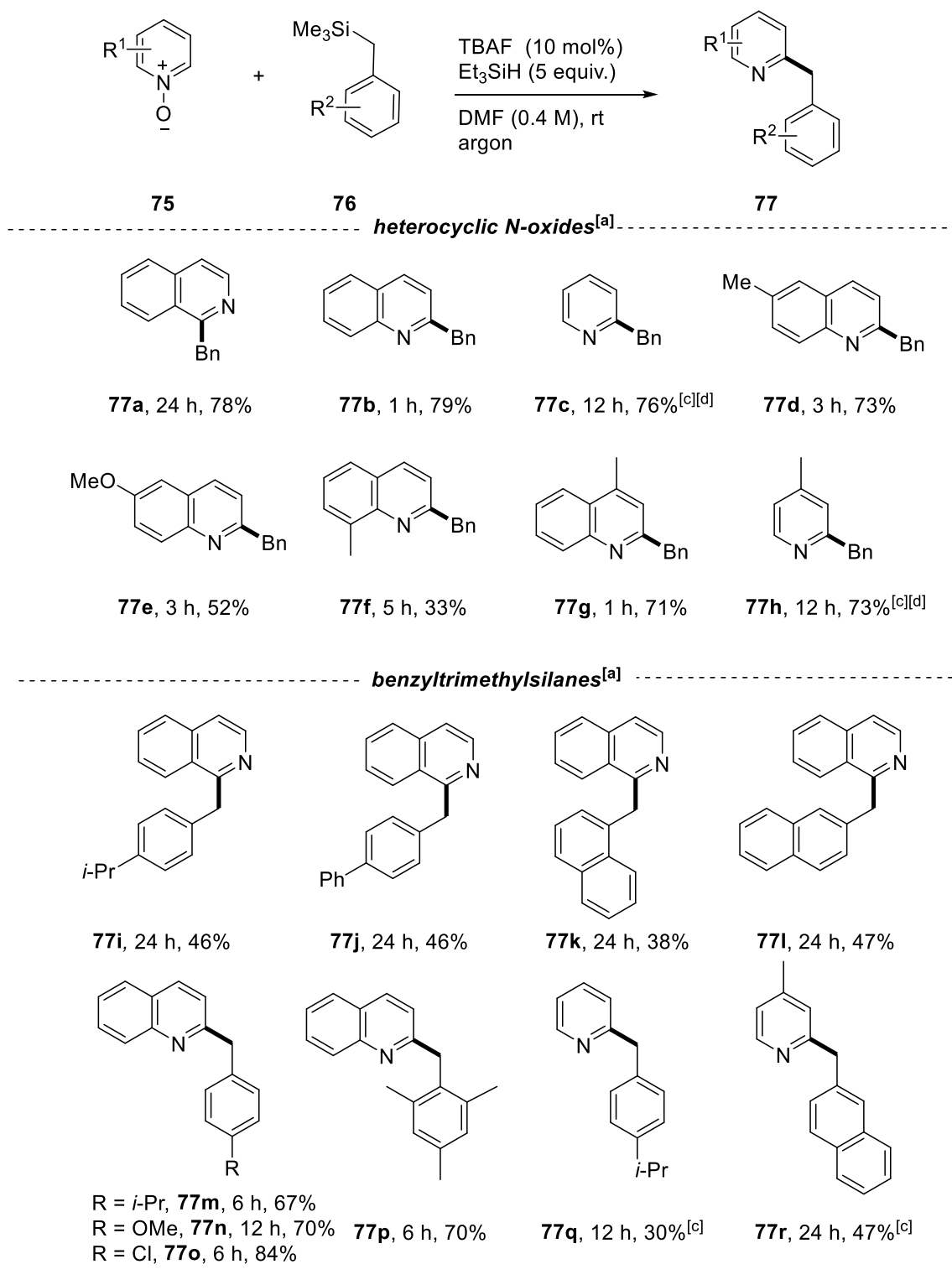
**Scheme 3.7** Preparation of benzyltrimethylsilanes

To evaluate the scope, respective *N*-oxides of isoquinoline, quinoline and pyridine were reacted with simple benzyltrimethylsilane initially. It was found that all three classes of these important nitrogen heterocycles provided the corresponding benzylated *N*-heterocyclic product in good yields. Isoquinoline *N*-oxide and quinoline *N*-oxide were reacted with benzyltrimethylsilane under standard conditions to obtain 78% and 79% of C<sub>1</sub>- and C<sub>2</sub>- benzylated products respectively (**77a** and **77b**). In case of pyridine *N*-oxide, better yield of product was obtained in the absence of triethylsilane additive (**77c**). But, the catalyst loading was increased from 10 mol% to 20 mol% for optimum product formation. Various substituted heterocyclic *N*-oxides were also examined. For instance, electron donating substituents on the C<sub>6</sub>- position of quinoline was well tolerated

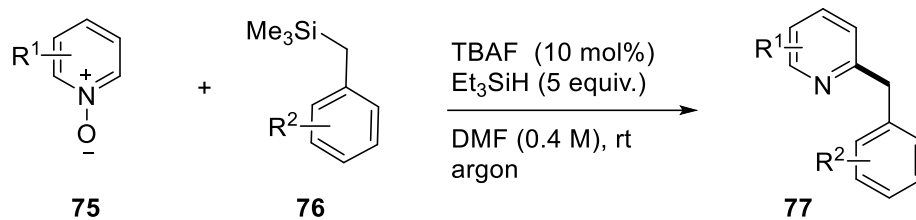
(**77d** and **77e**). Similarly, effects of substitutions at other positions of *N*-oxide compounds were also studied (**77f-77h**). With respect to the time taken to consume the starting materials, quinoline analogues were found to be faster to provide benzylated quinoline compounds, followed by pyridines and then isoquinolines.

Later on, different benzyltrimethylsilane analogues as substituted benzyl group donors were tested. In case of isoquinoline *N*-oxides, a *para*- isopropyl group and a *para*- phenyl group on the phenyl ring reacted to yield corresponding products in moderate yields (**77i** and **77j**). In addition, 1-naphthyl and 2-naphthyl derivatives were also successfully coupled with isoquinoline *N*-oxide (**77k** and **77l**). Synthesis of quinoline derivatives using developed protocol was superior to that of isoquinolines. For instance, substitutions on the *para*- position of the phenyl ring of the silane component had no significant deteriorating effect on the reaction performance. Electron donating groups such as methoxy, isopropyl group and electron withdrawing halogen were all compatible (**77m-77o**) under these conditions. Highly substituted trimethyl(2,4,6-trimethylbenzyl)silane effectively coupled with quinoline *N*-oxide to furnish **77p** in 70% yield in 6 hours. Furthermore, C<sub>2</sub>- substituted pyridine derivatives were synthesized by established cross-coupling protocol. For these products **77q** and **77r**, the reaction was catalyzed solely by tetrabutylammonium fluoride and use of additional triethylsilane as an additive was negated (Scheme 3.8).

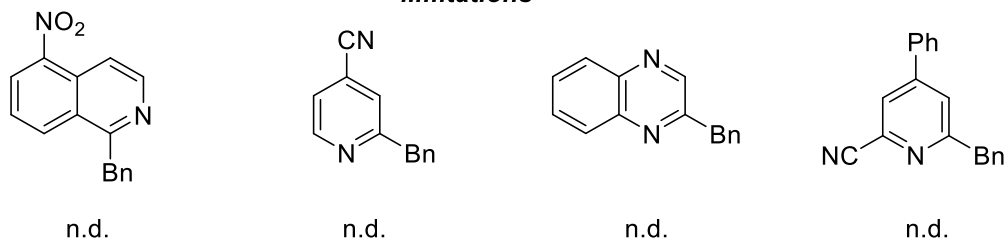
With respect to the limitations of this protocol, it was found that highly electron deficient heterocycles are not suited. This could be justified because of the decreased nucleophilicity of oxide functionality. A nitro- group or a cyano- group would decrease the electron density of heterocyclic *N*-oxide and thereby prevent the nucleophilic attack of the *N*-oxide group to activate silanes. This limitation however provides useful directions for the plausible mechanism of reaction (Scheme 3.9). Delightedly, the reaction scale-up was also found to be successful. 1 g scale reaction of isoquinoline *N*-oxide (**75a**) with benzyltrimethylsilane (**76a**) under optimized conditions provided 68% of isolated product (**77a**). No further modifications were required to the optimal conditions of the reaction (Scheme 3.10).



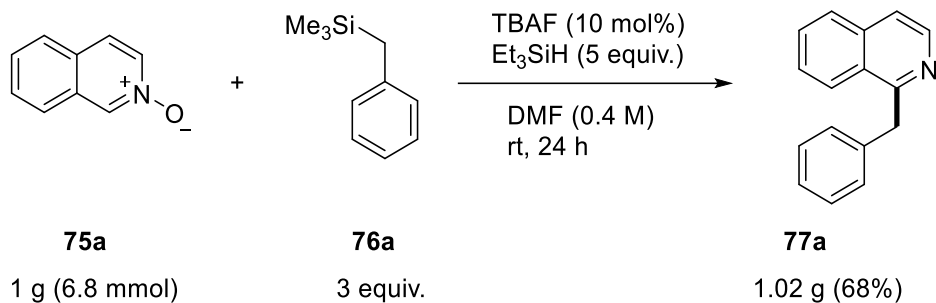
**Scheme 3.8** Scope of cross-coupling between heterocyclic *N*-oxides and organosilanes. <sup>[a]</sup>Reaction conditions: **75** (0.4 mmol), **76** (1.2 mmol, 3 equiv.), TBAF (10 mol%), DMF (0.4 M). <sup>[b]</sup>Yields are given for isolated products (**77**). <sup>[c]</sup>20 mol% of TBAF was used. <sup>[d]</sup>Without Et<sub>3</sub>SiH.



*limitations*



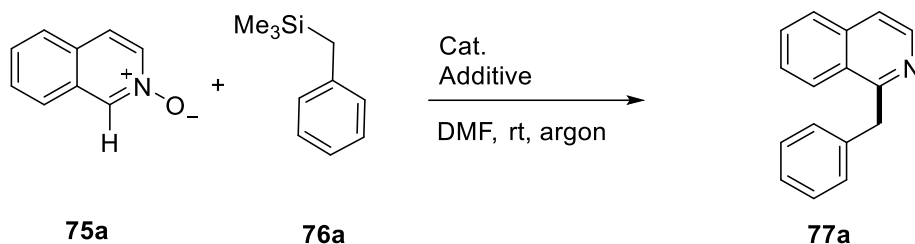
**Scheme 3.9** Limitations of cross-coupling methodology. n.d. = not detected



**Scheme 3.10** Scale-up experiment of the developed benzylation methodology

### 3.1.5 Mechanistic considerations

To understand the reaction mechanism various control experiments were performed (Table 3.2). Various fluoride sources catalyzed the reaction under standard conditions (entry 1-3). However, using a stoichiometric amount of base failed to initiate the transformation (entry 4). The starting materials remain unconsumed in the absence of any fluoride source (entry 5). This supported the initial thought of fluoride activation of silanes in the first step of reaction. The reaction happens in the absence of triethylsilane as additive but with lower yields (entry 6). To understand the role of triethylsilane in the reaction, a control experiment was carried out in the absence of a coupling partner, which is benzyltrimethylsilane. Interestingly, the *N*-oxide was simply reduced to yield isoquinoline **78** (Scheme 3.11). In this case, the necessity of addition of triethylsilane after addition of fluoride catalyst was understood. The role of triethylsilane was hypothesized to be a reducing

**Table 3.2** Control experiments for fluoride catalysis<sup>[a]</sup>

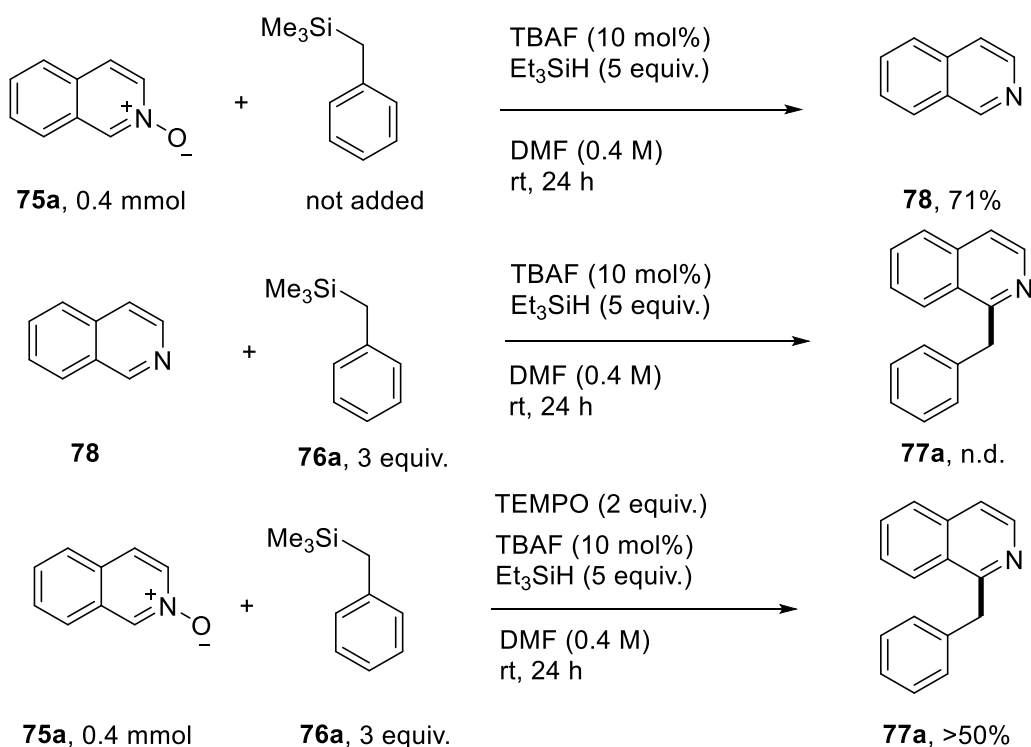
Entry	Cat.	Additives (5 equiv.)	Yield (%) <sup>[b]</sup>
1	TBAF (10 mol%)	Et <sub>3</sub> SiH	78
2	CsF (10 mol%)	Et <sub>3</sub> SiH	30
3	TBAT (10 mol%)	Et <sub>3</sub> SiH	29
4	KOtBu (2 equiv.)	Et <sub>3</sub> SiH	n.d.
5	-	Et <sub>3</sub> SiH	n.d.
6	TBAF (10 mol%)	-	45

<sup>[a]</sup>Reaction conditions: 75a (0.4 mmol), 76a (1.2 mmol, 3 equiv.), DMF (0.4 M), rt, argon. n.d. = not detected.

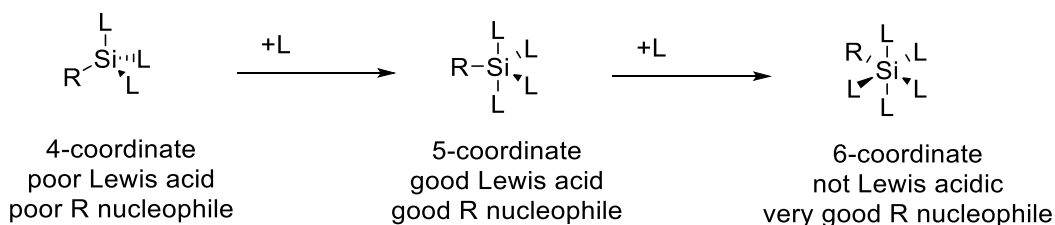
agent to transform C<sub>1</sub>-benzylated isoquinoline *N*-oxides to C<sub>1</sub>-benzylated isoquinoline. The pre-oxidation of heterocycle is necessary, because simple isoquinoline failed to react with the organosilanes coupling partner under fluoride catalysis to give coupling product. A high C<sub>1</sub> regioselectivity for isoquinolines and C<sub>2</sub> regioselectivity for quinolines and pyridines indicated a 1,2-migration type of mechanism as in the case of previously reported boronic acid coupling. However, to negate a radical mediated reaction, radical trap experiments were performed. The reaction performance had no significant decrease in presence of 2 equiv. of TEMPO as radical scavenger. These results from control experiments and the pattern of substrate scope suggested a reaction mechanism involving formation of a hypervalent silicon intermediate (Scheme 3.11).

Silicon can afford 4-,5- and 6- coordinate complexes. Benzyltrimethylsilane has a 4-coordinate silicon. This is a poor Lewis acid because it cannot accept a lone pair of electrons. The R group attached to 4-coordinate silicon is a poor nucleophile (Scheme 3.12). A nucleophilic attack of

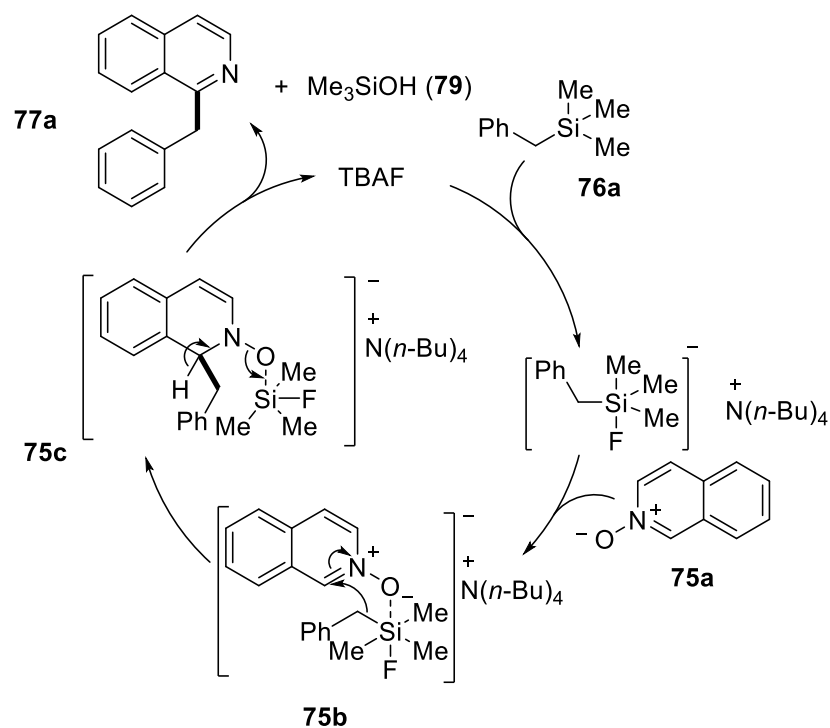
fluoride ion to benzyltrimethylsilane **76a** results in the formation of a 5-coordinate silicon **75b**. In comparison to the 4-coordinate silicon, pentacoordinate silicon is a good Lewis acid. Hence, the nucleophilic oxygen attacks the silicon which results in the formation of hexacoordinate silicon intermediate **75c**. The R group, which is a benzyl group attached to a hexacoordinate silicon, is a very good nucleophile. It will undergo a nucleophilic migration to the C<sub>1</sub> position of isoquinoline N-oxide. The following rearomatization step gives the desired product **77a**, with the regeneration of the catalyst. In the process, trimethylsilanol **79** is formed as a byproduct which will polymerize to form hexamethyldisiloxane and other polysiloxanes.<sup>[92-93]</sup>



**Scheme 3.11** Control experiments for mechanistic studies of benzylation.



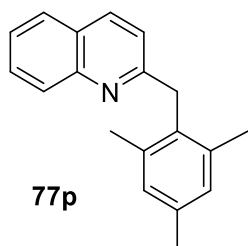
**Scheme 3.12** Characteristics of hypervalent silicon complexes



**Scheme 3.13** Proposed reaction mechanism of C<sub>1</sub>-benzylation

### 3.1.6 Identification of biological activity

Compound libraries of C<sub>1</sub>-benzylated isoquinoline were submitted to COMAS (Compound Management and Screening Centre) in Dortmund to screen for the biological activities. Cell-based assays to screen for autophagy inhibitor activities and hedgehog signaling pathway inhibition were carried out. After screening, the compound **77p** was identified as an Autophagy inhibitor in the low micro molar range. However, a rapamycin induced autophagy inhibition assay in presence of compound showed no activity.



Autophagy IC<sub>50</sub> = 6.86 μM

RAPA IC<sub>50</sub> = inactive



Furthermore, the phenotypic screening of compounds was also carried out using Cell painting assay which is highly useful for retrieving the biological information from morphological characteristics of cellular components.<sup>[94]</sup> From the library, 4 compounds were reported to have significant biosimilarity to reference compounds. However, the reference compounds for active hits were not very similar and the hit frequencies of these reference compounds are high. The compounds are suggested to possess the highest similarity to functional clusters of Lysosomotrop.

**Table 3.3** Representative results of cell painting assay

<b>Compound</b>	<b>Conc. [μM]</b>	<b>Activity</b>	<b>Induction [%]</b>	<b>Highest sim. to a reference [%]</b>	<b>Toxic</b>
<b>77p</b>	30	active	6.0	78.9	No
<b>77p</b>	10	inactive	1.2		No
<b>77k</b>	10	active	5.0	73.9	No
<b>77d</b>	10	active	11.1	84.4	No
<b>77h</b>		active	14.0	86.2	No

## 3.2 C–H Alkynylation

### 3.2.1 Introduction

Having success on developing a metal-free methodology for C(sp<sup>2</sup>)-C(sp<sup>3</sup>) bond formation, focus was diverted to other silanes which would make C(sp<sup>2</sup>)-C(sp<sup>2</sup>) and C(sp<sup>2</sup>)-C(sp) connections with *N*-heterocycles. In this regard, trimethyl(phenylethynyl)silane was first tested as a coupling partner because of the biological significance of C<sub>2</sub>-alkynylated scaffolds (Figure 3.2).

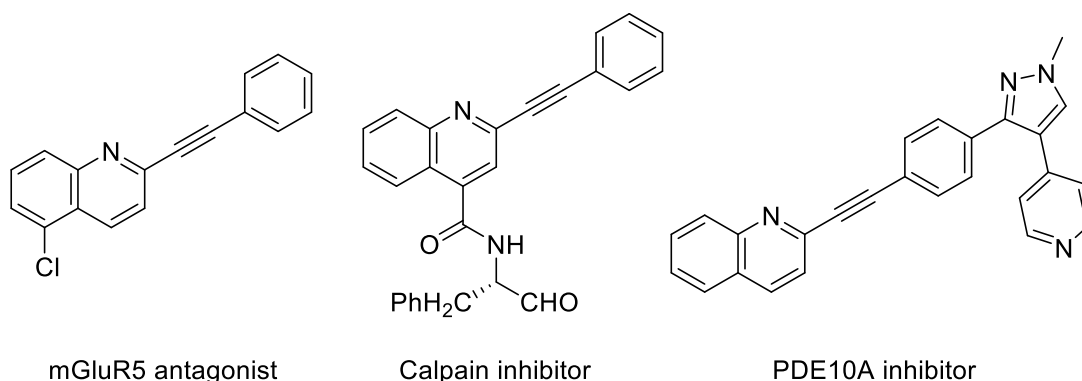
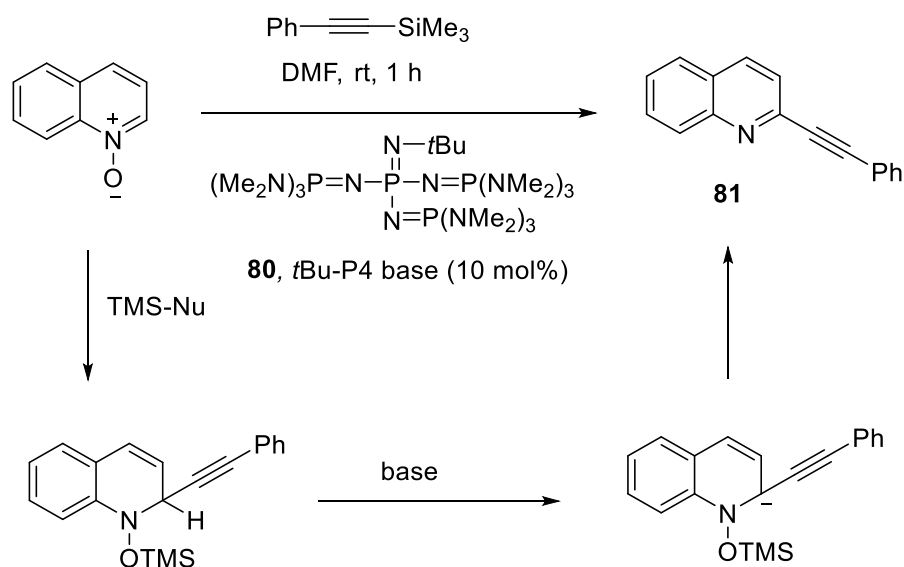


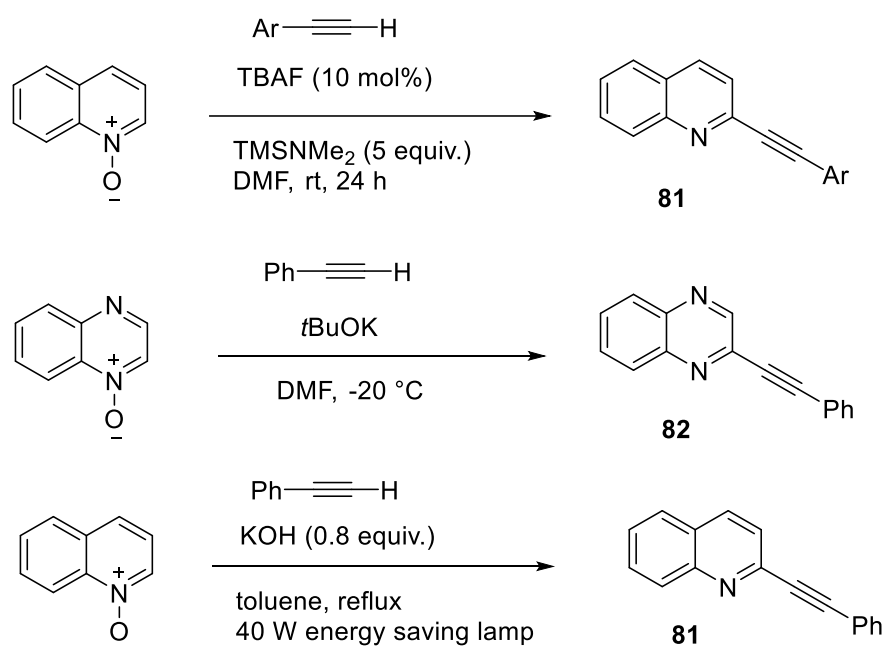
**Figure 3.2** Representative bioactive compounds having alkynyl substituted *N*-heterocycle



**Scheme 3.14** Deoxygenative alkylation of quinoline *N*-oxides using phosphazene super base

Kondo and co-workers elucidated a method for deoxygenative alkylation of quinoline *N*-oxides using phosphazene super base **80** as catalyst in presence of silylated nucleophiles (Scheme 3.14).

Afterwards, the same group modified the conditions and reported a procedure for coupling terminal alkynes with heteroaromatic *N*-oxides to provide 2-alkynyl substituted nitrogen heteroaromatics.<sup>[95]</sup> The phosphazene organic superbases were replaced by an onium amide base in this method and thereby improving the ease of access for reagents.<sup>[96]</sup> Chupakhin *et al.* had reported a complementary method to Sonogashira cross-coupling reaction for the synthesis of ethynylazines using potassium *tert*-butoxide. In the reaction, phenylacetylide of potassium is generated. Quinoxaline *N*-oxide readily reacts with this reagent at -20 °C in anhydrous DMF to yield corresponding ethynylazines.<sup>[97]</sup> Recently a potassium hydroxide catalyzed visible light mediated reaction has also been developed for selectively alkynylating the azine *N*-oxides (Scheme 3.15).<sup>[98]</sup>

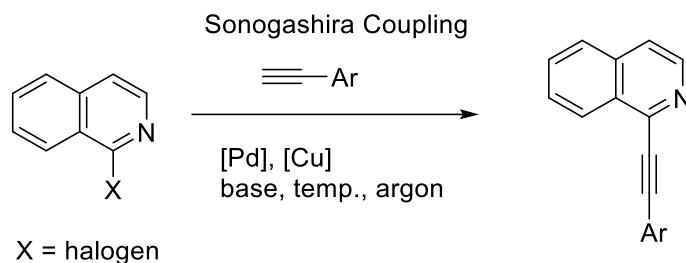


**Scheme 3.15** C–H functionalization methods 2-alkynyl substituted nitrogen heteroaromatics

### 3.2.2 Motivation and objectives

A most common approach for introducing alkynyl group is carrying out Sonogashira cross-coupling reactions. This reaction usually requires transition metal catalysts, base and harsh reaction conditions (Scheme 3.16).<sup>[99]</sup> Alternatively, aforementioned methods for the synthesis of alkynylated quinoline and pyridine are known. The reported methodologies are carried out in presence of strong bases such as phosphazene super base, potassium *tert*-butoxide, etc. So, there is still room for further improvements. Additionally, the synthesis of selectively C–H alkynylated

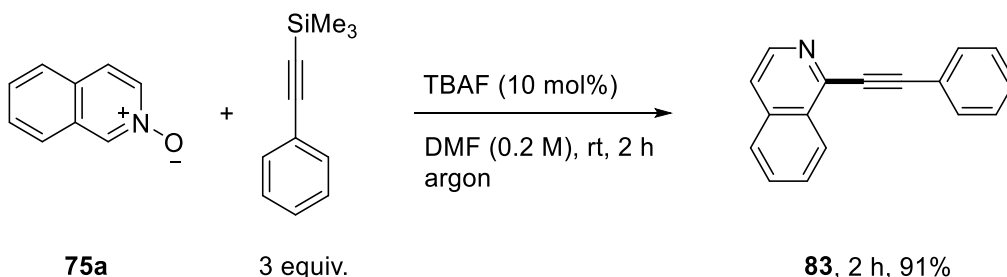
isoquinoline derivatives under transition metal-free conditions is not well studied. For these reasons, the feasibility of cross-coupling between isoquinoline *N*-oxide and trimethyl(phenylethynyl)silane was examined initially.



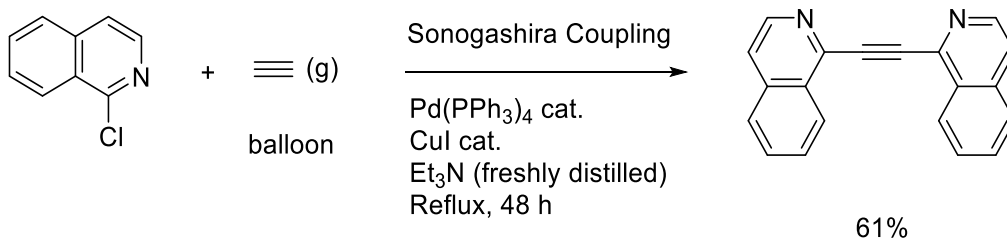
**Scheme 3.16** Sonogashira coupling for alkylation

### 3.2.3 Initial results and optimization

The cross-coupling reaction between isoquinoline *N*-oxide **75a** and trimethyl(phenylethynyl)silane proceeded smoothly to yield 91% of the coupled product **83** in just 2 hours (Scheme 3.17). Tetrabutylammonium fluoride was an efficient fluoride source for this transformation for carrying out the reaction in DMF at room temperature under argon atmosphere.



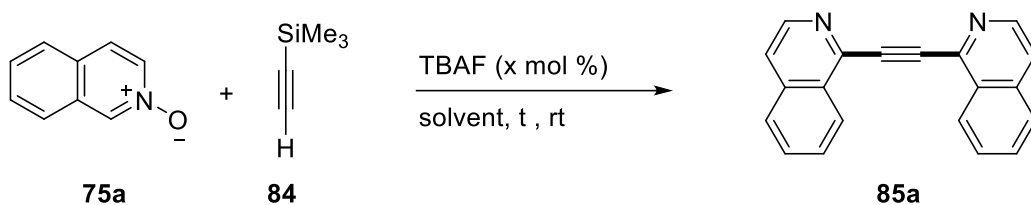
**Scheme 3.17** C–H alkylation of heterocyclic *N*-oxide using organosilanes



**Scheme 3.18** Sonogashira coupling for 1,2-diheteroarylacetylenes

Unexpectedly using ethynyltrimethylsilane as a coupling partner resulted in the formation of a double coupling product (Table 3.4). Symmetrically heteroaryl disubstituted acetylene **85a** was obtained under transition metal-free conditions. This observation was encouraging in the sense that, an alternative Sonogashira coupling takes place only in presence of metals such as copper and palladium and additionally a base has to be added. More importantly, handling of gaseous alkyne is required and reaction conditions were harsh and long as well (Scheme 3.18). With these initial observations, further optimization of the reaction conditions was carried out. THF found to be the only suitable solvent in this transformation while DMF, MeCN or DCE was found to be not suitable for this cross-coupling between compound **75a** and compound **84** (entry 1-6).

**Table 3.4** Representative conditions for the optimization of alkylation<sup>[a]</sup>



Entry	Equiv. of <b>84a</b>	TBAF (mol%)	Solvent (1 mL)	Time (h)	Yield of <b>85a</b> (%) <sup>b</sup>
1	3	10	THF	12	42
2	3	10	DMF	12	n.d.
3	3	10	MeCN	12	n.d.
4	3	10	DCE	12	n.d.
5	6	10	THF	12	72
6	6	5	THF	3	82
<b>7</b>	<b>4</b>	<b>5</b>	<b>THF</b>	<b>3</b>	<b>89</b>
8	4	3	THF	3	35
9	3	5	THF	3	36

<sup>[a]</sup>Reaction conditions: **75a** (0.2 mmol), solvent (0.2 M). <sup>[b]</sup>Isolated yields. n.d. = not detected.

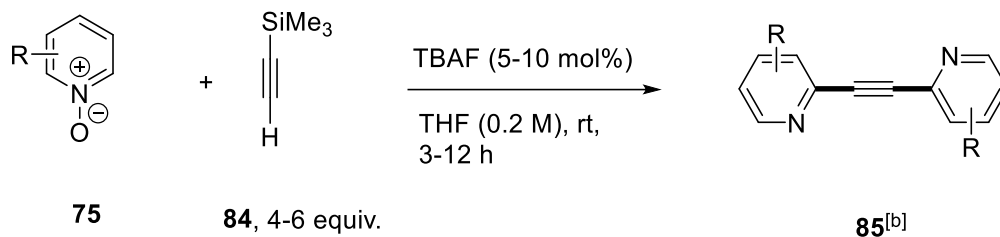
In case of synthesis of 1,2-di(isoquinolin-1-yl)ethyne, 5 mol% of TBAF and 6 equivalents of ethynyltrimethylsilane was found to be optimal. The reaction yielded 89% of the desired cross-coupled product at room temperature in just 3 hours (entry 7). This was really encouraging to see, because unlike the Sonogashira method, inexpensive catalysts and harsh reaction conditions were not required at all. Instead, reaction at room temperature using easy to handle reagents and simple laboratory set up was more than sufficient to obtain these interesting classes of compounds. Further experiments did not improve the yield of product **85a** (entry 8 and entry 9).

### 3.2.4 Scope of heterocyclic *N*-oxides

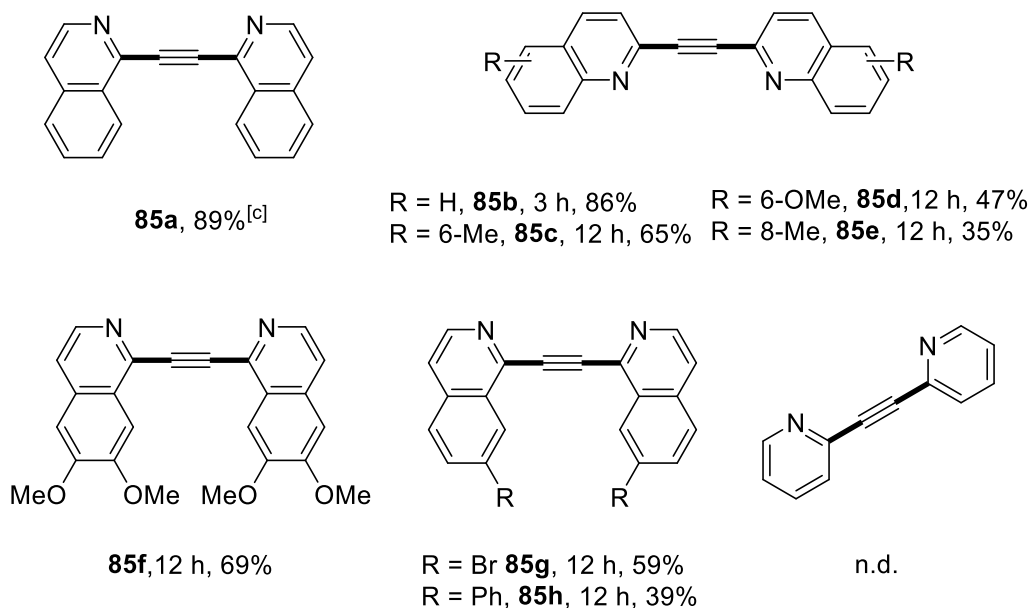
After the optimization of reaction conditions, the methodology was applied for the synthesis of different coupled products. Different isoquinoline and quinoline compounds were evaluated for their compatibility.

It was found that, in addition to the isoquinoline scaffold, various substituted quinoline heterocyclic *N*-oxides also undergo double deoxygenative coupling reaction to produce disubstituted acetylene compounds. A 6-methyl substituted quinoline *N*-oxide reacted with ethyne containing trimethylsilyl group at 1-position to yield 1,2-bis(6-methylquinolin-2-yl)ethyne under mild conditions. However, a slight increase of catalyst loading to 10 mol% was important to get 65% of the product (**85c**). A strong electron donating substituent at the same position was also tolerated (**85d**). Interestingly, *N*-oxide of isoquinoline ring possessing methoxy substitution at both 6 and 7 position reacted well with 6 equivalents of ethynyltrimethylsilane to provide the product **85f**. Also, R groups such as halogen or phenyl substitution of only 7-position of isoquinoline *N*-oxide substrate were also acceptable for the developed cross-coupling method (**85g** and **85h**). In short, the scope of reaction is good and this method proved to be a powerful alternative for Sonogashira type coupling reactions for such a class of compounds. Unfortunately, the methodology could not be applied for pyridine *N*-oxides.

More importantly, most of the reported compounds are synthesized for the first time and this will allow to unveil interesting applications of this 1,2-heteroarylsubstituted acetylene scaffold for various applications. The results are summarized in the scheme below (Scheme 3.19).<sup>[a] [b]</sup>



----- **scope and limitations** -----

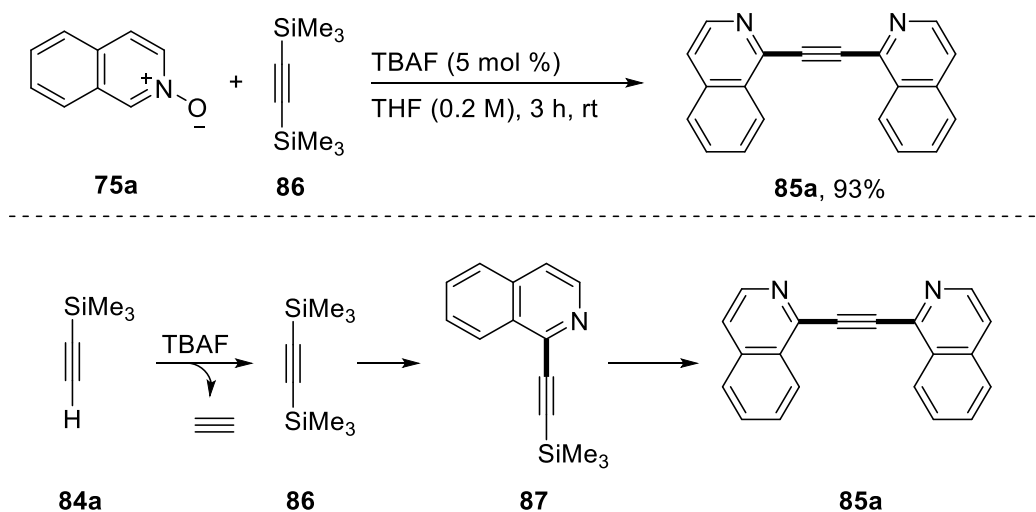


**Scheme 3.19** Scope of cross-coupling between heterocyclic *N*-oxides and organosilanes. <sup>[a]</sup>Reaction conditions: **75** (0.4 mmol), **84** (6 equiv.), TBAF (10 mol%), DMF (0.2 M). <sup>[b]</sup>Yields are given for isolated products (**77**). <sup>[c]</sup> 4 equiv. of **84** and 5 mol% TBAF was used. n.d = not detected.

### 3.2.5 Mechanistic considerations

A plausible mechanistic pathway was hypothesized in the scheme. Initially a proton abstraction from the terminal alkynes results in the generation of an alkynide ion. Fluoride ions act as a base in this process.<sup>[100]</sup> The nucleophilic attack of alkynide ion to the silicon of ethynyltrimethylsilane results in the generation of bis(trimethylsilyl)acetylene. A molecule of ethyne is eliminated as gas from the reaction mixture. This results in strong effervescence upon addition of catalyst. Also, requirement of excess acetylene partner could be justified for this reason (Scheme 3.20). Literature reports suggest that this type of sigma bond metathesis of terminal alkynes has been reported earlier as well.<sup>[101-102]</sup> Furthermore, a reaction starting with bis(trimethylsilyl)acetylene **86** and

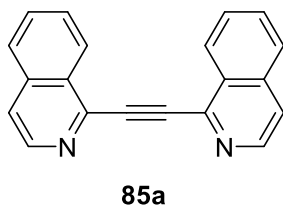
isoquinoline *N*-oxide proceeded smoothly to yield 93% of the double coupling product **85a**. Heteroaromatic *N*-oxide first couple with *in situ* generated bis(trimethylsilyl)acetylene **86** to give the mono coupling intermediate. Another molecule of *N*-oxide moiety then attacks this intermediate to eventually give a double coupled final product **85a**.



**Scheme 3.20** Mechanistic consideration of alkylation reaction methodology

### 3.2.6 Identification of biological activity

Compound libraries of symmetrically heteroaryl disubstituted acetylenes were submitted to COMAS (Compound Management and Screening Centre) in Dortmund to screen for the biological activities. Cell-based assays to screen for autophagy inhibitory activity and hedgehog signaling pathway inhibition were carried out. After screening, the compound **85a** was identified as a hedgehog pathway inhibitor in the low micro molar range.



Hh IC<sub>50</sub> = 0.26 μM

Furthermore, the phenotypic screening of compounds was also carried out using cell painting assay (Table 3.5). From the library, 2 compounds were reported to have significant biosimilarity to reference compounds. Unfortunately, 10 μM concentration of isoquinoline was toxic to the cells.



Lowering the concentration leads to loss of activity. In the case of quinoline analogue (COMAS compound Id 409532), 10  $\mu\text{M}$  solution showed a significant induction and similarity to the reference compound. Activity of reference compound suggests a potential to inhibit glucose transporter GLUT1. The frequency of this reference compound is only 0.16%, which is really good. But this compound also has a mild toxicity. Activity studies with lower concentration needs to be carried out.

**Table 3.5** Representative results of cell painting assay

Compound	Conc. [ $\mu\text{M}$ ]	Activity	Induction [%]	Highest sim. to a ref. [%]	Toxic
<b>85a</b>	10	active	31.4		Yes
<b>85a</b>	3	inactive	2.4		No
<b>85a</b>	1	inactive	0.7		No
<b>85b</b>	10	active	34.7	84.4	No



**Electrochemical Dehydrogenative Amination**

---

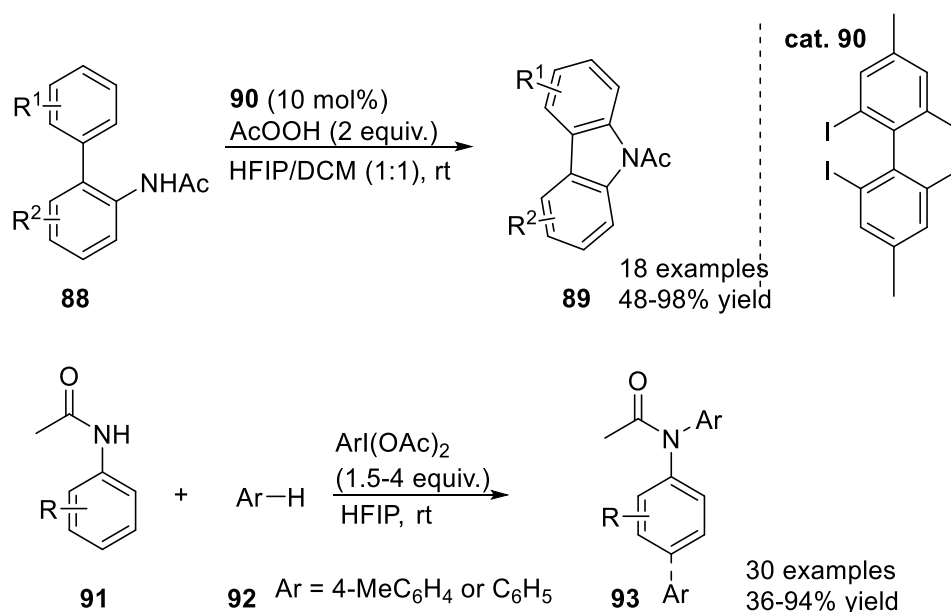
(Parts of this chapter have already been published: [Mahesh Puthanveedu](#), Vladislav Khamraev, Lukas Brieger, Carsten Strohmann, and Andrey P. Antonchick; *Chem. Eur. J.* **2021**, *27*, 8008-8012)



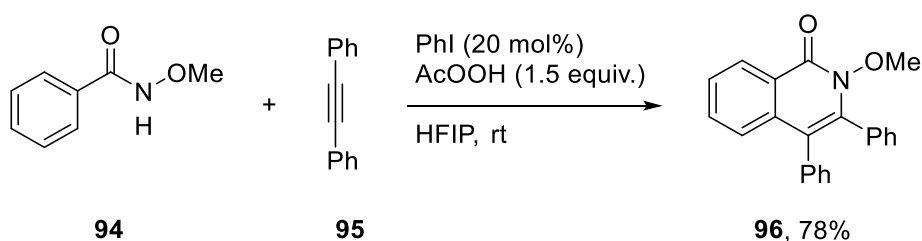
## 4 Electrochemical Dehydrogenative Amination

### 4.1 Introduction

Nitrenium ions are important intermediates in organic synthesis. Various transition metal-free C–H amination methodologies have been developed exploiting the high reactivity of *in situ* generated nitrenium ions. In this regard, Antonchick and co-workers discovered various oxidative annulation reactions and direct C–H bond amination reactions using hypervalent iodine reagents. For instance, an intramolecular C–H amination method towards carbazole scaffold (**89**) was developed under hypervalent iodine catalysis. The methodology was also applicable for the amination of unactivated arenes and also for diarylation of anilides (**91**) in presence of excess arene and stoichiometric amount of phenyliodine (III) diacetate (PIDA) (Scheme 4.1).<sup>[103]</sup>

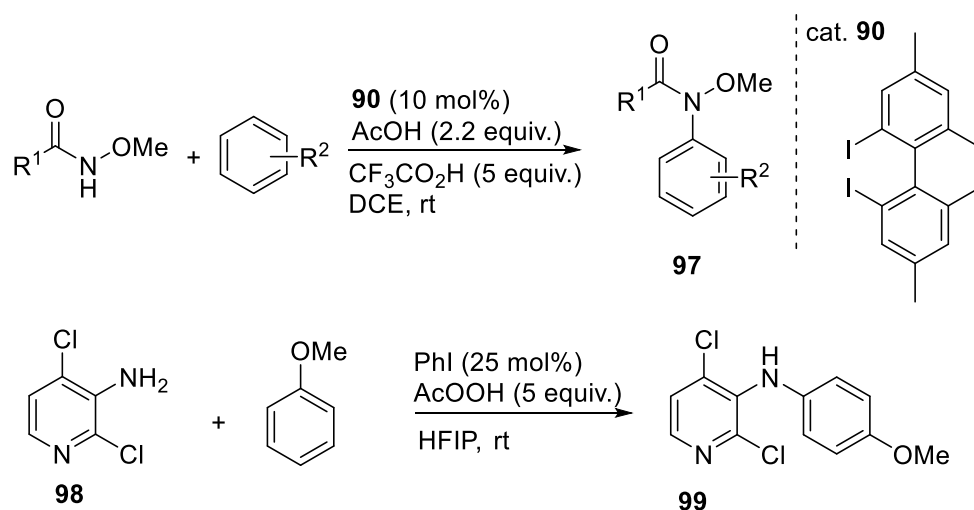


**Scheme 4.1** Hypervalent iodine mediated direct C–H bond aminations



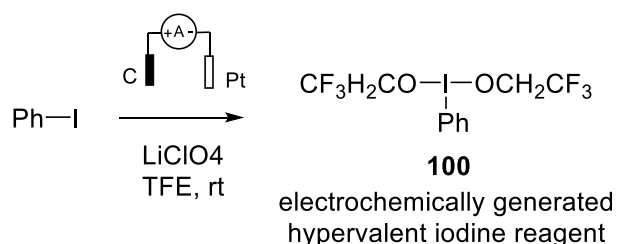
**Scheme 4.2** Organocatalytic annulation of benzamide compounds with alkynes

Also, an organocatalytic annulation of benzamide compounds with alkynes has been reported for the straight forward synthesis of isoquinolines (Scheme 4.2). The reaction was proposed to proceed *via* an *in-situ* generation of PIDA in presence of peracetic acid as an oxidant. The hypervalent iodine reagent then oxidizes the benzamide nitrogen to form electrophilic nitrenium ions. The attack of alkynes to the and followed nucleophilic attack of aryl ring results in isoquinoline scaffold.<sup>[104]</sup> Similarly, nucleophilic attack of aryl ring to the nitrenium intermediates of benzamide derivatives results in direct C–H bond amination of aromatic and heteroaromatic compounds (Scheme 4.3).<sup>[105-107]</sup>

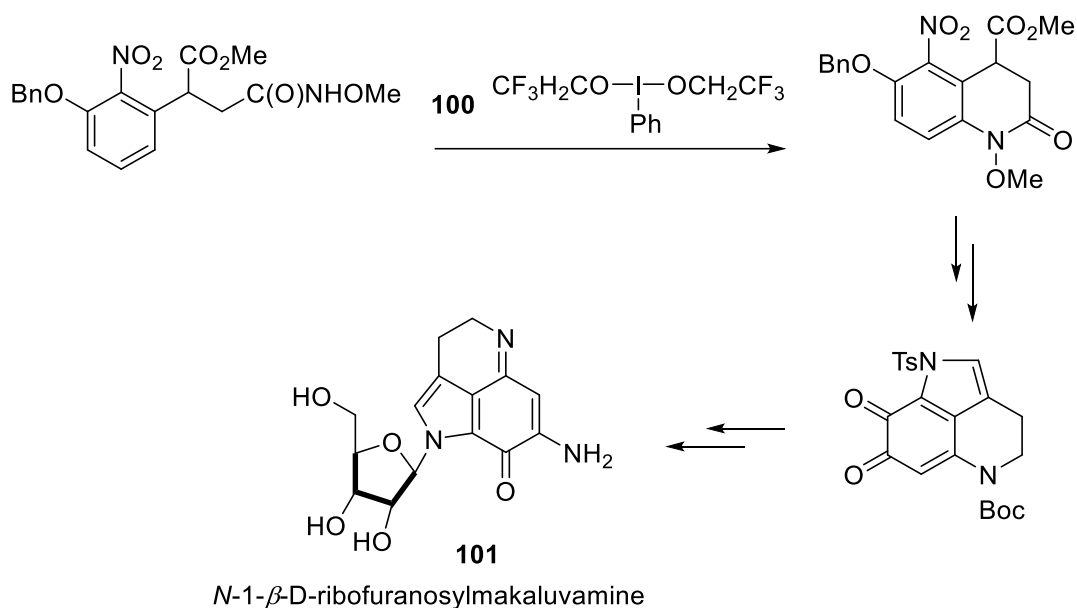


**Scheme 4.3** Intermolecular amination mediated by hypervalent iodine reagents

Owing to their broad applicability and unique advantages in organic synthesis, efforts have been made to combine electroorganic chemistry with transition metal-free C–H bond functionalization. Nishiyama and coworkers applied electrochemistry to oxidize iodine(I) precursors to iodine(III) reagents (**100**) and employed these electrogenerated hypervalent iodine reagents to C–H amination reactions involving nitrenium ion intermediates (Scheme 4.4).



**Scheme 4.4** Electrochemical generation of hypervalent iodine reagents



**Scheme 4.5** Electrochemical total synthesis of tetrahydropyrroloiminoquinone alkaloids

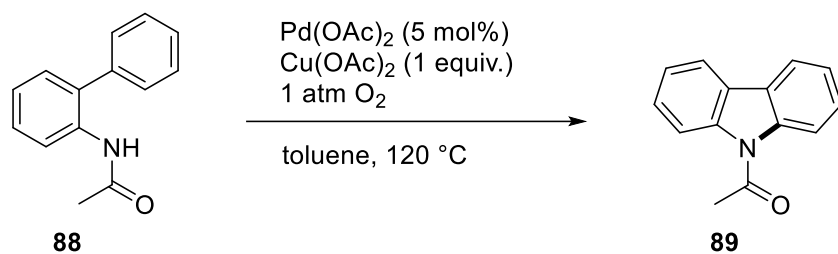
Moreover, the synthetic utility of these methods was demonstrated by applying them in the total synthesis of natural products such as tetrahydropyrroloiminoquinone alkaloids (**101**) (Scheme 4.5).<sup>[108]</sup>

## 4.2 Intramolecular amination

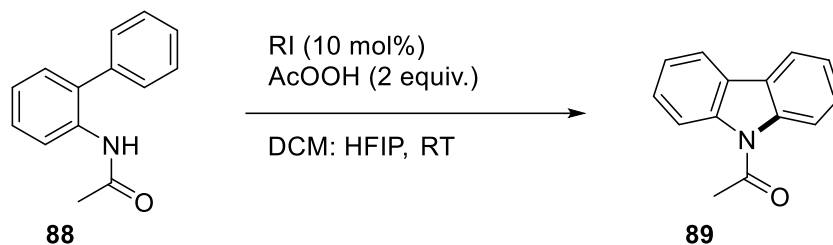
### 4.2.1 Motivation and objectives

Atom economy of organic reactions is an important parameter with respect to sustainable chemistry. Direct amination of C–H bonds is an atom economic method to synthesize nitrogen heterocyclic compounds. In case of carbazoles, Buchwald and coworkers reported a highly atom economic strategy to access this class of compounds. The method was a novel C–H activation approach catalyzed by expensive palladium catalysts in presence of copper(II) acetate as an oxidant.<sup>[109]</sup> Afterwards, numerous reactions of similar chemistry were reported using different transition metal catalysts such as copper, rhodium, iridium etc.<sup>[110-112]</sup> In 2011, Antonchick and coworkers reported a novel transition metal-free organocatalytic approach for intramolecular C–H bond amination. The approach was based on the generation of electrophilic nitrenium ion intermediate in presence of hypervalent iodine reagents.<sup>[103]</sup> This report later paved the way to the electrochemical synthesis of carbazole derivatives (Scheme 4.6).

Buchwald, 2005: Pd catalyzed

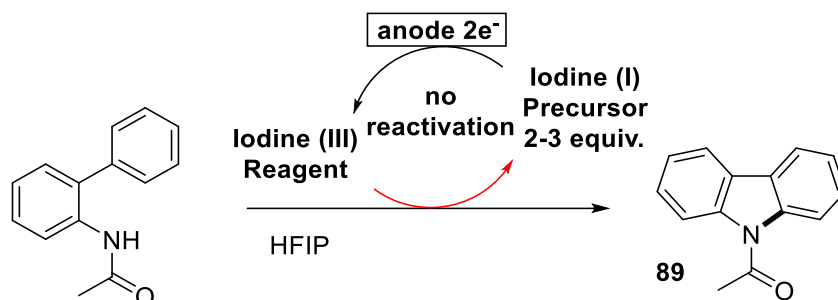


Antonchick, 2011: Hypervalent iodine catalyzed



**Scheme 4.6** Intramolecular amination of 2-amidobiphenyls towards carbazoles

It is claimed that direct electrochemical synthesis is hard because of overoxidation, homo coupling and electropolymerization reactions.<sup>[113-114]</sup> For these reasons, the existing methodologies use an indirect electrochemical approach. This method is otherwise called the *ex cell* approach. In an *ex cell* electrochemical synthesis using iodine based redox mediator as a precursor for hypervalent iodine reagent, at first the electrolysis of iodine precursor is carried out in presence of fluorinated solvents to generate the active hypervalent iodine reagent. Then the electric current is turned off and the substrate is added to the electrolytic solution and stirred under specified conditions.<sup>[115-116]</sup> In such reactions, it is mandatory to use a stoichiometric amount of redox mediator because the active catalyst is just consumed and not regenerated after (Scheme 4.7).

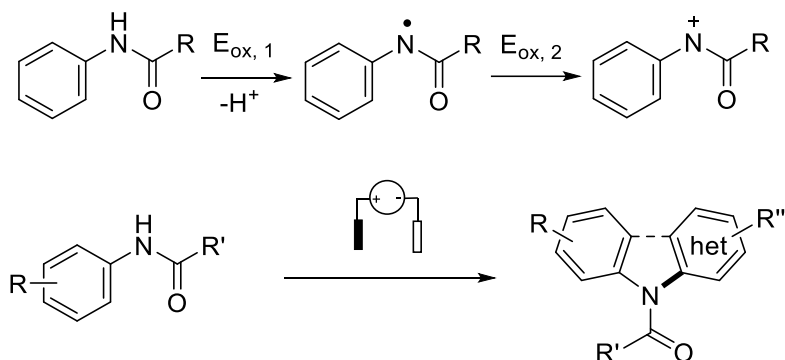


**Scheme 4.7** *Ex cell* electrochemical methods for amination reactions



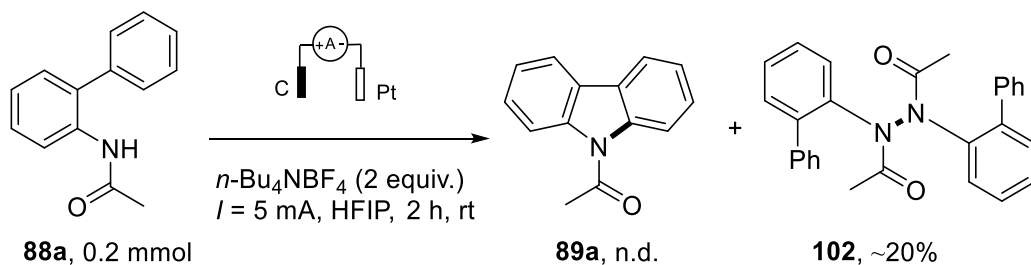
Also, in case of intermolecular reactions, it is found that an excess of coupling partners has to be used with stoichiometric quantities of supporting electrolytes. Even though using quantities of supporting electrolytes and non-friendly constant potential electrolysis, a very recent report has allowed *in cell* electrolysis for C–H amination using hypervalent iodine catalysts.<sup>[117]</sup>

An alternative could be the direct electrolysis of acetanilide derivatives to generate corresponding nitrenium ions. Waldvogel and co-workers delineated a possibility to generate nitrenium ion by a two-step oxidation of acetanilide. Not only they succeeded in the mechanistic investigations including a series of cyclic voltammetric studies to prove the two-step oxidation of nitrogen, but also demonstrated the utility by benzoxazole synthesis *via* intramolecular C–O bond formation.<sup>[118]</sup> However, a direct electrolytic strategy for such C–N bond formation remained unexplored. In this regard, a novel direct electrochemical strategy for intramolecular amination of C–H bonds mediated by nitrenium ion intermediate would be highly appreciated. This would open the door to more synthetic methods based on the direct electrochemical generation of nitrenium ions (Scheme 4.8).

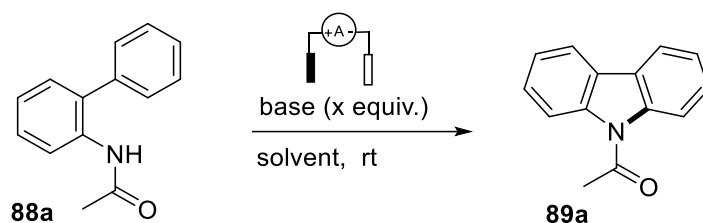


**Scheme 4.8** Proposed direct electrolytic approach to nitrenium ions

#### 4.2.2 Initial results and optimization



**Scheme 4.9** Initial results of direct electrolytic approach towards carbazole synthesis

**Table 4.1** Representative conditions for the optimization of intramolecular amination<sup>[a]</sup>

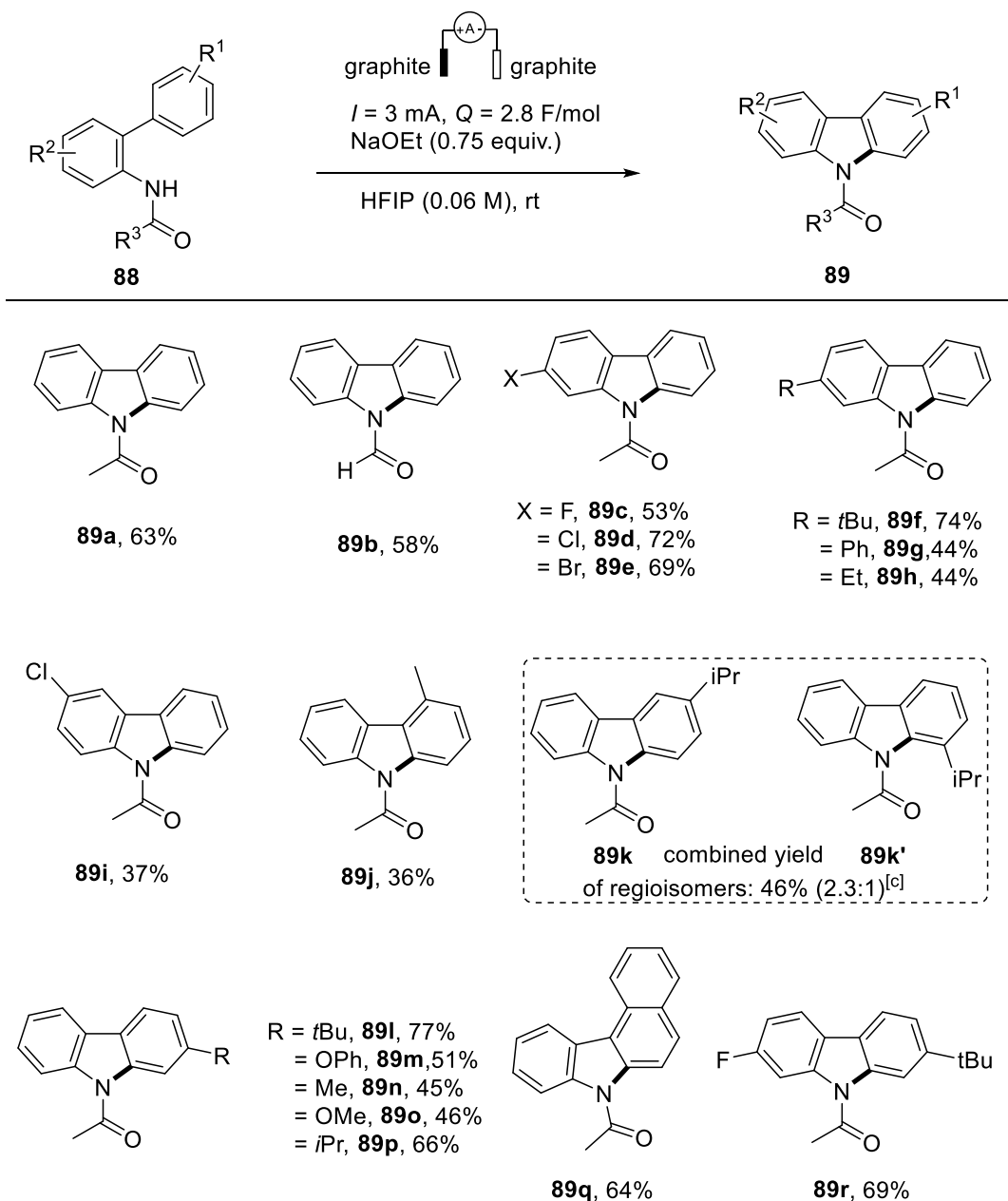
Entry	Base (equiv.)	Electrolyte (1 equiv.)	Solvent	Yield <sup>[b]</sup>
1 <sup>[c]</sup>	-	<i>n</i> -Bu <sub>4</sub> NBF <sub>4</sub>	HFIP	n.d.
2	-	<i>n</i> -Bu <sub>4</sub> NBF <sub>4</sub>	HFIP	trace
3	KOtBu (2)	<i>n</i> -Bu <sub>4</sub> NBF <sub>4</sub>	HFIP	57
4	KOtBu (2)	<i>n</i> -Bu <sub>4</sub> NBF <sub>4</sub>	toluene	n.d.
5	KOtBu (2)	<i>n</i> -Bu <sub>4</sub> NBF <sub>4</sub>	TFE	n.d.
6	KOtBu (2)	<i>n</i> -Bu <sub>4</sub> NBF <sub>4</sub>	DCE/HFIP (1:1)	40
7	KOtBu (2)	<i>n</i> -Bu <sub>4</sub> NBF <sub>4</sub>	MeCN/HFIP (1:1)	33
8	KOtBu (1)	<i>n</i> -Bu <sub>4</sub> NOAc	HFIP	43
9	KOtBu (1)	<i>n</i> -Bu <sub>4</sub> NOAc	HFIP	43
10	KOtBu (1)	<i>n</i> -Bu <sub>4</sub> NPF <sub>6</sub>	HFIP	47
11	KOtBu (1)	Et <sub>4</sub> NOTs	HFIP	45
12	KOtBu (1)	-	HFIP	52
13	LiOtBu (1)	-	HFIP	59
14	Et <sub>3</sub> N (2)	-	HFIP	56
15	DBU (2)	-	HFIP	45
16	NaOEt (1)	-	HFIP	60
<b>17<sup>[d]</sup></b>	<b>NaOEt (0.75)</b>	-	<b>HFIP</b>	<b>63</b>

<sup>[a]</sup> Reaction conditions: constant current electrolysis (5 mA) for 3 h (3.2 F/mol) using graphite electrodes: **88a** (0.2 mmol), solvent (0.06 M). <sup>[b]</sup> Isolated yield of **89a** <sup>[c]</sup> Glassy carbon anode and platinum plate cathode. <sup>[d]</sup> 3 mA current and 2.8 F/mol charge passed in 5 h. n.d. = not detected.

The initial efforts to realize a direct electrolytic approach to generate nitrenium ion intermediate and to initiate the intramolecular cyclization of 2-amidobiaryl compounds were not successful. Instead of the desired products, a dimerization of the starting material was consistently observed. This is due to the ready formation and high reactivity of *N*-acyl radicals upon electrolysis. The N–N radical dimerization was initially reported by Baran and co-workers as a key step in the synthesis of natural product Dixiamicine B.<sup>[119]</sup> In addition, mechanistic studies by Waldvogel, Moeller and co-workers have also reported methodologies based on N–N radical dimerization reactions (Scheme 4.9).<sup>[118]</sup> At this point, modification of reaction conditions was necessary to shift the reaction pathway from radical homo-coupling to intramolecular C–H amination (Table 4.1). Only switching to graphite electrodes did not provide useful results (entry 2). A detailed literature review led to a previous report from Zeng group in which a base mediated proton abstraction from amide was proposed as the first step of an electrochemical benzylic C–H amination.<sup>[120]</sup> Based on this, a base was added additionally to the reaction mixture for electrolysis. A constant current electrolysis using graphite electrodes in presence of 2 equivalents of potassium *tert*-butoxide in hexafluoroisopropanol solvent and tetrabutylammonium tetrafluoroborate as electrolyte provided a promising yield of 57% of desired product (entry 3). Various solvents including toluene, TFE and solvent mixtures were also screened (entry 4-7). Screening different electrolytes did not improve the yield of desired product (entry 8-11). However, using a base in an acidic solvent was found beneficial. Because it was found that the reaction still proceeds without huge resistance to render the reaction even in the absence of an external electrolyte (entry 12). Then further optimization revealed sodium ethoxide as a good choice (entry 13-16) which results in good yield of desired product with sub-stoichiometric quantities of base (entry 17).

### 4.2.3 Scope of intramolecular amination

To evaluate the substrate scope of the developed method, various substrates containing different substitutions at different positions of the aryl rings were prepared according to the known literature methods. Acetanilide derivatives were prepared using acetyl chlorides and triethylamine base. To make biaryl substrates, Suzuki coupling with respective boronic acids or palladium catalyzed *ortho* C–H activation was applied.<sup>[121-122]</sup> Afterwards, the synthesized substrates were examined for the compatibility of the developed electrochemical intramolecular amination reaction.



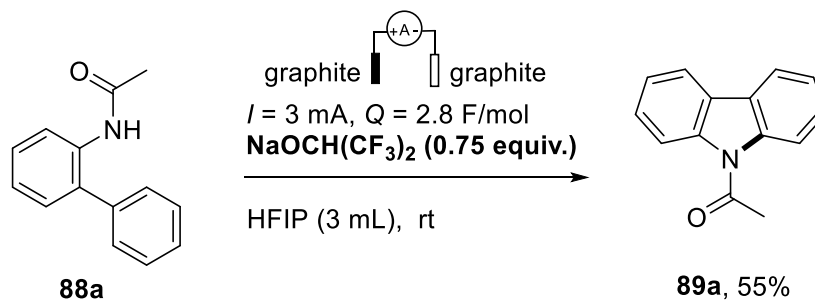
**Scheme 4.10.** <sup>[a]</sup> Reaction conditions: constant current electrolysis (5 mA) for 3 h (~ 3.2 F/mol) using graphite electrodes: **88** (0.2 mmol), solvent (0.06 M). <sup>[b]</sup> Isolated yield. <sup>[c]</sup> *n*-Bu<sub>4</sub>NBF<sub>4</sub> (0.2 mmol, 1 equiv.) as supporting electrolyte. <sup>[d]</sup> Glassy carbon anode and platinum plate cathode. <sup>[e]</sup> 3 mA current and 2.8 F/mol charge passed in 5 h. n.d. = not detected.

Delightedly, many substrates reacted under electrochemical oxidation in presence of base to yield corresponding carbazole derivatives (Scheme 4.10). In addition to the acetyl protection, a formyl protected 2-amidobiaryl was also examined. Contrary to previous reports, the current method selectively yielded a five membered carbazole product instead of the usual six membered

isoquinolone analogue (**89b**). Afterwards, substrates containing halogen substitution at 4- position of the biaryl ring was electrolyzed under standard conditions. All tested halogen containing substrates cyclized to yield *N*-protected 2-halocarbazoles (**89c-e**). Similarly, different 2-amidobiaryl derivatives containing 4-alkyl or 4-phenyl substitutions were also successful substrates for this intramolecular (**89f-h**) electrochemical C–H bond amination. Furthermore, the synthesis of 3-chlorocarbazole and 4-methyl carbazole derivatives were realized albeit in lower yields (**89i** and **89j**). 3'-isopropyl group containing biarylacetamide substrate resulted in a mixture of regioisomers as expected, with the combined yield of 46% in a ratio of 2.3 to 1 for two possible regioisomers (**89k** and **89k'**). However, all tested substrates with 4' electron donating substitutions such as *tert*-butyl, methoxy, etc. provided corresponding carbazoles in good yields (**89l-p**). Substrates containing polyaromatic rings such as 1-naphthyl were also found to be an excellent candidate for this electrosynthesis (**89q**). Also, biaryl compounds with more than one substitution were also tested and found successful (**89r**). Electron rich substitution on the phenyl ring decreases the redox potential of the substrate. In addition, it also increases the reactivity towards electron-poor nitrenium ions. This property is reflected clearly in the trend of substrate scope of reaction as well.

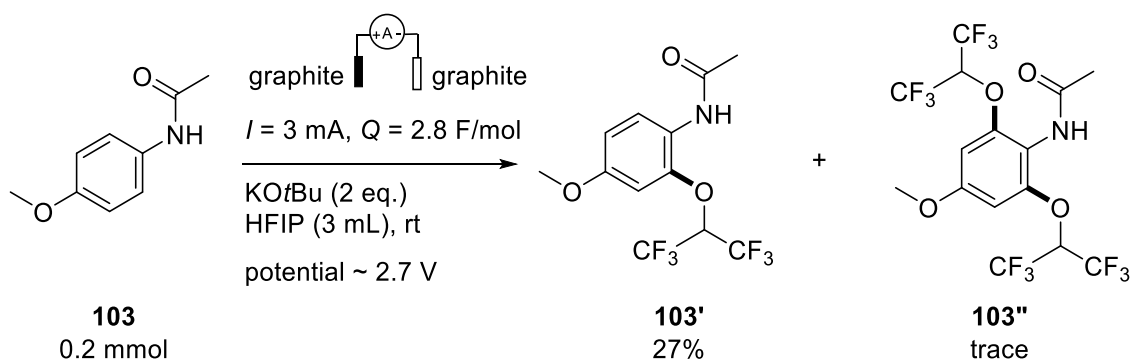
#### 4.2.4 Mechanistic considerations

Considering the pK<sub>a</sub> values of ethoxide ion and 1,1,1,3,3,3-hexafluoroethanol (pK<sub>a</sub> 16 and HFIP 9.3), the added base will react with solvent to form a salt. This salt negates the need of addition of external supporting electrolytes to carry out the electrolysis. This *in situ* electrolyte formation was further confirmed by carrying out the reaction using readily prepared sodium salt of HFIP as supporting electrolyte for the electrolysis (Scheme 4.11).<sup>[123]</sup>

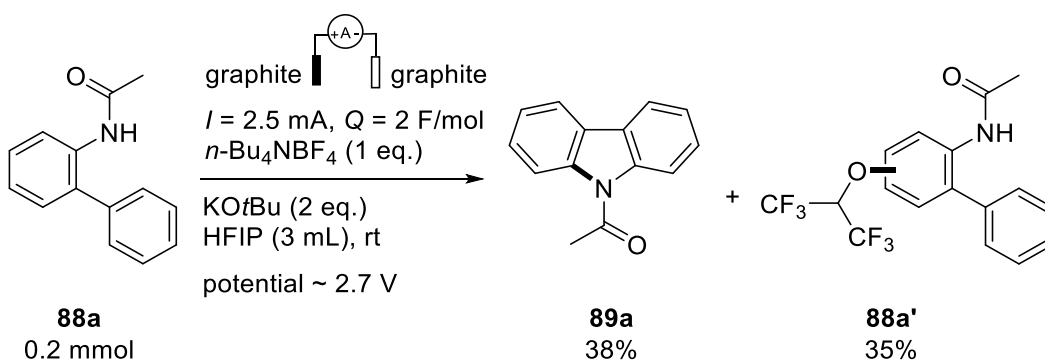


**Scheme 4.11** Sodium salt of HFIP as supporting electrolyte

Also, during the optimization and scope studies, much evidence for the nitrenium ion intermediate were observed. Most important being the consistent formation of HFIP adducts. A control experiment using 4-methoxy acetanilide in HFIP resulted in the formation of mono and di adduct of HFIP with the substrate.<sup>[124]</sup> Furthermore, the product **103'** was isolated and confirmed by NMR studies. The HFIP ether at both the *ortho*- positions of the substrate was also formed in trace amounts (**105**) (Scheme 4.12). Similarly, in case of intramolecular amination using potassium *tert*-butoxide as a base and tetrabutylammonium tetrafluoroborate as an electrolyte, almost 1:1 ratio of cyclized product (**89a**) and HFIP ether (**88a'**) of the biaryl compound was isolated (Scheme 4.13). It has to be noted that single electron transfer pathways for such compounds are not favored. Mostly, the HFIP ethers are formed by the nucleophilic addition reactions which strongly support the formation of nitrenium ions and following resonance structures.



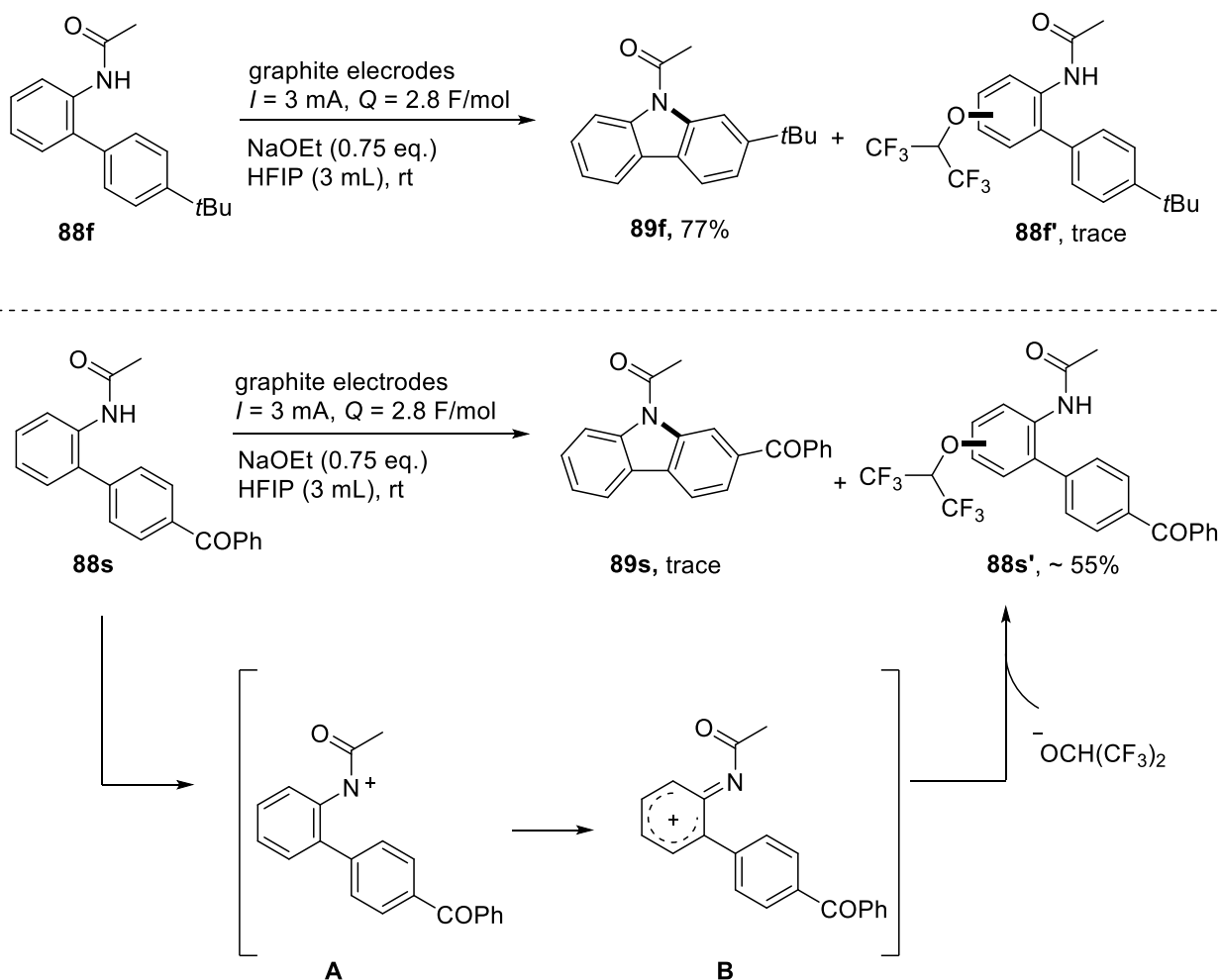
**Scheme 4.12** Mono and di adduct of HFIP with the acetamido substrate



**Scheme 4.13** Cyclized product and HFIP ether of the biaryl compound

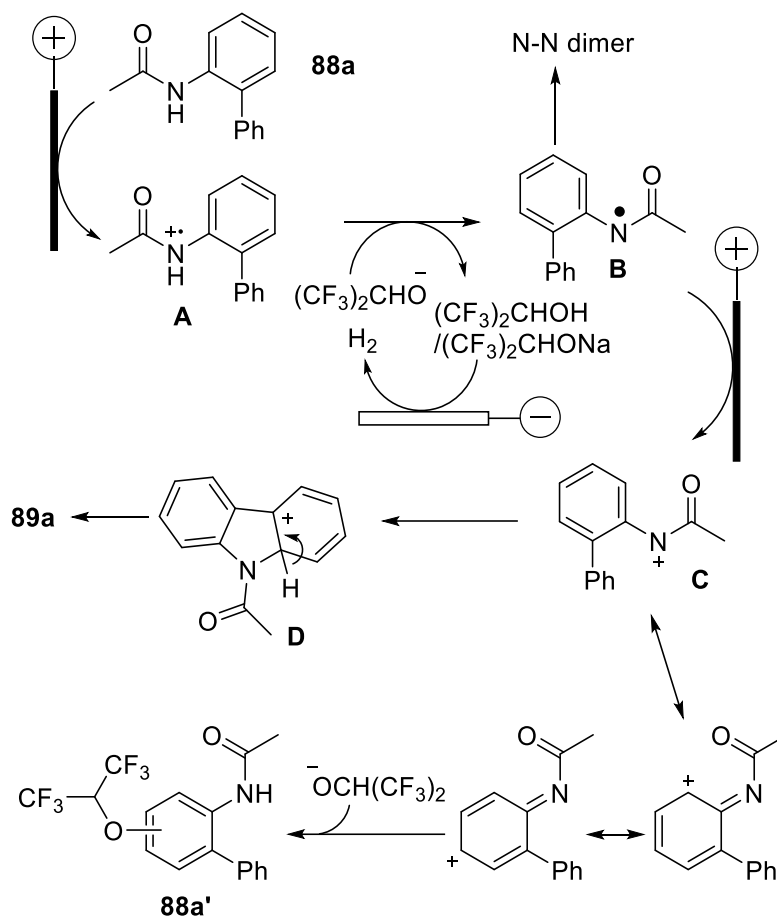
Moreover, electron rich arenes are easy to oxidize as they possess a low oxidation potential. Once the nitrenium ion is formed, they prefer carbazole formation *via* nucleophilic attack. The less

nucleophilic electron deficient arenes with higher oxidation potentials favored HFIP adduct formation (eg.: **88s'**) *via* positive charge delocalization. This indicates a strong dependence on the nature of substitution on aryl rings (Scheme 4.14). Afterwards, cyclic voltammetric studies were carried out to get more insights into the reaction mechanism. In the voltammogram of compound **88a** two distinct oxidation peaks are not visible (Figure 4.1). However, depending on the compounds and substitution pattern, the  $E_{ox,1}$  peak and  $E_{ox,2}$  can overlap with the current at the potential limit. The characteristic properties of the solvent 1,1,1,3,3,3-hexafluoroisopropanol (HFIP) play an important



**Scheme 4.14** Reaction pathway dependence on electron rich and poor substituents

role in this electrolysis. The ability to stabilize the charged intermediate, acidity to generate *in situ* electrolyte and an observed reduction of onset potential (1.45 V) are some of the important aspects to consider.<sup>[125]</sup>



**Scheme 4.15** Plausible mechanism of the reaction

Based on the control experiments and observations made during reaction development, a plausible mechanism has been outlined in the following scheme. A speculation was made considering the pKa values of involved chemicals. It suggests that a direct proton abstraction of amidyl nitrogen is possible only with a stronger base. However, the sodium ethoxide used here in the reaction mixture is small in quantity which would eventually form the salt with acidic solvent hexafluoroisopropanol. Also, the anion of solvent cannot directly abstract a proton from the substrate. For these reasons, it has to be believed that the reaction starts with an oxidation of 2-amidoaryl substrate at anode resulting in the formation of a cation radical **A**. This cation radical however is highly acidic in nature. The oxyanion of solvent then abstracts the proton to generate the highly reactive *N*-acyl radical intermediate **B**. Which actually can undergo homodimerization as observed in the initial screening reactions or would eventually undergo a second oxidation to



generate the key nitrenium ion intermediate **C**. A nucleophilic attack of the aryl ring to nitrenium ion to form **D** and following aromatization step provide the desired carbazole derivative **89a**. Another possibility is that the resonance of the positive charge results in a Wheland intermediate and form adduct **88a'** with hexafluoroisopropanol anion.

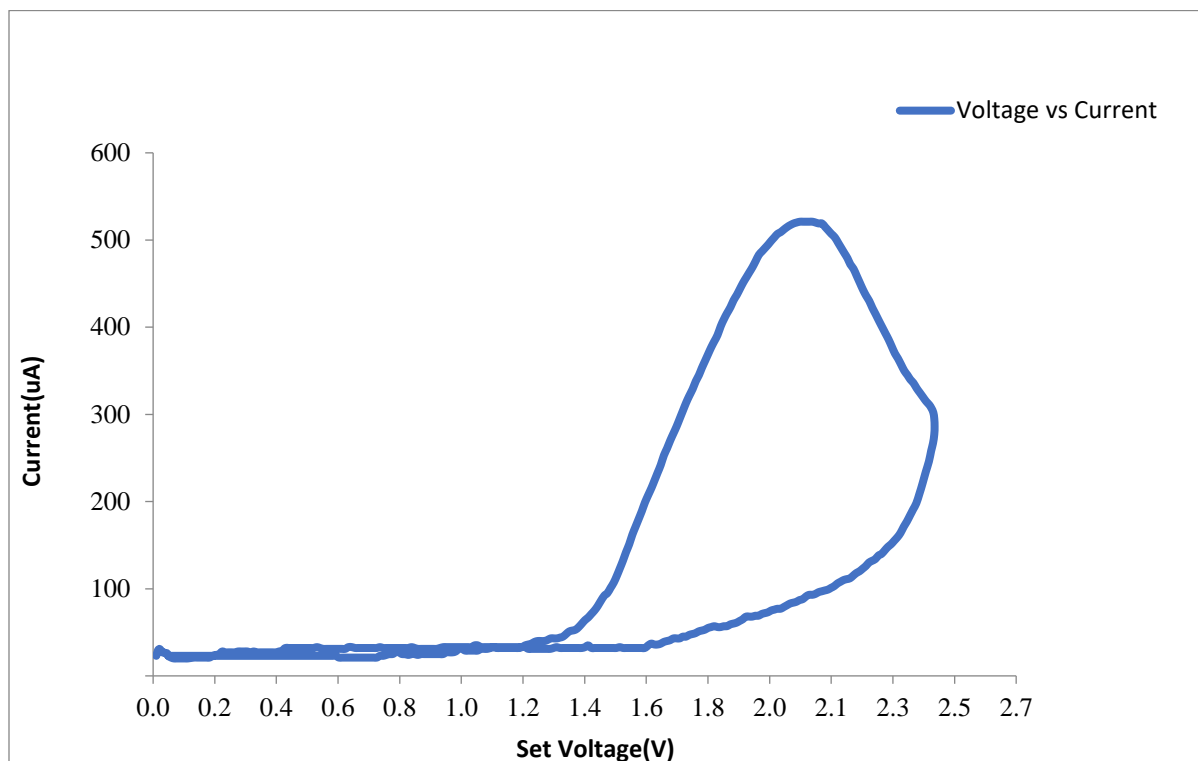


**Figure 4.1.** Cyclic voltammograms of **88a** (1 mM) and 0.75 equiv. NaOEt (21% solution in EtOH) in HFIP (3 mL) using supporting electrolyte *n*-Bu<sub>4</sub>NBF<sub>4</sub> (0.1 M). WE, Glassy Carbon; CE, Platinum plated electrode; RE; Ag/AgCl in 3 M aqueous KCl. Scan rate = 200 mV/S. X-axis, voltage (V); Y-axis, current (μA).

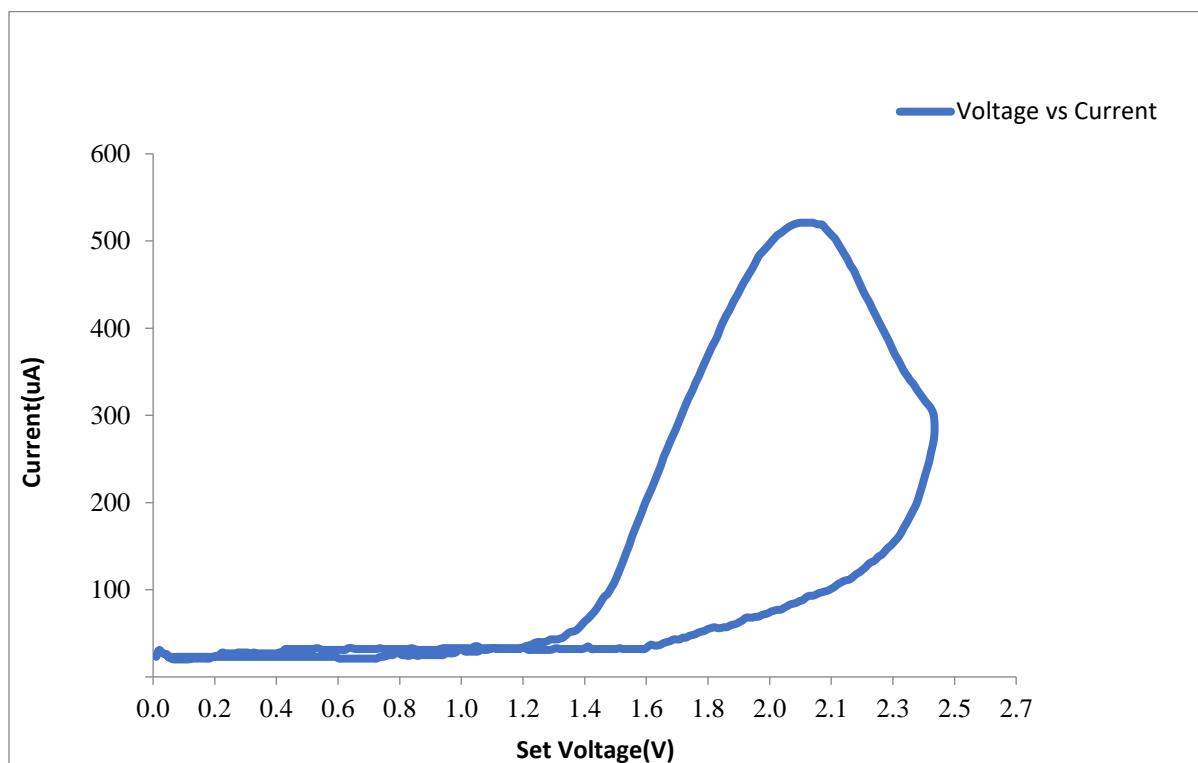
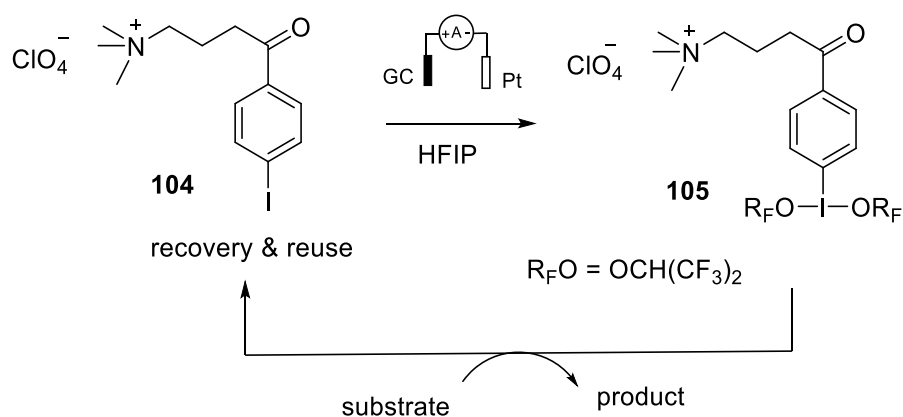


**Figure S3.** Cyclic voltammograms of **88a** (1 mM) and 0.75 equiv. NaOEt (21% solution in EtOH) in HFIP (3 mL) using supporting electrolyte *n*-Bu<sub>4</sub>NBF<sub>4</sub> (0.1 M). WE, Glassy Carbon; CE, Platinum plated electrode; RE; Ag/AgCl in 3 M aqueous KCl. Scan rate = 200 mV/S. X-axis, voltage (V); Y-axis, current (μA).

## 4.3 Intermolecular amination

### 4.3.1 Motivation and objectives

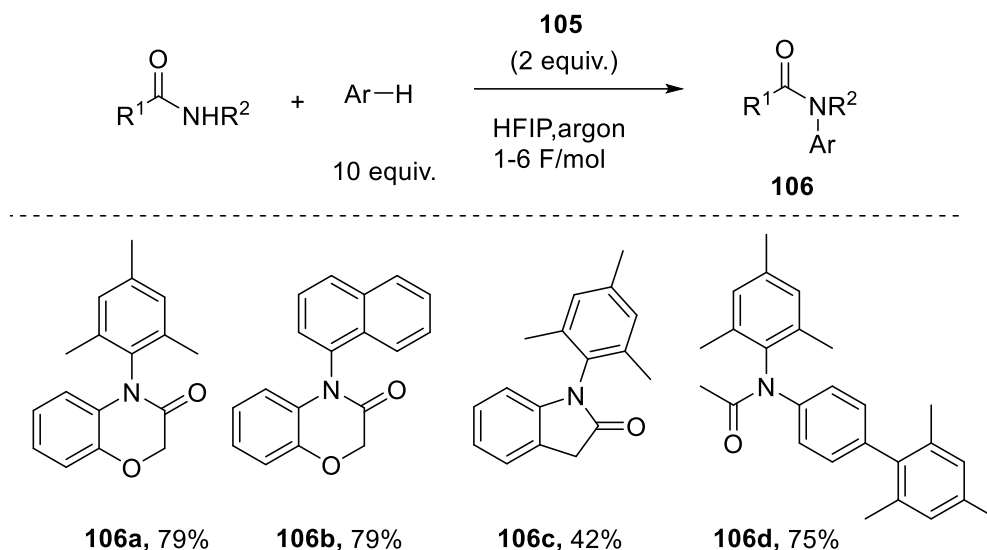
Direct amination of unactivated C–H bonds under electrochemical conditions is an appealing strategy to obtain *N*-arylated compounds in a sustainable manner. Francke and coworkers first reported a redox mediator mediated methodology towards this research. An interesting iodine-based mediator was designed and synthesized for this purpose with the characteristics of recyclability and reusability (Scheme 4.16). The iodine precursor **104** was also linked with an alkyl chain constituting a supporting electrolyte at the *para* position of the phenyl ring. The benzylic position was protected from oxidation by equipping a carbonyl group there. In this indirect electrosynthesis, the iodine(I) mediator was electrochemically oxidized to the active iodine(III) reagent **105** in HFIP (Scheme 4.16). Afterwards an excess of arene coupling partner along with the acetanilide derivatives were added to the pre-electrolyzed solution. This enabled the C–N coupling reaction between the coupling partners. After the reaction the mediator-salt is readily recovered and can be reused. Based on this appealing strategy, various *N*-heterocycles and acetanilide derivatives were arylated successfully (Scheme 4.17).<sup>[115]</sup>



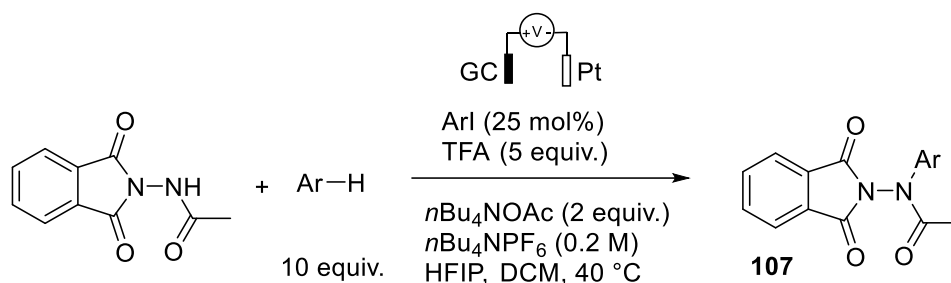
**Scheme 4.16** Indirect electrolysis using a recyclable mediator

Very recently, Powers *et al* came up with another method which enabled the catalytic use of iodine(I) reagent. In this redox mediated electrolysis, the iodine(I)/iodine(III) redox process was continuous over the whole reaction time by electrochemically reactivating the iodine(I) precursor. However, the reaction uses an undesired amount of two different electrolytes and 5 equivalents of acid additives under constant potential conditions (4.18).<sup>[117]</sup> A direct electrolytic approach similar

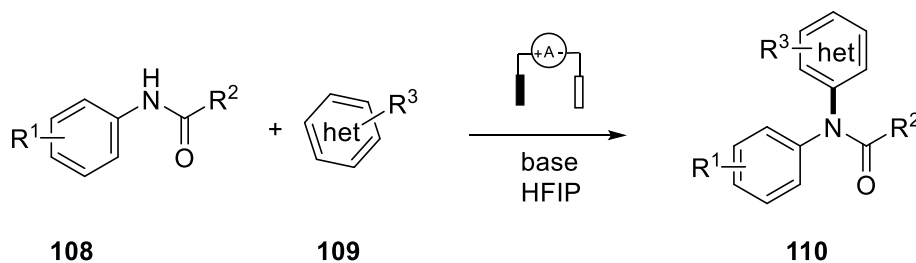
to aforementioned intramolecular amination methodology might drastically simplify the reaction conditions and improve the green characteristics. For these reasons, a constant current electrolytic cross-amination of arenes with in situ generated electrolyte using an easily available and simple inorganic base would be highly appealing (Scheme 4.19).



**Scheme 4.17** Indirect electrolysis for C–H amination of arenes



**Scheme 4.18** Hypervalent iodine catalyzed electrochemical amination

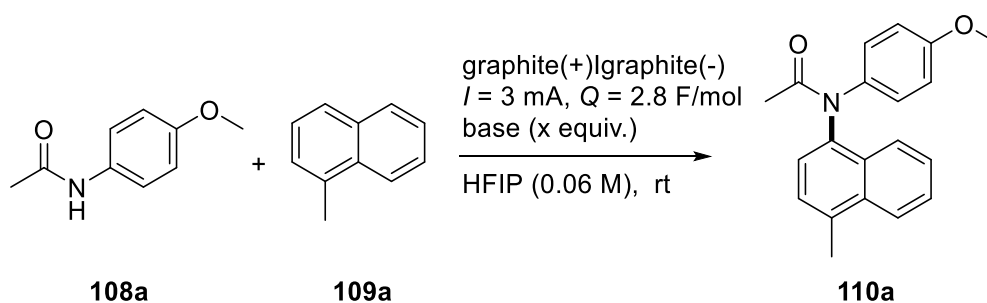


**Scheme 4.19** Proposed strategy for direct electrolytic intermolecular amination

### 4.3.2 Initial results and optimization

*N*-(4-methoxyphenyl)acetamide (**108a**) and 1-methylnaphthalene (**109a**) were initially tested under electrochemical conditions (Table 4.2). As for the intramolecular amination part, potassium *tert*-butoxide was first used as the base for this arylation of acetanilide substrate. Interestingly, a constant current electrolysis using graphite electrodes in hexafluoroisopropanol as solvent successfully cross-aminated the 1-methylnaphthalene in excellent yields (entry 1). So, the focus was given to reduce the amount of coupling partners for this reaction (entry 2). Indeed, 2 equivalents of aryl coupling partner was sufficient to react with acetanilide and provide the product **110a** in excellent yield of 92% (entry 3). Decreased amount of base had a slight impact on the reaction performance. Other bases and an electrolyte were also effective in this intermolecular coupling reaction even though with slightly lower efficiency (entry 4-6).

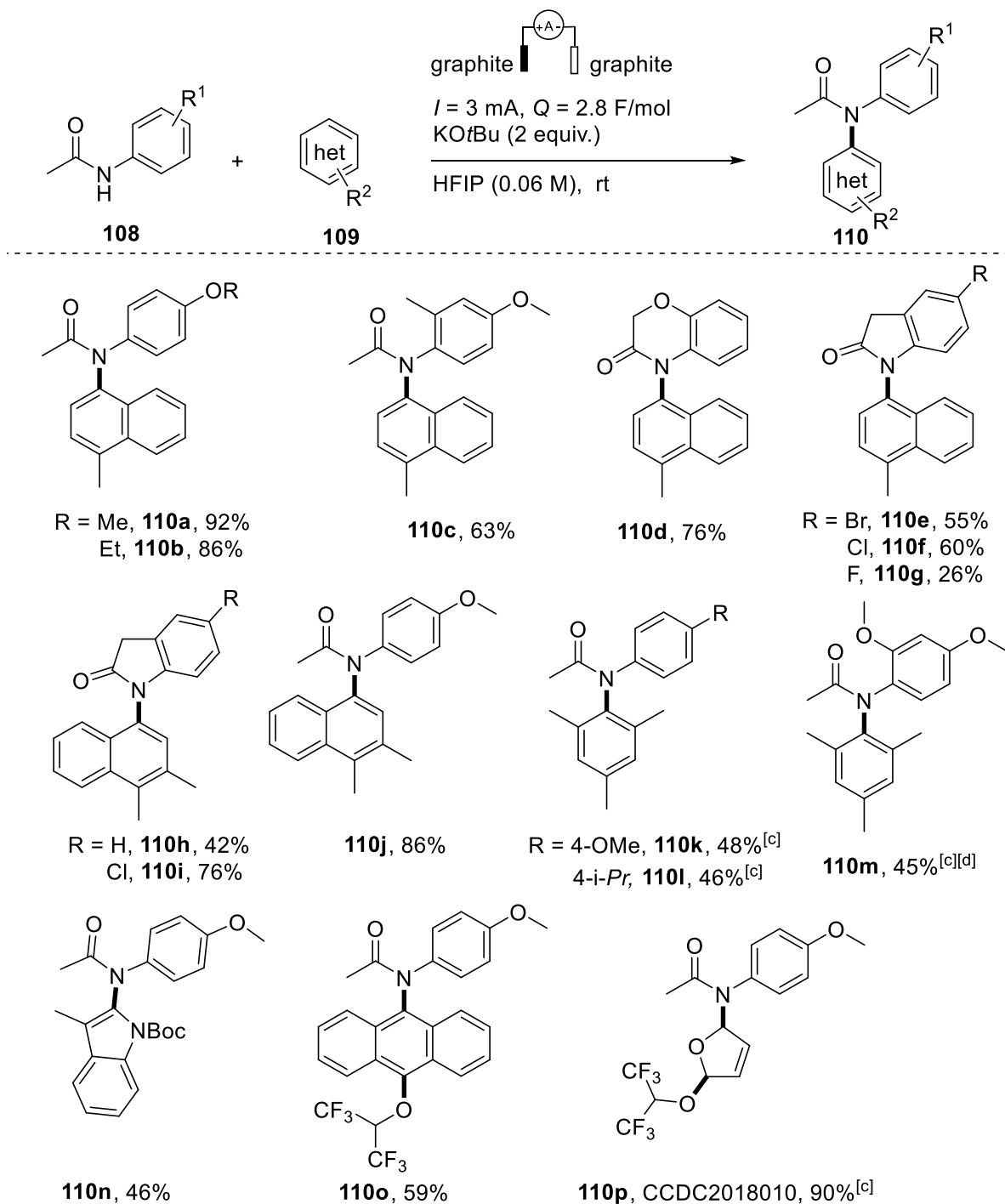
**Table 4.2** Representative conditions of the optimization for the cross-coupling.<sup>[a]</sup>



Entry	<b>109a</b> (equiv.)	Base (equiv.)	Yield <sup>[b]</sup> (%)
1	5	KOtBu (2)	90
2	2	<b>KOtBu (2)</b>	<b>92</b>
3	2	KOtBu (1)	88
4	2	NaOEt (2)	90
5	2	Et <sub>3</sub> N (2)	86
6 <sup>[c]</sup>	2	-	88

<sup>[a]</sup>Reaction conditions: constant current electrolysis (3 mA) until 2.8 F/mol charge was passed using graphite electrodes: **3a** (0.2 mmol), solvent (0.06 M, 3 mL) <sup>[b]</sup>Isolated yield. <sup>[c]</sup>*n*-Bu<sub>4</sub>NBF<sub>4</sub> (0.2 mmol, 1 equiv.) as supporting electrolyte. rt = room temperature.

### 4.3.3 Scope of intermolecular amination



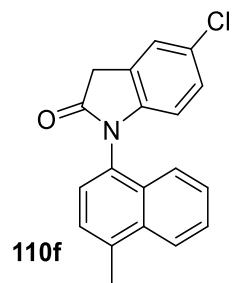
**Scheme 4.20** Substrate scope of intermolecular amination.<sup>[a][b]</sup> [a] Reaction conditions: constant current electrolysis ( $I = 3 \text{ mA}$ ) until 2.8 F/mol charge ( $Q$ ) was passed using graphite electrodes for ~ 5 h: **3** (0.2 mmol), **4** (0.4 mmol, 2 equiv.), potassium *tert*-butoxide (0.4 mmol, 2 equiv.), HFIP (0.06 M, 3 mL).<sup>[b]</sup> Isolated yield. <sup>[c]</sup> 5 equiv. of arene was used as coupling partner. <sup>[d]</sup> 1:1 DCM: HFIP (3 mL).

The optimized reaction conditions were then applied for the arylation and heteroarylation of numerous compounds (Scheme 4.20). Various *N*-phenylacetamide containing substitution at *para*-position undergo cross coupling reactions with 1-methylnaphthalene **109a** to give the corresponding products in moderate to excellent yields (**110a- 110c**). Heterocyclic compound benzoxazinone (**108d**) was also found to be a suitable coupling partner for the electrochemical arylation of *N*-containing compounds. In addition, oxindole derivatives such as 5-bromo, 5-chloro and 5-fluoro oxindole reacted with 1-methyl and 1,2-dimethylnaphthalene coupling partners under constant current electrolysis to yield products **110e-110i**. The yields of these products were also very good. Other arene and hetero(arene) coupling partners also partook in our electro-oxidative cross-amination method. However, in case of mesitylene as arylation partner, an excess of this partner was necessary to get decent yield. Similarly, conditions were slightly modified for arylation of substrate with 2,4-dimethoxy functionality (**110k-110m**). C<sub>2</sub>-arylation of *N*-Boc protected 3-methylindole was also achieved under standard conditions to give **110n**. Surprisingly, the electrochemical amination reaction of a polyaromatic ring containing anthracene resulted in the simultaneous formation of C–N and C–O bonds as a result of amination plus HFIP ether formation (**110o**). When furan was used as a partner for heteroarylation of acetanilide, an unprecedented dual C–H functionalization resulted in the formation of compound **110p**.

#### 4.3.4 Identification of biological activity

Compound libraries of electrochemical C–H amination were submitted to COMAS (Compound Management and Screening Centre) in Dortmund to screen for the biological activities. Cell-based assays to screen for autophagy inhibitory activity and hedgehog signaling pathway inhibition were carried out. After screening, the compound was identified as an autophagy inhibitor at low micromolar concentration.

Furthermore, the phenotypic screening of compounds was also carried out using cell painting assay. From the library, 2 compounds were reported to have significant biosimilarity to reference compounds. But in most of the cases the frequency of hits for these similar compounds is high. For instance, acetanilide compound had a similarity of 94.2 with a RNA polymerase inhibitor Dasabuvir. But the frequency percentage was as high as 3.45%. Also, lowering the concentration to 10  $\mu$ M leads to loss of activity.



Autophagy IC<sub>50</sub> = 4.01 μM

RAPA IC<sub>50</sub> = inactive

**Table 4.3** Representative results of cell painting assay

Compound	Conc. [μM]	Activity	Induction [%]	Highest sim. to a ref. [%]	Toxic
<b>110f</b>	50	active	52.5	81.7	No
<b>110f</b>	30	active	21.9	74.6	No
<b>110f</b>	10	inactive			No
<b>110c</b>	30	active	49.7	94.9	No
<b>110c</b>	10	inactive			No



**Synthesis of Bioactive Compounds *via* C–H Amination**

---

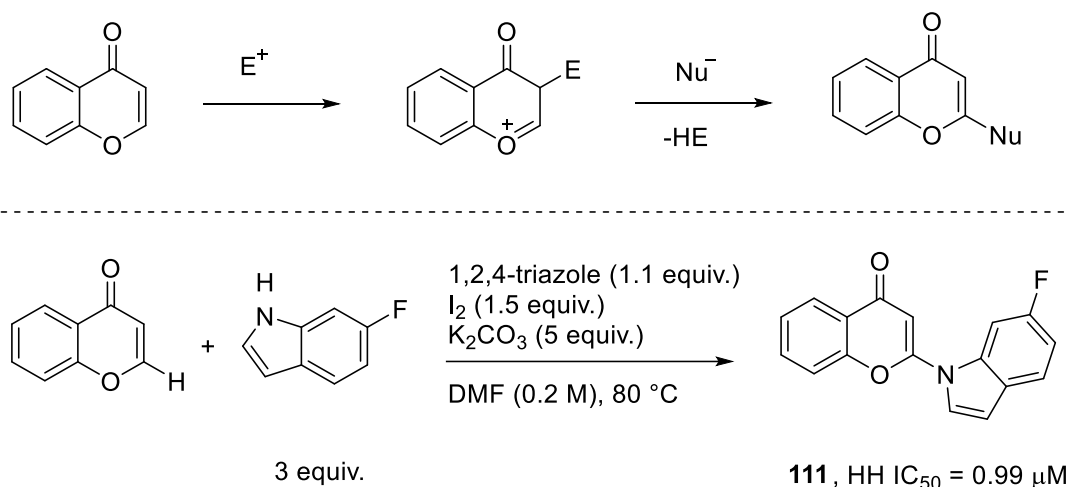


## 5 Synthesis of Bioactive Compounds *via* C-H Amination

### 5.1 Introduction

Inert C–H bond functionalization chemistry enables easy access to highly functionalized heterocyclic compounds. This in fact provides an opportunity to evaluate the biological properties of previously unknown chemical structures. This is an additional advantage of C–H bond functionalization chemistry. A novel methodology can supply solutions to synthetic chemistry challenges and additionally when the obtained novel chemical compound, when studied might possess interesting biological activities. That resembles a research at the interface of organic chemistry and biology, while the approach is purely chemistry driven. One such example was reported by Antonchick and co-workers in 2015.<sup>[126]</sup> The authors developed a novel regioselective amination method for chromones using azoles as the cross-coupling partner (Scheme 5.1). Afterwards, the compounds were evaluated for their bioactivities and found that these novel compounds are potent hedgehog signaling pathway inhibitors (HH inhibitors). Small molecule HH inhibitors are particularly important because of their role as potential anticancer agents. Mutations in the HH signaling pathway have been identified as causes of cancers such as basal cell carcinoma and medulloblastoma.<sup>[127]</sup>

**working hypothesis:**



**Scheme 5.1** Hedgehog signaling pathway inhibitors *via* C–H amination

Interestingly, the HH signaling pathway has close association with other biological signals like that of bone morphogenetic proteins (BMPs). Small molecule bone morphogenetic protein (BMP)

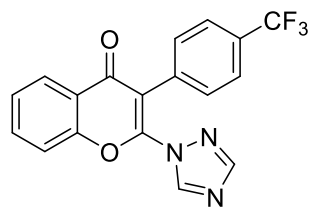
activators are also an important class of compounds in chemical biology and medicinal chemistry.

## 5.2 Identification of a novel osteogenic BMP activator chemotype

Bone Morphogenetic Proteins (BMPs) are a group of signalling molecules belonging to the Transforming Growth Factor- $\beta$  (TGF $\beta$ ) superfamily. They have crucial roles in various organ systems of the body such as in embryogenesis, adult tissue homeostasis and regeneration. BMPs help to differentiate mesenchymal stem cells to bone. So BMPs play a central role in bone and cartilage formation. Additionally, many processes in early development such as cell growth, apoptosis and cell differentiation are highly dependent on the BMP signaling pathway. BMPs have diverse functions in almost all organ systems and are known to be regulators throughout the body. Deficiency of these proteins have marked effects in various biological systems such as neurological, cardiovascular, skeletal system, etc.<sup>[128]</sup>

Because of their prominent role in osteogenesis, BMPs and small molecule activators of BMPs are highly relevant for the treatment of skeletal trauma and osteopenic diseases. The available treatments of difficult fractures are based on recombinant proteins. But they are costly and have various adverse effects mainly because of their 10,000-fold beyond doses when compared to physiological concentrations. Small molecules that can activate BMP signaling are highly desirable. BMP activator modalities have various applications in biotechnology, chemical biology and regenerative medicine. However, the discovery and development of such small molecule growth factor/cytokine activators is intrinsically challenging. In this regard, Schade *et al.* devised a physiological, morphogenic cellular screening system that is focused on the BMP pathway for the discovery of novel BMP activators. Using this stem cell-based screening method, almost 7000 compounds were screened for their bone morphogenetic activation abilities. These efforts furnished 4*H*-chromen-4-ones as a novel osteogenic BMP activator chemotype that potentiated BMP signaling outputs.

Interestingly this compound belongs to the compound library of previously reported HH inhibitor chemotype synthesized *via*. C–H bond amination. This is not surprising considering the close association between hedgehog signaling pathways and BMP signaling pathways. Based on this result, other similar compounds were also tested as potential activators of BMPs.

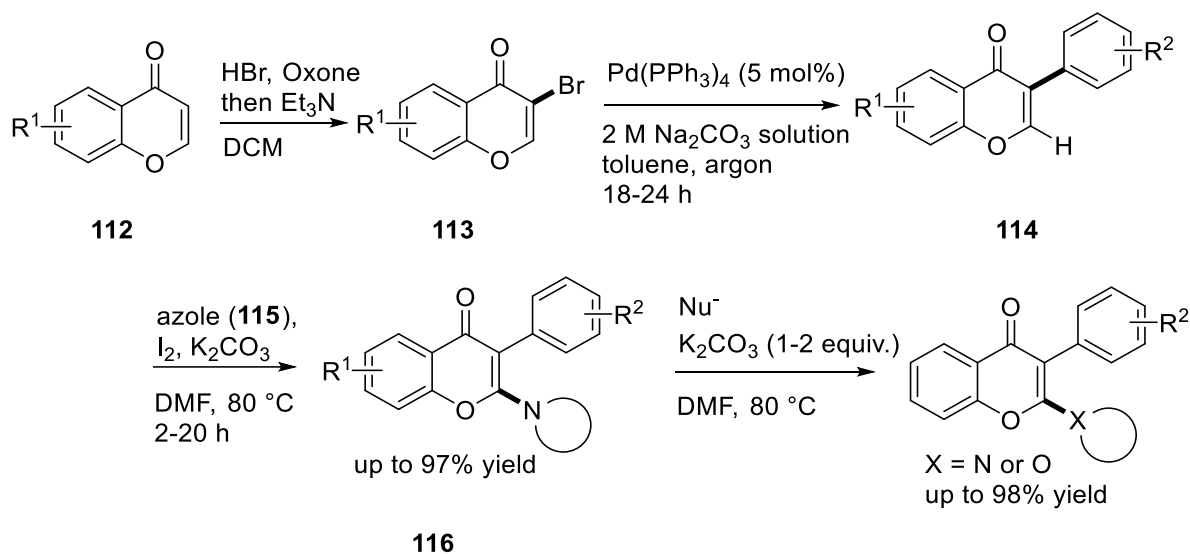


**116a**

$IC_{50}$  mESC =  $0.2 \pm 0.08$   $\mu$ M

### 5.3 Design, synthesis and biological evaluation of chromone derivatives

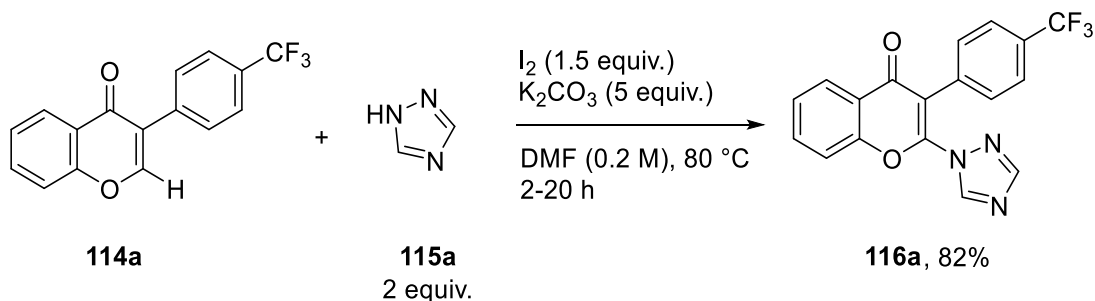
For the structure activity relationship studies, previously reported compounds as well as novel analogues were also evaluated. The synthetic route for the compounds is outlined in the following scheme. At first, the C<sub>3</sub> position of chromone **112** was brominated using hydrobromic acid, in presence of Oxone and triethylamine as base. This was followed by a palladium catalyzed cross-coupling with aryl halide to obtain the C<sub>3</sub>-arylated derivatives **114**. The key C–H functionalization at C<sub>2</sub>-position using corresponding azoles provided the required compounds **116** for biological studies. Additionally, the triazole ring at C<sub>2</sub>-position was replaced with stronger nucleophiles to obtain more structurally diverse analogues (Scheme 5.2).



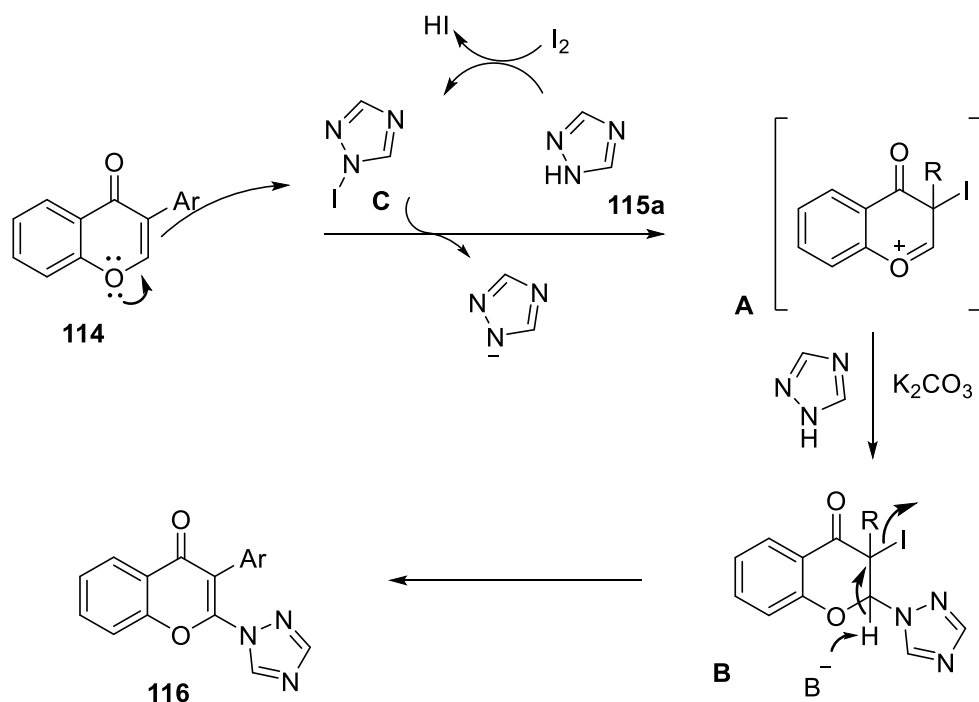
**Scheme 5.2** Synthetic route for bioactive chromones

The BMP hit chromenone (2-(1*H*-1,2,4-triazol-1-yl)-3-(4-(trifluoromethyl)phenyl)-4*H*-chromen-4-one) **116a** was prepared on a higher scale to produce the compound in sufficient quantity for

various biological assays and *in vivo* studies. The key amination step was carried out using potassium carbonate as base in presence of 1.5 equivalents of molecular iodine. Reaction with 1 mmol scale of chromone starting material yielded 82% of required compound **116a** (Scheme 5.3). With respect to the mechanism of this amination method, initially molecular iodine reacts with triazole **115a** to form an electrophilic iodine reagent **C**. Reaction between isoflavone and this reagent results in an oxonium ion intermediate **A**. Following nucleophilic substitution and dehydroiodination mediated by base results in the formation of product **116** (Scheme 5.4).

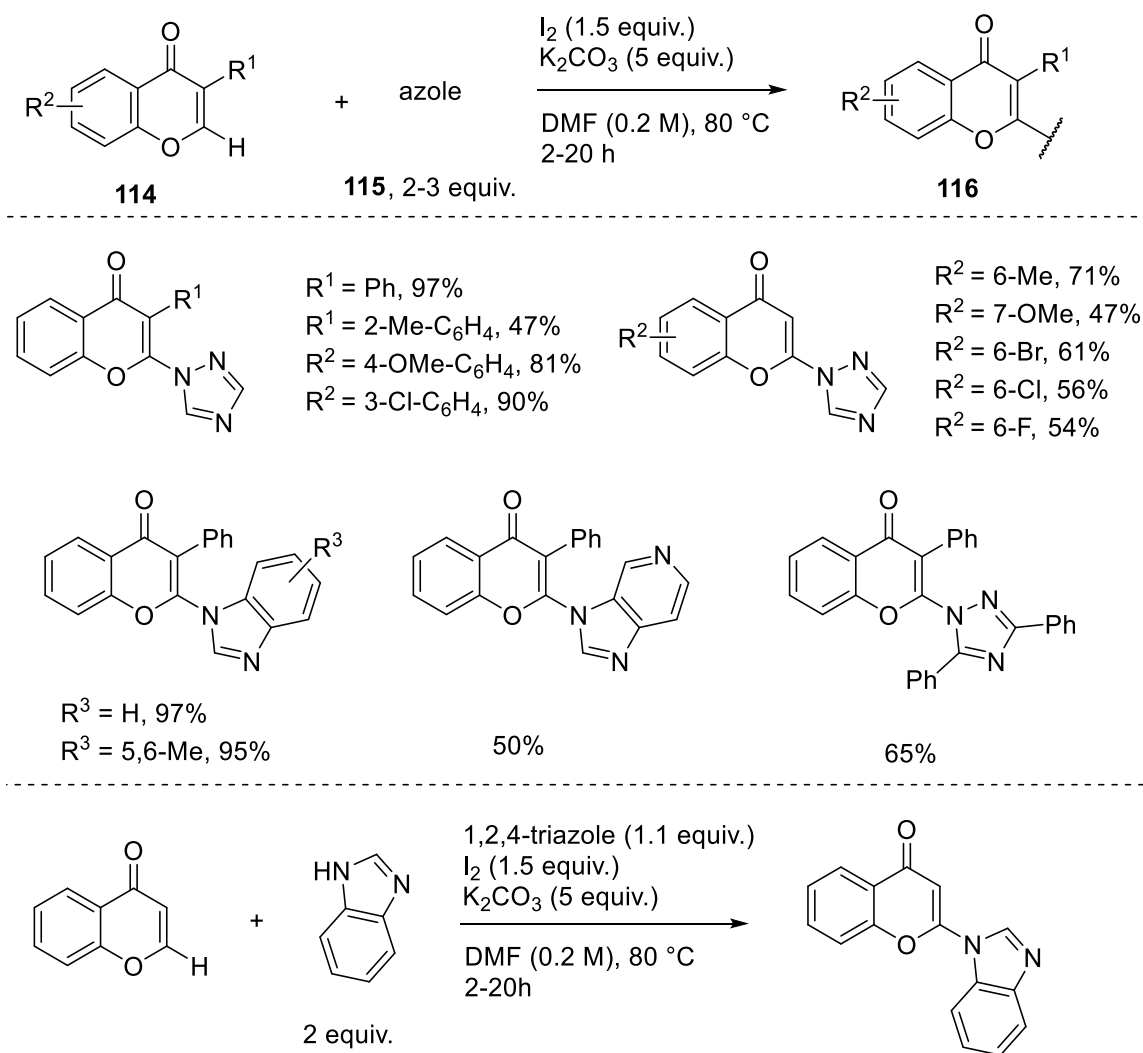


**Scheme 5.3** Scale-up synthesis of bioactive chromone **115a**



**Scheme 5.4** Mechanistic considerations of key C–H amination step

Following the same protocol, a number of analogues were also prepared previously by Antonchick *et al.* The general strategy for the cross-coupling is based on the cross-coupling reaction of various substituted and unsubstituted chromones with different types of azoles in presence of molecular iodine and a base.<sup>[126]</sup> In some cases, however, 1,2,4-triazole is used in addition to azole in excess quantities. Also, azole was replaced with more stronger nucleophiles by heating with a base to obtain more structurally diverse analogues. Some of these analogues were resynthesized whenever it was necessary to do so (Scheme 5.5).



**Scheme 5.5** Previously known analogues of chromones for resynthesis

Schade *et al.* conducted various biological experiments and fully validated chromone **116a** as a novel osteogenic BMP activator chemotype (Figure 5.1). Based on these encouraging results,

novel chromones mainly focusing on the 2- and 3-positions of the 4*H*-chromen-4-one scaffold were designed and synthesized as potential chemical biology tools for BMP signaling.

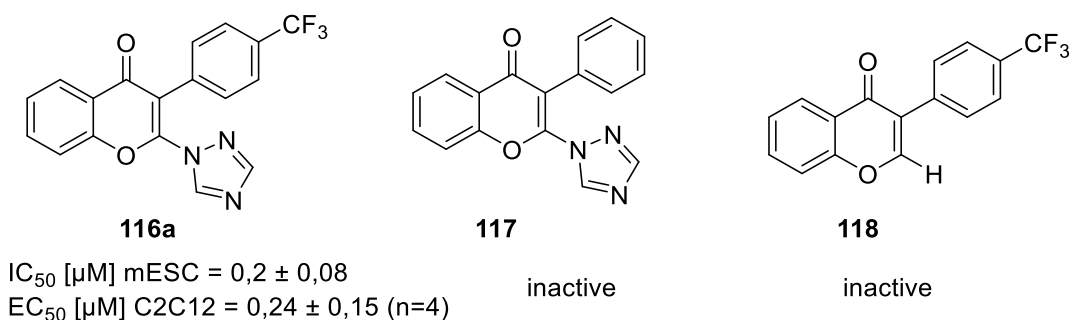
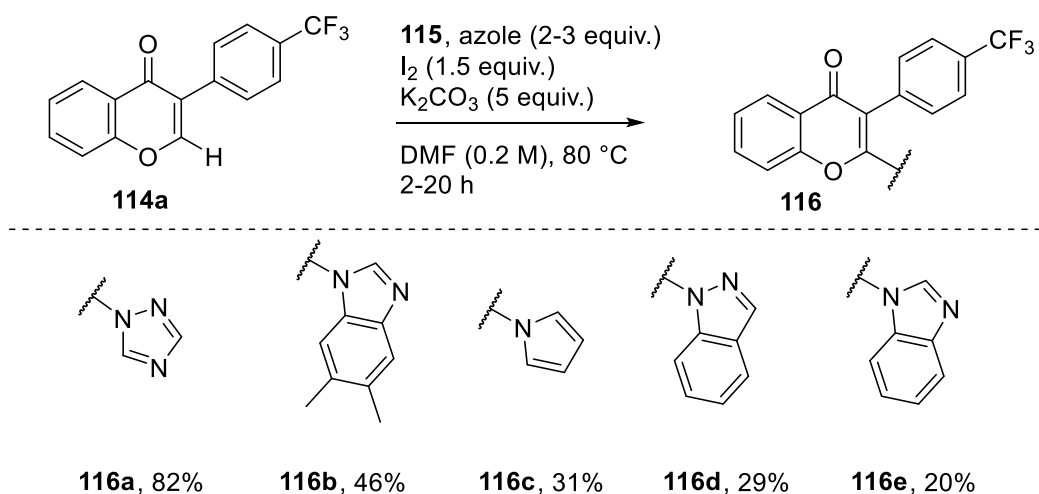


**Figure 5.1** Novel BMP activator analogue and closely related analogues

A total of 29 derivatives including newly synthesized analogues were profiled in the BMP-dependent morphogenic assays (Scheme 5.7 and Scheme 5.8). The data showed that the 3-substituent was quite essential for activity. Compounds containing no substituent at C2-position were inactive. Another analogue which has no *p*-trifluoromethyl moiety on the phenyl ring at C2-position was rendered inactive as well. Other similar compounds screened were also inactive, including compounds such as 4-methoxy phenyl, 3-chlorophenyl or 2-toluyyl chromones.

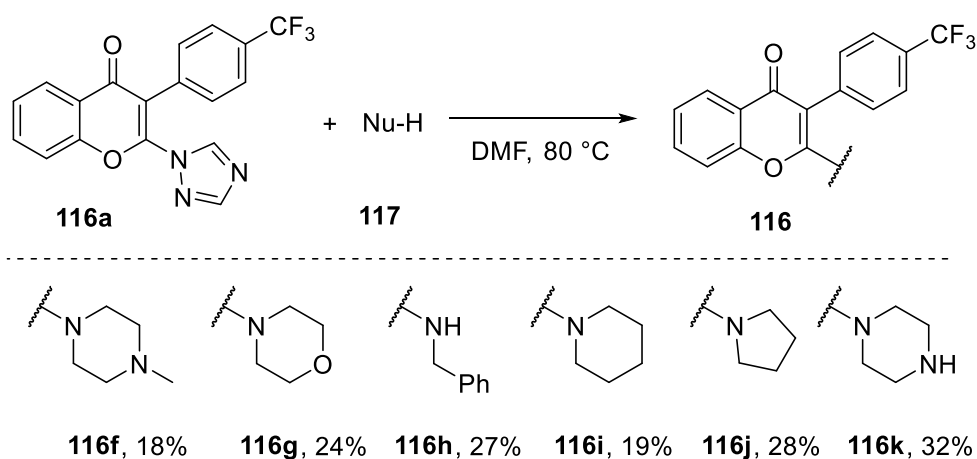


**Scheme 5.7** Synthesis of novel analogues *via* direct C–H amination

The 2-position also did not tolerate many alterations as the 2-(1,2,4-triazolyl) substituent turned out essential for robust biological activities and could only be replaced by a pyrrole substituent (**116c**), albeit with lower potency for this derivative. After that, other derivatives containing cyclic



aliphatic substituents containing nitrogen were also tested in addition to other big heterocyclic compounds (**116f-k**). Additional combinations that included variations in the six- and seven-position also did not furnish novel BMP activator characteristics. Although a vast number of derivatives were not tested, it was obvious that a small heteroaromatic triazole ring at C<sub>2</sub>-position and a *para* electron withdrawing group containing phenyl ring at C<sub>3</sub>- position were the most important pharmacophoric features. The other closely related chromones without these substitutions at respective positions would serve as important inactive probes for chemical biology applications. These compounds were evaluated in the human cells to understand their biological properties in the context of osteogenesis. Indeed, Chromone **116a**, but not its inactive analogues, efficiently enhanced BMP-4-induced mineralization of human SaoS-2 cells at a dose of 25 nM. Therefore 2,3-disubstituted 4*H*-chromen-4-ones were identified as a new chemotype of BMP potentiators with high potency and efficacy with a unique mode-of-action. This compound (**116a**) induced a pronounced, kinase-independent, negative TGF- $\beta$  feedback that enhanced nuclear BMP-Smad signaling outputs. These results provide novel BMP activators and important inactive chromones as novel chemical biology probes and potential therapeutic options.



**Scheme 5.8** Synthesis of novel analogues *via* nucleophilic substitution



## **Chapter 6**

---

### **Summary**

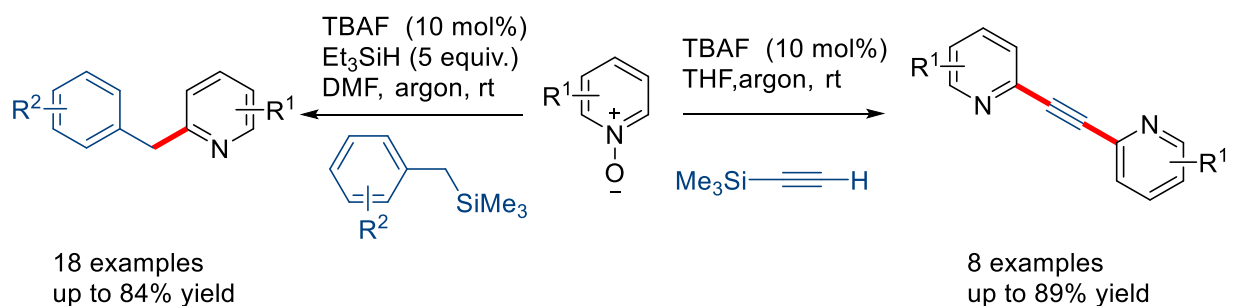
---



## 6 Summary

Development of novel transition metal-free C–H functionalization methods have enabled faster, selective and sustainable organic transformations. These methods are highly relevant when it comes to the direct functionalization of otherwise inert bonds and thereby providing useful solutions to the conventional organic chemistry challenges. Additionally, various oxidative and organocatalytic annulation methods give access to various heterocyclic molecules.

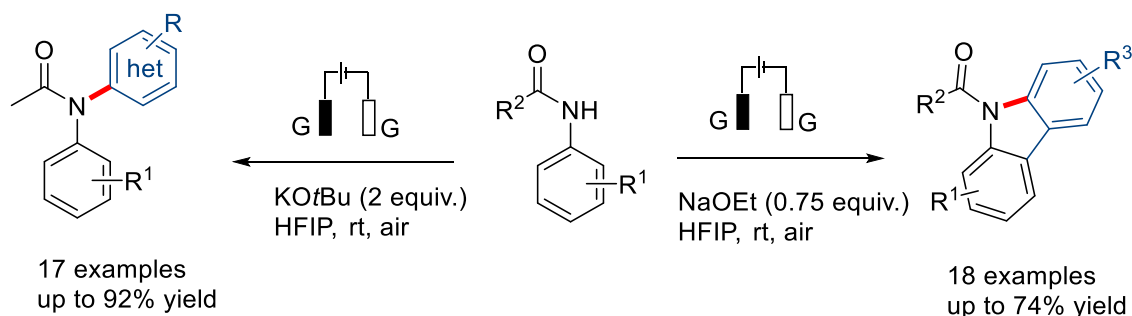
A novel regioselective organocatalytic cross-coupling between heteroaromatic *N*-oxides and organosilanes was developed. The methodology enabled synthesis of benzylated *N*-heterocyclic molecules in a transition metal-free manner. Tetrabutylammonium fluoride was found to be the best fluoride activator of organosilanes and triethylsilane as an additive was proved to be advantageous for the transformation. Scope and mechanistic studies of C–H benzylation reactions were also carried out. Based on these data, a plausible mechanism of the reaction has been proposed. Additionally, the versatility of the developed methodology was demonstrated by extending the method for site-selective deoxygenative C–H alkylation of isoquinoline and quinoline *N*-oxides.



**Scheme 6.1** Regioselective cross-coupling of *N*-oxides and organosilanes

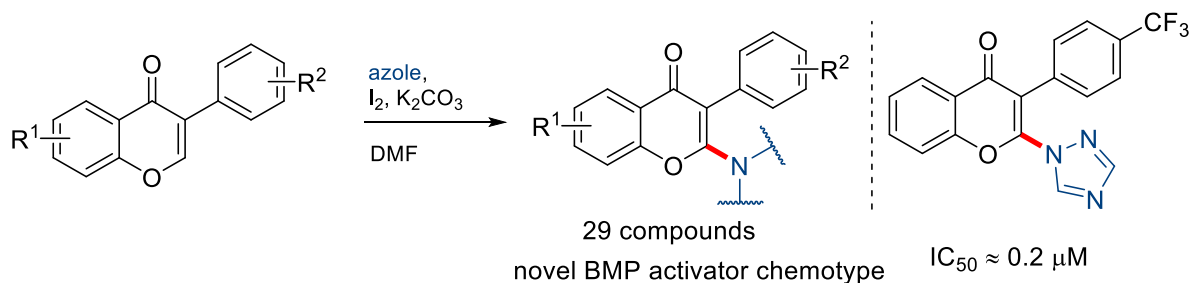
A sustainable electrochemical dehydrogenative C(sp<sup>2</sup>)-H amination involving an electrochemical oxidation-induced nitrenium ion intermediate has been established. The application of electrochemical methods was justified by the metal-free direct electrolytic synthesis of carbazole scaffold as well as direct cross-amination of aromatic and heteroaromatic compounds. The reaction used a simple and easy to use undivided cell. Direct electrolysis using cheap and easily available graphite electrodes provided a straight forward C–H amination method without the use of any expensive transition metals as catalysts or electrodes. Additionally, use of external supporting

electrolyte was not required in presence of added base and an acidic solvent which is HFIP. This is beneficial because the use of stoichiometric amount of external supporting electrolytes results in larger amount of waste from the reaction. Some of the compounds from this compound library were suggested to have some biological effects as well.



**Scheme 6.2** Electrochemical dehydrogenative C(sp<sup>2</sup>)-H amination method

Straight forward synthesis of novel bioactive chromones involving an oxidative C-H bond amination with azoles are also carried out. Based on the biological data of active analogues, novel derivatives are designed, synthesized and evaluated biologically for their potential bone morphogenetic protein activating abilities. Additional chromones lacking key substituents at C<sub>2</sub> and C<sub>3</sub> positions were also prepared as closely related probes for biological applications. A novel 2,3-disubstituted 4*H*-chromen-4-one induced a pronounced, kinase-independent, negative TGF- $\beta$  feedback that enhanced nuclear BMP-Smad signaling outputs.



**Scheme 6.3** Design, Synthesis and biological studies of chromone derivatives

In summary, novel metal-free C-H functionalization methods are developed for accessing biologically relevant heteroatoms containing organic molecules. Also, existing C-H functionalization methodologies are employed for the design and synthesis of known bioactive compounds as well as novel potential bioactive compounds.

---

## **Experimental Part**

---





## 7 Experimental Part

### 7.1 General

#### Reagents and solvents

Commercially available chemicals were purchased from *Sigma-Aldrich*, *Acros Organics*, *Alfa Aesar*, *Fluorochem*, *VWR Germany*, *ABCR* or *TCI Germany*. Unless otherwise noted, all commercially available compounds and solvents were used as provided without any further purification. Dry dichloromethane was purified by the solvent purification system *M-BRAUN SPS-800*. Solvents for chromatography were laboratory grade.

#### Chromatography

Analytical thin-layer chromatography (TLC) was performed on Merck silica gel 60 aluminium plates with F<sub>254</sub> indicator, visualized by irradiation with UV light (254 nm or 365 nm) or staining with KMnO<sub>4</sub>-solution (1.5 g KMnO<sub>4</sub>, 10 g K<sub>2</sub>CO<sub>3</sub>, 1.25 mL 10% NaOH in 150 mL H<sub>2</sub>O) or staining with *para*-anisaldehyde staining solution (5 mL glacial sulfuric acid, 1.5 mL glacial acetic acid and 3.7 mL *para*-anisaldehyde in 135 mL absolute EtOH).

Column chromatography was performed using silica gel Merck 60 (particle size 0.040-0.063 mm). Solvent mixtures are understood as volume/volume.

#### Mass spectrometry

Low resolution mass spectra (MS-EI, 70 eV) were collected using an *Agilent Technologies 7890A GC-System* (column: HP-5MS, 30 m × 0.250 mm × 0.25 μm) equipped with an *Agilent Technologies 5975C inert XL MSD with Triple-Axis Detector*. Otherwise Low-resolution mass spectra (MS-ESI) were collected using a *Agilent 1290 LC-MS system, Rapid resolution HD 2.1x50 mm 1.8 μm column*. High resolution mass spectra were recorded on an *LTQ Orbitrap* mass spectrometer coupled to an *Accela HPLC System* (HPLC column: Hypersyl GOLD, 50 mm × 1 mm, 1.9 μm). 122 Experimental |

#### Nuclear magnetic resonance spectroscopy (NMR)

<sup>1</sup>H-NMR, <sup>19</sup>F NMR, <sup>13</sup>C-NMR and 2D-NMR spectra were recorded on *Bruker DRX400* (400 MHz), *DRX500* (500MHz), *DRX600* (600MHz) and *DRX700* (700 MHz) spectrometers in

CD<sub>2</sub>Cl<sub>2</sub>, CDCl<sub>3</sub>, or (CD<sub>3</sub>)<sub>2</sub>SO. Data are reported in the following order: chemical shift ( $\delta$ ) in ppm; multiplicities are indicated s (singlet), d (doublet), dd (doublet of doublets), t (triplet), q (quartet), hept (heptet), m (multiplet); coupling constants ( $J$ ) are given in Hertz (Hz).

### **Fourier transform infrared spectroscopy**

Fourier transform infrared spectroscopy (FT-IR) spectra were obtained with a *Bruker Tensor 27* spectrometer (ATR, neat) and are reported in terms of frequency of absorption (cm<sup>-1</sup>).

### **Electrochemistry**

Unless otherwise noted, all reactions and cyclic voltametry (CV) studies were carried out in a 5 mL IKA Electrasyn 2.0 single reaction vial or carousel connected to Electrasyn 2.0. All the electrodes (52 x 5 mm) used for reactions and CV were purchased from IKA.

### **Biological Studies**

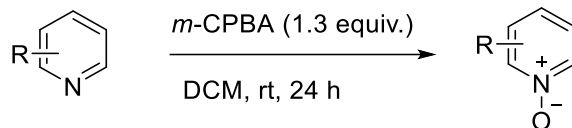
All biological experiments were carried out at the Compound Management and Screening Center (COMAS) in Dortmund or at their collaborator's labs.

## 7.2 Experimental part for the cross-coupling

### 7.2.1 General procedures

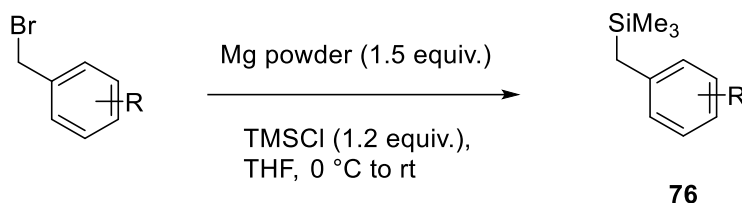
#### Preparation of heteroaromatic *N*-oxides

To a solution of quinoline, isoquinoline or pyridine (1 mmol) in dichloromethane (10 mL), 3-chloroperbenzoic acid (1.3 mmol) was added and the reaction was stirred for 24 h at room temperature. Afterwards, residual 3-chloroperbenzoic acid was removed by adding 1 M KOH solution. The aqueous phase was extracted three times with dichloromethane and the combined organic layers were dried over MgSO<sub>4</sub>. Column chromatography provided the pure product (eluent: DCM - MeOH).<sup>[28]</sup>



#### Preparation benzyltrimethylsilanes

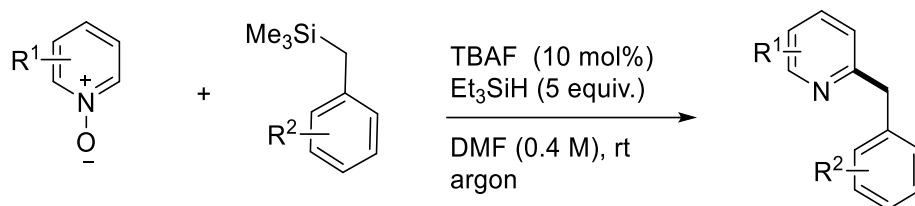
An oven-dried two neck round-bottom flask containing magnesium powder (0.18 g, 7.5 mmol, 1.5 equiv.) a grain of iodine and dry THF (20 mL) was cooled to 0 °C under nitrogen. Then trimethylsilyl chloride (0.6 mL, 1.2 equiv.) was added, followed by the dropwise addition of a solution of the bromide (5.0 mol, 1.0 equiv.) in THF (5 mL) over a period of 15 min. After the addition was completed, the reaction mixture was stirred overnight and poured 10 mL saturated NH<sub>4</sub>Cl. The resulting mixture was extracted with EtOAc (3 x 20 mL), the combined organic layers were washed with brine (20 mL), dried MgSO<sub>4</sub> and concentrated to obtain the residue. The residue was purified by flash column chromatography to give the benzyltrimethylsilanes.<sup>[91]</sup>



#### General procedures A for the benzylation of heteroaromatic *N*-oxides

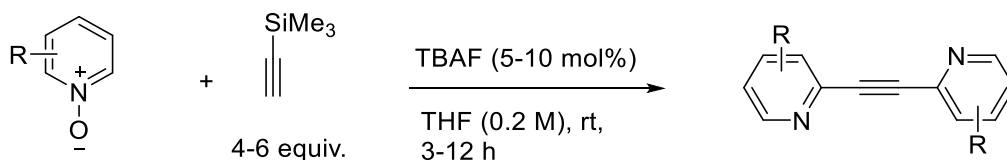
To a solution of *N*-oxide (0.4 mmol) in DMF (1 mL), **2a** (1.20 mmol, 233.15 μL) was added and the reaction vial was flushed with argon. TBAF (10 - 20 mol%, 40 - 80 μL) and Et<sub>3</sub>SiH (only in

case of isoquinoline and quinoline *N*-oxides) (2 mmol, 329.32  $\mu$ L) were added respectively, stirred at room temperature and monitored by TLC. After the complete consumption of *N*-oxide, column chromatography of the reaction mixture provided the pure product (Eluent: Petroleum ether-EtOAc).



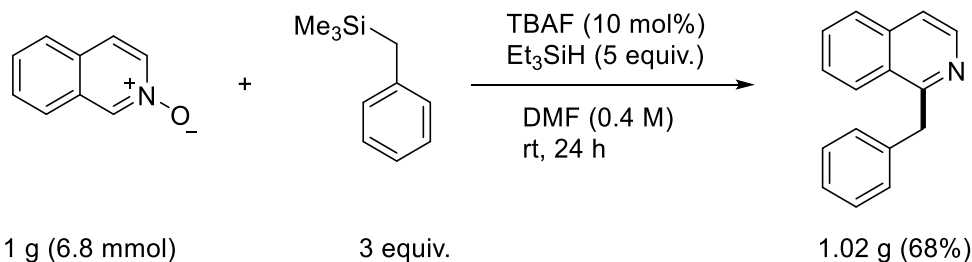
### General procedures B for the alkylation of heteroaromatic *N*-oxides

To a solution of *N*-oxide (0.2 mmol) in THF (1 mL), ethynyltrimethylsilane (0.8 - 1.2 mmol) was added and the reaction tube was flushed with argon, to which TBAF (5 - 10 mol%) was added using a micropipette (acetylene gas evolution might cause strong effervescence) and stirred at room temperature for specified time. Column chromatography provided the pure product (Eluent: DCM-MeOH).

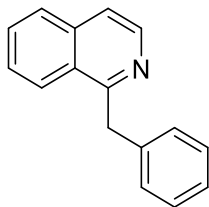


### Procedure for gram-scale C–H bond benzylation of isoquinoline *N*-oxide

To a solution of isoquinoline *N*-oxide (1g, 6.75 mmol) in DMF (17 mL), **2a** (3.9 mL, 20.25 mmol) was added and the reaction vial was flushed with argon. TBAF (10 mol%, 675  $\mu$ L) and Et<sub>3</sub>SiH (5.56 mL, 33.76 mmol) were added respectively, stirred at room temperature and monitored by TLC. After the complete consumption of isoquinoline *N*-oxide, column chromatography of the reaction mixture provided the pure product (Eluent: Petroleum ether-EtOAc = 10:1).

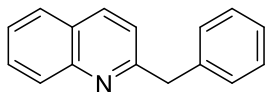


## 7.2.2 Physical data of products



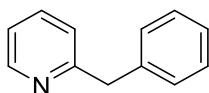
### 1-Benzylisoquinoline (77a)

Prepared according to general procedure A using isoquinoline *N*-oxide (0.4 mmol) and benzyltrimethylsilane (1.2 mmol). The product was isolated as yellow oil (69 mg, 0.31 mmol, 78%) after 24 h;  $R_f = 0.32$  (cyclohexane / ethyl acetate = 5:1);  $^1\text{H NMR}$  (400 MHz,  $\text{CDCl}_3$ )  $\delta$  8.49 (d,  $J = 5.8$  Hz, 1H), 8.13 (dd,  $J = 8.5, 1.1$  Hz, 1H), 7.79 (d,  $J = 8.2$  Hz, 1H), 7.63 – 7.59 (m, 1H), 7.57 – 7.47 (m, 2H), 7.29 – 7.20 (m, 4H), 7.18 – 7.11 (m, 1H), 4.67 ppm (s, 2H);  $^{13}\text{C NMR}$  (126 MHz,  $\text{CDCl}_3$ )  $\delta$  160.1, 141.8, 139.3, 136.6, 129.9, 128.6, 128.5, 127.3, 127.2, 127.2, 126.2, 125.8, 119.9, 41.9 ppm; **FT-IR**:  $\tilde{\nu} = 3027, 2959, 1673, 1560, 1385, 1153, 1002$   $\text{cm}^{-1}$ ; **HR-MS**: calc. for  $[\text{M}+\text{H}]^+$   $\text{C}_{16}\text{H}_{14}\text{N} = 220.1121$  found: 220.1120.



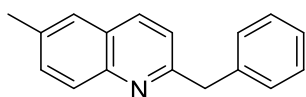
### 2-Benzylquinoline (77b)

Prepared according to general procedure A using quinoline *N*-oxide (0.4 mmol) and benzyltrimethylsilane (1.2 mmol). The product was isolated as yellow oil (69.5 mg, 0.31 mmol, 79%) after 1 h;  $R_f = 0.28$  (cyclohexane / ethyl acetate = 5:1);  $^1\text{H NMR}$  (500 MHz,  $\text{CD}_2\text{Cl}_2$ )  $\delta$  8.09 – 8.04 (m, 2H), 7.80 – 7.77 (m, 1H), 7.73 – 7.71 (m, 1H), 7.50 – 7.53 (m, 1H), 7.36 – 7.21 ppm (m, 6H), 4.33 ppm (s, 2H);  $^{13}\text{C NMR}$  (126 MHz,  $\text{CD}_2\text{Cl}_2$ )  $\delta$  161.6, 148.3, 139.9, 136.7, 129.7, 129.5, 129.3, 128.9, 127.9, 127.1, 126.7, 126.2, 121.9, 45.7 ppm; **FT-IR**:  $\tilde{\nu} = 3058, 2848, 2362, 1815, 1597, 1495, 1310, 1029$   $\text{cm}^{-1}$ ; **HR-MS**: calc. for  $[\text{M}+\text{H}]^+$   $\text{C}_{16}\text{H}_{14}\text{N} = 220.1121$  found: 220.1119.



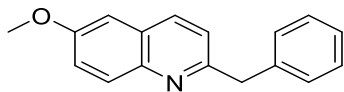
## 2-Benzylpyridine (77c)

Prepared according to general procedure A using pyridine *N*-oxide (0.4 mmol) and benzyltrimethylsilane (1.2 mmol). The product was isolated as yellow oil (51 mg, 0.3 mmol, 76%) after 12 h;  $R_f = 0.38$  (cyclohexane / ethyl acetate = 5:1);  $^1\text{H NMR}$  (600 MHz,  $\text{CDCl}_3$ )  $\delta$  8.53 – 8.49 (m, 1H), 7.55 – 7.52 (m, 1H), 7.29 – 7.20 (m, 4H), 7.20 – 7.15 (m, 1H), 7.09 – 7.04 (m, 2H), 4.13 ppm (s, 2H);  $^{13}\text{C NMR}$  (151 MHz,  $\text{CDCl}_3$ )  $\delta$  160.8, 149.0, 139.3, 136.5, 129.0, 128.5, 126.3, 123.0, 121.1, 44.5 ppm; **FT-IR**:  $\tilde{\nu} = 3061, 2922, 2314, 1879, 1588, 1568, 1309, 1049 \text{ cm}^{-1}$ ; **HR-MS**: calc. for  $[\text{M}+\text{H}]^+$   $\text{C}_{12}\text{H}_{12}\text{N} = 170.0964$  found: 170.0959.



## 2-Benzyl-6-methylquinoline (77d)

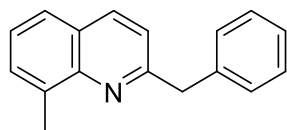
Prepared according to general procedure A using 6-methylquinoline *N*-oxide (0.4 mmol) and benzyltrimethylsilane (1.2 mmol). The product was isolated as yellow solid (68 mg, 0.29 mmol, 73%) after 3 h;  $R_f = 0.47$  (cyclohexane / ethyl acetate = 5:1);  $^1\text{H NMR}$  (500 MHz,  $\text{CD}_2\text{Cl}_2$ )  $\delta$  7.99 – 7.92 (m, 2H), 7.55 (d,  $J = 7.9 \text{ Hz}$ , 2H), 7.35 – 7.29 (m, 4H), 7.24 (dd,  $J = 7.4, 3.2 \text{ Hz}$ , 2H), 4.31 (s, 2H), 2.53 ppm (s, 3H);  $^{13}\text{C NMR}$  (126 MHz,  $\text{CD}_2\text{Cl}_2$ )  $\delta$  160.6, 146.8, 140.1, 136.2, 136.0, 131.9, 129.5, 128.9, 128.8, 127.1, 126.7, 126.7, 121.8, 45.6, 21.6 ppm; **FT-IR**:  $\tilde{\nu} = 3025, 2512, 1976, 1597, 1433, 1220, 1026 \text{ cm}^{-1}$ ; **HR-MS**: calc. for  $[\text{M}+\text{H}]^+$   $\text{C}_{17}\text{H}_{16}\text{N} = 234.1277$  found: 234.1273.



## 2-Benzyl-6-methoxyquinoline (77e)

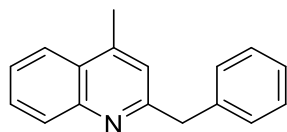
Prepared according to general procedure A using 6-methoxyquinoline *N*-oxide (0.4 mmol) and benzyltrimethylsilane (1.2 mmol). The product was isolated as pale orange solid (52 mg, 0.21 mmol, 52%) after 3 h;  $R_f = 0.32$  (cyclohexane / ethyl acetate = 5:1);  $^1\text{H NMR}$  (500 MHz,  $\text{CD}_2\text{Cl}_2$ )  $\delta$  7.97 (d,  $J = 8.4 \text{ Hz}$ , 1H), 7.93 (d,  $J = 9.2 \text{ Hz}$ , 1H), 7.34 (dd,  $J = 9.2, 2.8 \text{ Hz}$ , 1H), 7.33 – 7.27 (m, 4H), 7.25 – 7.19 (m, 2H), 7.08 (d,  $J = 2.9 \text{ Hz}$ , 1H), 4.28 (s, 2H), 3.91 ppm (s, 3H);  $^{13}\text{C NMR}$  (126 MHz,  $\text{CD}_2\text{Cl}_2$ )  $\delta$  159.0, 157.7, 144.2, 140.2, 135.5, 130.6, 129.4, 128.8, 128.0, 126.6, 122.2, 122.1,

105.5, 55.8, 45.4 ppm; **FT-IR**:  $\tilde{\nu}$  = 3082, 2962, 2362, 1664, 1493, 1374, 1289, 1071  $\text{cm}^{-1}$ ; **HR-MS**: calc. for  $[\text{M}+\text{H}]^+$   $\text{C}_{17}\text{H}_{16}\text{ON}$  = 250.1226 found: 250.1223.



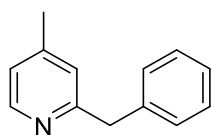
### 2-Benzyl-8-methylquinoline (77f)

Prepared according to general procedure A using 8-methylquinoline *N*-oxide (0.4 mmol) and benzyltrimethylsilane (1.2 mmol). The product was isolated as yellow oil (31 mg, 0.13 mmol, 33%) after 5 h;  $R_f$  = 0.72 (cyclohexane / ethyl acetate = 5:1);  **$^1\text{H}$  NMR** (500 MHz,  $\text{CD}_2\text{Cl}_2$ )  $\delta$  8.03 (d,  $J$  = 8.4 Hz, 1H), 7.62 (dd,  $J$  = 8.1, 1.5 Hz, 1H), 7.56 – 7.54 (m, 1H), 7.40 – 7.33 (m, 3H), 7.32 – 7.24 (m, 3H), 7.23 – 7.19 (m, 1H), 4.32 (s, 2H), 2.80 ppm (t,  $J$  = 0.8 Hz, 3H);  **$^{13}\text{C}$  NMR** (126 MHz,  $\text{CD}_2\text{Cl}_2$ )  $\delta$  160.3, 147.2, 140.1, 137.2, 136.9, 129.7, 129.5, 128.8, 128.8, 128.7, 126.9, 126.6, 125.9, 125.8, 125.7, 121.5, 45.9, 18.0 ppm; **FT-IR**:  $\tilde{\nu}$  = 3026, 2850, 1935, 1614, 1466, 1210, 972  $\text{cm}^{-1}$ ; **HR-MS**: calc. for  $[\text{M}+\text{H}]^+$   $\text{C}_{17}\text{H}_{16}\text{N}$  = 234.1277 found: 234.1275.



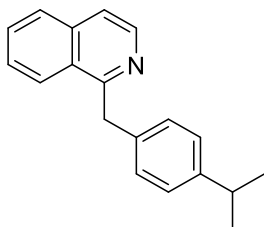
### 2-Benzyl-4-methylquinoline (77g)

Prepared according to general procedure A using 4-methylquinoline *N*-oxide (0.4 mmol) and benzyltrimethylsilane (1.2 mmol). The product was isolated as pale yellow solid (67 mg, 0.28 mmol, 71%) after 1 h;  $R_f$  = 0.4 (cyclohexane / ethyl acetate = 5:1);  **$^1\text{H}$  NMR** (500 MHz,  $\text{CD}_2\text{Cl}_2$ )  $\delta$  8.07 – 8.03 (m, 1H), 7.97 (dd,  $J$  = 8.3, 1.4 Hz, 1H), 7.72 – 7.68 (m, 1H), 7.55 – 7.52 (m, 1H), 7.37 – 7.28 (m, 4H), 7.26 – 7.20 (m, 1H), 7.13 (d,  $J$  = 1.1 Hz, 1H), 4.28 (s, 2H), 2.63 ppm (s, 3H);  **$^{13}\text{C}$  NMR** (126 MHz,  $\text{CD}_2\text{Cl}_2$ )  $\delta$  161.2, 148.1, 145.0, 140.0, 129.8, 129.5, 128.8, 128.8, 127.2, 126.7, 125.9, 124.0, 122.5, 45.7, 18.8 ppm; **FT-IR**:  $\tilde{\nu}$  = 3023, 2521, 1976, 1506, 1341, 1188, 1018  $\text{cm}^{-1}$ ; **HR-MS**: calc. for  $[\text{M}+\text{H}]^+$   $\text{C}_{17}\text{H}_{16}\text{N}$  = 234.1277 found: 234.1274.



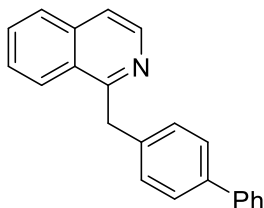
### 2-Benzyl-4-methylpyridine (77h)

Prepared according to general procedure A using 4-methylpyridine *N*-oxide (0.4 mmol) and benzyltrimethylsilane (1.2 mmol). The product was isolated as yellow oil (54 mg, 0.29 mmol, 73%) after 12 h;  $R_f = 0.25$  (cyclohexane / ethyl acetate = 5:1);  **$^1\text{H NMR}$**  (600 MHz,  $\text{CD}_2\text{Cl}_2$ )  $\delta$  8.36 (d,  $J = 5.1$  Hz, 1H), 7.33 – 7.24 (m, 4H), 7.24 – 7.15 (m, 1H), 6.98 (d,  $J = 1.7$  Hz, 1H), 6.95 (dd,  $J = 5.0, 1.6$  Hz, 1H), 4.08 ppm (s, 2H), 2.28 ppm (s, 3H);  **$^{13}\text{C NMR}$**  (151 MHz,  $\text{CD}_2\text{Cl}_2$ )  $\delta$  161.1, 149.4, 148.0, 140.5, 129.4, 128.8, 126.5, 124.2, 122.6, 44.8, 21.1 ppm; **FT-IR**:  $\tilde{\nu} = 3084, 2922, 2030, 1601, 1400, 1216, 1030$   $\text{cm}^{-1}$ ; **HR-MS**: calc. for  $[\text{M}+\text{H}]^+$   $\text{C}_{13}\text{H}_{14}\text{N} = 184.1121$  found: 184.1117.



### 1-(4-Isopropylbenzyl)isoquinoline (77i)

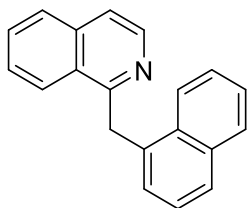
Prepared according to general procedure A using isoquinoline *N*-oxide (0.4 mmol) and 4-isopropylbenzyltrimethylsilane (1.2 mmol). The product was isolated as a yellow oil (48 mg, 0.18 mmol, 46%) after 24 h;  $R_f = 0.28$  (cyclohexane / ethyl acetate = 5:1);  **$^1\text{H NMR}$**  (600 MHz,  $\text{CD}_2\text{Cl}_2$ )  $\delta$  8.47 (d,  $J = 5.7$  Hz, 1H), 8.22 – 8.20 (m, 1H), 7.85 – 7.83 (m, 1H), 7.67 – 7.65 (m, 1H), 7.58 – 7.55 (m, 2H), 7.21 (d,  $J = 8.2$  Hz, 2H), 7.13 (d,  $J = 8.1$  Hz, 2H), 4.63 (s, 2H), 2.89 – 2.82 (m, 1H), 1.21 ppm (d,  $J = 7.0$  Hz, 6H);  **$^{13}\text{C NMR}$**  (151 MHz,  $\text{CD}_2\text{Cl}_2$ )  $\delta$  160.8, 147.2, 142.4, 137.3, 136.9, 130.1, 128.9, 127.7, 127.5, 127.4, 126.8, 126.0, 119.9, 41.7, 34.0, 24.1 ppm; **FT-IR**:  $\tilde{\nu} = 3009, 2957, 1907, 1585, 1419, 1290, 1153, 1018$   $\text{cm}^{-1}$ ; **HR-MS**: calc. for  $[\text{M}+\text{H}]^+$   $\text{C}_{19}\text{H}_{20}\text{N} = 262.1590$  found: 262.1587.



### 1-([1,1'-Biphenyl]-4-ylmethyl)isoquinoline (77j)

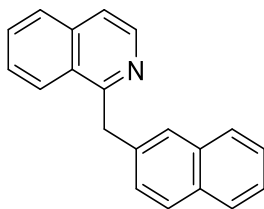


Prepared according to general procedure A using isoquinoline *N*-oxide (0.4 mmol) and ([1,1'-biphenyl]-4-ylmethyl)trimethylsilane (1.2 mmol). The product was isolated as a white solid (54 mg, 0.18 mmol, 46%) after 24 h;  $R_f = 0.26$  (cyclohexane / ethyl acetate = 5:1);  $^1\text{H NMR}$  (700 MHz,  $\text{CD}_2\text{Cl}_2$ )  $\delta$  8.50 (d,  $J = 5.7$  Hz, 1H), 8.23 (d,  $J = 8.5$  Hz, 1H), 7.86 (d,  $J = 8.2$  Hz, 1H), 7.69 – 7.66 (m, 1H), 7.62 – 7.55 (m, 4H), 7.54 – 7.50 (m, 2H), 7.42 (t,  $J = 7.7$  Hz, 2H), 7.37 (d,  $J = 8.0$  Hz, 2H), 7.33 (t,  $J = 7.4$  Hz, 1H), 4.72 ppm (s, 2H);  $^{13}\text{C NMR}$  (176 MHz,  $\text{CD}_2\text{Cl}_2$ )  $\delta$  160.5, 142.4, 141.1, 139.4, 139.2, 136.9, 130.2, 129.5, 129.1, 127.7, 127.6, 127.5, 127.4, 127.4, 127.2, 126.0, 120.0, 41.8 ppm; **FT-IR**:  $\tilde{\nu} = 3027, 2925, 2516, 1975, 1620, 1599, 1238, 1006$   $\text{cm}^{-1}$ ; **HR-MS**: calc. for  $[\text{M}+\text{H}]^+ \text{C}_{22}\text{H}_{18}\text{N} = 296.1434$  found: 296.1429.



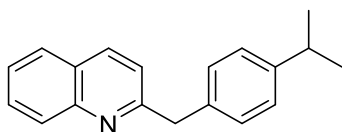
### 1-(Naphthalen-1-ylmethyl) isoquinoline (77k)

Prepared according to general procedure A using isoquinoline *N*-oxide (0.4 mmol) and trimethyl (naphthalen-1-ylmethyl) silane (1.2 mmol). The product was isolated as a pale yellow solid (41 mg, 0.15 mmol, 38%) after 24 h;  $R_f = 0.26$  (cyclohexane / ethyl acetate = 5:1);  $^1\text{H NMR}$  (600 MHz,  $\text{CD}_2\text{Cl}_2$ )  $\delta$  8.51 (d,  $J = 5.7$  Hz, 1H), 8.24 – 8.22 (m, 1H), 7.86 – 7.84 (m, 1H), 7.81 – 7.77 (m, 1H), 7.75 (dd,  $J = 10.8, 8.0$  Hz, 2H), 7.70 (d,  $J = 1.6$  Hz, 1H), 7.66 – 7.64 (m, 1H), 7.61 (dd,  $J = 5.7, 0.9$  Hz, 1H), 7.55 – 7.53 (m, 1H), 7.47 – 7.39 (m, 3H), 4.83 ppm (s, 2H);  $^{13}\text{C NMR}$  (151 MHz,  $\text{CD}_2\text{Cl}_2$ )  $\delta$  160.4, 142.4, 137.7, 136.9, 133.9, 132.5, 130.2, 128.3, 127.9, 127.8, 127.7, 127.7, 127.5, 127.5, 127.3, 126.3, 126.0, 125.8, 120.1, 42.4 ppm; **FT-IR**:  $\tilde{\nu} = 3016, 2959, 1976, 1599, 1389, 1238, 1067$   $\text{cm}^{-1}$ ; **HR-MS**: calc. for  $[\text{M}+\text{H}]^+ \text{C}_{20}\text{H}_{16}\text{N} = 270.1277$  found: 270.1276.



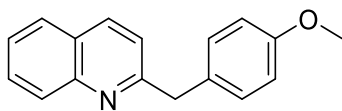
### 1-(Naphthalen-2-ylmethyl)isoquinoline (77l)

Prepared according to general procedure A using isoquinoline *N*-oxide (0.4 mmol) and Trimethyl(naphthalen-2-ylmethyl)silane (1.2 mmol). The product was isolated as a yellow oil (50 mg, 0.19 mmol, 47%) after 24 h;  $R_f = 0.26$  (cyclohexane / ethyl acetate = 5:1);  $^1\text{H NMR}$  (700 MHz,  $\text{CD}_2\text{Cl}_2$ )  $\delta$  8.45 (d,  $J = 5.7$  Hz, 1H), 8.24 – 8.19 (m, 1H), 8.17 (d,  $J = 8.5$  Hz, 1H), 7.93 – 7.86 (m, 2H), 7.76 (d,  $J = 8.2$  Hz, 1H), 7.68 (dd,  $J = 8.3, 6.8$  Hz, 1H), 7.61 (d,  $J = 5.7$  Hz, 1H), 7.55 – 7.51 (m, 3H), 7.33 (t,  $J = 7.6$  Hz, 1H), 7.07 (d,  $J = 7.1$  Hz, 1H), 5.13 ppm (s, 2H);  $^{13}\text{C NMR}$  (176 MHz,  $\text{CD}_2\text{Cl}_2$ )  $\delta$  160.3, 142.4, 136.7, 136.2, 134.2, 132.6, 130.3, 129.0, 127.8, 127.8, 127.6, 127.3, 127.2, 126.4, 126.0, 125.8, 125.8, 124.4, 120.0, 39.2 ppm; **FT-IR**:  $\tilde{\nu} = 3026, 2925, 1976, 1620, 1498, 1408, 1261, 1015$   $\text{cm}^{-1}$ ; **HR-MS**: calc. for  $[\text{M}+\text{H}]^+$   $\text{C}_{20}\text{H}_{16}\text{N} = 270.1277$  found: 270.1269.



### 2-(4-Isopropylbenzyl) quinoline (77m)

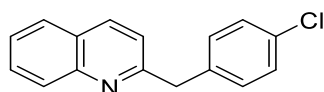
Prepared according to general procedure A using quinoline *N*-oxide (0.4 mmol) and 4-isopropylbenzyltrimethylsilane (1.2 mmol). The product was isolated as yellow oil (70 mg, 0.27 mmol, 67%) after 6 h;  $R_f = 0.40$  (cyclohexane / ethyl acetate = 5:1);  $^1\text{H NMR}$  (500 MHz,  $\text{CD}_2\text{Cl}_2$ )  $\delta$  8.10 – 8.03 (m, 2H), 7.80 (dd,  $J = 8.1, 1.5$  Hz, 1H), 7.73 – 7.69 (m, 1H), 7.53 – 7.50 (m, 1H), 7.31 – 7.24 (m, 3H), 7.22 – 7.17 (m, 2H), 4.30 (s, 2H), 2.89 (p,  $J = 6.9$  Hz, 1H), 1.24 ppm (d,  $J = 6.9$  Hz, 6H);  $^{13}\text{C NMR}$  (126 MHz,  $\text{CD}_2\text{Cl}_2$ )  $\delta$  161.8, 148.3, 147.4, 137.2, 136.6, 129.7, 129.4, 129.3, 127.9, 127.1, 126.9, 126.2, 121.9, 45.4, 34.1, 24.2 ppm; **FT-IR**:  $\tilde{\nu} = 3052, 2869, 1794, 1598, 1382, 1197, 1018$   $\text{cm}^{-1}$ ; **HR-MS**: calc. for  $[\text{M}+\text{H}]^+$   $\text{C}_{19}\text{H}_{20}\text{N} = 262.1590$  found: 262.1587.



### 2-(4-Methoxybenzyl)quinoline (77n)

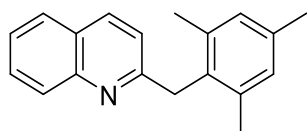
Prepared according to general procedure A using quinoline *N*-oxide (0.4 mmol) and 4-methoxybenzyltrimethylsilane (1.2 mmol). The product was isolated as yellow oil (70 mg, 0.28 mmol, 70%) after 12 h;  $R_f = 0.32$  (cyclohexane / ethyl acetate = 5:1);  $^1\text{H NMR}$  (500 MHz,  $\text{CD}_2\text{Cl}_2$ )

$\delta$  8.08 – 8.00 (m, 2H), 7.79 (dd,  $J = 8.2, 1.4$  Hz, 1H), 7.71 – 7.68 (m, 1H), 7.51 – 7.49 (m, 1H), 7.28 – 7.20 (m, 3H), 6.87 – 6.82 (m, 2H), 4.25 (s, 2H), 3.76 ppm (s, 3H);  $^{13}\text{C}$  NMR (126 MHz,  $\text{CD}_2\text{Cl}_2$ )  $\delta$  162.0, 158.7, 148.2, 136.6, 131.9, 130.4, 129.6, 129.2, 127.9, 127.1, 126.2, 121.8, 114.2, 55.5, 44.8 ppm; **FT-IR**:  $\tilde{\nu} = 3058, 2954, 2489, 1886, 1652, 1464, 1280, 1106$   $\text{cm}^{-1}$ ; **HR-MS**: calc. for  $[\text{M}+\text{H}]^+ \text{C}_{17}\text{H}_{16}\text{ON} = 250.1226$  found: 250.1224.



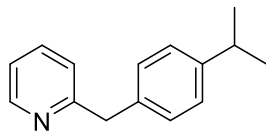
### 2-(4-Chlorobenzyl)quinoline (77o)

Prepared according to general procedure A using quinoline *N*-oxide (0.4 mmol) and 4-chlorobenzyltrimethylsilane (1.2 mmol). The product was isolated as yellow oil (86 mg, 0.34 mmol, 84%) after 6 h;  $R_f = 0.36$  (cyclohexane / ethyl acetate = 5:1);  $^1\text{H}$  NMR (500 MHz,  $\text{CD}_2\text{Cl}_2$ )  $\delta$  8.08 (d,  $J = 8.5$  Hz, 1H), 8.02 (dd,  $J = 8.3, 1.1$  Hz, 1H), 7.80 (dd,  $J = 8.1, 1.5$  Hz, 1H), 7.72 – 7.69 (m, 1H), 7.53 – 7.50 (m, 1H), 7.30 – 7.22 (m, 5H), 4.29 ppm (s, 2H);  $^{13}\text{C}$  NMR (126 MHz,  $\text{CD}_2\text{Cl}_2$ )  $\delta$  161.0, 148.3, 138.5, 136.9, 132.4, 130.9, 129.8, 129.2, 128.9, 127.9, 127.1, 126.4, 121.8, 44.9 ppm; **FT-IR**:  $\tilde{\nu} = 3037, 2962, 2490, 1818, 1599, 1374, 1220, 1154, 1014$   $\text{cm}^{-1}$ ; **HR-MS**: calc. for  $[\text{M}+\text{H}]^+ \text{C}_{16}\text{H}_{13}\text{N}^{35}\text{Cl} = 254.0731$  found: 254.0729;  $\text{C}_{16}\text{H}_{13}\text{N}^{37}\text{Cl} = 256.0701$  found: 256.0695.



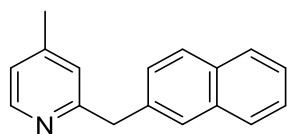
### 2-(2,4,6-Trimethylbenzyl)quinoline (77p)

Prepared according to general procedure A using quinoline *N*-oxide (0.4 mmol) and 2, 4, 6-trimethylbenzyltrimethylsilane (1.2 mmol). The product was isolated as white solid (73 mg, 0.28 mmol, 70%) after 6 h;  $R_f = 0.44$  (cyclohexane / ethyl acetate = 5:1);  $^1\text{H}$  NMR (500 MHz,  $\text{CD}_2\text{Cl}_2$ )  $\delta$  7.99 (dd,  $J = 8.5, 2.5$  Hz, 2H), 7.77 (dd,  $J = 8.2, 1.5$  Hz, 1H), 7.67 – 7.70 (m, 1H), 7.47 – 7.50 (m, 1H), 6.98 (d,  $J = 8.5$  Hz, 1H), 6.92 (s, 2H), 4.35 (s, 2H), 2.28 ppm (d,  $J = 14.0$  Hz, 9H);  $^{13}\text{C}$  NMR (126 MHz,  $\text{CD}_2\text{Cl}_2$ )  $\delta$  161.4, 148.3, 137.6, 136.6, 136.3, 133.2, 129.6, 129.2, 129.1, 127.8, 127.0, 126.0, 120.5, 39.0, 20.5 ppm; **FT-IR**:  $\tilde{\nu} = 2960, 2350, 1619, 1503, 1426, 1204, 1016$   $\text{cm}^{-1}$ ; **HR-MS**: calc. for  $[\text{M}+\text{H}]^+ \text{C}_{19}\text{H}_{20}\text{N} = 262.1590$  found: 262.1587.



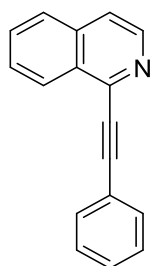
#### 2-(4-Isopropylbenzyl) pyridine (77q)

Prepared according to general procedure A using pyridine *N*-oxide (0.4 mmol) and isopropylbenzyltrimethylsilane (1.2 mmol). The product was isolated as yellow oil (25 mg, 0.12 mmol, 30%) after 12 h;  $R_f = 0.24$  (cyclohexane / ethylacetate = 5:1);  **$^1\text{H NMR}$**  (500 MHz,  $\text{CD}_2\text{Cl}_2$ )  $\delta$  8.50 – 8.49 (m, 1H), 7.60 – 7.57 (m, 1H), 7.20 – 7.13 (m, 5H), 7.12 – 7.09 (m, 1H), 4.08 (s, 2H), 2.90 - 2.84 (m, 1H), 1.22 ppm (d,  $J = 7.0$  Hz, 6H);  **$^{13}\text{C NMR}$**  (126 MHz,  $\text{CD}_2\text{Cl}_2$ )  $\delta$  161.6, 149.6, 147.3, 137.5, 136.7, 129.2, 126.8, 123.3, 121.5, 44.5, 34.0, 24.1 ppm; **FT-IR**:  $\tilde{\nu} = 3007, 2160, 1588, 1420, 1221, 1019$   $\text{cm}^{-1}$ ; **HR-MS**: calc. for  $[\text{M}+\text{H}]^+$   $\text{C}_{15}\text{H}_{18}\text{N} = 212.1434$  found: 212.1428.



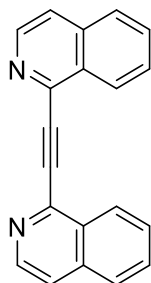
#### 4-Methyl-2-(naphthalen-2-ylmethyl) pyridine (77r)

Prepared according to general procedure A using 4-methylpyridine *N*-oxide (0.4 mmol) and trimethyl (naphthalen-2-ylmethyl) silane (1.2 mmol). The product was isolated as yellow oil (68 mg, 0.29 mmol, 72%) after 24 h;  $R_f = 0.16$  (cyclohexane / ethyl acetate = 5:1);  **$^1\text{H NMR}$**  (500 MHz,  $\text{CD}_2\text{Cl}_2$ )  $\delta$  8.37 (d,  $J = 5.0$  Hz, 1H), 7.83 – 7.75 (m, 4H), 7.73 – 7.69 (m, 1H), 7.49 – 7.38 (m, 4H), 4.25 (s, 2H), 2.27 ppm (s, 3H);  **$^{13}\text{C NMR}$**  (126 MHz,  $\text{CD}_2\text{Cl}_2$ )  $\delta$  160.9, 149.3, 137.9, 134.0, 132.5, 128.3, 128.0, 127.9, 127.8, 127.8, 127.6, 126.3, 125.7, 124.3, 122.6, 44.9, 21.0 ppm; **FT-IR**:  $\tilde{\nu} = 3179, 2920, 2158, 1668, 1437, 1270, 1017$   $\text{cm}^{-1}$ ; **HR-MS**: calc. for  $[\text{M}+\text{H}]^+$   $\text{C}_{17}\text{H}_{16}\text{N} = 234.1277$  found: 234.1275.



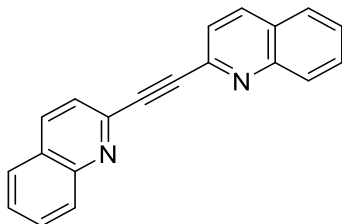
#### 1-(Phenylethynyl)isoquinoline (83)

To a mixture of isoquinoline *N*-oxide (0.2 mmol) in DMF (1 mL), trimethyl(phenylethynyl)silane (0.6 mmol) was added. The reaction vial was flushed with argon and then 10 mol% of TBAF was added and stirred for 2 h. Purification by column chromatography (EtOAc/Petroleum ether) yielded the desired product as a dark brown solid (41 mg, 0.18 mmol, 91%);  $R_f = 0.36$  (cyclohexane / ethyl acetate = 5:1);  $^1\text{H NMR}$  (500 MHz,  $\text{CDCl}_3$ )  $\delta$  8.56 (d,  $J = 5.7$  Hz, 1H), 8.53 – 8.51 (m, 1H), 7.88 – 7.83 (m, 1H), 7.77 – 7.63 (m, 5H), 7.44 – 7.41 ppm (m, 3H);  $^{13}\text{C NMR}$  (126 MHz,  $\text{CDCl}_3$ )  $\delta$  144.3, 142.8, 136.0, 132.3, 130.9, 129.4, 129.4, 128.6, 128.3, 128.2, 127.1, 127.0, 122.2, 120.8, 94.4, 86.7 ppm; **FT-IR**:  $\tilde{\nu} = 3055, 2514, 2159, 2030, 1596, 1353, 1315, 1014$   $\text{cm}^{-1}$ ; **HR-MS**: calc. for  $[\text{M}+\text{H}]^+ \text{C}_{17}\text{H}_{12}\text{N} = 230.0964$  found: 230.0961.



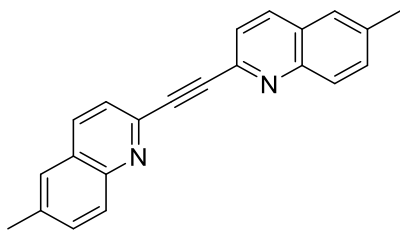
### 1,2-Di(isoquinolin-1-yl)ethyne (85a)

Prepared according to general procedure B using isoquinoline *N*-oxide (0.2 mmol) and ethynyltrimethylsilane (0.8 mmol); The product was obtained as a pale brown solid (25 mg, 0.09 mmol, 89%);  $R_f = 0.33$  (dichloromethane / methanol = 50:1);  $^1\text{H NMR}$  (400 MHz,  $\text{CD}_2\text{Cl}_2$ )  $\delta$  8.65 (dd,  $J = 9.2, 6.4$  Hz, 4H), 7.93 (d,  $J = 7.7$  Hz, 2H), 7.77 ppm (t,  $J = 6.6$  Hz, 6H);  $^{13}\text{C NMR}$  (101 MHz,  $\text{CD}_2\text{Cl}_2$ )  $\delta$  143.8, 143.6, 136.2, 131.1, 130.1, 128.8, 127.4, 127.1, 121.7, 90.6 ppm; **FT-IR**:  $\tilde{\nu} = 2924, 2853, 2510, 2159, 2030, 1976, 1204$   $\text{cm}^{-1}$ ; **HR-MS**: calc. for  $[\text{M}+\text{H}]^+ \text{C}_{20}\text{H}_{13}\text{N}_2 = 281.1073$  found: 281.1068.



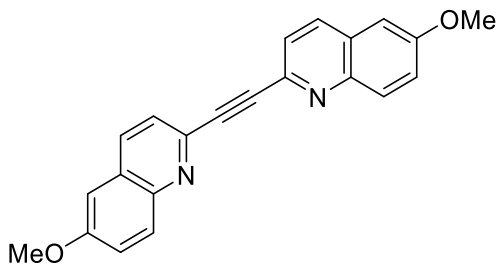
### 1,2-Di(quinolin-2-yl)ethyne (85b)

Prepared according to general procedure B using quinoline *N*-oxide (0.2 mmol) and ethynyltrimethylsilane (1.2 mmol). The product was obtained as a pale yellow solid (24 mg, 0.09 mmol, 86%);  $R_f = 0.4$  (dichloromethane / methanol = 50:1);  $^1\text{H NMR}$  (500 MHz,  $\text{CD}_2\text{Cl}_2$ )  $\delta$  8.23 (dd,  $J = 8.5, 0.8$  Hz, 2H), 8.11 (dd,  $J = 8.5, 1.1$  Hz, 2H), 7.88 (dd,  $J = 8.2, 1.4$  Hz, 2H), 7.80 – 7.77 (m, 2H), 7.73 (d,  $J = 8.4$  Hz, 2H), 7.63 – 7.60 ppm (m, 2H);  $^{13}\text{C NMR}$  (126 MHz,  $\text{CD}_2\text{Cl}_2$ )  $\delta$  148.3, 142.5, 136.3, 130.1, 129.3, 127.6, 127.5, 127.4, 124.4, 88.5 ppm; **FT-IR**:  $\tilde{\nu} = 3052, 2521, 2159, 2030, 1976, 1500, 1207$   $\text{cm}^{-1}$ ; **HR-MS**: calc. for  $[\text{M}+\text{H}]^+ \text{C}_{20}\text{H}_{13}\text{N}_2 = 281.1073$  found: 281.1068.



### 1,2-Bis(6-methylquinolin-2-yl)ethyne (85c)

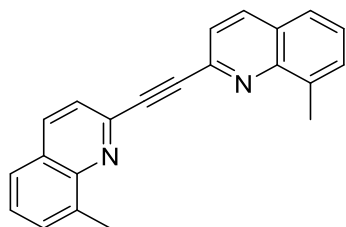
Prepared according to general procedure B using 6, 7-dimethoxyisoquinoline *N*-oxide (0.2 mmol) and ethynyltrimethylsilane (1.2 mmol). The product was obtained as a pale brown solid (20 mg, 0.07 mmol, 65%);  $R_f = 0.62$  (dichloromethane / methanol = 50:1);  $^1\text{H NMR}$  (400 MHz,  $\text{CDCl}_3$ )  $\delta$  8.07 (dd,  $J = 15.0, 8.8$  Hz, 4H), 7.74 (d,  $J = 8.4$  Hz, 2H), 7.62 – 7.55 (m, 4H), 2.55 ppm (s, 6H);  $^{13}\text{C NMR}$  (101 MHz,  $\text{CDCl}_3$ )  $\delta$  146.8, 141.8, 137.8, 135.8, 132.7, 129.1, 127.6, 126.5, 124.8, 89.0, 21.8 ppm; **FT-IR**:  $\tilde{\nu} = 3059, 2513, 2159, 2030, 1976, 1491, 1285, 1162$   $\text{cm}^{-1}$ ; **HR-MS**: calc. for  $[\text{M}+\text{H}]^+ \text{C}_{22}\text{H}_{17}\text{N}_2 = 309.1386$  found: 309.1386.



### 1,2-Bis(6-methoxyquinolin-2-yl)ethyne (85d)

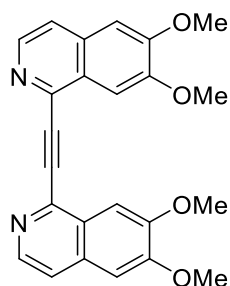
Prepared according to general procedure B using 6-methoxyquinoline *N*-oxide (0.2 mmol) and ethynyltrimethylsilane (1.2 mmol). The product was obtained as a brown solid (16 mg, 0.05 mmol, 47%);  $R_f = 0.33$  (dichloromethane / methanol = 50:1);  $^1\text{H NMR}$  (500 MHz,  $\text{CDCl}_3$ )  $\delta$  8.08 (d,  $J =$

8.8 Hz, 4H), 7.75 (d,  $J = 8.4$  Hz, 2H), 7.41 (dd,  $J = 9.2, 2.8$  Hz, 2H), 7.08 (d,  $J = 2.7$  Hz, 2H), 3.95 ppm (s, 6H);  $^{13}\text{C}$  NMR (126 MHz,  $\text{CDCl}_3$ )  $\delta$  158.8, 144.1, 139.9, 135.4, 130.7, 128.8, 125.2, 123.5, 105.0, 88.9, 55.8 ppm; FT-IR:  $\tilde{\nu} = 3002, 2964, 2518, 2159, 2026, 1976, 1305, 1148$   $\text{cm}^{-1}$ ; HR-MS: calc. for  $[\text{M}+\text{H}]^+ \text{C}_{22}\text{H}_{17}\text{O}_2\text{N}_2 = 341.1284$  found: 341.1287.



### 1,2-Bis(8-methylquinolin-2-yl)ethyne (85e)

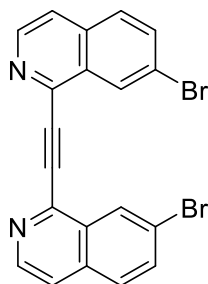
Prepared according to general procedure B using 8-methylquinoline *N*-oxide (0.2 mmol) and ethynyltrimethylsilane (1.2 mmol). The product was obtained as a white solid (10 mg, 0.04 mmol, 35%);  $R_f = 0.7$  (dichloromethane / methanol = 50:1);  $^1\text{H}$  NMR (400 MHz,  $\text{CD}_2\text{Cl}_2$ )  $\delta$  8.20 (d,  $J = 8.4$  Hz, 2H), 7.72 (t,  $J = 7.8$  Hz, 4H), 7.64 (d,  $J = 7.0$  Hz, 2H), 7.50 (t,  $J = 7.6$  Hz, 2H), 2.86 ppm (s, 6H);  $^{13}\text{C}$  NMR (126 MHz,  $\text{CD}_2\text{Cl}_2$ )  $\delta$  147.8, 141.8, 137.8, 136.9, 130.6, 127.8, 127.7, 126.0, 124.6, 88.8, 18.2 ppm; FT-IR:  $\tilde{\nu} = 3059, 2952, 2732, 2503, 2159, 1976, 1499, 1303, 1080$   $\text{cm}^{-1}$ ; HR-MS: calc. for  $[\text{M}+\text{H}]^+ \text{C}_{22}\text{H}_{17}\text{N}_2 = 309.1386$  found: 309.1381.



### 1,2-Bis(6,7-dimethoxyisoquinolin-1-yl)ethyne (85f)

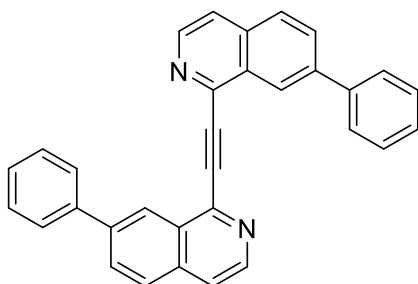
Prepared according to general procedure B using 6,7-dimethoxyisoquinoline *N*-oxide (0.2 mmol) and ethynyltrimethylsilane (1.2 mmol). The product was obtained as pale yellow solid (28 mg, 0.07 mmol, 69%);  $R_f = 0.36$  (dichloromethane / methanol = 50:1);  $^1\text{H}$  NMR (400 MHz,  $\text{CDCl}_3$ )  $\delta$  8.46 (d,  $J = 5.5$  Hz, 2H), 7.92 (s, 2H), 7.58 (d,  $J = 5.7$  Hz, 2H), 7.11 (s, 2H), 4.11 (s, 6H), 4.05 ppm (s, 6H);  $^{13}\text{C}$  NMR (101 MHz,  $\text{CDCl}_3$ )  $\delta$  153.4, 151.2, 141.2, 140.2, 132.8, 126.2, 119.9,

104.9, 104.5, 56.3, 56.0 ppm; **FT-IR**:  $\tilde{\nu}$  = 2931, 2518, 2159, 2027, 1976, 1426, 1027  $\text{cm}^{-1}$ ; **HR-MS**: calc. for  $[\text{M}+\text{H}]^+ \text{C}_{24}\text{H}_{21}\text{O}_4\text{N}_2 = 401.1496$  found: 401.1490.



### 1,2-Bis(7-bromoisoquinolin-1-yl)ethyne (85g)

Prepared according to general procedure B using 7-bromoisoquinoline *N*-oxide (0.2 mmol) and ethynyltrimethylsilane (1.2 mmol). The product was obtained as a pale brown solid (26 mg, 0.06 mmol, 59%);  $R_f = 0.33$  (dichloromethane / methanol = 50:1);  **$^1\text{H NMR}$**  (500 MHz,  $\text{CDCl}_3$ )  $\delta$  8.83 (d,  $J = 1.9$  Hz, 2H), 8.68 (d,  $J = 5.6$  Hz, 2H), 7.86 (dd,  $J = 8.7, 1.9$  Hz, 2H), 7.79 (d,  $J = 8.7$  Hz, 2H), 7.74 ppm (d,  $J = 5.7$  Hz, 2H);  **$^{13}\text{C NMR}$**  (126 MHz,  $\text{CDCl}_3$ )  $\delta$  142.9, 141.7, 134.7, 134.3, 129.1, 128.6, 122.7, 121.3, 90.3 ppm; **FT-IR**:  $\tilde{\nu}$  = 2918, 2495, 2159, 2031, 1976, 1541, 1373, 1012  $\text{cm}^{-1}$ ; **HR-MS**: calc. for  $[\text{M}+\text{H}]^+ \text{C}_{20}\text{H}_{11}\text{N}_2^{79}\text{Br}_2 = 436.9283$  found: 436.9282  $\text{C}_{20}\text{H}_{11}\text{N}_2^{79}\text{Br}^{81}\text{Br} = 438.9263$  found: 438.9258  $\text{C}_{20}\text{H}_{11}\text{N}_2^{81}\text{Br}_2 = 440.9243$  found: 440.9236.



### 1, 2-Bis (7-phenylisoquinolin-1-yl) ethyne (85h)

Prepared according to general procedure B using 7-phenylisoquinoline 2-oxide (0.2 mmol) and ethynyltrimethylsilane (1.2 mmol). The product was obtained as a pale brown solid (17 mg, 0.04 mmol, 39%);  $R_f = 0.64$  (dichloromethane / methanol = 50:1);  **$^1\text{H NMR}$**  (500 MHz,  $\text{CDCl}_3$ )  $\delta$  8.87 – 8.83 (m, 2H), 8.65 (d,  $J = 5.6$  Hz, 2H), 8.03 (dd,  $J = 8.5, 1.8$  Hz, 2H), 7.97 (d,  $J = 8.5$  Hz, 2H), 7.77 (d,  $J = 5.6$  Hz, 2H), 7.76 – 7.71 (m, 4H), 7.45 – 7.39 (m, 4H), 7.39 – 7.34 ppm (m, 2H);  **$^{13}\text{C NMR}$**  (126 MHz,  $\text{CDCl}_3$ )  $\delta$  143.5, 142.9, 141.9, 140.2, 135.5, 131.3, 130.4, 129.4, 128.4, 128.0,



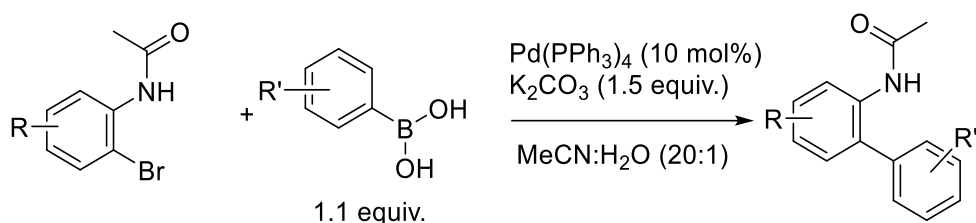
124.9, 121.7, 91.3 ppm; **FT-IR**:  $\tilde{\nu} = 2956, 2514, 2361, 2159, 2096, 1670, 1487, 1144 \text{ cm}^{-1}$ ; **HR-MS**: calc. for  $[\text{M}+\text{H}]^+ \text{C}_{32} \text{H}_{21} \text{N}_2 = 433.1699$  found: 433.1699.

## 7.3 Experimental part for the electrochemical amination

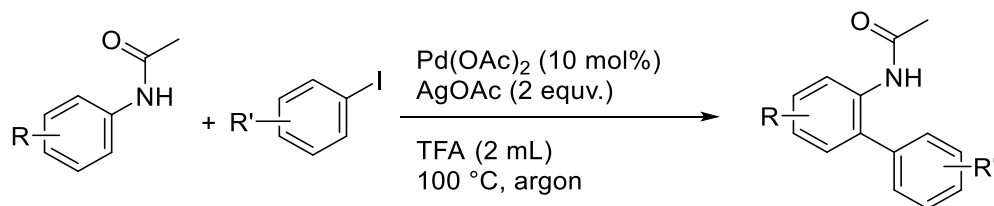
### 7.3.1 General procedures

#### General procedures for the preparation of biaryl acetanilides

To a solution of bromoacetanilide (0.25 mmol) in MeCN (10 mL) and H<sub>2</sub>O (0.5 mL), borate (0.28 mmol), K<sub>2</sub>CO<sub>3</sub> (0.38 mmol) and Pd(PPh<sub>3</sub>)<sub>4</sub> (0.025 mmol) were added and the reaction tube was flushed with argon. Degassing was done 3 times and stirred at 100 °C overnight. After the completion, reaction mixture was diluted with water, extracted with EtOAc, dried over anhydrous Na<sub>2</sub>SO<sub>4</sub>. The organic extracts were filtered and concentrated under reduced pressure. Purification by column-chromatography on silica gel afforded the pure product (Eluent: Petroleum ether-EtOAc).<sup>[116]</sup>



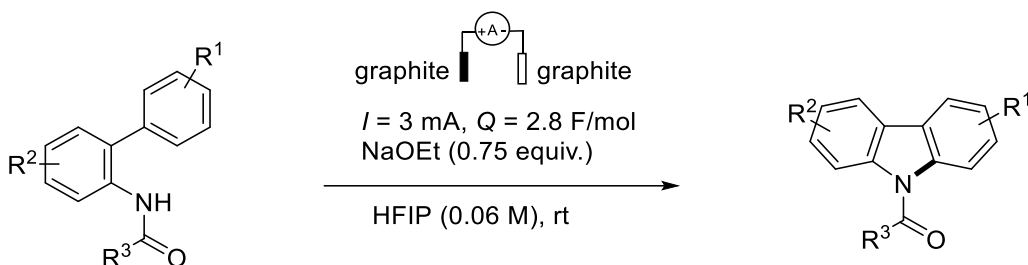
Anilides (1 mmol) were taken in TFA (2 mL). Then Pd(OAc)<sub>2</sub> (0.1 mmol) followed by AgOAc (2 mmol) were added to it. The reaction was heated at 110 °C for the maximum consumption of starting material. Then the reaction was quenched with aqueous sodium bicarbonate solution and extracted with EtOAc, washed with water, brine dried and purified by column chromatography (Eluent: Petroleum ether-EtOAc).<sup>[129]</sup>



#### General procedure A for intramolecular C–H amination

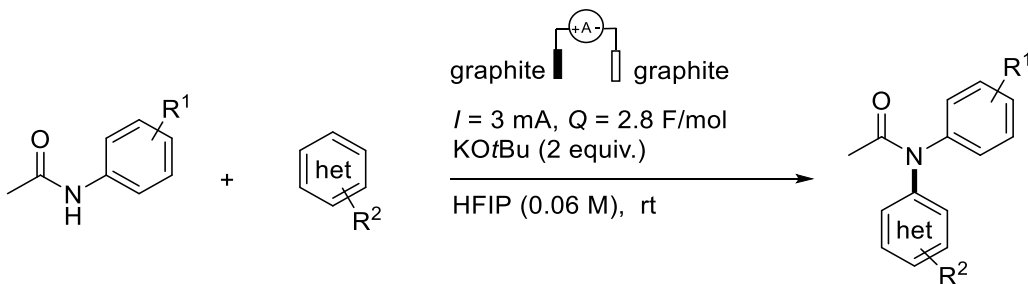
A 5 mL glass vial was charged with 2-amidobiaryl substrate (0.2 mmol, 1 equiv.) to which 1,1,1,3,3,3-hexfluoroisopropanol (0.06 M, 3 mL) followed by sodium ethoxide (21 wt. % solution in ethanol, 0.15 mmol, 0.75 equiv., 56  $\mu$ L) were added. Lid with graphite electrodes (52 x 5 mm)

was attached and electrolysis was carried out with a constant current of 3 mA until 2.8 F/mol charge was passed (~ 5 h) at room temperature. After the reaction, the reaction mixture was transferred to a 50 mL round bottom flask to which electrodes were washed with methanol. Solvents were evaporated under reduced pressure and the crude product was purified by silica gel column chromatography to obtain pure product (eluent: petroleum ether- ethyl acetate).



### General procedure B for intermolecular C–H amination

A 5 mL glass vial was charged with corresponding *N*-arylamide (0.2 mmol, 1 equiv.) and (hetero)arene partner (2-5 equiv.) to which 1,1,1,3,3,3-hexfluoroisopropanol (0.06 M, 3 mL) followed by potassium *tert*-butoxide (0.4 mmol, 2 equiv., 45.3 mg) were added. Lid with graphite electrodes (52 x 5 mm) was attached and electrolysis was carried out with a constant current of 3 mA until 2.8 F/mol charge was passed (~ 5 h) at room temperature. After the reaction, the reaction mixture was transferred to a 50 mL round bottom flask to which electrodes were washed with methanol. Solvents were evaporated under reduced pressure and the crude product was purified by silica gel column chromatography to obtain pure product (eluent: *n*-pentane- acetone or petroleum ether- ethyl acetate).



### General procedure for cyclovoltammetric (CV) studies

A 5 mL glass vial was charged with substrate (1 mM) and tetrabutylammonium tetrafluoroborate (0.1 M) in solvent (3 mL). Lid equipped with glassy carbon anode, reference electrode (Ag/AgCl

in 3 M aqueous KCl) and platinum plated cathode was attached to the vial and voltammograms were recorded with scan rates as mentioned.

### 7.3.2 Electrolytic parameters of reaction

Constant current,  $I = 3$  mA

Charge passed,  $Q = 2.8$  F/mol

Time,  $t$  for 0.2 mmol scale reaction = 5 h

Electrode materials for both WE and CE = Graphite electrodes

Maximum concentration of *in situ* generated electrolyte = 0.05 M for intramolecular aminations

= 0.13 M for intermolecular aminations

Voltage range of reactions for 3 mA CCE = 8 – 19 V for intramolecular aminations using NaOEt

= 3 – 9 V for intermolecular aminations using KO $t$ Bu

Charge (coulomb, C) = current (ampere, A)  $\times$  time (second, s) = 0.003  $\times$  18000 = 54 C

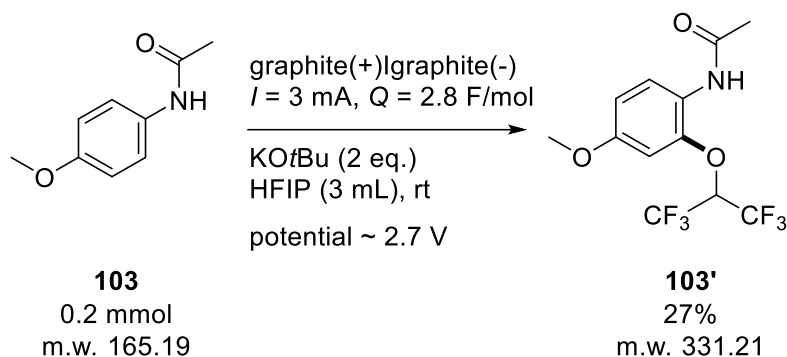
Faradaic efficiency range calculated = 26 – 55 %

$$\text{Faradaic efficiency} = \frac{Q_{\text{theoretical}}}{Q_{\text{experimental}}} \times \text{reaction yield \%}$$

Exposed surface area of electrodes calculated using  $A = 2(wl + hl + hw)$ , where  $l$  is exposed length (5 mm),  $h$  is exposed height (2 mm) and  $w$  is exposed width (16 mm). = 244 mm<sup>2</sup>

Current density = area of junction/current value = 244/3 = 0.012 mA/mm<sup>2</sup>

### 7.3.3 Evidences for nitrenium ion intermediate



The HFIP mono adduct was isolated and characterized from a reaction in the absence of any coupling partner. The formation of **103'** indicates a delocalization of positive charge of nitrenium ion in the aromatic ring. The HFIP di adduct was observed in GC-MS spectra for a reaction in the absence of any coupling partner. This indicates a delocalization of the positive charge of the nitrenium ion in the aromatic ring.

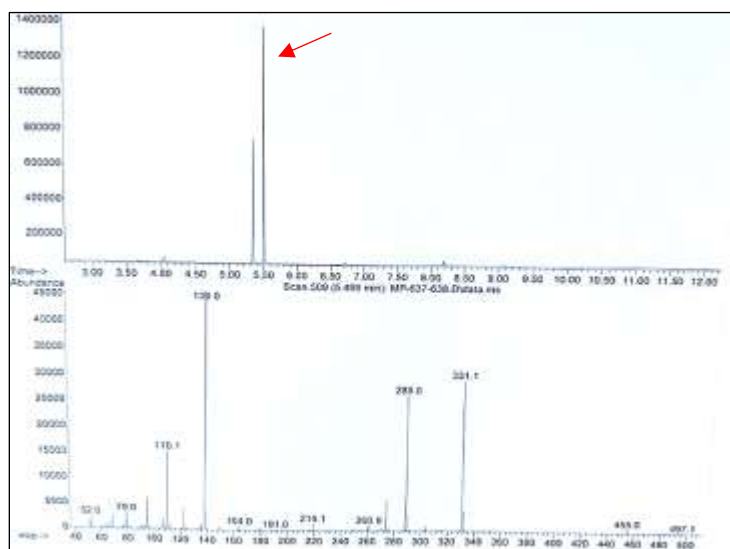
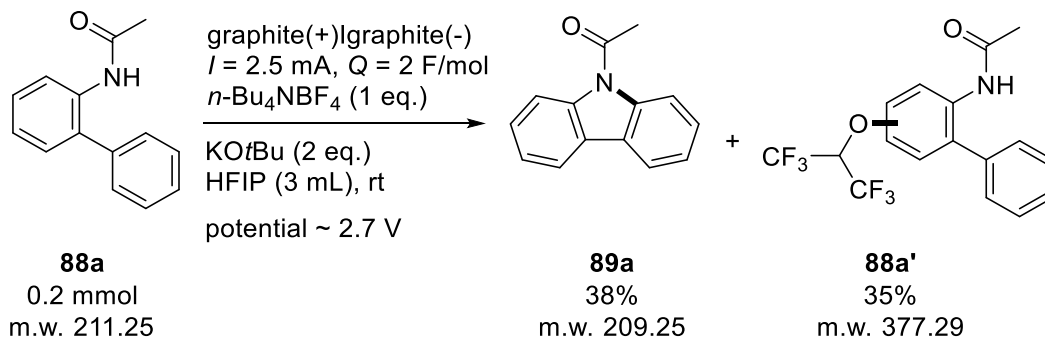


**Figure S4.** GC-MS-FID spectra for HFIP mono-adduct of **103**.



Competitive formation of the HFIP mono adduct was observed in GC-MS spectra for many intramolecular reactions as the major side product. Attempts to minimize this side product were mainly not successful. The formation of **88a'** indicates a delocalization of positive charge of the nitrenium ion in the aromatic ring.

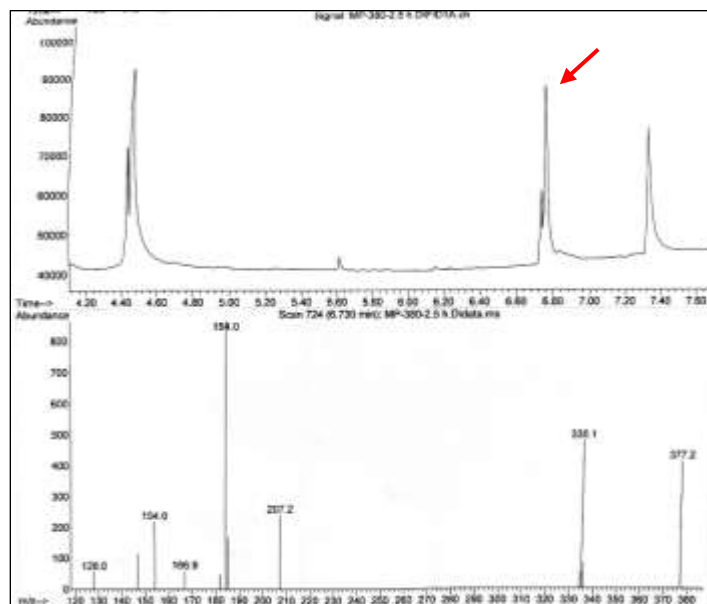
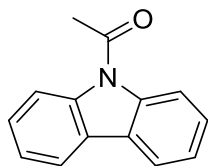


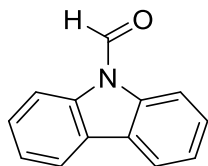
**Figure S5.** GC-MS-FID spectra for HFIP mono-adduct of **88a**.

### 7.3.4 Physical data of products



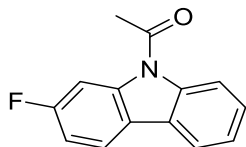
#### 1-(9H-carbazol-9-yl)ethan-1-one (89a)

Prepared according to general procedure A; The product was isolated as white solid (26 mg, 0.13 mmol, 63%) after electrolysis;  $R_f = 0.53$  (cyclohexane / ethyl acetate = 4:1);  $^1\text{H NMR}$  (500 MHz,  $\text{CD}_2\text{Cl}_2$ )  $\delta$  8.21 (d,  $J = 8.4$  Hz, 2H), 8.02 (d,  $J = 7.7$  Hz, 2H), 7.49 (t,  $J = 7.8$  Hz, 2H), 7.40 (t,  $J = 7.5$  Hz, 2H), 2.86 ppm (s, 3H);  $^{13}\text{C NMR}$  (126 MHz,  $\text{CD}_2\text{Cl}_2$ )  $\delta$  170.6, 139.2, 127.8, 126.8, 124.1, 120.3, 116.7, 28.1 ppm; **FT-IR**:  $\tilde{\nu} = 2924, 2531, 1977, 1678, 1430, 1295, 1236, 1151, 1122, 942$   $\text{cm}^{-1}$ ; **HR-MS**: calc. for  $[\text{M}+\text{H}]^+$   $\text{C}_{14}\text{H}_{12}\text{ON} = 210.0913$  found: 210.0913.



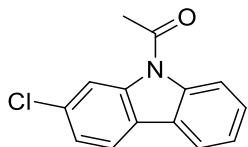
#### 9H-carbazole-9-carbaldehyde (89b)

Prepared according to general procedure A; The product was isolated as white solid (23 mg, 0.12 mmol, 58%) after electrolysis;  $R_f = 0.57$  (cyclohexane / ethyl acetate = 4:1);  $^1\text{H NMR}$  (700 MHz,  $\text{CDCl}_3$ )  $\delta$  9.69 (s, 1H), 8.58 (s, 1H), 7.98 (dd,  $J = 7.2, 3.6$  Hz, 2H), 7.71 (s, 1H), 7.53 – 7.45 (m, 2H), 7.43 ppm (t,  $J = 7.4$  Hz, 2H);  $^{13}\text{C NMR}$  (176 MHz,  $\text{CDCl}_3$ )  $\delta$  157.6, 137.9, 137.3, 127.9, 127.2, 126.3, 124.8, 124.5, 120.9, 120.0, 117.0, 110.1 ppm; **FT-IR**:  $\tilde{\nu} = 2927, 2514, 1977, 1673, 1589, 1361, 1302, 1216, 1081, 946$   $\text{cm}^{-1}$ ; **HR-MS**: calc. for  $[\text{M}+\text{H}]^+$   $\text{C}_{13}\text{H}_{10}\text{ON} = 196.0757$  found: 196.0759.



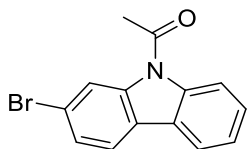
#### 1-(2-fluoro-9H-carbazol-9-yl)ethan-1-one (89c)

Prepared according to general procedure A; The product was isolated as pale yellow solid (24 mg, 0.11 mmol, 53%) after electrolysis;  $R_f = 0.47$  (cyclohexane / ethyl acetate = 4:1);  $^1\text{H NMR}$  (500 MHz,  $\text{CDCl}_3$ )  $\delta$  8.11 – 8.03 (m, 2H), 7.93 (dd,  $J = 7.7, 0.8$  Hz, 1H), 7.89 (dd,  $J = 8.5, 5.6$  Hz, 1H), 7.49 – 7.42 (m, 1H), 7.42 – 7.35 (m, 1H), 7.16 – 7.08 (m, 1H), 2.86 ppm (s, 3H);  $^{13}\text{C NMR}$  (126 MHz,  $\text{CDCl}_3$ )  $\delta$  170.1, 162.5 (d,  $J = 243.0$  Hz), 139.4 (d,  $J = 12.4$  Hz), 138.8, 127.0, 126.1, 124.0, 122.5, 120.5 (d,  $J = 10.1$  Hz), 119.8, 115.9, 111.7 (d,  $J = 24.0$  Hz), 104.6 (d,  $J = 29.4$  Hz), 27.7 ppm; **FT-IR**:  $\tilde{\nu} = 3049, 2159, 1977, 1692, 1382, 1365, 1131, 1062, 1022, 942$   $\text{cm}^{-1}$ ; **HR-MS**: calc. for  $[\text{M}+\text{H}]^+ \text{C}_{14}\text{H}_{11}\text{ONF} = 228.0819$  found: 228.0820.



### 1-(2-chloro-9H-carbazol-9-yl)ethan-1-one (89d)

Prepared according to general procedure A; The product was isolated as pale yellow solid (35 mg, 0.14 mmol, 72%) after electrolysis;  $R_f = 0.50$  (cyclohexane / ethyl acetate = 4:1);  $^1\text{H NMR}$  (500 MHz,  $\text{CDCl}_3$ )  $\delta$  8.32 (s, 1H), 8.06 (d,  $J = 8.4$  Hz, 1H), 7.93 (d,  $J = 7.7$  Hz, 1H), 7.84 (d,  $J = 8.2$  Hz, 1H), 7.51 – 7.44 (m, 1H), 7.40 – 7.33 (m, 2H), 2.85 ppm (s, 3H);  $^{13}\text{C NMR}$  (126 MHz,  $\text{CDCl}_3$ )  $\delta$  170.0, 139.3, 138.7, 133.2, 127.6, 125.9, 124.9, 124.3, 124.0, 120.5, 120.1, 117.1, 116.0, 27.8 ppm; **FT-IR**:  $\tilde{\nu} = 3142, 2159, 1689, 1595, 1468, 1451, 1364, 1271, 1187, 913$   $\text{cm}^{-1}$ ; **HR-MS**: calc. for  $[\text{M}+\text{H}]^+ \text{C}_{14}\text{H}_{11}\text{O N}^{35}\text{Cl} = 244.0524$  found: 244.0525  $\text{C}_{14}\text{H}_{11}\text{ON}^{37}\text{Cl} = 246.0494$  found: 246.0495.

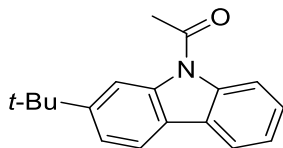


### 1-(2-bromo-9H-carbazol-9-yl)ethan-1-one (89e)

Prepared according to general procedure A; The product was isolated as pale yellow solid (40 mg, 0.14 mmol, 69%) after electrolysis;  $R_f = 0.63$  (cyclohexane / ethyl acetate = 4:1);  $^1\text{H NMR}$  (500 MHz,  $\text{CDCl}_3$ )  $\delta$  8.49 (s, 1H), 8.06 (d,  $J = 8.5$  Hz, 1H), 7.94 (d,  $J = 7.7$  Hz, 1H), 7.83 – 7.77 (m, 1H), 7.53 – 7.46 (m, 2H), 7.39 (t,  $J = 7.5$  Hz, 1H), 2.85 (s, 3H) ppm;  $^{13}\text{C NMR}$  (126 MHz,  $\text{CDCl}_3$ )  $\delta$  170.0, 139.5, 138.5, 127.8, 127.1, 125.8, 125.2, 124.0, 121.1, 120.8, 120.1, 119.9, 116.0, 27.8

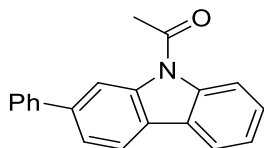


ppm; **FT-IR**:  $\tilde{\nu}$  = 3132, 2924, 2526, 1976, 1594, 1409, 1325, 1274, 1034, 906  $\text{cm}^{-1}$ ; **HR-MS**: calc. for  $[\text{M}+\text{H}]^+$   $\text{C}_{14}\text{H}_{11}\text{ON}^{79}\text{Br}$  = 288.0018 found: 288.0023  $\text{C}_{14}\text{H}_{11}\text{ON}^{81}\text{Br}$  = 289.9998 found: 290.0002.



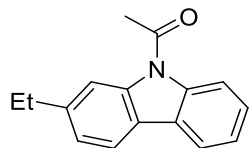
### 1-(2-(*tert*-butyl)-9H-carbazol-9-yl)ethan-1-one (89f)

Prepared according to general procedure A; The product was isolated as white solid (39 mg, 0.15 mmol, 74%) after electrolysis;  $R_f$  = 0.59 (cyclohexane / ethyl acetate = 4:1);  **$^1\text{H}$  NMR** (500 MHz,  $\text{CD}_2\text{Cl}_2$ )  $\delta$  8.30 (s, 1H), 8.18 (d,  $J$  = 8.4 Hz, 1H), 7.98 (dd,  $J$  = 7.7, 1.4 Hz, 1H), 7.93 (d,  $J$  = 8.1 Hz, 1H), 7.51 – 7.42 (m, 2H), 7.41 – 7.34 (m, 1H), 2.87 (s, 3H), 1.44 ppm (s, 9H);  **$^{13}\text{C}$  NMR** (126 MHz,  $\text{CD}_2\text{Cl}_2$ )  $\delta$  170.7, 151.6, 139.6, 139.4, 127.3, 126.8, 124.3, 124.0, 121.9, 120.1, 119.7, 116.7, 113.6, 35.9, 32.0, 28.2 ppm; **FT-IR**:  $\tilde{\nu}$  = 2961, 2159, 1691, 1601, 1497, 1460, 1325, 1206, 1018, 860  $\text{cm}^{-1}$ ; **HR-MS**: calc. for  $[\text{M}+\text{H}]^+$   $\text{C}_{14}\text{H}_{12}\text{ON}$  = 266.1539 found: 266.1541.



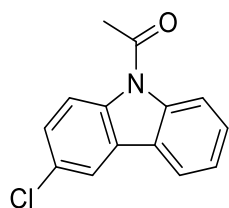
### 1-(2-phenyl-9H-carbazol-9-yl)ethan-1-one (89g)

Prepared according to general procedure A; The product was isolated as pale yellow solid (25 mg, 0.09 mmol, 44%) after electrolysis;  $R_f$  = 0.47 (cyclohexane / ethyl acetate = 4:1);  **$^1\text{H}$  NMR** (500 MHz,  $\text{CDCl}_3$ )  $\delta$  8.51 (d,  $J$  = 1.5 Hz, 1H), 8.19 (d,  $J$  = 8.4 Hz, 1H), 8.06 – 8.01 (m, 2H), 7.72 – 7.69 (m, 2H), 7.64 (dd,  $J$  = 8.0, 1.5 Hz, 1H), 7.52 – 7.47 (m, 3H), 7.43 – 7.37 (m, 2H), 2.93 ppm (s, 3H);  **$^{13}\text{C}$  NMR** (126 MHz,  $\text{CDCl}_3$ )  $\delta$  170.3, 141.6, 141.0, 139.4, 139.1, 129.0, 127.7, 127.6, 127.4, 126.4, 125.6, 123.9, 123.3, 120.1, 120.1, 116.3, 115.3, 28.0 ppm; **FT-IR**:  $\tilde{\nu}$  = 2924, 2159, 1977, 1695, 1459, 1448, 1306, 1265, 1013, 913  $\text{cm}^{-1}$ ; **HR-MS**: calc. for  $[\text{M}+\text{H}]^+$   $\text{C}_{20}\text{H}_{16}\text{ON}$  = 286.1226 found: 286.1229.



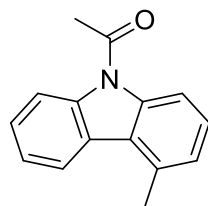
### 1-(2-ethyl-9H-carbazol-9-yl)ethan-1-one (89h)

Prepared according to general procedure A using a (0.2 mmol); The product was isolated as pale yellow solid (21 mg, 0.14 mmol, 44%) after electrolysis;  $R_f = 0.53$  (cyclohexane / ethyl acetate = 4:1);  **$^1\text{H NMR}$**  (500 MHz,  $\text{CDCl}_3$ )  $\delta$  8.15 (d,  $J = 8.4$  Hz, 1H), 8.09 (s, 1H), 7.95 (d,  $J = 7.2$  Hz, 1H), 7.89 (d,  $J = 7.9$  Hz, 1H), 7.48 – 7.41 (m, 1H), 7.40 – 7.33 (m, 1H), 7.24 (d,  $J = 7.9$  Hz, 1H), 2.88 (s, 3H), 2.84 (q,  $J = 7.6$  Hz, 2H), 1.34 ppm (t,  $J = 7.6$  Hz, 3H);  **$^{13}\text{C NMR}$**  (126 MHz,  $\text{CDCl}_3$ )  $\delta$  170.3, 144.3, 139.2, 138.7, 126.9, 126.7, 124.4, 123.9, 123.7, 119.7, 119.7, 116.2, 115.8, 29.9, 28.0, 16.4 ppm; **FT-IR**:  $\tilde{\nu} = 2965, 2866, 2116, 1621, 1421, 1325, 1292, 1192, 1057, 922$   $\text{cm}^{-1}$ ; **HR-MS**: calc. for  $[\text{M}+\text{H}]^+$   $\text{C}_{16}\text{H}_{16}\text{ON} = 238.1226$  found: 238.1228.



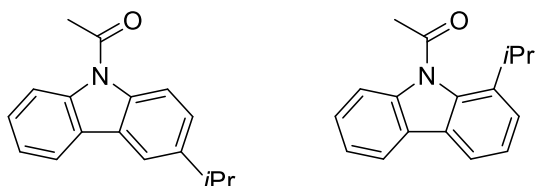
### 1-(3-chloro-9H-carbazol-9-yl)ethan-1-one (89i)

Prepared according to general procedure A; The product was isolated as yellow solid (18 mg, 0.07 mmol, 37%) after electrolysis;  $R_f = 0.50$  (cyclohexane / ethyl acetate = 4:1);  **$^1\text{H NMR}$**  (400 MHz,  $\text{CDCl}_3$ )  $\delta$  8.22 (d,  $J = 8.9$  Hz, 1H), 8.08 (d,  $J = 8.5$  Hz, 1H), 7.94 – 7.90 (m, 2H), 7.52 – 7.48 (m, 1H), 7.42 – 7.37 (m, 2H), 2.85 ppm (s, 3H);  **$^{13}\text{C NMR}$**  (101 MHz,  $\text{CDCl}_3$ )  $\delta$  169.9, 139.0, 137.2, 129.5, 128.1, 127.8, 127.4, 125.5, 124.0, 120.3, 119.7, 117.8, 116.1, 27.8 ppm; **FT-IR**:  $\tilde{\nu} = 3060, 2933, 2510, 1616, 1582, 1484, 1329, 1128, 1022, 982$   $\text{cm}^{-1}$ ; **HR-MS**: calc. for  $[\text{M}+\text{H}]^+$   $\text{C}_{14}\text{H}_{11}\text{ON}^{35}\text{Cl} = 244.0524$  found: 244.0525  $\text{C}_{14}\text{H}_{11}\text{ON}^{37}\text{Cl} = 246.0494$  found: 246.0495.



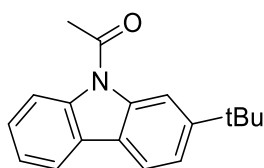
### 1-(4-methyl-9*H*-carbazol-9-yl)ethan-1-one (89j)

Prepared according to general procedure A; The product was isolated as pale white solid (16 mg, 0.07 mmol, 36%) after electrolysis;  $R_f = 0.57$  (cyclohexane / ethyl acetate = 4:1);  $^1\text{H NMR}$  (400 MHz,  $\text{CD}_2\text{Cl}_2$ )  $\delta$  8.29 (d,  $J = 8.5$  Hz, 1H), 8.16 (d,  $J = 7.7$  Hz, 1H), 8.07 (d,  $J = 8.5$  Hz, 1H), 7.54 – 7.45 (m, 1H), 7.46 – 7.34 (m, 2H), 7.19 (d,  $J = 7.4$  Hz, 1H), 2.87 (s, 3H), 2.84 ppm (s, 3H);  $^{13}\text{C NMR}$  (101 MHz,  $\text{CD}_2\text{Cl}_2$ )  $\delta$  170.8, 139.4, 139.3, 133.8, 127.6, 127.3, 127.1, 126.0, 125.0, 124.0, 123.1, 116.5, 114.1, 28.4, 21.5 ppm; **FT-IR**:  $\tilde{\nu} = 2923, 2515, 1479, 1456, 1448, 1434, 1416, 1313, 1247, 983$   $\text{cm}^{-1}$ ; **HR-MS**: calc. for  $[\text{M}+\text{H}]^+$   $\text{C}_{15}\text{H}_{14}\text{ON} = 224.1070$  found: 224.1070.



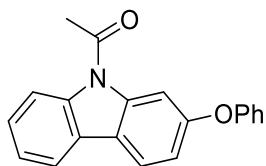
### 1-(isopropyl-9*H*-carbazol-9-yl)ethan-1-one (89k) and 1-(1-isopropyl-9*H*-carbazol-9-yl)ethan-1-one (89k')

Prepared according to general procedure A; Combined yield of regioisomers = 46% (23 mg, 0.09 mmol, ratio of isolated isomers is 2.3:1); Pale yellow oils;  $R_{f(2i)} = 0.53$  (cyclohexane / ethyl acetate = 4:1);  $^1\text{H NMR}$  (500 MHz,  $\text{CDCl}_3$ )  $\delta$  8.24 (d,  $J = 8.4$  Hz, 1H), 8.09 (d,  $J = 8.6$  Hz, 1H), 8.00 (dd,  $J = 7.6, 0.7$  Hz, 1H), 7.85 (d,  $J = 1.8$  Hz, 1H), 7.49 – 7.44 (m, 1H), 7.41 – 7.34 (m, 2H), 3.09 (hept,  $J = 7.2$  Hz, 1H), 2.87 (s, 3H), 1.36 ppm (d,  $J = 6.9$  Hz, 6H);  $^{13}\text{C NMR}$  (126 MHz,  $\text{CDCl}_3$ )  $\delta$  170.1, 144.7, 139.1, 137.1, 127.3, 126.7, 126.2, 123.7, 119.8, 117.4, 116.5, 116.1, 34.1, 27.8, 24.5 ppm. **FT-IR**:  $\tilde{\nu} = 3071, 2961, 2851, 2666, 1452, 1368, 1240, 1026, 982$   $\text{cm}^{-1}$ ; **HR-MS**: calc. for  $[\text{M}+\text{H}]^+$   $\text{C}_{17}\text{H}_{18}\text{ON} = 252.1383$  found: 252.1385;  $R_{f(2i')} = 0.69$  (cyclohexane / ethyl acetate = 4:1);  $^1\text{H NMR}$  (500 MHz,  $\text{CDCl}_3$ )  $\delta$  8.00 – 7.92 (m, 2H), 7.82 (dd,  $J = 7.0, 1.8$  Hz, 1H), 7.49 – 7.34 (m, 4H), 3.30 (hept,  $J = 6.8$  Hz, 1H), 2.67 (s, 3H), 1.32 ppm (d,  $J = 6.8$  Hz, 6H);  $^{13}\text{C NMR}$  (126 MHz,  $\text{CDCl}_3$ )  $\delta$  172.3, 140.3, 137.8, 137.7, 128.2, 127.2, 126.9, 125.2, 125.0, 123.6, 120.0, 117.5, 114.8, 30.5, 26.8, 23.8 ppm.



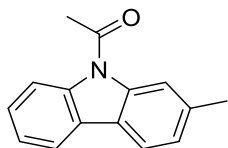
### 1-(2-(tert-butyl)-9H-carbazol-9-yl)ethan-1-one (89l)

Prepared according to general procedure A; The product was isolated as white solid (41 mg, 0.16 mmol, 77%) after electrolysis;  $R_f = 0.59$  (cyclohexane / ethyl acetate = 4:1);  $^1\text{H NMR}$  (500 MHz,  $\text{CD}_2\text{Cl}_2$ )  $\delta$  8.30 (s, 1H), 8.18 (d,  $J = 8.4$  Hz, 1H), 7.98 (dd,  $J = 7.7, 1.4$  Hz, 1H), 7.93 (d,  $J = 8.1$  Hz, 1H), 7.51 – 7.42 (m, 2H), 7.41 – 7.34 (m, 1H), 2.87 (s, 3H), 1.44 ppm (s, 9H);  $^{13}\text{C NMR}$  (126 MHz,  $\text{CD}_2\text{Cl}_2$ )  $\delta$  170.7, 151.6, 139.6, 139.4, 127.3, 126.8, 124.3, 124.0, 121.9, 120.1, 119.7, 116.7, 113.6, 35.9, 32.0, 28.2 ppm; **FT-IR**:  $\tilde{\nu} = 2961, 2159, 1691, 1601, 1497, 1460, 1325, 1206, 1018, 860$   $\text{cm}^{-1}$ ; **HR-MS**: calc. for  $[\text{M}+\text{H}]^+ \text{C}_{14}\text{H}_{12}\text{ON} = 266.1539$  found: 266.1541. All physical data are also given above (2g).



### 1-(2-phenoxy-9H-carbazol-9-yl)ethan-1-one (89m)

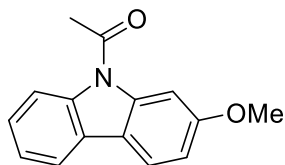
Prepared according to general procedure A; The product was isolated as white solid (31 mg, 0.10 mmol, 51%) after electrolysis;  $R_f = 0.57$  (cyclohexane / ethyl acetate = 4:1);  $^1\text{H NMR}$  (500 MHz,  $\text{CD}_2\text{Cl}_2$ )  $\delta$  8.12 (d,  $J = 8.3$  Hz, 1H), 8.02 – 7.93 (m, 3H), 7.51 – 7.42 (m, 1H), 7.42 – 7.35 (m, 3H), 7.19 – 7.11 (m, 1H), 7.11 – 7.04 (m, 3H), 2.80 ppm (s, 3H);  $^{13}\text{C NMR}$  (126 MHz,  $\text{CD}_2\text{Cl}_2$ )  $\delta$  170.6, 158.1, 157.4, 140.3, 139.4, 130.4, 127.1, 126.6, 124.2, 123.9, 122.5, 121.0, 120.0, 119.2, 116.4, 115.8, 108.2, 28.1 ppm; **FT-IR**:  $\tilde{\nu} = 2925, 2364, 2031, 1704, 1584, 1420, 1369, 1297, 1036, 827$   $\text{cm}^{-1}$ ; **HR-MS**: calc. for  $[\text{M}+\text{H}]^+ \text{C}_{20}\text{H}_{16}\text{O}_2\text{N} = 302.1176$  found: 302.1178.



### 1-(2-methyl-9H-carbazol-9-yl)ethan-1-one (89n)

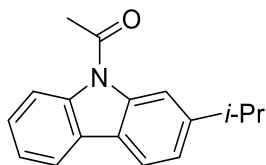
Prepared according to general procedure A; The product was isolated as white solid (20 mg, 0.09 mmol, 45%) after electrolysis;  $R_f = 0.47$  (cyclohexane / ethyl acetate = 4:1);  $^1\text{H NMR}$  (500 MHz,  $\text{CD}_2\text{Cl}_2$ )  $\delta$  8.18 (d,  $J = 8.4$  Hz, 1H), 8.05 (s, 1H), 7.99 – 7.95 (m, 1H), 7.88 (d,  $J = 7.8$  Hz, 1H), 7.48 – 7.41 (m, 1H), 7.41 – 7.34 (m, 1H), 7.24 – 7.21 (m, 1H), 2.85 (s, 3H), 2.54 ppm (s, 3H);  $^{13}\text{C}$

**NMR** (126 MHz, CD<sub>2</sub>Cl<sub>2</sub>)  $\delta$  170.7, 139.6, 139.2, 138.2, 127.2, 126.9, 125.3, 124.4, 124.0, 120.0, 119.9, 117.1, 116.7, 28.2, 22.6 ppm; **FT-IR**:  $\tilde{\nu}$  = 2918, 2519, 2029, 1977, 1600, 1459, 1369, 1196, 982, 808 cm<sup>-1</sup>; **HR-MS**: calc. for [M+H]<sup>+</sup> C<sub>15</sub>H<sub>14</sub>ON = 224.1070 found: 224.1070.



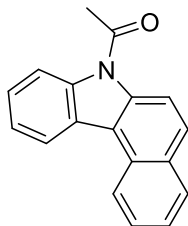
### 1-(2-methoxy-9H-carbazol-9-yl)ethan-1-one (89o)

Prepared according to general procedure A; The product was isolated as pale yellow solid (22 mg, 0.09 mmol, 46%) after electrolysis;  $R_f$  = 0.43 (cyclohexane / ethyl acetate = 4:1); **<sup>1</sup>H NMR** (400 MHz, CDCl<sub>3</sub>)  $\delta$  8.03 (d,  $J$  = 7.7 Hz, 1H), 7.93 – 7.86 (m, 2H), 7.83 (d,  $J$  = 8.5 Hz, 1H), 7.43 – 7.32 (m, 2H), 6.97 (dd,  $J$  = 8.5, 2.3 Hz, 1H), 3.92 (s, 3H), 2.85 ppm (s, 3H); **<sup>13</sup>C NMR** (101 MHz, CDCl<sub>3</sub>)  $\delta$  170.3, 159.9, 140.2, 138.5, 126.8, 126.0, 123.8, 120.3, 119.8, 119.3, 115.9, 111.5, 102.1, 55.9, 27.8 ppm; **FT-IR**:  $\tilde{\nu}$  = 3150, 2182, 1597, 1498, 1372, 1278, 1201, 1163, 1025, 945 cm<sup>-1</sup>; **HR-MS**: calc. for [M+H]<sup>+</sup> C<sub>15</sub>H<sub>14</sub>O<sub>2</sub>N = 240.1019 found: 240.1020.



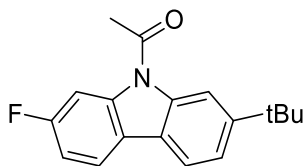
### 1-(2-isopropyl-9H-carbazol-9-yl)ethan-1-one (89p)

Prepared according to general procedure A; The product was isolated as pale yellow solid (33 mg, 0.13 mmol, 66%) after electrolysis;  $R_f$  = 0.59 (cyclohexane / ethyl acetate = 4:1); **<sup>1</sup>H NMR** (500 MHz, CDCl<sub>3</sub>)  $\delta$  8.15 (d,  $J$  = 7.9 Hz, 2H), 7.96 (d,  $J$  = 7.5 Hz, 1H), 7.90 (d,  $J$  = 7.9 Hz, 1H), 7.47 – 7.42 (m, 1H), 7.39 – 7.34 (m, 1H), 7.29 (dd,  $J$  = 7.9, 1.4 Hz, 1H), 3.10 (hept,  $J$  = 6.9 Hz, 1H), 2.89 (s, 3H), 1.36 ppm (d,  $J$  = 6.9 Hz, 6H); **<sup>13</sup>C NMR** (126 MHz, CDCl<sub>3</sub>)  $\delta$  170.3, 149.1, 139.2, 138.8, 126.9, 126.7, 124.5, 123.7, 122.5, 119.7, 119.7, 116.2, 114.5, 35.1, 28.0, 24.5 ppm; **FT-IR**:  $\tilde{\nu}$  = 2958, 2867, 2160, 1695, 1496, 1422, 1284, 1241, 1104, 936 cm<sup>-1</sup>; **HR-MS**: calc. for [M+H]<sup>+</sup> C<sub>17</sub>H<sub>18</sub>ON = 252.1383 found: 252.1385.



### 1-(7H-benzo[c]carbazol-7-yl)ethan-1-one (89q)

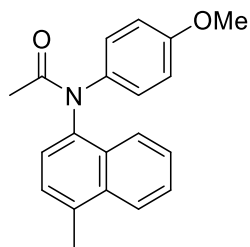
Prepared according to general procedure A; The product was isolated as white solid (33 mg, 0.13 mmol, 64%) after electrolysis;  $R_f = 0.35$  (cyclohexane / ethyl acetate = 4:1);  $^1\text{H NMR}$  (400 MHz,  $\text{CD}_2\text{Cl}_2$ )  $\delta$  8.82 (d,  $J = 8.5$  Hz, 1H), 8.63 – 8.55 (m, 1H), 8.48 (d,  $J = 9.2$  Hz, 1H), 8.33 – 8.25 (m, 1H), 8.03 (d,  $J = 8.2$  Hz, 1H), 7.95 (d,  $J = 9.1$  Hz, 1H), 7.79 – 7.70 (m, 1H), 7.62 – 7.48 (m, 3H), 2.95 ppm (s, 3H);  $^{13}\text{C NMR}$  (101 MHz,  $\text{CD}_2\text{Cl}_2$ )  $\delta$  171.0, 138.7, 137.5, 131.3, 129.5, 129.2, 128.8, 127.9, 127.3, 126.6, 125.3, 124.3, 124.2, 122.7, 119.7, 116.5, 116.4, 28.6 ppm; **FT-IR**:  $\tilde{\nu} = 3049, 2159, 1977, 1692, 1382, 1365, 1131, 1062, 1022, 942$   $\text{cm}^{-1}$ ; **HR-MS**: calc. for  $[\text{M}+\text{H}]^+$   $\text{C}_{18}\text{H}_{14}\text{ON}$  = 260.1070 found: 260.1072.



### 1-(2-(tert-butyl)-7-fluoro-9H-carbazol-9-yl)ethan-1-one (89r)

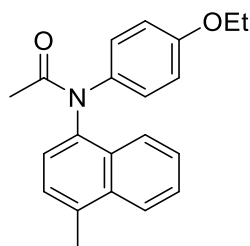
Prepared according to general procedure A; The product was isolated as pale yellow solid (39 mg, 0.14 mmol, 69%) after electrolysis;  $R_f = 0.67$  (cyclohexane / ethyl acetate = 4:1);  $^1\text{H NMR}$  (500 MHz,  $\text{CD}_2\text{Cl}_2$ )  $\delta$  8.12 (d,  $J = 1.6$  Hz, 1H), 8.04 (dd,  $J = 11.1, 2.4$  Hz, 1H), 7.94 – 7.83 (m, 2H), 7.52 – 7.44 (m, 1H), 7.18 – 7.06 (m, 1H), 2.85 (s, 3H), 1.43 ppm (s, 9H);  $^{13}\text{C NMR}$  (126 MHz,  $\text{CD}_2\text{Cl}_2$ )  $\delta$  170.6, 162.6 (d,  $J = 241.5$  Hz), 151.2, 140.1 (d,  $J = 12.4$  Hz), 139.7, 123.9, 123.0, 122., 120.7 (d,  $J = 10.1$  Hz), 119.6, 113.2, 111.7 (d,  $J = 23.9$  Hz), 104.8 (d,  $J = 29.4$  Hz), 35.8, 32.0, 28.1 ppm; **FT-IR**:  $\tilde{\nu} = 2952, 2865, 1996, 1498, 1367, 1264, 1020, 1009, 952$   $\text{cm}^{-1}$ ; **HR-MS**: calc. for  $[\text{M}+\text{H}]^+$   $\text{C}_{18}\text{H}_{19}\text{ONF}$  = 284.1445 found: 284.1449.

*Note: Compounds 110a-110p exist as rotamers because of the restricted rotation around C–N bond. Major rotamer peaks are reported except for 110m.*



### ***N*-(4-methoxyphenyl)-*N*-(4-methylnaphthalen-1-yl)acetamide (110a)**

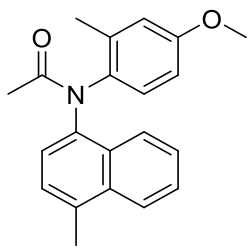
Prepared according to general procedure B using *N*-(4-methoxyphenyl)acetamide (**108a**, 0.2 mmol, 1 equiv.) and 1-methylnaphthalene (**109a**, 0.4 mmol, 2 equiv.); The product was isolated as pale yellow oil (56.1 mg, 0.18 mmol, 92%) after electrolysis;  $R_f = 0.22$  (pentane / acetone = 4:1);  **$^1\text{H NMR}$**  (500 MHz,  $\text{CD}_2\text{Cl}_2$ )  $\delta$  8.12 – 8.00 (m, 2H), 7.63 – 7.54 (m, 2H), 7.45 – 7.27 (m, 4H), 6.84 (dd,  $J = 34.0, 8.6$  Hz, 2H), 3.73 (s, 3H), 2.73 (s, 3H), 1.88 ppm (s, 3H); major rotamer  **$^{13}\text{C NMR}$**  (126 MHz,  $\text{CD}_2\text{Cl}_2$ )  $\delta$  171.4, 157.8, 138.5, 136.2, 134.4, 131.2, 129.0, 127.6, 127.4, 127.2, 127.0, 126.9, 125.5, 123.9, 114.2, 56.0, 23.7, 19.8 ppm; **FT-IR**:  $\tilde{\nu} = 3001, 2836, 2121, 1710, 1667, 1507, 1440, 1421, 1320, 1243, 986$   $\text{cm}^{-1}$ ; **HR-MS**: calc. for  $[\text{M}+\text{H}]^+$   $\text{C}_{20}\text{H}_{20}\text{O}_2\text{N} = 306.1489$  found: 306.1490.



### ***N*-(4-ethoxyphenyl)-*N*-(4-methylnaphthalen-1-yl)acetamide (110b)**

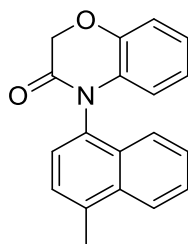
Prepared according to general procedure B using *N*-(4-ethoxyphenyl)acetamide (**108b**, 0.2 mmol, 1 equiv.) and 1-methylnaphthalene (**109a**, 0.4 mmol, 2 equiv.); The product was isolated as white solid (55 mg, 0.17 mmol, 56%) after electrolysis;  $R_f = 0.28$  (pentane / acetone = 4:1);  **$^1\text{H NMR}$**  (500 MHz,  $\text{CD}_2\text{Cl}_2$ )  $\delta$  8.10 – 8.03 (m, 2H), 7.63 – 7.56 (m, 2H), 7.44 – 7.27 (m, 4H), 6.89 – 6.75 (m, 2H), 4.01 – 3.93 (m, 2H), 2.73 – 2.61 (m, 3H), 2.20 – 1.86 (m, 3H), 1.41 – 1.32 (m, 3H) ppm; major rotamer  **$^{13}\text{C NMR}$**  (126 MHz,  $\text{CD}_2\text{Cl}_2$ )  $\delta$  171.5, 157.3, 138.5, 136.2, 134.4, 131.2, 129.0, 127.7, 127.3, 127.2, 127.0, 127.0, 125.5, 123.9, 114.8, 64.2, 23.7, 19.8, 15.1 ppm; **FT-IR**:  $\tilde{\nu} =$

2978, 2384, 1990, 1596, 1421, 1390, 1241, 1107, 1044, 922  $\text{cm}^{-1}$ ; **HR-MS**: calc. for  $[\text{M}+\text{H}]^+$   $\text{C}_{21}\text{H}_{22}\text{O}_2\text{N} = 320.1645$  found: 320.1647.



#### ***N*-(4-methoxy-2-methylphenyl)-*N*-(4-methylnaphthalen-1-yl)acetamide (110c)**

Prepared according to general procedure B using *N*-(4-methoxy-2-methylphenyl)acetamide (**108c**, 0.2 mmol, 1 equiv.) and 1-methylnaphthalene (**109a**, 0.4 mmol, 2 equiv.); The product was isolated as white solid (40.2 mg, 0.13 mmol, 63%) after electrolysis;  $R_f = 0.23$  (pentane / acetone = 4:1);  **$^1\text{H}$  NMR** (500 MHz,  $\text{CD}_2\text{Cl}_2$ )  $\delta$  8.17 – 7.97 (m, 2H), 7.69 – 7.54 (m, 2H), 7.37 – 7.20 (m, 2H), 7.15 – 6.95 (m, 1H), 6.83 (d,  $J = 2.9$  Hz, 1H), 6.54 (dd,  $J = 8.8, 2.9$  Hz, 1H), 3.78 and 3.73 (two s, total 3H), 2.71 and 2.66 (two s, total 3H), 2.44 – 1.90 ppm (m, 6H);  **$^{13}\text{C}$  NMR** (151 MHz,  $\text{CD}_2\text{Cl}_2$ )  $\delta$  171.3, 158.7, 137.0, 135.8, 134.3, 127.7, 127.4, 127.1, 126.9, 126.8, 126.4, 125.6, 125.4, 124.3, 124.1, 116.6, 112.2, 55.8, 31.2, 23.2, 19.8 ppm; **FT-IR**:  $\tilde{\nu} = 3053, 2836, 1977, 1666, 1596, 1389, 1294, 1180, 917$   $\text{cm}^{-1}$ ; **HR-MS**: calc. for  $[\text{M}+\text{H}]^+$   $\text{C}_{21}\text{H}_{22}\text{O}_2\text{N} = 320.1645$  found: 320.1647.

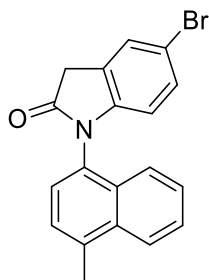


#### **4-(4-methylnaphthalen-1-yl)-2H-benzo[*b*][1,4]oxazin-3(4H)-one (110d)**

Prepared according to general procedure B using 2H-benzo[*b*][1,4]oxazin-3(4H)-one (**108d**, 0.2 mmol, 1 equiv.) and 1-methylnaphthalene (**109a**, 0.4 mmol, 2 equiv.); The product was isolated as yellow solid (43.9 mg, 0.15 mmol, 76%) after electrolysis;  $R_f = 0.44$  (pentane / acetone = 4:1);  **$^1\text{H}$  NMR** (500 MHz,  $\text{CD}_2\text{Cl}_2$ )  $\delta$  8.14 (d,  $J = 8.5$  Hz, 1H), 7.69 – 7.56 (m, 2H), 7.55 – 7.45 (m, 2H), 7.40 (d,  $J = 7.4$  Hz, 1H), 7.11 (dd,  $J = 8.1, 1.2$  Hz, 1H), 7.02 – 6.95 (m, 1H), 6.85 – 6.63 (m, 1H), 6.25 (dd,  $J = 8.1, 1.3$  Hz, 1H), 4.92 (d,  $J = 15.0$  Hz, 1H), 4.86 (d,  $J = 15.0$  Hz, 1H), 2.80 ppm (s,

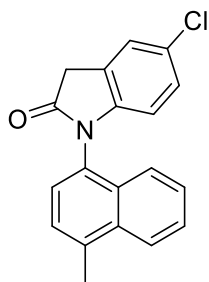


3H);  $^{13}\text{C NMR}$  (126 MHz,  $\text{CD}_2\text{Cl}_2$ )  $\delta$  165.0, 145.3, 137.2, 134.3, 131.4, 131.2, 130.5, 127.7, 127.5, 127.1, 127.1, 125.7, 124.5, 123.2, 123.1, 117.4, 117.2, 68.9, 19.9 ppm; **FT-IR**:  $\tilde{\nu}$  = 2873, 2349, 2114, 1996, 1686, 1592, 1459, 1394, 1377, 1265, 1221, 1193, 930  $\text{cm}^{-1}$ ; **HR-MS**: calc. for  $[\text{M}+\text{H}]^+$   $\text{C}_{19}\text{H}_{16}\text{O}_2\text{N}$  = 290.1176 found: 290.1178.



### 5-bromo-1-(4-methylnaphthalen-1-yl)indolin-2-one (110e)

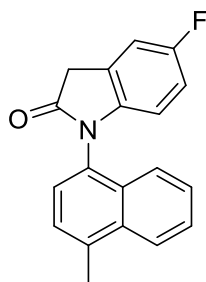
Prepared according to general procedure B using 5-bromoindolin-2-one (**108e**, 0.2 mmol, 1 equiv.) and 1-methylnaphthalene (**109a**, 0.4 mmol, 2 equiv.); The product was isolated as pale yellow solid (38.7 mg, 0.11 mmol, 55%) after electrolysis;  $R_f$  = 0.45 (pentane / acetone = 4:1);  $^1\text{H NMR}$  (500 MHz,  $\text{CD}_2\text{Cl}_2$ )  $\delta$  8.13 (d,  $J$  = 8.4 Hz, 1H), 7.64 – 7.57 (m, 2H), 7.52 – 7.46 (m, 3H), 7.39 (d,  $J$  = 7.4 Hz, 1H), 7.27 – 7.23 (m, 1H), 6.22 (d,  $J$  = 8.4 Hz, 1H), 3.87 (d,  $J$  = 22.5 Hz, 1H), 3.79 (d,  $J$  = 22.5 Hz, 1H), 2.78 ppm (s, 3H);  $^{13}\text{C NMR}$  (126 MHz,  $\text{CD}_2\text{Cl}_2$ )  $\delta$  174.7, 146.1, 137.2, 134.2, 131.2, 130.1, 129.6, 128.2, 127.2, 127.1, 127.1, 127.0, 126.6, 125.62, 123.5, 115.4, 111.5, 36.4, 19.9 ppm; **FT-IR**:  $\tilde{\nu}$  = 2915, 2848, 2385, 2115, 1994, 1721, 1462, 1350, 1239, 969  $\text{cm}^{-1}$ ; **HR-MS**: calc. for  $[\text{M}+\text{H}]^+$   $\text{C}_{19}\text{H}_{15}\text{ON}^{79}\text{Br}$  = 352.0331 found: 352.0333  $\text{C}_{19}\text{H}_{15}\text{ON}^{81}\text{Br}$  = 354.0311 found: 354.0312.



### 5-chloro-1-(4-methylnaphthalen-1-yl)indolin-2-one (110f)

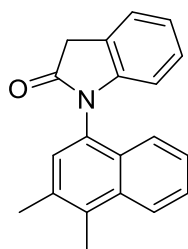
Prepared according to general procedure B using 5-chloroindolin-2-one (**108f**, 0.2 mmol, 1 equiv.) and 1-methylnaphthalene (**109a**, 0.4 mmol, 2 equiv.); The product was isolated as white solid (36.8

mg, 0.12 mmol, 60%) after electrolysis;  $R_f = 0.31$  (pentane / acetone = 4:1);  $^1\text{H NMR}$  (500 MHz,  $\text{CDCl}_3$ )  $\delta$  8.12 – 8.08 (m, 1H), 7.61 – 7.56 (m, 2H), 7.50 – 7.43 (m, 2H), 7.41 – 7.34 (m, 2H), 7.09 (dd,  $J = 8.3, 2.1$  Hz, 1H), 6.27 (d,  $J = 8.4$  Hz, 1H), 3.89 (d,  $J = 22.5$  Hz, 1H), 3.82 (d,  $J = 22.5$  Hz, 1H), 2.77 ppm (s, 3H);  $^{13}\text{C NMR}$  (126 MHz,  $\text{CDCl}_3$ )  $\delta$  174.7, 145.0, 136.8, 133.9, 129.7, 129.0, 128.1, 128.1, 127.0, 126.7, 126.2, 125.9, 125.2, 125.1, 123.1, 110.9, 36.1, 19.7 ppm; **FT-IR**:  $\tilde{\nu} = 2664, 2116, 1719, 1512, 1481, 1356, 1270, 1195, 1110, 1023, 943$   $\text{cm}^{-1}$ ; **HR-MS**: calc. for  $[\text{M}+\text{H}]^+$   $\text{C}_{19}\text{H}_{15}\text{ON}^{35}\text{Cl} = 308.0837$  found: 308.0836  $\text{C}_{19}\text{H}_{15}\text{ON}^{37}\text{Cl} = 310.0807$  found: 310.0807.



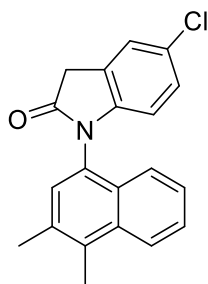
#### 5-fluoro-1-(4-methylnaphthalen-1-yl)indolin-2-one (110g)

Prepared according to general procedure B using 5-fluoroindolin-2-one (**108g**, 0.2 mmol, 1 equiv.) and 1-methylnaphthalene (**109a**, 0.4 mmol, 2 equiv.); The product was isolated as yellow solid (15 mg, 0.05 mmol, 26%) after electrolysis;  $R_f = 0.34$  (pentane / acetone = 4:1);  $^1\text{H NMR}$  (500 MHz,  $\text{CD}_2\text{Cl}_2$ )  $\delta$  8.16 – 8.10 (m, 1H), 7.64 – 7.57 (m, 2H), 7.52 – 7.45 (m, 2H), 7.39 (d,  $J = 7.3$  Hz, 1H), 7.17 – 7.11 (m, 1H), 6.87 – 6.79 (m, 1H), 6.26 (dd,  $J = 8.6, 4.4$  Hz, 1H), 3.87 (d,  $J = 22.4$  Hz, 1H), 3.79 (d,  $J = 22.6$  Hz, 1H), 2.78 ppm (s, 3H);  $^{13}\text{C NMR}$  (126 MHz,  $\text{CD}_2\text{Cl}_2$ )  $\delta$  175.1, 159.7 (d,  $J = 239.4$  Hz), 143.0, 137.1, 134.3, 130.1 (d,  $J = 34.9$  Hz), 127.2, 127.0, 127.0, 126.6, 126.6, 126.5, 125.6, 123.6, 114.5 (d,  $J = 23.5$  Hz), 112.9 (d,  $J = 25.0$  Hz), 110.5 (d,  $J = 8.3$  Hz), 36.9, 19.9 ppm; **FT-IR**:  $\tilde{\nu} = 2915, 2349, 1724, 1480, 1357, 1216, 1110, 1061, 983$   $\text{cm}^{-1}$ ; **HR-MS**: calc. for  $[\text{M}+\text{H}]^+$   $\text{C}_{19}\text{H}_{15}\text{ONF} = 292.1132$  found: 292.1134.



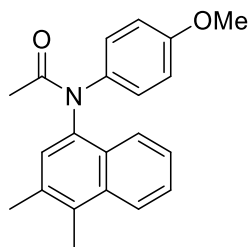
#### 1-(3,4-dimethylnaphthalen-1-yl)indolin-2-one (110h)

Prepared according to general procedure B using indolin-2-one (**108h**, 0.2 mmol, 1 equiv.) and 1,2-dimethylnaphthalene (**109b**, 0.4 mmol, 2 equiv.); The product was isolated as yellow solid (24.1 mg, 0.08 mmol, 42%) after electrolysis;  $R_f = 0.22$  (cyclohexane / ethyl acetate = 4:1);  **$^1\text{H}$  NMR** (500 MHz,  $\text{CDCl}_3$ )  $\delta$  8.13 (d,  $J = 8.6$  Hz, 1H), 7.59 (d,  $J = 8.5$  Hz, 1H), 7.57 – 7.51 (m, 1H), 7.41 – 7.34 (m, 3H), 7.15 – 7.04 (m, 2H), 6.35 (d,  $J = 7.6$  Hz, 1H), 3.90 (d,  $J = 22.4$  Hz, 1H), 3.83 (d,  $J = 22.5$  Hz, 1H), 2.67 (s, 3H), 2.53 ppm (s, 3H);  **$^{13}\text{C}$  NMR** (126 MHz,  $\text{CDCl}_3$ )  $\delta$  175.5, 146.6, 134.2, 133.7, 133.6, 129.4, 128.6, 128.5, 128.1, 126.6, 125.8, 124.7, 124.6, 124.4, 123.1, 122.8, 110.0, 36.3, 20.9, 14.9 ppm; **FT-IR**:  $\tilde{\nu} = 3667, 2976, 2398, 2115, 1994, 1718, 1512, 1486, 1385, 1299, 1192, 980$   $\text{cm}^{-1}$ ; **HR-MS**: calc. for  $[\text{M}+\text{H}]^+ \text{C}_{20}\text{H}_{18}\text{ON} = 288.1383$  found: 288.1384.



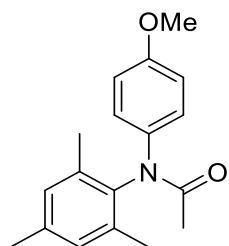
### 5-chloro-1-(3,4-dimethylnaphthalen-1-yl)indolin-2-one (**110i**)

Prepared according to general procedure B using 5-chloroindolin-2-one (**108f**, 0.2 mmol, 1 equiv.) and 1,2-dimethylnaphthalene (**109b**, 0.4 mmol, 2 equiv.); The product was isolated as white solid (49 mg, 0.15 mmol, 76%) after electrolysis;  $R_f = 0.28$  (cyclohexane / ethyl acetate = 4:1);  **$^1\text{H}$  NMR** (500 MHz,  $\text{CDCl}_3$ )  $\delta$  8.13 (d,  $J = 8.6$  Hz, 1H), 7.58 – 7.50 (m, 2H), 7.43 – 7.36 (m, 1H), 7.36 – 7.34 (m, 1H), 7.33 (s, 1H), 7.11 – 7.06 (m, 1H), 6.26 (d,  $J = 8.4$  Hz, 1H), 3.89 (d,  $J = 22.5$  Hz, 1H), 3.81 (d,  $J = 22.5$  Hz, 1H), 2.67 (s, 3H), 2.53 ppm (s, 3H);  **$^{13}\text{C}$  NMR** (126 MHz,  $\text{CDCl}_3$ )  $\delta$  174.8, 145.1, 134.2, 133.9, 133.7, 129.4, 128.3, 128.2, 128.1, 128.1, 126.7, 125.9, 125.9, 125.0, 124.8, 122.9, 110.9, 36.2, 21.2, 15.0 ppm; **FT-IR**:  $\tilde{\nu} = 2922, 2546, 1977, 1609, 1512, 1386, 1286, 1194, 1069, 999$   $\text{cm}^{-1}$ ; **HR-MS**: calc. for  $[\text{M}+\text{H}]^+ \text{C}_{20}\text{H}_{17}\text{ON}^{35}\text{Cl} = 322.0993$  found = 322.0995,  $\text{C}_{20}\text{H}_{17}\text{ON}^{37}\text{Cl} = 324.0964$  found = 324.0964.



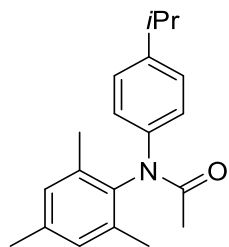
### *N*-(3,4-dimethylnaphthalen-1-yl)-*N*-(4-methoxyphenyl)acetamide (**110j**)

Prepared according to general procedure B using *N*-(4-methoxyphenyl)acetamide (**108a**, 0.2 mmol, 1 equiv.) and 1, 2-dimethylnaphthalene (**109b**, 0.4 mmol, 2 equiv.); The product was isolated as white solid (55 mg, 0.17 mmol, 86%) after electrolysis;  $R_f = 0.16$  (cyclohexane / ethyl acetate = 4:1); major rotamer  $^1\text{H NMR}$  (500 MHz,  $\text{CDCl}_3$ )  $\delta$  8.09 (d,  $J = 8.2$  Hz, 1H), 8.02 (d,  $J = 8.1$  Hz, 1H), 7.59 – 7.48 (m, 2H), 7.33 (d,  $J = 9.3$  Hz, 3H), 6.81 (d,  $J = 9.0$  Hz, 2H), 3.74 (s, 3H), 2.63 (s, 3H), 2.49 (s, 3H), 1.92 ppm (s, 3H);  $^{13}\text{C NMR}$  (126 MHz,  $\text{CDCl}_3$ )  $\delta$  171.6, 157.4, 137.5, 135.9, 134.2, 133.7, 132.7, 129.9, 129.6, 128.4, 126.6, 126.3, 124.6, 123.3, 114.1, 55.5, 23.6, 20.9, 14.9 ppm; **FT-IR**:  $\tilde{\nu} = 2931, 2835, 2089, 1667, 1598, 1506, 1461, 1367, 1293, 1121, 909$   $\text{cm}^{-1}$ ; **HR-MS**: calc. for  $[\text{M}+\text{H}]^+$   $\text{C}_{21}\text{H}_{22}\text{O}_2\text{N} = 320.1645$  found = 320.1647.



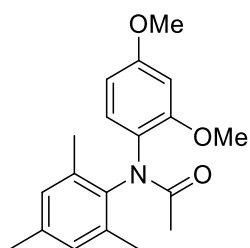
### *N*-mesityl-*N*-(4-methoxyphenyl)acetamide (**110k**)

Prepared according to general procedure B using *N*-(4-methoxyphenyl)acetamide (**108a**, 0.2 mmol, 1 equiv.) and mesitylene (**109c**, 1 mmol, 5 equiv.); The product was isolated as yellow oil (27.1 mg, 0.09 mmol, 46%) after electrolysis;  $R_f = 0.32$  (pentane / acetone = 4:1); major rotamer  $^1\text{H NMR}$  (500 MHz,  $\text{CD}_2\text{Cl}_2$ )  $\delta$  7.20 – 7.15 (m, 2H), 6.98 (s, 2H), 6.81 – 6.76 (m, 2H), 3.75 (s, 3H), 2.31 (s, 3H), 2.15 (s, 6H), 1.83 (s, 3H);  $^{13}\text{C NMR}$  (126 MHz,  $\text{CD}_2\text{Cl}_2$ )  $\delta$  170.7, 157.0, 138.8, 136.7, 134.6, 130.4, 127.9, 125.5, 113.9, 55.9, 23.7, 21.3, 18.3 ppm; **FT-IR**:  $\tilde{\nu} = 2915, 2349, 1995, 1667, 1585, 1482, 1367, 1294, 1197, 1111, 1033$   $\text{cm}^{-1}$ ; **HR-MS**: calc. for  $[\text{M}+\text{H}]^+$   $\text{C}_{18}\text{H}_{22}\text{O}_2\text{N} = 284.1645$  found: 284.1647.



### *N*-(4-isopropylphenyl)-*N*-mesitylacetamide (**110l**)

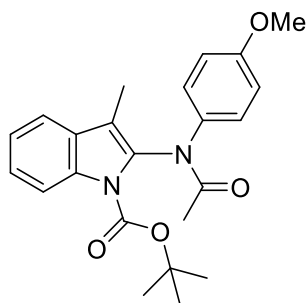
Prepared according to general procedure B using *N*-(4-isopropylphenyl)acetamide (**108i**, 0.2 mmol, 1 equiv.) and mesitylene (**109c**, 1 mmol, 5 equiv.); The product was isolated as yellow oil (27.1 mg, 0.09 mmol, 46%) after electrolysis;  $R_f = 0.43$  (pentane / acetone = 4:1);  $^1\text{H NMR}$  (500 MHz,  $\text{CDCl}_3$ )  $\delta$  7.21 – 7.14 (m, 2H), 7.13 – 7.04 (m, 2H), 6.97 (s, 2H), 2.84 (hept,  $J = 6.9$  Hz, 1H), 2.32 (s, 3H), 2.17 (s, 6H), 1.89 (s, 3H), 1.20 ppm (d,  $J = 6.9$  Hz, 6H);  $^{13}\text{C NMR}$  (126 MHz,  $\text{CDCl}_3$ )  $\delta$  170.7, 145.3, 138.5, 138.3, 138.3, 136.3, 130.0, 126.5, 123.4, 33.6, 24.1, 23.8, 21.2, 18.2 ppm; **FT-IR**:  $\tilde{\nu} = 2959, 1672, 1509, 1481, 1366, 1296, 1192, 1056, 982$   $\text{cm}^{-1}$ ; **HR-MS**: calc. for  $[\text{M}+\text{H}]^+$   $\text{C}_{20}\text{H}_{26}\text{ON} = 296.2009$  found: 296.2011.



### *N*-(2,4-dimethoxyphenyl)-*N*-mesitylacetamide (**110m**)

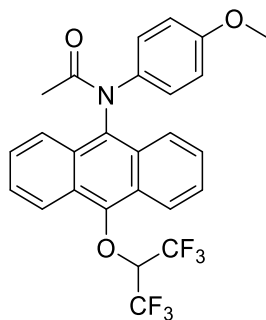
Prepared according to general procedure B using *N*-(2,4-dimethoxyphenyl)acetamide (**108j**, 0.2 mmol, 1 equiv.) and mesitylene (**109c**, 1 mmol, 5 equiv.) in 1:1 DCM:HFIP mixture (0.06 M, 3 mL); The product was isolated as yellow oil (28 mg, 0.09 mmol, 45%) after electrolysis;  $R_f = 0.20$  (pentane / acetone = 4:1); 1:1 rotamers  $^1\text{H NMR}$  (500 MHz,  $\text{CDCl}_3$ )  $\delta$  6.96 – 6.71 (m, 3H), 6.53 (dd,  $J = 4.0, 2.7$  Hz, 1H), 6.39 – 6.31 (m, 1H), 3.89 and 3.88 (two s, total 3H), 3.78 and 3.75 (two s, 3H), 2.30 and 2.28 (two s, total 3H), 2.24, 2.21 and 2.12 (three s, total 6H), 1.97 and 1.91 ppm (two s, total 3H);  $^{13}\text{C NMR}$  (126 MHz,  $\text{CDCl}_3$ )  $\delta$  172.2, 170.4, 159.2, 159.1, 155.1, 154.8, 139.3, 139.2, 137.6, 136.8, 136.3, 136.0, 135.2, 130.0, 129.8, 129.3, 127.1, 126.4, 124.7, 123.6, 104.8, 104.6, 100.0, 99.4, 56.0, 55.6, 55.6, 55.5, 22.7, 21.6, 21.1, 19.0, 18.2, 17.9 ppm; **FT-IR**:  $\tilde{\nu} = 2921,$

2841, 2160, 1668, 1586, 1452, 1294, 1160, 938, 877  $\text{cm}^{-1}$ ; **HR-MS**: calc. for  $[\text{M}+\text{H}]^+$   $\text{C}_{19}\text{H}_{24}\text{O}_3\text{N}$  = 314.1751 found: 314.1752.



***tert*-butyl 2-(*N*-(4-methoxyphenyl)acetamido)-3-methyl-1*H*-indole-1-carboxylate (110n)**

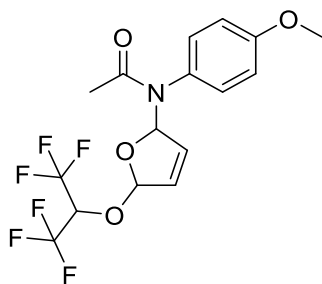
Prepared according to general procedure B using *N*-(4-methoxyphenyl)acetamide (**108a**, 0.2 mmol, 1 equiv.) and *tert*-butyl 3-methyl-1*H*-indole-1-carboxylate (**109d**, 0.4 mmol, 2 equiv.); Yellow solid; The product was isolated as yellow oil (36 mg, 0.09 mmol, 46%) after electrolysis;  $R_f = 0.22$  (cyclohexane / ethyl acetate = 4:1);  $^1\text{H NMR}$  (500 MHz,  $\text{CD}_2\text{Cl}_2$ )  $\delta$  8.15 (d,  $J = 8.4$  Hz, 1H), 7.54 (d,  $J = 7.7$  Hz, 1H), 7.41 – 7.35 (m, 1H), 7.32 – 7.23 (m, 3H), 6.85 – 6.79 (m, 2H), 3.76 (s, 3H), 2.20 (s, 3H), 2.04 (s, 3H), 1.57 ppm (s, 9H);  $^{13}\text{C NMR}$  (126 MHz,  $\text{CD}_2\text{Cl}_2$ )  $\delta$  171.6, 157.8, 149.9, 135.0, 134.9, 133.6, 128.7, 126.4, 125.9, 123.4, 119.8, 116.1, 115.6, 114.1, 85.1, 55.9, 28.4, 23.5, 8.5 ppm; **FT-IR**:  $\tilde{\nu} = 2930, 2836, 2116, 1991, 1685, 1476, 1395, 1286, 936 \text{ cm}^{-1}$ ; **HR-MS**: calc. for  $[\text{M}+\text{H}]^+$   $\text{C}_{23}\text{H}_{27}\text{O}_4\text{N}_2 = 395.1965$  found = 395.1964.



***N*-(10-((1,1,1,3,3,3-hexafluoropropan-2-yl)oxy)anthracen-9-yl)-*N*-(4-methoxyphenyl)acetamide (110o)**

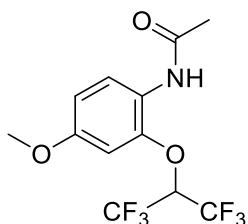
Prepared according to general procedure B using *N*-(4-methoxyphenyl)acetamide (**108a**, 0.2 mmol, 1 equiv.) and anthracene (**109e**, 0.4 mmol, 2 equiv.); The product was isolated as yellow oil (60.1 mg, 0.12 mmol, 60%) after electrolysis;  $R_f = 0.38$  (pentane / acetone = 4:1);  $^1\text{H NMR}$

(400 MHz, CD<sub>2</sub>Cl<sub>2</sub>) δ 8.36 (dd, *J* = 7.5, 2.5 Hz, 2H), 8.22 – 8.13 (m, 2H), 7.69 – 7.59 (m, 4H), 7.29 (dd, 2H), 6.76 (dd, 2H), 5.40 (h, *J* = 5.5 Hz, 1H), 3.71 (s, 3H), 1.70 (s, 3H); <sup>13</sup>C NMR (126 MHz, CDCl<sub>3</sub>) δ 171.7, 157.1, 147.8, 135.4, 132.4, 130.0, 128.3, 127.0, 125.5, 124.1, 123.8, 123.4, 121.7, 121.4 (q, *J* = 284.7 Hz), 114.0, 55.5, 23.7 ppm; <sup>19</sup>F NMR (565 MHz, CDCl<sub>3</sub>) δ -71.42 ppm; **FT-IR**:  $\tilde{\nu}$  = 2937, 2844, 2349, 1991, 1671, 1509, 1439, 1376, 1223, 1054, 905 cm<sup>-1</sup>; **HR-MS**: calc. for [M+H]<sup>+</sup> C<sub>26</sub>H<sub>20</sub>O<sub>3</sub>NF<sub>6</sub> = 508.1342 found: 508.1335.



***N*-5-((1,1,1,3,3,3-hexafluoropropan-2-yl)oxy)-2,5-dihydrofuran-2-yl)-*N*-(4-methoxyphenyl)acetamide (110p)**

Prepared according to general procedure B using *N*-(4-methoxyphenyl)acetamide (**108a**, 0.2 mmol, 1 equiv.) and furan (**109f**, 1 mmol, 5 equiv.); The product was isolated as pale yellow solid (72 mg, 0.18 mmol, 90%) after electrolysis; *R*<sub>f</sub> = 0.23 (cyclohexane / ethyl acetate = 4:1); <sup>1</sup>H NMR (500 MHz, CDCl<sub>3</sub>) δ 7.47 – 7.42 (m, 1H), 7.14 (s, 1H), 6.91 (s, 1H), 6.86 (d, *J* = 7.8 Hz, 2H), 6.03 (d, *J* = 5.8 Hz, 1H), 5.82 – 5.75 (m, 2H), 4.50 (hept, *J* = 5.8 Hz, 1H), 3.81 (s, 3H), 1.83 ppm (s, 3H); <sup>13</sup>C NMR (126 MHz, CDCl<sub>3</sub>) δ 172.1, 159.7, 133.8, 131.2, 130.5, 129.2, 121.7 (d, *J* = 284.2 Hz), 114.5, 107.7, 90.3, 70.9 (hept, *J* = 32.7 Hz), 55.5, 23.3 ppm (*see crystal data*); **FT-IR**:  $\tilde{\nu}$  = 3149, 2850, 2361, 2159, 1977, 1667, 1513, 1373, 1279, 1096, 963 cm<sup>-1</sup>; **HR-MS**: calc. for [M+H]<sup>+</sup> C<sub>16</sub>H<sub>16</sub>O<sub>4</sub>NF<sub>6</sub> = 400.0978 found = 400.0976.

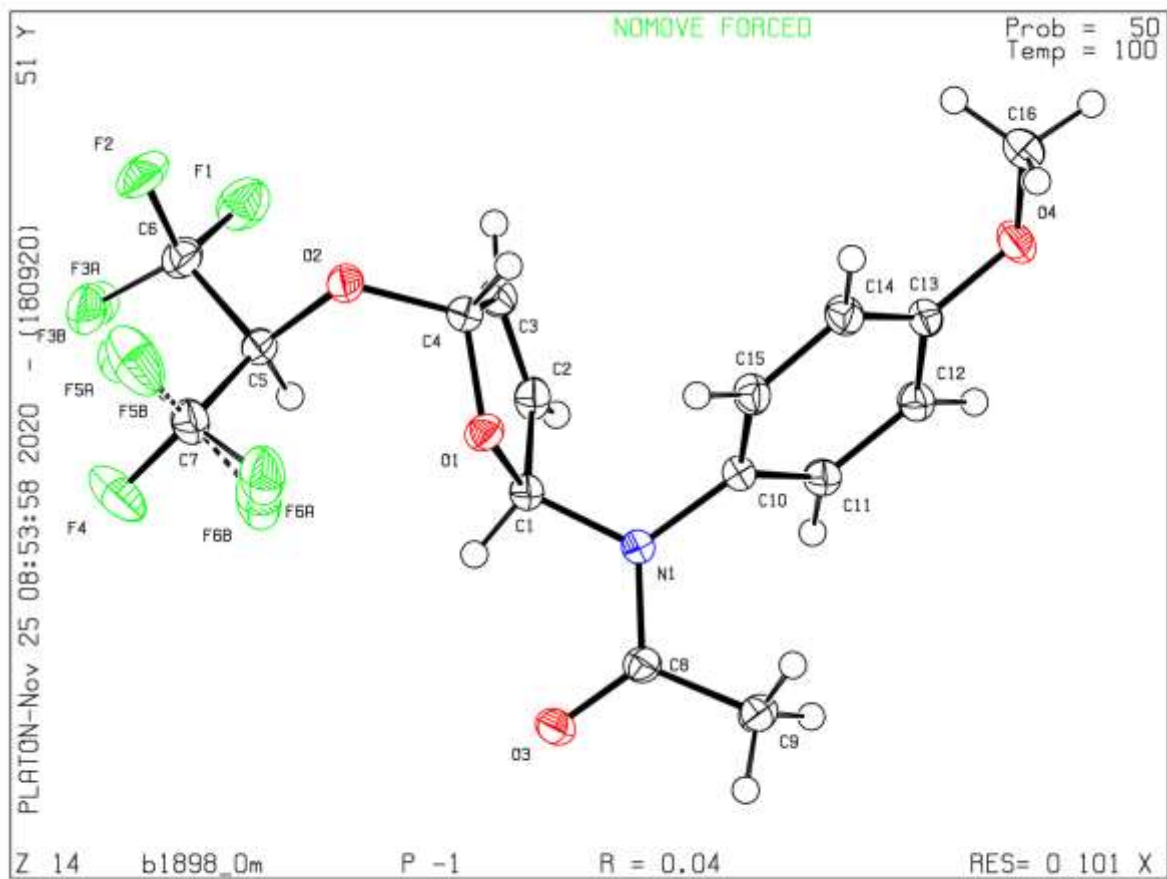


***N*-(2-((1,1,1,3,3,3-hexafluoropropan-2-yl)oxy)-4-methoxyphenyl)acetamide (103')**

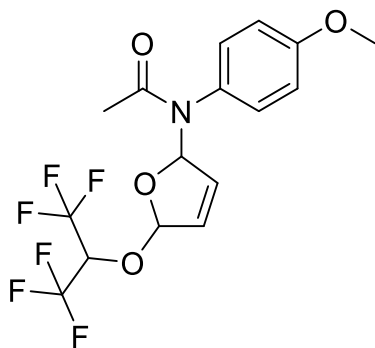
Physical data of **103'**: **<sup>1</sup>H NMR** (500 MHz, CDCl<sub>3</sub>) δ 8.17 (d, *J* = 9.0 Hz, 1H), 7.34 (s, 1H), 6.69 (dd, *J* = 9.0, 2.7 Hz, 1H), 6.58 (d, *J* = 2.7 Hz, 1H), 4.84 (hept, *J* = 5.7 Hz, 1H), 3.79 (s, 3H), 2.18 ppm (s, 3H); **<sup>13</sup>C NMR** (126 MHz, CDCl<sub>3</sub>) δ 168.3, 156.7, 147.4, 123.4, 122.5, 121.0 (q, *J* = 284.8 Hz), 109.1, 102.7, 76.7 (hept, *J* = 33.6 Hz), 55.8, 24.5 ppm.



### 7.3.5 Crystal data



CCDC 2018010

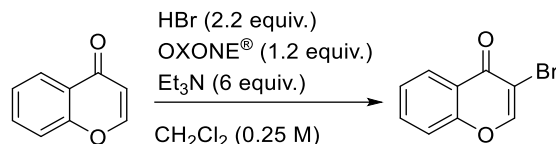


Compound	<b>110p</b>
CCDC	2018010
Data block name	data_b1898_0m
Identification code	B1898_0m
Empirical formula	C <sub>16</sub> H <sub>15</sub> F <sub>6</sub> NO <sub>4</sub>
Formula weight	399.29
Temperature/K	100.0
Crystal system	triclinic
Space group	P-1
a/Å	7.3160(5)
b/Å	11.3203(9)
c/Å	11.6708(10)
α/°	112.918(3)
β/°	92.672(4)
γ/°	107.503(3)
Volume/Å <sup>3</sup>	834.17(12)
Z	2
ρ <sub>calc</sub> /cm <sup>3</sup>	1.590
μ/mm <sup>-1</sup>	0.156
F(000)	408.0
Crystal size/mm <sup>3</sup>	0.749 × 0.505 × 0.144
Radiation	MoKα (λ = 0.71073)
2θ range for data collection/°	4.314 to 61.056
Index ranges	-10 ≤ h ≤ 10, -16 ≤ k ≤ 16, -16 ≤ l ≤ 16
Reflections collected	56063
Independent reflections	5096 [R <sub>int</sub> = 0.0275, R <sub>sigma</sub> = 0.0160]
Data/restraints/parameters	5096/0/333
Goodness-of-fit on F <sup>2</sup>	1.040
Final R indexes [I ≥ 2σ (I)]	R <sub>1</sub> = 0.0359, wR <sub>2</sub> = 0.0938
Final R indexes [all data]	R <sub>1</sub> = 0.0402, wR <sub>2</sub> = 0.0977
Largest diff. peak/hole / e Å <sup>-3</sup>	0.48/-0.30

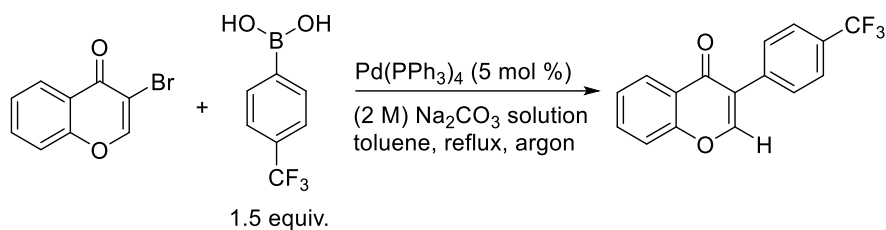
## 7.4 Experimental part for the synthesis of bioactive chromones

### 7.4.1 General procedures

#### Preparation of key building blocks as starting materials

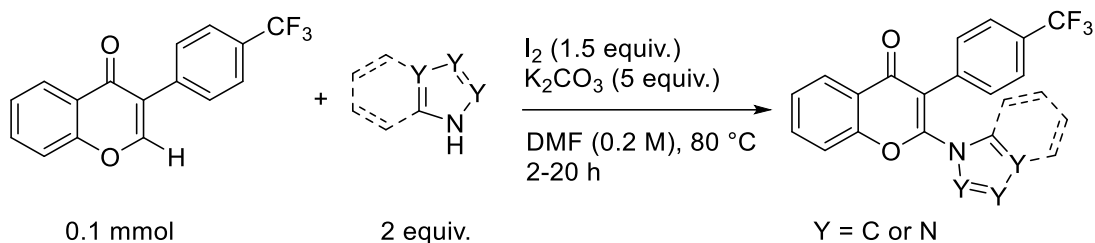


3-bromo-4H-chromen-4-one was prepared according to literature known procedure by addition of hydrobromic acid to the mixture of chromone and OXONE<sup>®</sup> in CH<sub>2</sub>Cl<sub>2</sub> followed by treatment of Et<sub>3</sub>N in moderate to good yields. The analytical data was identical with the reported.<sup>[130]</sup>



3-(4-(trifluoromethyl)phenyl)-4H-chromen-4-one was prepared according to literature known procedure following a palladium catalyzed cross-coupling reaction. The analytical data was identical with the reported.<sup>[126]</sup>

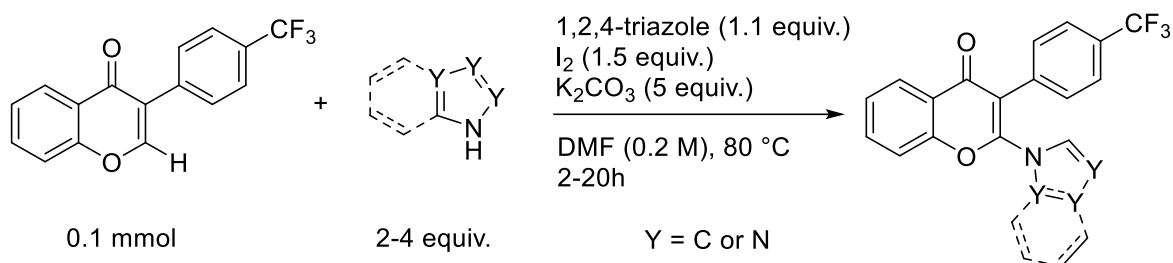
#### Procedure A for the coupling between chromone and azoles



Isoflavone (0.1 mmol) and azole (0.2 mmol) were dissolved in a 4 mL screw-capped vial with 0.5 mL of anhydrous DMF. Then molecular iodine (0.15 mmol), followed by anhydrous K<sub>2</sub>CO<sub>3</sub> were added at room temperature. The reaction mixture was stirred at 80 °C for 12 h. The reaction mixture was quenched with a saturated solution of sodium thiosulphate and extracted with

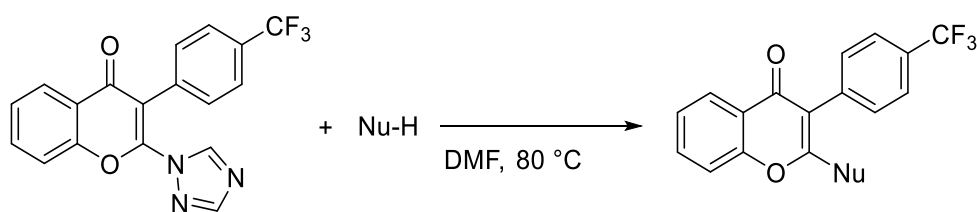
dichloromethane, washed with water, brine and dried over anhydrous  $\text{Na}_2\text{SO}_4$ . The organic extracts were filtered and concentrated under reduced pressure. Purification by column-chromatography on silica gel afforded the pure product.

### Procedure B for the coupling between chromone and azoles



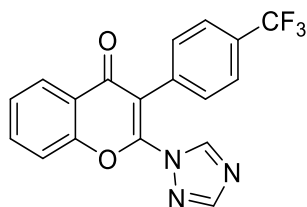
Chromone (0.1 mmol) and triazole (0.11 mmol) were dissolved in a 4 mL screw-capped vial with 0.5 mL of anhydrous DMF. Then molecular iodine (0.15 mmol) was added at room temperature and the reaction mixture was stirred at 80 °C for 12 h. Azole (0.2-0.4 mmol) followed by anhydrous  $\text{K}_2\text{CO}_3$  were added to the reaction mixture and the reaction was continued for 3-14 h. Then the reaction mixture was quenched with saturated solution of sodium thiosulphate and extracted with dichloromethane, washed with water, brine, dried over anhydrous  $\text{Na}_2\text{SO}_4$ . The organic extracts were filtered and concentrated under reduced pressure. Purification by column chromatography on silica gel afforded the pure product.

### General procedure C for the nucleophilic substitution



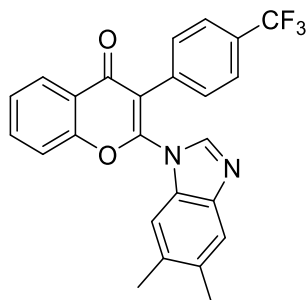
1 equiv. of 2-(1H-1,2,4-triazol-1-yl)-4H-chromen-4-one was transferred to a vial followed by the addition of dry DMF (0.1 M). After that 2 equiv. of nucleophile was added. The mixture was heated at the mentioned temperature. The progress of the reaction was monitored by TLC. Upon completion, the reaction mixture was diluted with EtOAc (10 mL) and washed 3 times with  $\text{H}_2\text{O}$  (3\*10 mL). The organic phase was dried by sodium sulfate and concentrated in vacuo. The pure product was obtained by column chromatography.

## 7.4.2 Physical data of products



### 2-(1*H*-1,2,4-triazol-1-yl)-3-(4-(trifluoromethyl)phenyl)-4*H*-chromen-4-one (116a)

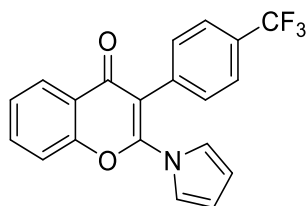
Prepared according to general procedure A. The product was isolated as white solid (31.8 mg, 0.09 mmol, 89%);  $R_f = 0.28$  (cyclohexane / ethyl acetate = 3:2);  $^1\text{H NMR}$  (500 MHz,  $\text{CD}_2\text{Cl}_2$ )  $\delta$  8.29 (d,  $J = 8.0$  Hz, 1H), 8.09 (d,  $J = 14.5$  Hz, 2H), 7.81 (t,  $J = 7.7$  Hz, 1H), 7.61 (dd,  $J = 13.0, 8.2$  Hz, 3H), 7.54 (t,  $J = 7.6$  Hz, 1H), 7.33 (d,  $J = 8.0$  Hz, 2H) ppm;  $^{13}\text{C NMR}$  (126 MHz,  $\text{CDCl}_3$ )  $\delta$  176.8, 154.4, 153.2, 149.7, 144.9, 135.2, 133.3, 130.9 (d,  $J = 32.7$  Hz), 130.5, 126.7 (d,  $J = 8.8$  Hz), 125.8 (q,  $J = 3.6$  Hz), 125.0, 123.0, 122.8, 118.1, 116.6 ppm; **FT-IR**:  $\tilde{\nu} = 3120, 1643, 1613, 1579, 1503, 1468, 1422, 1381, 1330, 1291, 1273, 1241, 1124, 1106, 1071$   $\text{cm}^{-1}$ ; **HR-MS**: calc. for  $[\text{M}+\text{H}]^+$   $\text{C}_{18}\text{H}_{11}\text{O}_2\text{N}_3\text{F}_3$ : 358.0798 found: 358.0799.



### 2-(5,6-dimethyl-1*H*-benzo[*d*]imidazol-1-yl)-3-(4-(trifluoromethyl)phenyl)-4*H*-chromen-4-one (116b)

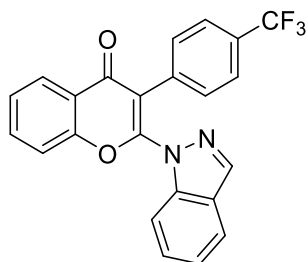
Prepared according to general procedure A. The product was isolated as pale yellow solid (20 mg, 0.05 mmol, 46%);  $R_f = 0.30$  (cyclohexane / ethyl acetate = 3:2);  $^1\text{H NMR}$  (500 MHz,  $\text{CD}_2\text{Cl}_2$ )  $\delta$  8.30 (dd,  $J = 8.1, 1.7$  Hz, 1H), 7.87 – 7.80 (m, 1H), 7.63 (dd,  $J = 8.6, 1.0$  Hz, 1H), 7.60 – 7.54 (m, 3H), 7.51 (s, 2H), 7.40 – 7.33 (m, 3H), 2.37 ppm (s, 6H);  $^{13}\text{C NMR}$  (126 MHz,  $\text{CD}_2\text{Cl}_2$ )  $\delta$  177.1, 154.9, 151.9, 142.3, 141.2, 135.2, 135.0, 133.9, 131.2, 131.2, 130.6 (d,  $J = 32.3$  Hz), 126.9, 126.8, 126.0 (q,  $J = 3.8$  Hz), 125.6, 123.7, 123.5, 121.2, 118.4, 115.8, 112.7, 20.8, 20.5 ppm; **FT-IR**  $\tilde{\nu} =$

3631, 2925, 2514, 2028, 1977, 1641, 1571, 1508, 1397, 1266, 1160, 960  $\text{cm}^{-1}$ ; **HR-MS**: calc. for  $[\text{M}+\text{H}]^+$   $\text{C}_{25}\text{H}_{18}\text{O}_2\text{N}_2\text{F}_3 = 435.1315$  found: 435.1311.



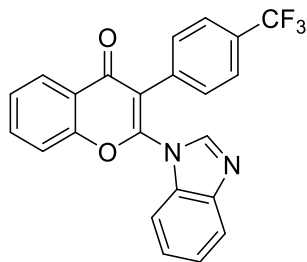
### 2-(1*H*-pyrrol-1-yl)-3-(4-(trifluoromethyl)phenyl)-4*H*-chromen-4-one (116c)

Prepared according to general procedure B. The product was isolated as yellow solid (11 mg, 0.03 mmol, 31%);  $R_f = 0.42$  (cyclohexane / ethyl acetate = 3:2);  **$^1\text{H NMR}$**  (700 MHz,  $\text{CD}_2\text{Cl}_2$ )  $\delta$  8.29 – 8.20 (m, 1H), 7.80 (d,  $J = 7.6$  Hz, 1H), 7.70 – 7.49 (m, 7H), 7.35 (d,  $J = 7.6$  Hz, 2H), 6.37 ppm (d,  $J = 4.3$  Hz, 1H).;  **$^{13}\text{C NMR}$**  (176 MHz,  $\text{CD}_2\text{Cl}_2$ )  $\delta$  177.5, 154.8, 153.0, 143.5, 135.8, 135.1, 131.8, 131.3, 130.2 (q,  $J = 32.5$  Hz), 126.8, 126.6, 125.6 (q,  $J = 4.0$  Hz), 123.6, 118.5, 114.7, 109.1 ppm; **FT-IR**:  $\tilde{\nu} = 3676, 2988, 2159, 1726, 1632, 1573, 1464, 1321, 1161, 1067, 908$   $\text{cm}^{-1}$ ; **HR-MS**: calc. for  $[\text{M}+\text{H}]^+$   $\text{C}_{20}\text{H}_{13}\text{O}_2\text{NF}_3 = 356.0893$  found: 357.0847.



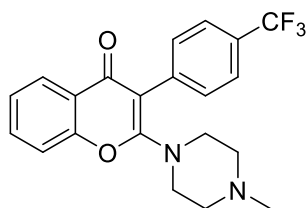
### 2-(1*H*-indazol-1-yl)-3-(4-(trifluoromethyl)phenyl)-4*H*-chromen-4-one (116d)

Prepared according to general procedure A. The product was isolated as yellow solid (12 mg, 0.03 mmol, 30%);  $R_f = 0.53$  (cyclohexane / ethyl acetate = 3:2);  **$^1\text{H NMR}$**  (500 MHz,  $\text{CD}_2\text{Cl}_2$ )  $\delta$  8.19 (dd,  $J = 7.9, 1.5$  Hz, 1H), 7.78 (d,  $J = 8.1$  Hz, 2H), 7.67 (m, 6H), 7.48 – 7.43 (m, 1H), 7.40 (d,  $J = 8.4$  Hz, 1H), 7.32 – 7.26 (m, 1H), 6.96 ppm (s, 1H);  **$^{13}\text{C NMR}$**  (126 MHz,  $\text{CD}_2\text{Cl}_2$ )  $\delta$  175.1, 157.1, 153.6, 140.0, 136.0, 134.5, 133.7, 133.6, 132.1, 131.7, 130.5 (d,  $J = 32.5$  Hz), 126.7 (q,  $J = 3.8$  Hz), 126.1, 125.7, 123.8, 123.6, 123.6, 117.4, 116.7, 106.5, 103.9 ppm; **FT-IR**:  $\tilde{\nu} = 2923, 2522, 2362, 2159, 1977, 1617, 1419, 1399, 1237, 1122, 1020$   $\text{cm}^{-1}$ ; **HR-MS**: calc. for  $[\text{M}+\text{H}]^+$   $\text{C}_{23}\text{H}_{14}\text{O}_2\text{N}_2\text{F}_3 = 407.1002$  found: 407.1000.



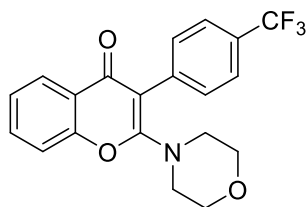
### 2-(1*H*-benzo[d]imidazol-1-yl)-3-(4-(trifluoromethyl)phenyl)-4*H*-chromen-4-one (116e)

Prepared according to general procedure A. The product was isolated as pale-yellow solid (8 mg, 0.02 mmol, 20%);  $R_f = 0.30$  (cyclohexane / ethyl acetate = 3:2);  $^1\text{H NMR}$  (500 MHz,  $\text{CD}_2\text{Cl}_2$ )  $\delta$  8.30 (dd,  $J = 7.9, 1.7$  Hz, 1H), 7.86 – 7.82 (m, 1H), 7.79 – 7.76 (m, 1H), 7.65 – 7.54 (m, 6H), 7.41 – 7.37 ppm (m, 4H);  $^{13}\text{C NMR}$  (126 MHz,  $\text{CD}_2\text{Cl}_2$ )  $\delta$  177.1, 154.9, 151.5, 143.8, 142.1, 135.3, 134.8, 132.8, 131.2, 130.7 (q,  $J = 32.5$  Hz), 127.2 (d,  $J = 18.9$  Hz), 126.9, 126.9, 126.1 (q,  $J = 3.8$  Hz), 125.5, 124.7, 123.6, 121.3, 118.4, 116.2, 112.6 ppm; **FT-IR**:  $\tilde{\nu} = 2672, 2384, 2115, 1991, 1624, 1503, 1353, 1292, 1162, 960$   $\text{cm}^{-1}$ ; **HR-MS**: calc. for  $[\text{M}+\text{H}]^+$   $\text{C}_{23}\text{H}_{14}\text{O}_2\text{N}_2\text{F}_3 = 407.1002$  found: 407.0999.



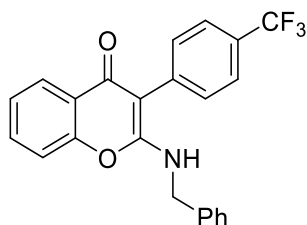
### 2-(4-methylpiperazin-1-yl)-3-(4-(trifluoromethyl)phenyl)-4*H*-chromen-4-one (116f)

Prepared according to general procedure C. The product was isolated as pale yellow solid (7 mg, 0.02 mmol, 18%);  $R_f = 0.50$  (dichloromethane / methanol = 9:1);  $^1\text{H NMR}$  (700 MHz,  $\text{CDCl}_3$ )  $\delta$  8.19 (dd,  $J = 7.8, 1.7$  Hz, 1H), 7.66 (d,  $J = 8.1$  Hz, 2H), 7.62 – 7.59 (m, 1H), 7.56 (d,  $J = 8.0$  Hz, 2H), 7.39 – 7.33 (m, 2H), 3.28 (t,  $J = 5.0$  Hz, 4H), 2.36 (t,  $J = 5.0$  Hz, 4H), 2.27 ppm (s, 3H);  $^{13}\text{C NMR}$  (176 MHz,  $\text{CDCl}_3$ )  $\delta$  176.1, 161.6, 153.4, 138.1, 132.8, 131.1, 129.0 (q,  $J = 32.3$  Hz), 126.4, 125.3 (q,  $J = 3.7$  Hz), 125.3, 123.6, 123.1, 116.6, 103.5, 54.5, 47.7, 46.1 ppm; **FT-IR**:  $\tilde{\nu} = 2925, 2029, 1615, 1548, 1464, 1293, 1162, 1019, 879$   $\text{cm}^{-1}$ ; **HR-MS**: calc. for  $[\text{M}+\text{H}]^+$   $\text{C}_{21}\text{H}_{20}\text{O}_2\text{N}_2\text{F}_3 = 389.1471$  found: 389.1473.



### 2-morpholino-3-(4-(trifluoromethyl)phenyl)-4H-chromen-4-one (116g)

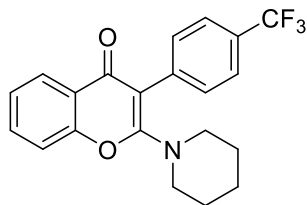
Prepared according to general procedure C. The product was isolated as pale yellow solid (5 mg, 0.01 mmol, 24%);  $R_f = 0.35$  (cyclohexane / ethyl acetate = 3:2);  **$^1\text{H NMR}$**  (500 MHz,  $\text{CDCl}_3$ )  $\delta$  8.20 (dd,  $J = 7.9, 1.6$  Hz, 1H), 7.67 (d,  $J = 8.1$  Hz, 2H), 7.65 – 7.58 (m, 1H), 7.58 (d,  $J = 8.0$  Hz, 2H), 7.40 – 7.34 (m, 2H), 3.66 – 3.60 (m, 4H), 3.28 – 3.22 ppm (m, 4H);  **$^{13}\text{C NMR}$**  (126 MHz,  $\text{CDCl}_3$ )  $\delta$  176.1, 161.4, 153.4, 137.8, 132.9, 131.1, 129.2 (d,  $J = 32.6$  Hz), 126.8, 126.5, 125.5 (q,  $J = 3.9$  Hz), 125.2, 123.0, 116.6, 103.7, 66.4, 48.1 ppm; **FT-IR**:  $\tilde{\nu} = 2921, 2854, 2090, 1614, 1515, 1406, 1320, 1161, 999, 898$   $\text{cm}^{-1}$ ; **HR-MS**: calc. for  $[\text{M}+\text{H}]^+$   $\text{C}_{20}\text{H}_{17}\text{O}_3\text{NF}_3 = 376.1155$  found: 376.1156.



### 2-(benzylamino)-3-(4-(trifluoromethyl)phenyl)-4H-chromen-4-one (116h)

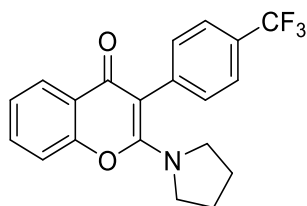
Prepared according to general procedure C. The product was isolated as brown solid (6 mg, 0.02 mmol, 27%);  $R_f = 0.45$  (cyclohexane / ethyl acetate = 3:2);  **$^1\text{H NMR}$**  (700 MHz,  $\text{CDCl}_3$ )  $\delta$  8.21 (dd,  $J = 7.8, 1.7$  Hz, 1H), 7.69 (d,  $J = 8.0$  Hz, 2H), 7.62 – 7.57 (m, 1H), 7.54 (d,  $J = 8.0$  Hz, 2H), 7.39 – 7.35 (m, 4H), 7.34 – 7.29 (m, 3H), 5.31 (t,  $J = 6.1$  Hz, 1H), 4.64 ppm (d,  $J = 6.1$  Hz, 2H);  **$^{13}\text{C NMR}$**  (176 MHz,  $\text{CDCl}_3$ )  $\delta$  173.8, 160.6, 153.0, 137.5, 136.6, 132.3, 131.6, 129.8 (q,  $J = 32.5$  Hz), 129.2, 128.7, 128.2, 127.4, 126.4, 126.3 (q,  $J = 3.7$  Hz), 125.2, 123.4, 116.5, 99.9, 45.8 ppm; **FT-IR**:  $\tilde{\nu} = 3741, 3032, 2921, 2850, 2115, 1736, 1698, 1581, 1484, 1319, 1166, 909$   $\text{cm}^{-1}$ ; **HR-MS**: calc. for  $[\text{M}+\text{H}]^+$   $\text{C}_{23}\text{H}_{17}\text{O}_2\text{NF}_3 = 396.1206$  found: 396.1200.





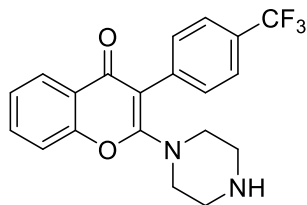
### 2-(piperidin-1-yl)-3-(4-(trifluoromethyl)phenyl)-4*H*-chromen-4-one (116i)

Prepared according to general procedure C. The product was isolated as pale yellow solid (7 mg, 0.02 mmol, 19%);  $R_f = 0.54$  (cyclohexane / ethyl acetate = 3:2);  $^1\text{H NMR}$  (700 MHz,  $\text{CDCl}_3$ )  $\delta$  8.19 (dd,  $J = 7.6, 1.9$  Hz, 1H), 7.65 (d,  $J = 7.8$  Hz, 2H), 7.60 – 7.55 (m, 3H), 7.37 – 7.33 (m, 2H), 3.22 – 3.19 (m, 4H), 1.62 – 1.56 (m, 2H), 1.52 (p,  $J = 5.7$  Hz, 4H).  $^{13}\text{C NMR}$  (176 MHz,  $\text{CDCl}_3$ )  $\delta$  176.0, 162.1, 153.4, 138.7, 132.6, 130.9, 128.6 (q,  $J = 32.4$  Hz), 126.4, 125.2 (q,  $J = 3.8$  Hz), 124.9, 123.7, 123.2, 116.5, 103.0, 49.3, 25.7, 24.2 ppm; **FT-IR**:  $\tilde{\nu} = 2928, 2841, 1732, 1614, 1542, 1425, 1250, 1106, 1068, 955, 893$   $\text{cm}^{-1}$ ; **HR-MS**: calc. for  $[\text{M}+\text{H}]^+$   $\text{C}_{21}\text{H}_{19}\text{O}_2\text{NF}_3 = 374.1362$  found: 374.1363.



### 2-(pyrrolidin-1-yl)-3-(4-(trifluoromethyl)phenyl)-4*H*-chromen-4-one (116j)

Prepared according to general procedure C. The product was isolated as pale yellow solid (10 mg, 0.03 mmol, 28%);  $R_f = 0.43$  (cyclohexane / ethyl acetate = 3:2);  $^1\text{H NMR}$  (700 MHz,  $\text{CDCl}_3$ )  $\delta$  8.19 (dd,  $J = 7.8, 1.7$  Hz, 1H), 7.64 – 7.60 (m, 2H), 7.58 – 7.53 (m, 1H), 7.51 – 7.45 (m, 2H), 7.35 – 7.31 (m, 2H), 3.26 – 3.21 (m, 4H), 1.95 – 1.60 ppm (m, 4H);  $^{13}\text{C NMR}$  (176 MHz,  $\text{CDCl}_3$ )  $\delta$  175.4, 159.4, 153.4, 138.6, 132.4, 132.2, 128.7 (q,  $J = 32.3$  Hz), 126.3, 125.3, 124.6 (q,  $J = 3.7$  Hz), 123.7, 122.9, 116.2, 100.7, 50.1, 25.5 ppm; **FT-IR**:  $\tilde{\nu} = 2665, 2384, 2118, 1996, 1727, 1614, 1512, 1468, 1357, 1222, 1098, 954, 883$   $\text{cm}^{-1}$ ; **HR-MS**: calc. for  $[\text{M}+\text{H}]^+$   $\text{C}_{20}\text{H}_{17}\text{O}_2\text{NF}_3 = 360.1206$  found: 360.1207.



**2-(piperazin-1-yl)-3-(4-(trifluoromethyl)phenyl)-4H-chromen-4-one (116k)**

Prepared according to general procedure C. The product was isolated as pale yellow solid (12 mg, 0.03 mmol, 32%);  $R_f = 0.44$  (dichloromethane / methanol = 9:1);  $^1\text{H NMR}$  (700 MHz,  $\text{CDCl}_3$ )  $\delta$  8.20 (dd,  $J = 7.8, 1.7$  Hz, 1H), 7.66 (d,  $J = 8.1$  Hz, 2H), 7.63 – 7.58 (m, 1H), 7.57 (d,  $J = 8.0$  Hz, 2H), 7.39 – 7.33 (m, 2H), 3.64 (s, 1H), 3.27 – 3.23 (m, 4H), 2.85 – 2.81 ppm (m, 4H);  $^{13}\text{C NMR}$  (176 MHz,  $\text{CDCl}_3$ )  $\delta$  176.1, 161.7, 153.4, 138.1, 132.8, 131.1, 128.9 (q,  $J = 32.4$  Hz), 126.4, 125.3 (q,  $J = 3.7$  Hz), 125.1, 123.6, 123.1, 116.6, 103.5, 48.9, 45.7 ppm; **FT-IR**:  $\tilde{\nu} = 2954, 2854, 2359, 2159, 1976, 1727, 1677, 1597, 1466, 1425, 1342, 1276, 1068, 1020, 942$   $\text{cm}^{-1}$ ; **HR-MS**: calc. for  $[\text{M}+\text{H}]^+$   $\text{C}_{20}\text{H}_{18}\text{O}_2\text{N}_2\text{F}_3 = 375.1315$  found: 375.1315.

## 8 References

- [1] A. E. Shilov, G. B. Shul'pin, *Chem. Rev.* **1997**, *97*, 2879-2932.
- [2] L. Guillemard, N. Kaplaneris, L. Ackermann, M. J. Johansson, *Nat. Rev. Chem.* **2021**, *5*, 522-545.
- [3] T. Rogge, N. Kaplaneris, N. Chatani, J. Kim, S. Chang, B. Punji, L. L. Schafer, D. G. Musaev, J. Wencel-Delord, C. A. Roberts, R. Sarpong, Z. E. Wilson, M. A. Brimble, M. J. Johansson, L. Ackermann, *Nat. Rev. Methods Primers* **2021**, *1*, DOI: 10.1038/s43586-43021-00041-43582.
- [4] S. D. Friis, M. J. Johansson, L. Ackermann, *Nat. Chem.* **2020**, *12*, 511-519.
- [5] M. S. Chen, M. C. White, *Science* **2007**, *318*, 783-787.
- [6] X. S. Xue, P. Ji, B. Zhou, J. P. Cheng, *Chem. Rev.* **2017**, *117*, 8622-8648.
- [7] Z. Chen, B. Wang, J. Zhang, W. Yu, Z. Liu, Y. Zhang, *Org. Chem. Front.* **2015**, *2*, 1107-1295.
- [8] U. Dutta, S. Maiti, T. Bhattacharya, D. Maiti, *Science* **2021**, *372*, DOI: 10.1126/science.abd5992; .
- [9] C. G. Newton, S.-G. Wang, C. C. Oliveira, N. Cramer, *Chem. Rev.* **2017**, *117*, 8908-8976.
- [10] P. Gandeepan, T. Müller, D. Zell, G. Cera, S. Warratz, L. Ackermann, *Chem. Rev.* **2018**, *119*, 2192-2452.
- [11] T. Dalton, T. Faber, F. Glorius, *ACS Cent. Sci.* **2021**, *7*, 245-261.
- [12] R. Samanta, K. Matcha, A. P. Antonchick, *Eur. J. Org. Chem.* **2013**, *2013*, 5769-5804.
- [13] R. Narayan, K. Matcha, A. P. Antonchick, *Chem. Eur. J.* **2015**, *21*, 14678-14693.
- [14] C. L. Sun, Z. J. Shi, *Chem. Rev.* **2014**, *114*, 9219-9280.
- [15] Y. Qin, L. Zhu, S. Luo, *Chem. Rev.* **2017**, *117*, 9433-9520.
- [16] A. Wiebe, T. Gieshoff, S. Mohle, E. Rodrigo, M. Zirbes, S. R. Waldvogel, *Angew. Chem. Int. Ed.* **2018**, *57*, 5594-5619; *Angew. Chem.* **2018**, *130*, 5694-5721.
- [17] R. Cannalire, S. Pelliccia, L. Sancineto, E. Novellino, G. C. Tron, M. Giustiniano, *Chem. Soc. Rev.* **2021**, *50*, 766-897.
- [18] L. Bering, S. Manna, A. P. Antonchick, *Chem. Eur. J.* **2017**, *23*, 10936-10946.
- [19] A. P. Pulis, D. J. Procter, *Angew. Chem. Int. Ed.* **2016**, *55*, 9842-9860; *Angew. Chem.* **2016**, *128*, 9996-10014.
- [20] A. Bhunia, S. R. Yetra, A. T. Biju, *Chem. Soc. Rev.* **2012**, *41*, 3140-3152.
- [21] R. Rossi, M. Lessi, C. Manzini, G. Marianetti, F. Bellina, *Adv. Synth. Catal.* **2015**, *357*, 3777-3814.
- [22] S. Roscales, A. G. Csaky, *Chem. Soc. Rev.* **2014**, *43*, 8215-8225.
- [23] E. Shirakawa, T. Hayashi, *Chem. Lett.* **2012**, *41*, 130-134.
- [24] A. V. Kutasevich, V. P. Perevalov, V. S. Mityanov, *Eur. J. Org. Chem.* **2020**, *3*, 357-373.
- [25] P. S. Fier, J. F. Hartwig, *J. Am. Chem. Soc.* **2014**, *136*, 10139-10147.
- [26] D. Wang, L. Désaubry, G. Li, M. Huang, S. Zheng, *Adv. Synth. Catal.* **2020**, *363*, 2-39.
- [27] A. T. Londregan, S. Jennings, L. Wei, *Org. Lett.* **2010**, *12*, 5254-5257.
- [28] A. T. Londregan, K. Burford, E. L. Conn, K. D. Hesp, *Org. Lett.* **2014**, *16*, 3336-3339.
- [29] A. T. Londregan, S. Jennings, L. Wei, *Org. Lett.* **2011**, *13*, 1840-1843.
- [30] S. E. Wengryniuk, A. Weickgenannt, C. Reiher, N. A. Strotman, K. Chen, M. D. Eastgate, P. S. Baran, *Org. Lett.* **2013**, *15*, 792-795.

- [31] H. Xiong, A. T. Hoye, K. H. Fan, X. Li, J. Clemens, C. L. Horchler, N. C. Lim, G. Attardo, *Org. Lett.* **2015**, *17*, 3726-3729.
- [32] B. S. Shaibu, R. K. Kawade, R. S. Liu, *Org. Biomol. Chem.* **2012**, *10*, 6834-6839.
- [33] D. H. Jones, S. T. Kay, J. A. McLellan, A. R. Kennedy, N. C. O. Tomkinson, *Org. Lett.* **2017**, *19*, 3512-3515.
- [34] T. Nishida, H. Ida, Y. Kuninobu, M. Kanai, *Nat. Commun.* **2014**, *5*, 1-6.
- [35] L.-Y. Xie, Y. Duan, L.-H. Lu, Y.-J. Li, S. Peng, C. Wu, K.-J. Liu, Z. Wang, W.-M. He, *ACS Sustain. Chem. Eng.* **2017**, *5*, 10407-10412.
- [36] K. Sun, X. L. Chen, X. Li, L. B. Qu, W. Z. Bi, X. Chen, H. L. Ma, S. T. Zhang, B. W. Han, Y. F. Zhao, C. J. Li, *Chem. Commun.* **2015**, *51*, 12111-12114.
- [37] F. Xu, Y. Li, X. Huang, X. Fang, Z. Li, H. Jiang, J. Qiao, W. Chu, Z. Sun, *Adv. Synth. Catal.* **2018**, *361*, 520-525.
- [38] H. Wang, X. Cui, Y. Pei, Q. Zhang, J. Bai, D. Wei, Y. Wu, *Chem. Commun.* **2014**, *50*, 14409-14411.
- [39] M.-T. Chen, X. You, L.-G. Bai, Q.-L. Luo, *Org. Biomol. Chem.* **2017**, *15*, 3165-3169.
- [40] J. M. Keith, *J. Org. Chem.* **2008**, *73*, 327-330.
- [41] J. M. Keith, *J. Org. Chem.* **2010**, *75*, 2722-2725.
- [42] J. M. Keith, *J. Org. Chem.* **2012**, *77*, 11313-11318.
- [43] X. Chen, X. Cui, F. Yang, Y. Wu, *Org. Lett.* **2015**, *17*, 1445-1448.
- [44] H. Wang, Y. Pei, J. Bai, J. Zhang, Y. Wu, X. Cui, *RSC Adv.* **2014**, *4*, 26244-26246.
- [45] P. Ghosh, N. Y. Kwon, S. Han, S. Kim, S. H. Han, N. K. Mishra, Y. H. Jung, S. J. Chung, I. S. Kim, *Org. Lett.* **2019**, *21*, 6488-6493.
- [46] W. Jo, J. Kim, S. Choi, S. H. Cho, *Angew. Chem. Int. Ed.* **2016**, *55*, 9690-9694; *Angew. Chem.* **2016**, *128*, 9842-9846.
- [47] S. Han, P. Chakrasali, J. Park, H. Oh, S. Kim, K. Kim, A. K. Pandey, S. H. Han, S. B. Han, I. S. Kim, *Angew. Chem. Int. Ed.* **2018**, *57*, 12737-12740; *Angew. Chem.* **2018**, *130*, 12919-12922.
- [48] R. Kumar, I. Kumar, R. Sharma, U. Sharma, *Org. Biomol. Chem.* **2016**, *14*, 2613-2617.
- [49] H. Xia, Y. Liu, P. Zhao, S. Gou, J. Wang, *Org. Lett.* **2016**, *18*, 1796-1799.
- [50] G. E. Crisenza, E. M. Dauncey, J. F. Bower, *Org. Biomol. Chem.* **2016**, *14*, 5820-5825.
- [51] C. Raminelli, Z. Liu, R. C. Larock, *J. Org. Chem.* **2006**, *71*, 4689-4691.
- [52] M. Lai, Y. Li, Z. Wu, M. Zhao, X. Ji, P. Liu, X. Zhang, *Asian J. Org. Chem.* **2018**, *7*, 1118-1123.
- [53] E. J. Horn, B. R. Rosen, P. S. Baran, *ACS Cent. Sci.* **2016**, *2*, 302-308.
- [54] A. Wiebe, T. Gieshoff, S. Möhle, E. Rodrigo, M. Zirbes, S. R. Waldvogel, *Angew. Chem. Int. Ed.* **2018**, *57*, 5594-5619; *Angew. Chem.* **2018**, *130*, 5694-5721.
- [55] C. Zhu, N. W. J. Ang, T. H. Meyer, Y. Qiu, L. Ackermann, *ACS Cent. Sci.* **2021**, *7*, 415-431.
- [56] M. D. Kärkäs, *Chem. Soc. Rev.* **2018**, *47*, 5786-5865.
- [57] H.-T. Tang, J.-S. Jia, Y.-M. Pan, *Org. Biomol. Chem.* **2020**, *18*, 5315-5333.
- [58] Y. Kawamata, K. Hayashi, E. Carlson, S. Shaji, D. Waldmann, B. J. Simmons, J. T. Edwards, C. W. Zapf, M. Saito, P. S. Baran, *J. Am. Chem. Soc.* **2021**.
- [59] M. Faraday, *Annalen der Physik* **1834**, *109*, 481-520.
- [60] H. Kolbe, *Liebigs Ann.* **1848**, *64*, 339-341.
- [61] R. Francke, R. D. Little, *Chem. Soc. Rev.* **2014**, *43*, 2492-2521.
- [62] Q. Jing, K. D. Moeller, *Acc. Chem. Res.* **2020**, *53*, 135-143.

- [63] J.-i. Yoshida, K. Nishiwaki, *J. Chem. Soc., Dalton Trans.* **1998**, 2589-2596.
- [64] J. C. Siu, N. Fu, S. Lin, *Acc. Chem. Res.* **2020**, *53*, 547-560.
- [65] S. Tang, Y. Liu, A. Lei, *Chem* **2018**, *4*, 27-45.
- [66] M. Yan, Y. Kawamata, P. S. Baran, *Chem. Rev.* **2017**, *117*, 13230-13319.
- [67] T. Noël, Y. Cao, G. Laudadio, *Acc. Chem. Res.* **2019**, *52*, 2858-2869.
- [68] M. Elsherbini, T. Wirth, *Acc. Chem. Res.* **2019**, *52*, 3287-3296.
- [69] T. Shen, T. H. Lambert, *J. Am. Chem. Soc.* **2021**, *143*, 8597-8602.
- [70] H.-C. Xu, K. D. Moeller, *J. Am. Chem. Soc.* **2008**, *130*, 13542-13543.
- [71] T. Morofuji, A. Shimizu, J.-i. Yoshida, *J. Am. Chem. Soc.* **2013**, *135*, 5000-5003.
- [72] L.-B. Zhang, R.-S. Geng, Z.-C. Wang, G.-Y. Ren, L.-R. Wen, M. Li, *Green Chem.* **2020**, *22*, 16-21.
- [73] T. Shono, Y. Matsumura, S. Katoh, K. Takeuchi, K. Sasaki, T. Kamada, R. Shimizu, *J. Am. Chem. Soc.* **1990**, *112*, 2368-2372.
- [74] Q. Wang, P. Wang, X. Gao, D. Wang, S. Wang, X. Liang, L. Wang, H. Zhang, A. Lei, *Chem. Sci.* **2020**, *11*, 2181-2186.
- [75] J. C. Siu, G. S. Sauer, A. Saha, R. L. Macey, N. Fu, T. Chauvire, K. M. Lancaster, S. Lin, *J. Am. Chem. Soc.* **2018**, *140*, 12511-12520.
- [76] J. C. Siu, J. B. Parry, S. Lin, *J. Am. Chem. Soc.* **2019**, *141*, 2825-2831.
- [77] Z. W. Hou, Z. Y. Mao, Y. Y. Melcamu, X. Lu, H. C. Xu, *Angew. Chem. Int. Ed.* **2018**, *57*, 1636-1639; *Angew. Chem.* **2018**, *130*, 1652-1655.
- [78] T. Siu, A. K. Yudin, *J. Am. Chem. Soc.* **2002**, *124*, 530-531.
- [79] J. Chen, W. Q. Yan, C. M. Lam, C. C. Zeng, L. M. Hu, R. D. Little, *Org. Lett.* **2015**, *17*, 986-989.
- [80] Y. Amano, S. Nishiyama, *Tetrahedron Lett.* **2006**, *47*, 6505-6507.
- [81] M. Gong, J. M. Huang, *Chem. Eur. J.* **2016**, *22*, 14293-14296.
- [82] A. A. Folgueziras-Amador, K. Philipps, S. Guilbaud, J. Poelakker, T. Wirth, *Angew. Chem. Int. Ed.* **2017**, *56*, 15446-15450; *Angew. Chem.* **2017**, *129*, 15648-15653.
- [83] L. Xu, F.-Y. Liu, Q. Zhang, W.-J. Chang, Z.-L. Liu, Y. Lv, H.-Z. Yu, J. Xu, J.-J. Dai, H.-J. Xu, *Nat. Catal.* **2021**, *4*, 71-78.
- [84] E. O. Pentsak, D. B. Eremin, E. G. Gordeev, V. P. Ananikov, *ACS Catal.* **2019**, *9*, 3070-3081.
- [85] T.-H. Wang, W.-C. Lee, T.-G. Ong, *Adv. Synth. Catal.* **2016**, *358*, 2751-2758.
- [86] F. Minisci, R. Bernardi, F. Bertini, R. Galli, M. Perchinummo, *Tetrahedron* **1971**, *27*, 3575-3579.
- [87] R.-J. Tang, L. Kang, L. Yang, *Adv. Synth. Catal.* **2015**, *357*, 2055-2060.
- [88] M. Wan, H. Lou, L. Liu, *Chem. Commun.* **2015**, *51*, 13953-13956.
- [89] H. Vorbrueggen, *Acc. Chem. Res.* **1995**, *28*, 509-520.
- [90] W. Zhou, T. Miura, M. Murakami, *Angew. Chem. Int. Ed.* **2018**, *57*, 5139-5142; *Angew. Chem.* **2018**, *130*, 5233-5236.
- [91] W. Li, G. Gao, Y. Gao, C. Yang, W. Xia, *Chem. Commun.* **2017**, *53*, 5291-5293.
- [92] L. Bering, A. P. Antonchick, *Org. Lett.* **2015**, *17*, 3134-3137.
- [93] R. J. P. Corriu, R. Perz, C. Reye, *Tetrahedron* **1983**, *39*, 999-1009.
- [94] M.-A. Bray, S. Singh, H. Han, C. T. Davis, B. Borgeson, C. Hartland, M. Kost-Alimova, S. M. Gustafsdottir, C. C. Gibson, A. E. Carpenter, *Nat. Protoc.* **2016**, *11*, 1757-1774.
- [95] Y. Araki, K. Kobayashi, M. Yonemoto, Y. Kondo, *Org. Biomol. Chem.* **2011**, *9*, 78-80.

- [96] K. Inamoto, Y. Araki, S. Kikkawa, M. Yonemoto, Y. Tanaka, Y. Kondo, *Org. Biomol. Chem.* **2013**, *11*, 4438-4441.
- [97] A. M. Prokhorov, M. Małkosza, O. N. Chupakhin, *Tetrahedron Lett.* **2009**, *50*, 1444-1446.
- [98] X. Chen, F. Yang, X. Cui, Y. Wu, *Adv. Synth. Catal.* **2017**, *359*, 3922-3926.
- [99] R. Chinchilla, C. Najera, *Chem. Rev.* **2007**, *107*, 874-922.
- [100] J. H. Clark, *Chem. Rev.* **1980**, *80*, 429-452.
- [101] J. Wang, Y. Gurevich, M. Botoshansky, M. S. Eisen, *J. Am. Chem. Soc.* **2006**, *128*, 9350-9351.
- [102] A. A. Toutov, K. N. Betz, D. P. Schuman, W. B. Liu, A. Fedorov, B. M. Stoltz, R. H. Grubbs, *J. Am. Chem. Soc.* **2017**, *139*, 1668-1674.
- [103] A. P. Antonchick, R. Samanta, K. Kulikov, J. Lategahn, *Angew. Chem. Int. Ed.* **2011**, *50*, 8605-8608; *Angew. Chem.* **2018**, *130*, 5694-5721.
- [104] S. Manna, A. P. Antonchick, *Angew. Chem. Int. Ed.* **2014**, *53*, 7324-7327; *Angew. Chem.* **2014**, *126*, 7452-7455.
- [105] R. Samanta, J. Lategahn, A. P. Antonchick, *Chem. Commun.* **2012**, *48*, 3194-3196.
- [106] S. Manna, P. O. Serebrennikova, I. A. Utepova, A. P. Antonchick, O. N. Chupakhin, *Org. Lett.* **2015**, *17*, 4588-4591.
- [107] R. Samanta, J. O. Bauer, C. Strohmman, A. P. Antonchick, *Org. Lett.* **2012**, *14*, 5518-5521.
- [108] K. Inoue, Y. Ishikawa, S. Nishiyama, *Org. Lett.* **2010**, *12*, 436-439.
- [109] W. P. Tsang, N. Zheng, S. L. Buchwald, *J. Am. Chem. Soc.* **2005**, *127*, 14560-14561.
- [110] J. A. Jordan-Hore, C. C. Johansson, M. Gulias, E. M. Beck, M. J. Gaunt, *J. Am. Chem. Soc.* **2008**, *130*, 16184-16186.
- [111] K. Takamatsu, K. Hirano, T. Satoh, M. Miura, *Org. Lett.* **2014**, *16*, 2892-2895.
- [112] S. Choi, T. Chatterjee, W. J. Choi, Y. You, E. J. Cho, *ACS Catal.* **2015**, *5*, 4796-4802.
- [113] M. Ates, N. Uludag, *J. Solid State Electrochem.* **2016**, *20*, 2599-2612.
- [114] J. F. Ambrose, R. F. Nelson, *J. Electrochem. Soc.* **1968**, *115*, 1159.
- [115] T. Broese, R. Francke, *Org. Lett.* **2016**, *18*, 5896-5899.
- [116] D. Kajiyama, K. Inoue, Y. Ishikawa, S. Nishiyama, *Tetrahedron* **2010**, *66*, 9779-9784.
- [117] A. Maity, B. L. Frey, N. D. Hoskinson, D. C. Powers, *J. Am. Chem. Soc.* **2020**, *142*, 4990-4995.
- [118] T. Gieshoff, A. Kehl, D. Schollmeyer, K. D. Moeller, S. R. Waldvogel, *J. Am. Chem. Soc.* **2017**, *139*, 12317-12324.
- [119] B. R. Rosen, E. W. Werner, A. G. O'Brien, P. S. Baran, *J. Am. Chem. Soc.* **2014**, *136*, 5571-5574.
- [120] M.-Y. Lin, K. Xu, Y.-Y. Jiang, Y.-G. Liu, B.-G. Sun, C.-C. Zeng, *Adv. Synth. Catal.* **2018**, *360*, 1665-1672.
- [121] H. R. Bjørsvik, V. Elumalai, *Eur. J. Org. Chem.* **2016**, *33*, 5474-5479.
- [122] O. Daugulis, V. G. Zaitsev, *Angew. Chem. Int. Ed.* **2005**, *44*, 4046-4048; *Angew. Chem.* **2005**, *117*, 4114-4116.
- [123] K. K. Ghosh, A. Uttry, A. Koldemir, M. Ong, M. van Gemmeren, *Org. Lett.* **2019**, *21*, 7154-7157.
- [124] M. Dörr, J. L. Röckl, J. Rein, D. Schollmeyer, S. R. Waldvogel, *Chem. Eur. J.* **2020**, *26*, 10195-10198.

- [125] I. Colomer, A. E. Chamberlain, M. B. Haughey, T. J. Donohoe, *Nat. Rev. Chem.* **2017**, *1*, 1-12.
- [126] R. Samanta, R. Narayan, J. O. Bauer, C. Strohmann, S. Sievers, A. P. Antonchick, *Chem. Commun.* **2015**, *51*, 925-928.
- [127] J. M. Ng, T. Curran, *Nat. Rev. Cancer* **2011**, *11*, 493-501.
- [128] R. N. Wang, J. Green, Z. Wang, Y. Deng, M. Qiao, M. Peabody, Q. Zhang, J. Ye, Z. Yan, S. Denduluri, O. Idowu, M. Li, C. Shen, A. Hu, R. C. Haydon, R. Kang, J. Mok, M. J. Lee, H. L. Luu, L. L. Shi, *Genes Dis.* **2014**, *1*, 87-105.
- [129] L. Su, D.-D. Guo, B. Li, S.-H. Guo, G.-F. Pan, Y.-R. Gao, Y.-Q. Wang, *ChemCatChem* **2017**, *9*, 2001-2008.
- [130] K.-M. Kim, I.-H. Park, *Synthesis* **2004**, *16*, 2641-2644.





---

## **Appendix**

---



## 9 Appendix

### 9.1 List of Abbreviations

Å	Ångström
Ac	acetyl
anhyd.	anhydrous
aq.	aqueous
Ar	argon
BDD	boron doped diamond
BDE	bond dissociation energy
BMP	bone morphogenetic protein
Bn	benzyl
Boc	<i>tert</i> -butyloxycarbonyl
Bu	butyl
Bz	benzoyl
calc.	calculated
cat.	catalyst
CDC	cross dehydrogenative coupling
CE	counter electrode
COMAS	Compound Management and Screening Center
conc.	concentration
const.	constant
conv.	conversion
CV	cyclic voltammetry
DCE	1,2-dichloroethane
DCM	dichloromethane
DDQ	2,3-dichloro-5,6-dicyano-1,4-benzoquinone
DIPEA	diisopropylethylamine
DMF	dimethylformamide
DMSO	dimethylsulfoxide
EC <sub>50</sub>	half maximal effective concentration

EDG	electron-donating group
ESI	electrospray ionization
Et	ethyl
<i>et al.</i>	<i>et alii</i> (and others)
Et <sub>3</sub> N	triethylamine
Et <sub>2</sub> O	diethylether
EtOAc	ethyl acetate
equiv.	equivalent
EWG	electron withdrawing group
F	Faraday
FT-IR	Fourier-Transform Infrared spectroscopy
G	graphite
GC	glassy carbon
h	hour
HFIP	1,1,1,3,3,3-hexafluoro-2-propanol
Hh	hedgehog
HPLC	high-performance liquid chromatography
HR-MS	high resolution mass spectrometry
Hz	Hertz
<i>I</i>	current
IC <sub>50</sub>	half-maximal inhibitory concentration
<i>i</i> Pr	iso-propyl
<i>J</i>	coupling constants
K <sub>2</sub> CO <sub>3</sub>	potassium carbonate
<i>m</i> -	meta
Me	methyl
MeCN	acetonitrile
mESCs	Mouse embryonic stem cells
NaOEt	sodium ethoxide
n.d.	not detected
NMR	nuclear magnetic resonance

Nu	nucleophile
<i>o</i> -	ortho
OAc	acetate
<i>p</i> -	para
Ph	phenyl
PIDA	iodosobenzene diacetate
PIFA	iodosobenzene bis(trifluoroacetate)
PPh <sub>3</sub>	triphenylphosphine
ppm	parts per million
rt	room temperature
<i>p</i> -TsOH	<i>para</i> -toluenesulfonic acid
<i>Q</i>	charge passed
<i>R<sub>f</sub></i>	retention factor
RVC	reticulated vitreous carbon
SAR	structure-activity relationship
SCE	saturated calomel electrode
SET	single electron transfer
sat.	saturated
TBAF	tetrabutylammonium fluoride
<i>t</i> Bu	<i>tert</i> -butyl
temp.	temperature
THF	tetrahydrofuran
TM	transition metal
<i>t<sub>R</sub></i>	retention time
Ts	<i>para</i> -tosyl
TsCl	<i>para</i> -toluenesulfonyl chloride
TS	transitionstate
<i>V</i>	voltage
WE	working electrode



## 9.2 Acknowledgement

First of all, I would like to gratefully acknowledge Prof. Dr. Dr. h.c. Herbert Waldmann for giving me the opportunity to pursue doctoral studies in his group and his willingness to be the first examiner of my thesis. His very constructive feedback and suggestions through the years had an important impact on the achieved work.

My biggest thanks go to my supervisor and mentor Dr. Andrey P. Antonchick. I would like to express my honest gratitude for his support and guidance. Working with him was always respectful, honest, and productive, ever since I joined his group. I can honestly say that he helped me evolve as a better scientist and more importantly as a better person. I extend my thanks for his immediate willingness to be my second examiner.

I would like to thank Dr. Andreas Brunschweiger for his valuable suggestions during my thesis advisory committee meetings. I would like to gratefully acknowledge Dr. Sonja Sievers and the COMAS Dortmund team for testing my compounds and providing valuable biological results. Also, I am thankful to Prof. Dennis Schade, Fabian Wesseler and all members of the 'BMP' team for the great collaboration.

I thank Dr. Sukdev Bag, Dr. Okan Yildirim, Caitlin Davies and Amrutha Krishnan for their support during thesis writing and for proof reading my thesis.

I am grateful to all of my current and former colleagues, particularly Dr. Okan Yildirim, Vasiliki Polychronidou, Hui Chun-ngai, Dr. Saad Shabaan, Dr. Luis Bering and Dr. Michael Grigalunas for their help, support and cooperation. I am very grateful for every friend I met during my academic journey. Without their direct and indirect support in each stage of my life, I would not be where I am today.

In addition, I would like to thank the analytical team, especially Christiane Heitbrink, Svetlana Gerdt, Jens Warmers, Mr. Bernhard Griewel and Dr. Petra Janning. I am thankful to IMPRS coordinators: Dr. Lucia Sironi and Christa Hornemann as well as TU staff including Ms. Maria Sergani. I am also thankful to Prof. Carsten Strohmann and Lukas Brieger for X-ray measurements.

I am highly indebted to Dr. Indu Bhusan Deb, Dr. Aniket Mishra and Tripta Kumari Vats for teaching me everything and for the constant encouragement to do research.

I am also thankful to Dr. Y. V. Madhavi and Dr. Sreya Gupta for their support. I am thankful to all my teachers and all my friends.

I would like to express my heartfelt gratitude to Dr. Bijisha KC for her support, encouragement and unconditional love in my life.

Finally, I want to express my profound gratitude to the members of my family; father, mother, brother and sis-in-law for their support, love and constant encouragement. This is as much my mother's thesis as it is mine.

Thank you!



## 9.3 Curriculum Vitae

### Personal Data

Name Mahesh Puthanveedu

Date of birth 12.06.1993

Place of birth Mannarkkad, India

### Education

2018- 2021 Ph.D. Chemistry and Chemical Biology

Advisors: Prof. Assoc. Andrey Antonchick and Prof. Herbert Waldmann  
Max Planck Institute of Molecular Physiology, TU Dortmund University,  
Germany.

Research Project: Development of Transition Metal-free Direct C–H  
Functionalization Methods.

2015-2017 M. S.(pharm) Medicinal Chemistry

Advisor: Dr. Indu Bhusan Deb

CSIR- Indian Institute of Chemical Biology (IICB), NIPER-Kolkata, India.

Research Project: Rhodium catalyzed C–H activation methodologies for the  
direct functionalization of nitrogen heterocycles.

2010-2014 Bachelor of Pharmacy

Kerala University of Health Sciences, Kerala, India.

### Publications

1. Puthanveedu, M.; Khamraev, V.; Brieger, L.; Strohmman, C.; Antonchick, A. P.,  
Electrochemical Dehydrogenative C(sp<sup>2</sup>)-H Amination. *Chem. Eur. J.* 2021, 27,  
8008.
2. Wesseler, F.; Riege, D.; Puthanveedu, M.; Halver, J.; Müller, E.; Bertrand, J.;  
Mercola, M.; Antonchick, A. P.; Ziegler, S.; Sievers, S.; Waldmann, H.; Schade,  
D., Probing embryonic mesodermal differentiation enables identification of small  
molecule bone morphogenetic protein activators (*manuscript submitted*).

3. Puthanveedu, M.; Antonchick A. P. Aromatic C–H Functionalization with Iodine(I/III) Catalysts or Iodine (III) Reagents in *Iodine Catalysis in Organic Synthesis*, co-edited by Kazuaki Ishihara and Kilian Muñiz. Wiley-VCH. 2020 (*book chapter in press*).
4. Puthanveedu, M.; Polychronidou, V.; Antonchick, A. P., Catalytic Selective Metal-Free Cross-Coupling of Heteroaromatic *N*-Oxides with Organosilanes. *Org. Lett.* 2019, 21, 3407-3411.
5. Mishra, A.; Vats, T. K.; Puthanveedu, M.; Das, A.; Deb, I., Rhodium-Catalyzed  $sp^2$  C–H Acetoxylation of *N*-Aryl Azaindoles/*N*-Heteroaryl Indolines. *J. Org. Chem.* 2017, 82, 12406–12415.

### Conferences

- 04/2021 Mahesh Puthanveedu, Vladislav Khamraev, Lukas Brieger, Carsten Strohmann, Andrey P. Antonchick “Electrochemical Dehydrogenative C(sp<sup>2</sup>)-H Amination” 8<sup>th</sup> IMPRS-LM student symposium, Dortmund, Germany, April 2021 (poster presentation)
- 07/2019 Mahesh Puthanveedu, Vasiliki Polychronidou, Andrey P. Antonchick “Catalytic Metal-Free Cross-Coupling of Heteroaromatic *N*-Oxides with Organosilanes” European Symposium on Organic Chemistry, Vienna, Austria, July 2019 (poster presentation)
- 03/2016 Mahesh Puthanveedu, Aniket Mishra, Tripta Kumari Vats, Indu Bhusan Deb “Rhodium-Catalyzed  $sp^2$  C–H Acetoxylation of *N*-Aryl Azaindoles” International Symposium on Chemical Biology and Drug Discovery, Kolkata, India, March 2016 (poster presentation)

### Honors & Awards

International Max Planck Research School Graduate School Fellowship, 2018  
 Dr. B.C. Pal Award for Medicinal Chemistry, 2017  
 Scholarships from NIPER, AICTE, India, 2015

## 9.4 Eidesstattliche Versicherung (Affidavit)

### Eidesstattliche Versicherung (Affidavit)

Putharveedu, Mahesh

Name, Vorname  
(Surname, first name)

215726

Matrikel-Nr.  
(Enrolment number)

**Belehrung:**

Wer vorsätzlich gegen eine die Täuschung über Prüfungsleistungen betreffende Regelung einer Hochschulprüfungsordnung verstößt, handelt ordnungswidrig. Die Ordnungswidrigkeit kann mit einer Geldbuße von bis zu 50.000,00 € geahndet werden. Zuständige Verwaltungsbehörde für die Verfolgung und Ahndung von Ordnungswidrigkeiten ist der Kanzler/die Kanzlerin der Technischen Universität Dortmund. Im Falle eines mehrfachen oder sonstigen schwerwiegenden Täuschungsversuches kann der Prüfling zudem exmatrikuliert werden, § 63 Abs. 5 Hochschulgesetz NRW.

Die Abgabe einer falschen Versicherung an Eides statt ist strafbar.

Wer vorsätzlich eine falsche Versicherung an Eides statt abgibt, kann mit einer Freiheitsstrafe bis zu drei Jahren oder mit Geldstrafe bestraft werden, § 156 StGB. Die fahrlässige Abgabe einer falschen Versicherung an Eides statt kann mit einer Freiheitsstrafe bis zu einem Jahr oder Geldstrafe bestraft werden, § 161 StGB.

Die oben stehende Belehrung habe ich zur Kenntnis genommen:

**Official notification:**

Any person who intentionally breaches any regulation of university examination regulations relating to deception in examination performance is acting improperly. This offence can be punished with a fine of up to EUR 50,000.00. The competent administrative authority for the pursuit and prosecution of offences of this type is the chancellor of the TU Dortmund University. In the case of multiple or other serious attempts at deception, the candidate can also be unenrolled, Section 63, paragraph 5 of the Universities Act of North Rhine-Westphalia.

The submission of a false affidavit is punishable.

Any person who intentionally submits a false affidavit can be punished with a prison sentence of up to three years or a fine, Section 156 of the Criminal Code. The negligent submission of a false affidavit can be punished with a prison sentence of up to one year or a fine, Section 161 of the Criminal Code.

I have taken note of the above official notification.

Dortmund

Ort, Datum  
(Place, date)

Unterschrift  
(Signature)

Titel der Dissertation:  
(Title of the thesis)

Novel Transition Metal-Free C-H bond functionalization for

Biologically Important Heterocycles

Ich versichere hiermit an Eides statt, dass ich die vorliegende Dissertation mit dem Titel selbstständig und ohne unzulässige fremde Hilfe angefertigt habe. Ich habe keine anderen als die angegebenen Quellen und Hilfsmittel benutzt sowie wörtliche und sinngemäße Zitate kenntlich gemacht.

Die Arbeit hat in gegenwärtiger oder in einer anderen Fassung weder der TU Dortmund noch einer anderen Hochschule im Zusammenhang mit einer staatlichen oder akademischen Prüfung vorgelegen.

I hereby swear that I have completed the present dissertation independently and without inadmissible external support. I have not used any sources or tools other than those indicated and have identified literal and analogous quotations.

The thesis in its current version or another version has not been presented to the TU Dortmund University or another university in connection with a state or academic examination."

\*Please be aware that solely the German version of the affidavit ("Eidesstattliche Versicherung") for the PhD thesis is the official and legally binding version.

Ort, Datum  
(Place, date)

Unterschrift  
(Signature)

